A THEORETICAL ANALYSIS OF FIRE DEVELOPMENT AND FLAME SPREAD IN UNDERGROUND TRAINS

A THESIS SUBMITTED TO
THE GRADUATE SCHOOL OF NATURAL AND APPLIED SCIENCES
OF
MIDDLE EAST TECHNICAL UNIVERSITY

BY

EREN MUSLUOĞLU

IN PARTIAL FULFILLMENT OF THE REQUIREMENTS
FOR
THE DEGREE OF DOCTOR OF PHILOSOPHY
IN
MECHANICAL ENGINEERING

AUGUST 2009

Approval of the thesis:

A THEORETICAL ANALYSIS OF FIRE DEVELOPMENT AND FLAME SPREAD IN UNDERGROUND TRAINS

submitted by **EREN MUSLUOĞLU** in partial fulfillment of the requirements for the degree of
Doctor of Philosophy in Mechanical Engineering Department, Middle East Technical University by,

Prof. Dr. Canan Özgen _____
Dean, Graduate School of **Natural and Applied Sciences**

Prof. Dr. Suha Oral _____
Head of Department, **Mechanical Engineering**

Prof. Dr. O. Cahit Eralp _____
Supervisor, **Mechanical Engineering Department**

Examining Committee Members:

Prof. Dr. Y. Samim Ünlüsoy
Mechanical Engineering, METU _____

Prof. Dr. O. Cahit Eralp
Mechanical Engineering, METU _____

Prof. Dr. Kahraman Albayrak
Mechanical Engineering, METU _____

Prof. Dr. Ali Durmaz
Mechanical Engineering, Gazi University _____

Prof. Dr. Birol Kılkış
Mechanical Engineering, Başkent University _____

Date: _____

I hereby declare that all information in this document has been obtained and presented in accordance with academic rules and ethical conduct. I also declare that, as required by these rules and conduct, I have fully cited and referenced all material and results that are not original to this work.

Name, Last Name: EREN MUSLUOĞLU

Signature :

ABSTRACT

A THEORETICAL ANALYSIS OF FIRE DEVELOPMENT AND FLAME SPREAD IN UNDERGROUND TRAINS

Musluoğlu, Eren
Ph.D., Department of Mechanical Engineering
Supervisor : Prof. Dr. O. Cahit Eralp

August 2009, 312 pages

The fire development and flame spread in the railway carriages are investigated by performing a set of simulations using a widely accepted simulation software called 'Fire Dynamics Simulator'.

Two different rolling stock models; representing a train made up of physically separated carriages, and a 4-car train with open wide gangways; have been built to examine the effects of train geometry on fire development and smoke spread within the trains. The simulations incorporate two different ignition sources; a small size arson fire, and a severe baggage fire incident. The simulations have been performed incorporating variations of parameters including tunnel geometry, ventilation and evacuation strategies, and combustible material properties.

The predictions of flame spread within the rolling stock and values of the peak heat release rates are reported for the simulated incident cases. In addition, for a set of base cases the onboard conditions are discussed and compared against the tenability criteria given by the international standards.

The predictions of heat release rate and the onboard conditions from the Fire Dynamics Simulator case studies have been checked against the empirical methods such as Duggan's method and other simulation softwares such as CFAST program.

Keywords: Train Fire, Fire Development, Flame Spread, Heat Release Rate, Fire Dynamics Simulator (FDS)

ÖZ

METRO TRENLERİNDE YANGIN GELİŞİMİNİN VE YAYILMASININ TEORİK ANALİZİ

Musluoğlu, Eren
Doktora, Makina Mühendisliği Bölümü
Tez Yöneticisi : Prof. Dr. O. Cahit Eralp

Ağustos 2009, 312 sayfa

Yeraltı trenlerinde yangın gelişimi ve yayılması endüstride geniş bir kitle tarafından kabul gören 'Fire Dynamics Simulator' programı kullanılarak yapılan bir dizi simülasyonla incelenmiştir.

Trenin yapısı ve geometrisinin, tren içerisindeki yangın gelişimi ve duman yayılması üzerindeki etkisini incelemek üzere iki farklı tren modeli; birbirinden fiziksel olarak ayrılmış vagonlardan oluşan bir treni temsil eden bir vagon, ve birbiri arasında geçiş yapılabilen açık aralıklı dört vagonlu bir tren modeli hazırlanmıştır. Simülasyonlarda, düşük güce sahip bir kundaklama ve yüksek güçlü bir bagaj yangını olmak üzere iki farklı ateşleme kaynağı kullanılmıştır. Yapılan simülasyonlarda, tünelin geometrisi, havalandırma ve yolcu tahliyesi stratejileri, ve yanıcı madde özellikleri gibi birçok değişkenin yangın gelişimi üzerindeki etkileri de incelenmiştir.

Simülasyonlar sonucunda elde edilen tren içerisindeki yangının yayılma alanı ve ortaya çıkan ısıl güç değerleri bu tezde raporlanmıştır. Ayrıca, seçilen bir dizi simülasyon çalışması için tren içerisindeki koşullar tartışılmış ve bunlar uluslararası standartlarca belirlenen yaşam için dayanılabilirlik limitleri ile karşılaştırılmıştır.

Fire Dynamics Simulator programı kullanılarak elde edilen tren içerisindeki koşullar ve ortaya çıkan ısıl güç değerleri diğer simülasyon programları, örneğin CFAST, ve basit aritmetik yöntemler, örneğin Duggan methodu, ile karşılaştırılıp doğrulanmıştır.

Anahtar Kelimeler: Tren Yangını, Yangın Gelişimi, Alev Yayılması, Isıl Güç Değeri, Fire Dynamics Simulator (FDS)

To My Family

ACKNOWLEDGMENTS

I would like to express my sincere gratitude to Prof. Dr. O. Cahit Eralp for his guidance and insight throughout this research. I wish to thank him especially for his empathy and trust in me completing my thesis work.

I also wish to express my gratitude to my managers at Mott MacDonald Ltd., especially Robin Hall and Bill Gray, for their support, and invaluable suggestions and comments on my research work.

I would like to thank Dave Tooley of Bombardier Transportation UK Ltd. and Cathy Hunsley from Transport for London for providing vital information on the rolling stock design and for allowing me to publish this research study.

I also would like to thank my colleagues at Mott MacDonald, Dr. Mikel Alonso, Edward Draper, and Alec Gregory for their moral support and sharing the most needed computational power during the thesis work.

I am grateful to my friends at Middle East Technical University, Serkan Kayılı, Tolga Köktürk, and Ekin Özgirgin Bingöl for their friendship and support at the university.

Finally, I would like to appreciate my parents for their encouragement, endless support, and patience throughout my thesis work.

TABLE OF CONTENTS

ABSTRACT iv

ÖZ vi

DEDICATON viii

ACKNOWLEDGMENTS ix

TABLE OF CONTENTS x

LIST OF TABLES xvi

LIST OF FIGURES xviii

CHAPTERS

1 INTRODUCTION 1

1.1 INTRODUCTION 1

1.2 FIRE DEVELOPMENT AND DETERMINATION OF FIRE SCENARIOS 2

1.2.1 STATISTICS OF FIRES IN UNDERGROUND TRAINS 3

1.2.2 HISTORY OF TUNNEL FIRES 4

1.2.3 SELECTION OF FIRE SCENARIOS 7

1.3 AIM OF THE THESIS 8

2 GOVERNING EQUATIONS 9

2.1 BURNING OF SOLIDS 9

2.2 FLAME SPREAD OVER SOLIDS 12

2.2.1 SURFACE ORIENTATION 12

2.2.2 PROPERTIES OF THE FUEL 15

2.2.3 GEOMETRICAL FEATURES OF THE FUEL 15

2.2.4 ENVIRONMENTAL CONDITIONS 16

2.3 BURNING OF LIQUIDS 18

2.4 FLASHOVER PHENOMENON 19
3 LARGE EDDY SIMULATION (LES) APPROACH 24
3.1 INTRODUCTION 24
3.2 FIRE DYNAMICS SIMULATOR (FDS) SOFTWARE 25
3.2.1 INTRODUCTION 25
3.2.2 GOVERNING EQUATIONS IN FDS 26
3.2.2.1 FUNDAMENTAL CONSERVATION EQUATIONS 26
3.2.2.2 COMBUSTION MODELLING EQUATIONS 28
3.2.2.3 THERMAL RADIATION MODELLING EQUATIONS 31
3.2.2.4 CONVECTION MODELLING EQUATIONS 33
3.2.2.5 PYROLYSIS MODELLING EQUATIONS . . 33
3.2.3 ASSUMPTIONS AND INPUTS IN FDS FIRE MODELLING 35
3.2.4 VALIDATION OF FDS SOFTWARE 36
4 FIRE DYNAMICS SIMULATOR (FDS) SIMULATIONS 41
4.1 INTRODUCTION 41
4.2 MODELLING APPROACH 42
4.2.1 ROLLING STOCK GEOMETRY 42
4.2.2 TUNNEL GEOMETRY 43
4.2.3 IGNITION SOURCES 44
4.2.4 VENTILATION 46
4.2.5 MATERIALS 47
4.2.6 COMPUTATIONAL DOMAIN 52
4.3 SIMULATIONS 55
5 INITIAL SIMULATIONS 59
5.1 INTRODUCTION 59
5.2 CASE-01: 1-CAR, 80kW SOURCE, SINGLE-TRACK TUNNEL . 60
5.2.1 FIRE DEVELOPMENT 60
5.2.2 ONBOARD CONDITIONS 62
5.3 CASE-02: 1-CAR, 80kW SOURCE, TWIN-TRACK TUNNEL . . . 66

5.3.1 FIRE DEVELOPMENT 66
5.3.2 ONBOARD CONDITIONS 68
5.4 CASE-03: 4-CAR, 80kW SOURCE, SINGLE-TRACK TUNNEL . 73
5.4.1 FIRE DEVELOPMENT 73
5.4.2 ONBOARD CONDITIONS 75
5.5 CASE-04: 4-CAR, 80kW SOURCE, TWIN-TRACK TUNNEL . . . 80
5.5.1 FIRE DEVELOPMENT 80
5.5.2 ONBOARD CONDITIONS 82
5.6 CASE-05: 1-CAR, 1.5MW SOURCE, SINGLE-TRACK TUNNEL . 86
5.6.1 FIRE DEVELOPMENT 86
5.6.2 ONBOARD CONDITIONS 89
5.7 CASE-06: 1-CAR, 1.5MW SOURCE, TWIN-TRACK TUNNEL . . 93
5.7.1 FIRE DEVELOPMENT 93
5.7.2 ONBOARD CONDITIONS 96
5.8 CASE-07: 4-CAR, 1.5MW SOURCE, SINGLE-TRACK TUNNEL . 100
5.8.1 FIRE DEVELOPMENT 100
5.8.2 ONBOARD CONDITIONS 103
5.9 CASE-08: 4-CAR, 1.5MW SOURCE, TWIN-TRACK TUNNEL . . 107
5.9.1 FIRE DEVELOPMENT 107
5.9.2 ONBOARD CONDITIONS 111
5.10 DISCUSSION ON PREDICTIONS OF INITIAL SIMULATIONS . 116
6 PARAMETRIC SENSITIVITY STUDIES 122
6.1 INTRODUCTION 122
6.2 THE TUNNEL LENGTH 123
6.3 THE LOCATION OF IGNITION SOURCE 127
6.4 THE IGNITION SOURCE CHARACTERISTIC 130
6.5 THE WINDOW FAILURE 135
6.6 THE NUMBER OF OPEN DOORS 142
6.7 THE MECHANICAL VENTILATION 151
6.8 MESH SENSITIVITY 159

6.9 CONCLUDING REMARKS FROM SENSITIVITY SIMULATIONS 167
TUNNEL LENGTH 167
LOCATION OF IGNITION SOURCE 168
IGNITION SOURCE CHARACTERISTICS . 168
WINDOW FAILURE 169
NUMBER OF OPEN DOORS 170
MECHANICAL VENTILATION 171
MESH SENSITIVITY 171
7 FINAL SIMULATIONS 176
7.1 INTRODUCTION 176
7.2 SIMULATION RESULTS 177
7.2.1 A TEST CASE; CASE-16: 1-CAR, 1.5MW SOURCE, SINGLE-TRACK TUNNEL 177
7.2.2 CALIBRATION OF MATERIAL PROPERTIES REVISITED 181
7.2.3 COMBUSTION REACTION REVISITED 187
7.2.4 CASE-17: 1-CAR, 80kW SOURCE, SINGLE-TRACK TUNNEL 190
7.2.5 CASE-18: 4-CAR, 1.5MW SOURCE IN SECOND CARRIAGE, SINGLE-TRACK TUNNEL 191
7.2.6 CASE-19: 4-CAR, 1.5MW SOURCE, SINGLE-TRACK TUNNEL, LIMITED WINDOW FAILURE 193
7.2.7 SENSITIVITY ON FINAL SIMULATIONS 198
7.2.7.1 WINDOW FAILURE CRITERION 198
7.2.7.2 CONE CALORIMETER MODELLING . . . 202
7.3 CONCLUDING REMARKS FROM FINAL SIMULATIONS 209
8 EMPIRICAL METHODS APPROACH 213
8.1 DUGGAN'S METHOD 213
8.1.1 BACKGROUND INFORMATION 213
8.1.2 DUGGAN'S METHOD TO VERIFY FDS PREDICTIONS OF HEAT RELEASE RATE 214
8.2 CFAST SIMULATIONS 223

8.2.1 BACKGROUND INFORMATION 223
8.2.2 CFAST SIMULATIONS TO VERIFY FDS PREDICTIONS OF ONBOARD CONDITIONS 224
8.2.2.1 80kW IGNITION SOURCE 225
1-CAR, SINGLE-TRACK TUNNEL 227
4-CAR, TWIN-TRACK TUNNEL 229
8.2.2.2 1.5MW IGNITION SOURCE 232
1-CAR, SINGLE-TRACK TUNNEL 232
1-CAR, TWIN-TRACK TUNNEL 235
4-CAR, SINGLE-TRACK TUNNEL 238
4-CAR, TWIN-TRACK TUNNEL 241
8.2.2.3 CONCLUDING REMARKS 244
9 DISCUSSION & CONCLUSION 245
9.1 INTRODUCTION 245
9.2 COMMENTS ON FDS SIMULATIONS 246
9.2.1 INITIAL SIMULATIONS 246
9.2.1.1 FIRE DEVELOPMENT 246
9.2.1.2 ONBOARD CONDITIONS 247
9.2.2 SENSITIVITY SIMULATIONS 248
9.2.2.1 TUNNEL LENGTH 249
9.2.2.2 LOCATION OF IGNITION SOURCE 249
9.2.2.3 IGNITION SOURCE CHARACTERISTICS . 250
9.2.2.4 WINDOW FAILURES 250
9.2.2.5 NUMBER OF OPEN DOORS 251
9.2.2.6 MECHANICAL VENTILATION 252
9.2.2.7 MESH SENSITIVITY 253
9.2.3 FINAL SIMULATIONS 254
9.3 COMMENTS ON EMPIRICAL METHODS 257
9.3.1 DUGGAN'S METHOD 257
9.3.2 CFAST SIMULATIONS 258

9.4 CONCLUDING REMARKS 260

REFERENCES 265

A BOMBARDIER CLASS-378 ROLLING STOCK 268

A.1 SECTIONAL AND PLAN VIEWS OF THE MODELLED ROLLING STOCK 268

B FIGURES: INITIAL SIMULATION RESULTS 273

B.1 CASE-01: 1-CAR, 80kW SOURCE, SINGLE-TRACK TUNNEL . 274

B.2 CASE-02: 1-CAR, 80kW SOURCE, TWIN-TRACK TUNNEL . . . 277

B.3 CASE-03: 4-CAR, 80kW SOURCE, SINGLE-TRACK TUNNEL . 280

B.4 CASE-04: 4-CAR, 80kW SOURCE, TWIN-TRACK TUNNEL . . . 283

B.5 CASE-05: 1-CAR, 1.5MW SOURCE, SINGLE-TRACK TUNNEL . 286

B.6 CASE-06: 1-CAR, 1.5MW SOURCE, TWIN-TRACK TUNNEL . . 289

B.7 CASE-07: 4-CAR, 1.5MW SOURCE, SINGLE-TRACK TUNNEL . 292

B.8 CASE-08: 4-CAR, 1.5MW SOURCE, TWIN-TRACK TUNNEL . . 295

C CONE CALORIMETER MODELLING 298

C.1 CONE CALORIMETER MODELLING 298

VITA 312

LIST OF TABLES

TABLES

Table 1.1 History of tunnel fires [21, 39] 5

Table 4.1 Material properties used in the initial and sensitivity simulations 51

Table 4.2 Exposure temperature limits for tenability given by NFPA 130 56

Table 4.3 Exposure air carbon-monoxide content limits for tenability given by NFPA 130 57

Table 5.1 Summary of the initial simulations with predicted peak heat release rates . 120

Table 6.1 Data set for incident cases involving liquid fuel 133

Table 6.2 Predicted peak heat release rate and duration of fire incidents for cases involving liquid fuel 134

Table 6.3 Labels and nominal edge lengths of the mesh sensitivity cases 160

Table 6.4 Summary of the sensitivity simulations with predicted peak heat release rates 174

Table 7.1 Calibrated material properties through FDS Cone Calorimeter simulations . 183

Table 7.2 Calibrated material properties through FDS Cone Calorimeter simulations, 5mm and 8mm grid sizes 203

Table 7.3 Summary of the final simulations with predicted peak heat release rates . . 212

Table 8.1 Areas of combustibles in the FDS model of DMOS carriage 216

Table 8.2 Comparison of CFAST and FDS predictions of temperature for 1-car model with 1 end door open 228

Table 8.3 Comparison of CFAST and FDS predictions of temperature for 4-car model with 8 side doors open 230

Table C.1 Comparison of grid sizes between the train fire domain and the Cone Calorimeter domain 302
Table C.2 Cone Calorimeter wall temperatures and predicted surface heat fluxes on specimen 303
Table C.3 Material properties used in the final simulations 308

LIST OF FIGURES

FIGURES

Figure 2.1 Mass burning rate of polyoxymethylene as a function of mole fraction of oxygen with no external heat flux [5] 10

Figure 2.2 Mass burning rate of polyoxymethylene as a function of external heat flux in air (η_{O_2} = 0.21)[5] 11

Figure 2.3 Variation of rate of flame spread over a thin fuel (computer card) as a function of angle of inclination (a) θ = -90° to θ = 0°; (b) θ = 0° to θ = 30° [5] 13

Figure 2.4 Interaction between a spreading flame and the surface of a (thick) combustible solid for different angles of inclination: (a) -90° ; (b) -45° ; (c) 0° ; (d) +45° ; (e) +90°. (a)-(c) are counter-current spread, while (d) and (e) are co-current spread. [5] 14

Figure 2.5 Upward spread of flame on a vertical strip of fabric (a) showing the burning (pyrolysis) zone of length l_p; (b) increase of rate of upward spread with increasing length of the pyrolysis zone. Cotton broadcloth (103 g/m^2) of width 0.457m and length 1.524m [5] 14

Figure 2.6 Rate of downward spread of flame on edges and in corners (a) Definition of the angle (θ) at an edge; (b) Variation of V for 20° $\leq$ θ $\leq$ 180°; (c) Definition of θ for a corner [5] 16

Figure 3.1 Results of the Validation & Verification of the Selected Fire Models by NUREG [26] 39

Figure 4.1 Views of the single car FDS model 43

Figure 4.2 Cross-sections for single and twin-track tunnels 44

Figure 4.3 Fire development curve for baggage fire source 45

Figure 4.4 Grid distribution for single-car model in twin-track tunnel 54

Figure 5.1 Fire spread, 1-car, 80kW source, single-track tunnel 61

Figure 5.2 Heat release rate, 1-car, 80kW source, single-track tunnel 62

Figure 5.3 Case-01: Temperature variation at 1.5m above the floor level 63

Figure 5.4 Case-01: Temperature variation at 1.0m above the floor level 63

Figure 5.5 Case-01: Visibility variation at 1.5m above the floor level 64

Figure 5.6 Case-01: Visibility variation at 1.0m above the floor level 64

Figure 5.7 Case-01: Carbon-monoxide concentration at 1.5m above the floor level . . 65

Figure 5.8 Case-01: Carbon-monoxide concentration at 1.0m above the floor level . . 65

Figure 5.9 Heat release rate, 1-car, 80kW source, twin-track tunnel 66

Figure 5.10 Fire spread, 1-car, 80kW source, twin-track tunnel 67

Figure 5.11 Case-02: Temperature variation at 1.5m above the floor level 68

Figure 5.12 Case-02: Temperature variation at 1.0m above the floor level 69

Figure 5.13 Case-02: Visibility variation at 1.5m above the floor level 70

Figure 5.14 Case-02: Visibility variation at 1.0m above the floor level 70

Figure 5.15 Case-02: Carbon-monoxide concentration at 1.5m above the floor level . . 72

Figure 5.16 Case-02: Carbon-monoxide concentration at 1.0m above the floor level . . 72

Figure 5.17 Heat release rate, 4-car, 80kW source, single-track tunnel 73

Figure 5.18 Fire spread, 4-car, 80kW source, single-track tunnel 74

Figure 5.19 Case-03: Temperature variation at 1.5m above the floor level 75

Figure 5.20 Case-03: Temperature variation at 1.0m above the floor level 76

Figure 5.21 Case-03: Visibility variation at 1.5m above the floor level 77

Figure 5.22 Case-03: Visibility variation at 1.0m above the floor level 77

Figure 5.23 Case-03: Carbon-monoxide concentration at 1.5m above the floor level . . 79

Figure 5.24 Case-03: Carbon-monoxide concentration at 1.0m above the floor level . . 79

Figure 5.25 Heat release rate, 4-car, 80kW source, twin-track tunnel 80

Figure 5.26 Fire spread, 4-car, 80kW source, twin-track tunnel 81

Figure 5.27 Case-04: Temperature variation at 1.5m above the floor level 82

Figure 5.28 Case-04: Temperature variation at 1.0m above the floor level 83
Figure 5.29 Case-04: Visibility variation at 1.5m above the floor level 84
Figure 5.30 Case-04: Visibility variation at 1.0m above the floor level 84
Figure 5.31 Case-04: Carbon-monoxide concentration at 1.5m above the floor level . . 85
Figure 5.32 Case-04: Carbon-monoxide concentration at 1.0m above the floor level . . 85
Figure 5.33 Heat release rate, 1-car, 1.5MW source, single-track tunnel 87
Figure 5.34 Fire spread, 1-car, 1.5MW source, single-track tunnel 88
Figure 5.35 Case-05: Temperature variation at 1.5m above the floor level 89
Figure 5.36 Case-05: Temperature variation at 1.0m above the floor level 90
Figure 5.37 Case-05: Visibility variation at 1.5m above the floor level 91
Figure 5.38 Case-05: Visibility variation at 1.0m above the floor level 91
Figure 5.39 Case-05: Carbon-monoxide concentration at 1.5m above the floor level . . 92
Figure 5.40 Case-05: Carbon-monoxide concentration at 1.0m above the floor level . . 92
Figure 5.41 Heat release rate, 1-car, 1.5MW source, twin-track tunnel 94
Figure 5.42 Fire spread, 1-car, 1.5MW source, twin-track tunnel 95
Figure 5.43 Case-06: Temperature variation at 1.5m above the floor level 96
Figure 5.44 Case-06: Temperature variation at 1.0m above the floor level 97
Figure 5.45 Case-06: Visibility variation at 1.5m above the floor level 97
Figure 5.46 Case-06: Visibility variation at 1.0m above the floor level 98
Figure 5.47 Case-06: Carbon-monoxide concentration at 1.5m above the floor level . . 99
Figure 5.48 Case-06: Carbon-monoxide concentration at 1.0m above the floor level . . 99
Figure 5.49 Heat release rate, 4-car, 1.5MW source, single-track tunnel 101
Figure 5.50 Fire spread, 4-car, 1.5MW source, single-track tunnel 102
Figure 5.51 Case-07: Temperature variation at 1.5m above the floor level 104
Figure 5.52 Case-07: Temperature variation at 1.0m above the floor level 104
Figure 5.53 Case-07: Visibility variation at 1.5m above the floor level 105
Figure 5.54 Case-07: Visibility variation at 1.0m above the floor level 105
Figure 5.55 Case-07: Carbon-monoxide concentration at 1.5m above the floor level . . 106
Figure 5.56 Case-07: Carbon-monoxide concentration at 1.0m above the floor level . . 107

Figure 5.57 Heat release rate, 4-car, 1.5MW source, twin-track tunnel 109

Figure 5.58 Fire spread, 4-car, 1.5MW source, twin-track tunnel 110

Figure 5.59 Case-08: Temperature variation at 1.5m above the floor level 112

Figure 5.60 Case-08: Temperature variation at 1.0m above the floor level 112

Figure 5.61 Case-08: Visibility variation at 1.5m above the floor level 113

Figure 5.62 Case-08: Visibility variation at 1.0m above the floor level 113

Figure 5.63 Case-08: Carbon-monoxide concentration at 1.5m above the floor level . . 115

Figure 5.64 Case-08: Carbon-monoxide concentration at 1.0m above the floor level . . 115

Figure 6.1 Heat release rate, 1-car, 1.5MW source, twin-track tunnel, 120m long domain 123

Figure 6.2 Heat release rate, 1-car, 1.5MW source, single-track tunnel, 120m long domain 124

Figure 6.3 Fire spread, 1-car, 1.5MW source, 120m long single-track tunnel 126

Figure 6.4 Heat release rate, 4-car, 1.5MW source, single-track tunnel, different ignition locations 128

Figure 6.5 Fire spread, 4-car, 1.5MW source, single-track tunnel, ignition at second car 129

Figure 6.6 Comparison of fire development curves for ignition sources reaching 1.0MW and 1.5MW 131

Figure 6.7 Heat release rate, 1-car, single-track tunnel, 1.0MW and 1.5MW sources . 131

Figure 6.8 Heat release rate, 1-car, single-track tunnel, incidents involving liquid fuel 134

Figure 6.9 Fire spread, 1-car, single-track tunnel, 10lt gasoline fuel spilled to 0.5m^2 area 135

Figure 6.10 Heat release rate, 1-car, 1.5MW source, single-track tunnel, limited window failure 137

Figure 6.11 Fire spread, 1-car, 1.5MW source, single-track tunnel, limited window failure 138

Figure 6.12 Heat release rate, 4-car, 1.5MW source, single-track tunnel, limited window failure 140

Figure 6.13 Fire spread, 4-car, 1.5MW source, single-track tunnel, limited window failure 141

Figure 6.14 Heat release rate, 1-car, 1.5MW source, twin-track tunnel, 4-doors open . 143

Figure 6.15 Temperature predictions for Case-06 and Case-13a at the center of the carriage 143

Figure 6.16 Fire spread, 1-car, 1.5MW source, twin-track tunnel, 4-doors open 144

Figure 6.17 Heat release rate, 4-car, 1.5MW source, single-track tunnel, all doors closed 146

Figure 6.18 Case-13b: Carbon-monoxide concentration at 1.5m above the floor level . 146

Figure 6.19 Heat release rate, 1-car, 1.5MW source, twin-track tunnel, doors opening at 3 min. or 6 min. 148

Figure 6.20 Fire spread, 1-car, 1.5MW source, twin-track tunnel, doors open at 6 minutes 150

Figure 6.21 Airflow velocity predictions at a longitudinal plane through the center of the incident carriage, 1-car, mechanical ventilation 153

Figure 6.22 Heat release rate, 1-car, 1.5MW source, twin-track tunnel, mechanical ventilation 153

Figure 6.23 Fire spread, 1-car, 1.5MW source, twin-track tunnel, mechanical ventilation 154

Figure 6.24 Heat release rate, 4-car, 1.5MW source, single-track tunnel, mechanical ventilation 155

Figure 6.25 Temperature predictions at a longitudinal plane through the center of the rolling stock, 4-car, mechanical ventilation 156

Figure 6.26 Fire spread, 4-car, 1.5MW source, single-track tunnel, mechanical ventilation 157

Figure 6.27 Visibility predictions at a longitudinal plane through the center of the rolling stock, 4-car, mechanical ventilation 158

Figure 6.28 Fire spread, 1-car, single-track tunnel, mesh sensitivity analysis, Case-15a (left) and Case-15b (right) 162

Figure 6.29 Heat release rate, 1-car, single-track tunnel, mesh sensitivity analysis . . . 163

Figure 6.30 Fire spread, 1-car, twin-track tunnel, mesh sensitivity analysis, Case-06 (left) and Case-15c (right) 165

Figure 6.31 Heat release rate, 1-car, twin-track tunnel, mesh sensitivity analysis 166

Figure 7.1 Heat release rate, 1-car, 1.5MW source, single-track tunnel, revised material properties 178

Figure 7.2 Fire spread, 1-car, 1.5MW source, single-track tunnel, revised material properties 179

Figure 7.3 Comparison of the calibrated and the initial material properties used in the simulations 180

Figure 7.4 Heat release rate per unit area, Seat material with lower ignition temperature, FDS Cone Calorimeter calibration 184

Figure 7.5 Heat release rate per unit area, Floor material with lower ignition temperature, FDS Cone Calorimeter calibration 184

Figure 7.6 Heat release rate, 1-car, 1.5MW source, single-track tunnel, revised material properties with lower ignition temperatures 185

Figure 7.7 Fire spread, 1-car, 1.5MW source, single-track tunnel, revised material properties with lower ignition temperatures 186

Figure 7.8 Fire spread, 1-car, 1.5MW source, single-track tunnel, combustibles with lower ignition temperatures and combustion reaction written for seats 189

Figure 7.9 Heat release rate, 1-car, 1.5MW source, single-track tunnel, combustibles with lower ignition temperatures and combustion reaction written for seats 190

Figure 7.10 Heat release rate, 1-car, 80kW source, single-track tunnel, calibrated material properties 191

Figure 7.11 Heat release rate, 4-car, 1.5MW source, single-track tunnel, ignition at second car, revised material properties 193

Figure 7.12 Fire spread, 4-car, 1.5MW source, single-track tunnel, ignition at second car, revised material properties 194

Figure 7.13 Heat release rate, 4-car, 1.5MW source, single-track tunnel, limited window failure, revised material properties 196

Figure 7.14 Fire spread, 4-car, 1.5MW source, single-track tunnel, limited window failure, revised material properties 197

Figure 7.15 Heat release rate, 4-car, 1.5MW source, single-track tunnel, ignition at second car, revised material properties and window failure criterion 198

Figure 7.16 Fire spread, 4-car, 1.5MW source, single-track tunnel, ignition at second car, revised material properties and window failure criterion 199

Figure 7.17 Heat release rate, 4-car, 1.5MW source, single-track tunnel, limited window failure, revised material properties and window failure criterion 200

Figure 7.18 Fire spread, 4-car, 1.5MW source, single-track tunnel, limited window failure, revised material properties and window failure criterion 201

Figure 7.19 Heat release rate per unit area, Seat material, FDS Cone Calorimeter calibration with 8mm grid size 204

Figure 7.20 Heat release rate per unit area, Floor material, FDS Cone Calorimeter calibration with 8mm grid size 204

Figure 7.21 Heat release rate, 1-car, 1.5MW source, single-track tunnel, combustible material properties Set 2 and Set 3 206

Figure 7.22 Heat release rate, 1-car, 1.5MW source, single-track tunnel, combustible material properties calibrated using cone calorimeter model with 8mm grid size . 206

Figure 7.23 Fire spread, 1-car, 1.5MW source, single-track tunnel, combustible material properties calibrated using cone calorimeter model with 8mm grid size 207

Figure 8.1 Cone calorimeter results used in verification of FDS simulations by Duggan's method 215

Figure 8.2 Predicted heat release rate variation using Duggan's method for single car, 1.5MW source, single-track tunnel 217

Figure 8.3 Comparison of the predicted heat release rate variations from the FDS simulation and the Duggan's analysis, 1-car model 218

Figure 8.4 Hypothetical combination of curves in Duggan's analysis to match FDS predictions 219

Figure 8.5 Predicted heat release rate variation using Duggan's method for 4-car rolling stock, 1.5MW source, single-track tunnel 221

Figure 8.6 Comparison of the predicted heat release rate variations from the FDS simulation and the Duggan's analysis, 4-car model 222

Figure 8.7 Layer height predictions for 1-car and 4-car models in a single-track tunnel 226

Figure 8.8 Layer height predictions for 1-car and 4-car models in a twin-track tunnel 226

Figure 8.9 Comparison of CFAST and FDS predictions of temperature for 1-car model with 1 end door open 227

Figure 8.10 Comparison of CFAST and FDS predictions of the upper layer temperature for 4-car model with 8 side doors open 229

Figure 8.11 Comparison of CFAST and FDS predictions of the lower layer temperature for 4-car model with 8 side doors open 230

Figure 8.12 The heat release rate histories obtained from the FDS and CFAST simulations for baggage fire in a 1-car model in the single-track tunnel 233

Figure 8.13 Layer height prediction for 1-car model in a single-track tunnel for baggage fire incident 233

Figure 8.14 Comparison of CFAST and FDS predictions of temperature for a baggage fire incident in 1-car model in a single-track tunnel 234

Figure 8.15 The heat release rate histories obtained from the FDS and CFAST simulations for baggage fire in a 1-car model in the twin-track tunnel 235

Figure 8.16 Layer height prediction for 1-car model in a twin-track tunnel for baggage fire incident 236

Figure 8.17 Comparison of CFAST and FDS predictions of temperature for a baggage fire incident in 1-car model in a twin-track tunnel 236

Figure 8.18 The heat release rate histories obtained from the FDS and CFAST simulations for baggage fire in a 4-car model in the single-track tunnel 238

Figure 8.19 Layer height prediction for 4-car model in a single-track tunnel for baggage fire incident 239

Figure 8.20 Comparison of CFAST and FDS predictions of the upper layer temperature for a baggage fire incident in 4-car model in a single-track tunnel 240

Figure 8.21 Comparison of CFAST and FDS predictions of the lower layer temperature for a baggage fire incident in 4-car model in a single-track tunnel 240

Figure 8.22 The heat release rate histories obtained from the FDS and CFAST simulations for baggage fire in a 4-car model in the twin-track tunnel 241
Figure 8.23 Layer height prediction for 4-car model in a twin-track tunnel for baggage fire incident 242
Figure 8.24 Comparison of CFAST and FDS predictions of the upper layer temperature for a baggage fire incident in 4-car model in a twin-track tunnel 242
Figure 8.25 Comparison of CFAST and FDS predictions of the lower layer temperature for a baggage fire incident in 4-car model in a twin-track tunnel 243

Figure 9.1 Parameters that affect fire development and their relation to risk of flashover 264

Figure A.1 Sectional view of the typical carriage 268
Figure A.2 Overall view of the rolling stock 269
Figure A.3 Plan view of the DMOS type carriage 270
Figure A.4 Plan view of the MOS type carriage 271
Figure A.5 Plan view of the PTOS type carriage 272

Figure B.1 Temperature, 1-car, 80kW source, Single-track tunnel 274
Figure B.2 Visibility, 1-car, 80kW source, Single-track tunnel 275
Figure B.3 Carbon-monoxide concentration, 1-car, 80kW source, Single-track tunnel 276
Figure B.4 Temperature, 1-car, 80kW source, Twin-track tunnel 277
Figure B.5 Visibility, 1-car, 80kW source, Twin-track tunnel 278
Figure B.6 Carbon-monoxide concentration, 1-car, 80kW source, Twin-track tunnel . 279
Figure B.7 Temperature, 4-car, 80kW source, Single-track tunnel 280
Figure B.8 Visibility, 4-car, 80kW source, Single-track tunnel 281
Figure B.9 Carbon-monoxide concentration, 4-car, 80kW source, Single-track tunnel 282
Figure B.10 Temperature, 4-car, 80kW source, Twin-track tunnel 283
Figure B.11 Visibility, 4-car, 80kW source, Twin-track tunnel 284
Figure B.12 Carbon-monoxide concentration, 4-car, 80kW source, Twin-track tunnel . 285
Figure B.13 Temperature, 1-car, 1.5MW source, Single-track tunnel 286
Figure B.14 Visibility, 1-car, 1.5MW source, Single-track tunnel 287

Figure B.15 Carbon-monoxide concentration, 1-car, 1.5MW source, Single-track tunnel 288
Figure B.16 Temperature, 1-car, 1.5MW source, Twin-track tunnel 289
Figure B.17 Visibility, 1-car, 1.5MW source, Twin-track tunnel 290
Figure B.18 Carbon-monoxide concentration, 1-car, 1.5MW source, Twin-track tunnel 291
Figure B.19 Temperature, 4-car, 1.5MW source, Single-track tunnel 292
Figure B.20 Visibility, 4-car, 1.5MW source, Single-track tunnel 293
Figure B.21 Carbon-monoxide concentration, 4-car, 1.5MW source, Single-track tunnel 294
Figure B.22 Temperature, 4-car, 1.5MW source, Twin-track tunnel 295
Figure B.23 Visibility, 4-car, 1.5MW source, Twin-track tunnel 296
Figure B.24 Carbon-monoxide concentration, 4-car, 1.5MW source, Twin-track tunnel 297

Figure C.1 General view of the Cone Calorimeter [7] 299
Figure C.2 Sectional view through the heater [1] 300
Figure C.3 Overall view of Cone Calorimeter apparatus [1] 300
Figure C.4 Views of the FDS Cone Calorimeter model 302
Figure C.5 Heat release rate per unit area, Seat material, FDS Cone Calorimeter calibration 306
Figure C.6 Heat release rate per unit area, Floor material, FDS Cone Calorimeter calibration 307

CHAPTER 1

INTRODUCTION

1.1 INTRODUCTION

The interest in fire life safety in underground transportation systems increased considerably in recent years. New regulations and guidelines are being set by the railroad administrations on fire life safety addressing rail car design, flammability and smoke emission performance criteria of the materials, fire detection and suppression systems, passenger evacuation and their interaction. Research projects involving small scale tests to determine fire characteristics of individual materials were performed, however there is not much information on real-scale fire incidents involving the whole railroad car.

In the majority of fire cases, the most crucial question that can be asked by the person responsible for fire protection is: ”What is the heat release rate of this fire?” Heat release rate is a measure of the amount of energy that a material produces while burning. For a given confined space (e.g. rail car interior), the air temperature increases as the heat release rate increases. If passengers do not come into direct contact with the fire, they would most likely be injured from the high temperatures, high heat fluxes, and large amounts of toxic gases emitted by the materials involved in the fire. Accordingly, the life threat to passengers of these materials can be directly correlated to the heat release rate of a real fire.

The prediction of the heat release rate variation in an underground train fire has also vital importance on the design of the underground ventilation systems. The heat release rate is one of the main parameters that define the magnitude of the critical velocity. The airflow velocities provided by the tunnel ventilation fans shall be greater than the calculated critical velocity in order to provide a smoke free evacuation path for the passengers. The required

airflow velocity over the train on fire in a tunnel determines the airflow capacities of the tunnel ventilation fans. The value of critical velocity depends on the design heat release rate, in other words the design fire size. Therefore, for a higher value of design heat release rate, higher ventilation capacities for the fans are required provided that all the other parameters affecting the magnitude of the critical velocity kept constant. For the incidents in the stations, the heat release rate variation with the flame spread pattern determines the temperature and smoke distributions in the station, which may lead to the prediction of the limiting evacuation times for the passengers.

1.2 FIRE DEVELOPMENT AND DETERMINATION OF FIRE SCENARIOS

In a typical fire development process in an underground train, the fire starts with the ignition source, which might be in the interior or exterior of the carriage. If the fire is unattended or not suppressed, and there is sufficient amount of ventilation and fuel, fire would grow in intensity. For interior car fire, the first item ignited by the ignition source would be the back of a seat or the face panel in the driver console assembly depending on the fire scenario considered. For an exterior fire, the first item ignited is likely to be the wiring under the car.

Fires grow in size either by increased burning rate, by flame spread over the first ignited item, or by ignition of nearby surfaces. With sufficient amount of ventilation and fuel, the fire could progress to involve the entire carriage in which all exposed combustible surfaces ignite simultaneously, with a very rapid increase in heat release rate. This very rapid and sudden transition from a growing fire to a fully developed fire is called the flashover. However, not all fires would flashover, and there are certain conditions for fuel and ventilation within the incident carriage that shall be satisfied for the fire to flashover. The flashover phenomenon is examined further in the following chapters in this thesis.

The most probable fire scenario must be defined through the statistics of the most relevant fires which have occurred within the Railway Companies. The analysis of the most important reported fires which have happened in the last decade show that in recent years significant fires in railway vehicles have decreased in a substantial way. This is often due to renewal of the railway vehicles with materials in conformity with more severe standards about fire safety.

The statistics of train fires and selection of fire scenarios are summarized in Sub-sections 1.2.1 to 1.2.3.

1.2.1 STATISTICS OF FIRES IN UNDERGROUND TRAINS

Analyzing the statistical data in the literature revealed that beside the electrical faults, for interior fire scenarios, the ignition sources ranged from discarded cigarettes to flammable liquid; and the locations of ignition sources were usually on the seat or on the floor. For exterior fire scenarios, short circuit and overheating of equipment in the undercarriage were the main causes of fires.

Statistical analysis of the fires occurring in interior of railway carriages by Briggs et al. [9] indicated that fires caused by arson on a seat due to a cigarette lighter or burning newspaper were the most probable. They have also identified high temperature in electrical equipment due to electrical defects as one of the common fire scenarios.

It is also reported by Chiam [20] that the interior fire due to arson is the most probable scenario with a percentage of 68% among the various causes of fires. It can be concluded that there are mainly three causes of fire:

1. Arson (interior fire scenario),
2. Electrical faults (interior or exterior fire scenarios), and
3. An accident due to derailment or a collision followed by an electrical short circuit.

Fire due to a derailment or a collision followed by an electrical short circuit is the least probable and only observed in very old systems. Consequently, fire due to electrical faults and arson are more frequent as the main causes of metro train fires which inline with the statistical data found in literature.

1.2.2 HISTORY OF TUNNEL FIRES

The railway systems clearly have a much higher potential for many casualties in the event of a fire, compared to fires in road tunnels, since incidents generally involve trains, each with the capacity for several hundred passengers. Two incidents in the last 15 years have highlighted the dreadful scale of possible consequences of fires in metro systems: nearly 200 people died following an arson attack on an underground railway train in South Korea (2003) and over 200 people died following an electrical fault on an underground railway train in Azerbaijan (1995).

Fire disasters have also occurred on conventional and funicular railways. In 2000, a fire started on a funicular railway near Kaprun in Austria. The fire was directly responsible for the deaths of 155 people due to the confines of the tunnel. The handful of survivors were those who fled down the tunnel, past the fire; those trying to escape the fire by going up the tunnel were all killed by the smoke.

The reports on the Kaprun incident indicate that the majority of the passengers on the train did not manage to get off the train before they were unable to resist against the poisonous smoke. This was also the case in the fire incident on a Baku underground railway train in 1995. 220 passengers were found on the train itself while a further 80 passengers died due to the fumes while making their way along the tracks towards the station.

In both these cases the lack of a safety management system was partly responsible for the number of deaths; in the Kaprun incident the train was held to be 'fire-proof' so the consequences of a fire onboard had never been considered, and the possibility that the passengers could be carrying flammable materials, at least in the form of clothing, also appears to have never been considered. In the Baku incident the lack of communication and the ad hoc operation of the ventilation system also led to fatalities; some 15 minutes after the fire started the emergency ventilation system was switched on which directed the smoke towards the majority of the passengers - those in the control room had no idea what was going on at the fire. [21]

Aside from these incidents, large-scale fires rarely happen on passenger trains; there is comparatively little fuel to burn and usually many people are able to extinguish the fire while it is still small.

Some of the rail tunnel fire incidents occurred in the last decade are listed in Table 1.1.

Table 1.1: History of tunnel fires [21, 39]

2008, Channel Tunnel, France/UK The fire was reported on 11 September 2008, on a Eurotunnel shuttle train carrying heavy goods vehicles 11 kilometers from the French entrance in the North Tunnel. The blaze spread to other trucks on the train during the evening, destroying six carriages and one locomotive. The fire continued to burn overnight and lasted for 16 hours. More than 300 fire-fighters from both sides of the English Channel helped tackle the blaze. 32 people on-board the train were led to safety down a separate service tunnel; 14 people suffered minor injuries, including smoke inhalation.
2003, Jungangno underground railway station, Daegu, South Korea An arson attack on an underground railway train in Jungangno Station, near Daegu city center, led to the deaths of at least 189 people. The arsonist used a small quantity of petrol and a cigarette lighter to start the fire on a stationary train in the station. The fire quickly spread to all six carriages of the train within 2 minutes due to the highly flammable interior of the train. After the underground railway operators were aware of the fire, a second train entered the station and stopped near to the train on fire; the doors of this train did not open. The fire spread to the second train where most of the fatalities occurred.
2003, Mornay Tunnel, France In 2003, a fire broke out in a passenger carriage on an 'autorail' train. Once the fire as detected the train stopped automatically, about 300m from the tunnel portal. The tunnel, constructed in 1877, is a single-tube, single-track tunnel with no lighting and no ventilation system. All of the 17 passengers on board were able to self-rescue before the arrival of the fire brigade. On arrival, however, the fire brigade had to overcome major problems to fight the fire. The fire took five hours to control.
2003, Guadarrama rail tunnel, Spain An accident occurred in 2003 on a train near the tunnel portal. The crew on the train escaped the tunnel before the smoke became too thick. Some 34 workers were trapped about 3km inside the tunnel by heavy smoke for 5 hours before they were rescued. They took refuge in an air pocket in the tunnel.

Table 1.1 Cont'd: History of tunnel fires [21, 39]

2002, Motorway tunnel on A86, Versailles, France In 2002, the engine of a train, carrying construction materials into a partially built motorway tunnel, exploded and started a fire which burned for 6 hours. The 19 construction workers who were in the tunnel at the time took refuge in an airtight compartment in the 200m long tunnelling machine. Approximately 150 fire-fighters attended the scene and none of the construction workers were injured.
2001, Howard Street Tunnel, Baltimore, USA In 2001, a freight train passing through a tunnel in downtown Baltimore had an 'emergency brake application'. Following standard procedure, the drivers detached the locomotives from the train and removed them from the tunnel. Of the 60 cars that made up the train, eight were carrying hazardous materials, chemicals and various solvents. It took four days to remove all the wreckage. The fire resulted in gridlock on the roads to Baltimore as all the major routes were closed to traffic for about 12 hours.
2001, Düsseldorf underground railway tunnel, Germany The roof of an underground railway train caught fire. There were two reported injuries.
2001, Kurt Schumacher Platz station, Berlin, Germany In 2001, a fire was started by an arc lamp in the rear carriage of a 100m long train. Despite the small size of the fire, the amount of smoke inside the carriage and the tunnel area was considerable. No injuries were reported.
2000, Kitzsteinhorn funicular tunnel, Kaprun, Austria In 2000, a fire broke out at the rear of the ascending train shortly after leaving the lower terminal. The train stopped automatically 600m inside the tunnel. The doors of the train failed to open. Twelve passengers escaped by smashing the windows and fleeing down the tunnel. The remaining 150 people on the train died on the train or attempting to flee up the smoke-filled tunnel. The fire on the supposedly fireproof train is thought to have started by hydraulic oil leaking into the heater in the rear driver's cab and spread via the clothes and baggage of the passengers on the train.

Table 1.1 Cont'd: History of tunnel fires [21, 39]

2000, New York City underground railway, USA In 2000, two fires broke out in the electrical supply of the New York underground railway system. All passengers were safely evacuated before the tunnels filled with smoke, but the fire-fighting operations took over 2 hours and 20 underground stations were closed for over 3 hours.
2000, Montreal underground railway, Canada In 2000, a cable fire led to complete closure of the Montreal underground system for 6 hours. The fire filled several tunnels with smoke, triggered three explosions and brought about the failure of the electrical, communication and ventilation systems on the entire underground railway network. There were no recorded injuries.
2000, Toronto underground railway, Canada In 2000, a fire broke out on an underground railway train being used to collect refuse from Old Mill station on the Bloor-Danforth line of the Toronto Underground system (TTC). Three people were treated for smoke inhalation. The line was closed for 24 hours.

It should be noted that Table 1.1 includes some of the tunnel fires reported from 2000 to date. The details of many train fire incidents in and before 1999 can be found in the handbook of tunnel fire safety. [21]

1.2.3 SELECTION OF FIRE SCENARIOS

The list of fire incidents in the rail tunnels, given in Table 1.1, show that the causes of fires vary between engine failures to arson attacks. As discussed in Sub-section 1.2.1, arson attacks are reported to be the most probable scenario among the various causes of fires in the railway carriages.

In this thesis, a set of different ignition sources, ranging from a small-scale arson fire to a more severe baggage fire ignition source, will be simulated. The small-scale arson fire source would represent the ignition of a newspaper-filled trash bag, and will be placed on a passenger

seat. The baggage fire source would have much higher intensity and would be placed on the floor of the chosen carriage in a rolling stock.

The incidents will be assumed to occur under natural ventilation conditions. However, a set of simulations will be performed to investigate the effects of ventilation on fire development within the carriages.

The Class-378 rolling stock will be used in this study. The manufacturer's claimed that all the electricity cables and boxes would be fire resistant and fail-safe. In addition, it is reported that the under-carriage and the passenger compartment are separated by a fire resistant partition. Consequently, the under-carriage fires, and the onboard fires due to an electrical fault are not considered in this thesis. The details of all the simulated fire incidents are given in Chapter 4.

1.3 AIM OF THE THESIS

This study is focused on fire incidents within the passenger compartments of the underground railway carriages. The main purpose of the study is to investigate fire development and flame spread within the underground rolling stock using 3-dimensional simulation methods with a set of different initial and boundary conditions. The simulations will be used to identify the cases where the fire would develop to involve the entire incident carriage, and cases with fire spreading further to the adjacent carriages.

The predictions would clarify the conditions promoting or preventing the flame spread, and help developing strategies that would minimize fire development within the rolling stock therefore minimizing the damage to the rolling stock itself and to the infrastructure.

The predictions of fire development, along with the peak heat release rate values and the time it takes to achieve these peak heat release rates, would be used indicatively in commenting on the timescales for evacuation of passengers and suppression of fire by the local fire brigade.

Train onboard conditions will also be provided for the selected fire scenarios as a supplementary information. The study will give an indication of the temperature, carbon-monoxide concentration, and visibility levels within the rolling stock. The onboard conditions will be linked to the evacuation of passengers, and the likelihood of survival of the passengers onboard will be briefly touched on.

CHAPTER 2

GOVERNING EQUATIONS

2.1 BURNING OF SOLIDS

In an underground train fire, the combustible materials are generally solid, and flame spread over the solid surfaces. The simulation softwares that predict the fire development and flame spread in an enclosure, such as the Fire Dynamics Simulator (FDS), assume that the fire is an infinitely-fast reaction between fuel and oxygen. This reaction is not dependent on the surrounding gas temperature. The softwares also assume that the reaction zone is an infinitely thin sheet with fuel on one side and oxygen on the other. Consequently, the main part of the governing equations is the relations derived for burning of solids.

The burning of a solid fuel requires chemical decomposition to produce fuel vapors which can escape from the surface to burn in the flame. While the composition of the fuel vapors has direct relevance to the combustion process and product formation, fire safety engineers normally bypass this complexity by relying on the results of small-scale tests to provide relatively simple data which could be used in the assessment of the fire hazard of a given material. The best known example is the Cone Calorimeter, but the performance of the material in the test must be interpreted correctly. This requires a thorough understanding of the fire process and careful analysis of the test results obtained using the test procedures defined by the standards. A more detailed explanation on Cone Calorimeter is given in Chapter 4 under Clause C.1.

The rate of burning of solid materials can be expressed as:

$$\dot{m}'' = \frac{\dot{Q}''_a - \dot{Q}''_L}{L_v} \tag{2.1}$$

where $\dot{Q}''_L$ represents the heat losses, and L_v is the latent heat of gasification. $\dot{Q}''_a$ is the heat fluxes on the material, which will be discussed further in the text.

Surface temperatures of burning solids tend to be high, typically > 350°C, so that radiative heat loss from the surface is significant. The heat required to produce the volatiles or "heat of gasification" (L_v) is considerably greater for solids, as chemical decomposition is involved.

$\dot{Q}''_a$ can be written in terms of its components, $\dot{Q}''_F$ and $\dot{Q}''_E$ which refer to the heat fluxes to the surface from the flame and from the external radiant heaters respectively. The rate of burning can be rewritten as:

$$\dot{m}'' = \frac{\dot{Q}''_F + \dot{Q}''_E - \dot{Q}''_L}{L_v} \tag{2.2}$$

As the rate of burning is strongly dependent on the oxygen concentration, it can be defined that $\dot{Q}''_F = \xi\, \eta_{O_2}{}^{\alpha'}$, where ξ and α' are constants, and η_{O_2} is the mole fraction of oxygen in the surrounding atmosphere. It was found that when $\dot{Q}''_E$ was held constant, $\dot{m}''$ is a linear function of η_{O_2} (i.e. $\alpha' = 1$) over a range of oxygen concentrations of 12% to 22% (Refer to Figure 2.1). The slope of the line in the figure gives a value for $\frac{\xi}{L_v}$ provided that $\frac{(\dot{Q}''_E - \dot{Q}''_L)}{L_v}$ is constant. The equation for burning rate becomes:

$$\dot{m}'' = \frac{\xi\, \eta_{O_2}}{L_v} + \frac{\dot{Q}''_E - \dot{Q}''_L}{L_v} \tag{2.3}$$

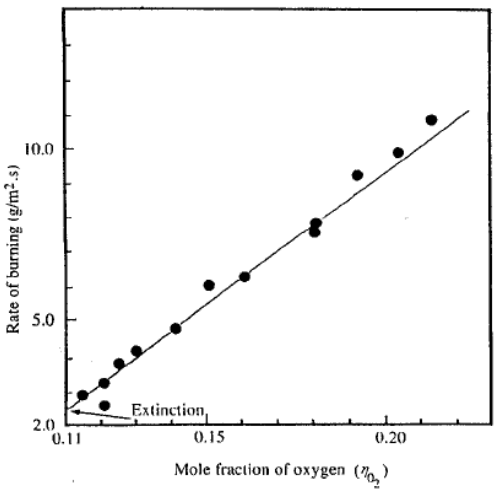

Figure 2.1: Mass burning rate of polyoxymethylene as a function of mole fraction of oxygen with no external heat flux [5]

Similarly, if η_{O_2} is held constant, then a plot of $\dot{m}''$ against $\dot{Q}''_E$ will give a straight line, which has a slope of $\frac{1}{L_v}$ (Refer to Figure 2.2).

Comparison of the value of heat transferred from the flame to surface of the fuel, $\dot{Q}''_F$, with those of $\dot{Q}''_L$ which have been calculated from Equation 2.2, identifies materials which will not burn unless an external heat flux is applied to render the numerator of the equation positive.

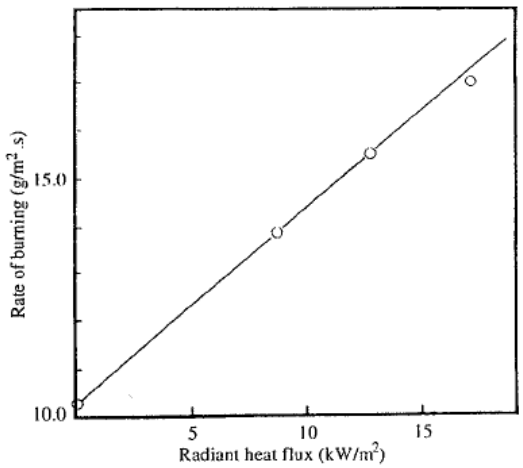

Figure 2.2: Mass burning rate of polyoxymethylene as a function of external heat flux in air (η_{O_2} = 0.21)[5]

It is proposed that the quantity:

$$\dot{m}''_{ideal} = \frac{\dot{Q}''_F}{L_v} \tag{2.4}$$

be used as a measure of the "burning intensity" of a material, i.e. the maximum burning rate that a material could achieve if all heat losses were reduced to zero or exactly compensated by an imposed heat flux $\dot{Q}''_E = \dot{Q}''_L$. While this gives results that appear to correlate reasonably well with data from existing fire tests in literature, it would be more logical if heat loss by surface re-radiation was included in $\dot{m}''_{ideal}$. This would seem to provide a means of calculating burning rates under different heat gain and loss regimes, thus:

$$\dot{m}'' = \dot{m}''_{ideal} + \frac{\dot{Q}''_E - \dot{Q}''_L}{L_v} \tag{2.5}$$

In the event of a fire in an underground train, it can be considered that the combustible materials burn in an enclosure, in which the heat flux to the surface comes from general burning

within the space. Therefore, the rate of heat release due to the combustion of the fuels in the compartment can be expressed in terms of the burning rate of materials as follows:

$$\dot{Q}_c = \dot{m}'' \, \chi \, \Delta H_c \, A_F \tag{2.6}$$

where ΔH_c is the heat of combustion of the volatiles, χ is an efficiency factor that takes into account incomplete combustion, and A_F is the fuel surface area. Writing $\dot{Q}''_{net}$ as the net heat flux entering the surface, Equation 2.6 may be rewritten as follows:

$$\dot{Q}_c = \frac{\dot{Q}''_{net}}{L_v} \, \chi \, \Delta H_c \, A_F \tag{2.7}$$

The ratio of heat of combustion to the heat of gasification, $\frac{\Delta H_c}{L_v}$, in Equation 2.7 is also known as the 'combustibility ratio'. It is given in the literature that χ, the combustion efficiency, lies in the range of 0.4 to 0.7 for most of the solid fuels. Therefore, the combustibility ratio plays an important role in the generated heat release rate during combustion.

2.2 FLAME SPREAD OVER SOLIDS

Unlike liquid fuels, the surface of a solid fuel can be at any orientation, which can have a dominating effect on fire behavior. This is particularly true for the phenomenon of flame spread as it is controlled by the mechanism by which heat is transferred ahead of the burning zone. This is strongly influenced by the surface geometry and inclination.

The rate of flame spread over the solids also depends on the thickness of the fuel, the properties of the fuel; such as density, thermal capacity, and thermal conductivity; and the environmental conditions; such as composition of the atmosphere and the imposed radiant heat flux. These are briefly discussed in this section of the thesis.

2.2.1 SURFACE ORIENTATION

In general, solid surfaces can burn in any orientation, but flame spread is most rapid if it is directed upwards on a vertical surface. Downward propagation is much slower, and the rate less sensitive to change in orientation.

Results of experiments with computer cards as thin fuel showed that the rate of spread is approximately constant as the angle of orientation was changed from -90° (vertically downwards) to -30°, while increasing more than threefold when the angle was changed from -30° to 0° (horizontal) (Refer to Figure 2.3).

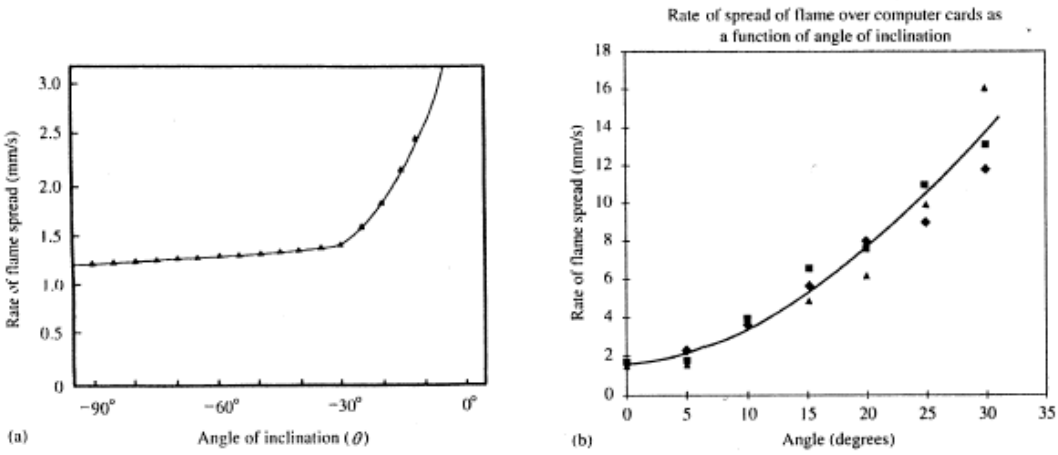

Figure 2.3: Variation of rate of flame spread over a thin fuel (computer card) as a function of angle of inclination (a) θ = -90° to θ = 0°; (b) θ = 0° to θ = 30° [5]

Quite different behavior is observed with physically thick fuels. At intermediate orientations, enhancement of upward spread is observed only when the inclination of the surface is increased above 15-20°. It is also reported that there is a switch from counter-current spread at inclinations below about 15°, to concurrent spread which is certainly operating at inclinations of 25° and above. The critical angle depends on the geometry (Refer to Figure 2.4). [5]

Markstein and de Ris [5] observed that following an ignition at the bottom edge of the freely suspended strips of fabric, there is a short period of laminar burning which quickly develops turbulence as the flame size increases. They also reported that downward spread (-90°) achieves a slow, steady rate of propagation almost immediately, but upward spread (+90°) accelerates toward a quasi-steady state. It was shown that the instantaneous rate of flame spread was dependent on the length of the pyrolyzing zone, i.e. the zone from which the volatiles were being released. As the rate of flow of volatiles determines the height of the flame, it also determines the extent of preheating of the unaffected fabric which in turn determines how quickly the fuel is brought to the firepoint. It is reported that:

$$V_p \propto l_p{}^n \tag{2.8}$$

where V_p is the rate of vertical spread, l_p is the length of the pyrolysis zone, and n is a constant, approximately equal to 0.5 (Refer to Figure 2.5).

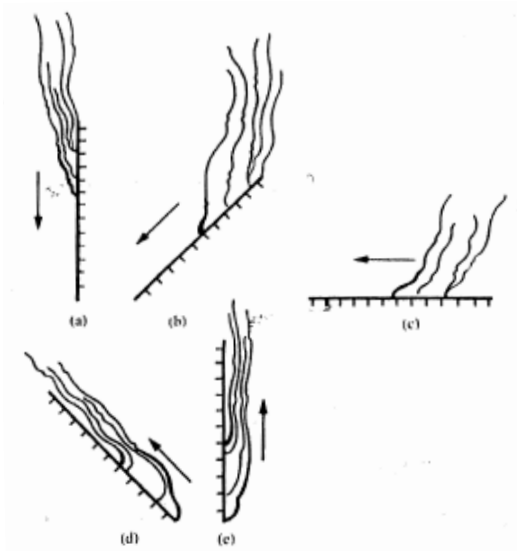

Figure 2.4: Interaction between a spreading flame and the surface of a (thick) combustible solid for different angles of inclination: (a) -90° ; (b) -45° ; (c) 0° ; (d) +45° ; (e) +90°. (a)-(c) are counter-current spread, while (d) and (e) are co-current spread. [5]

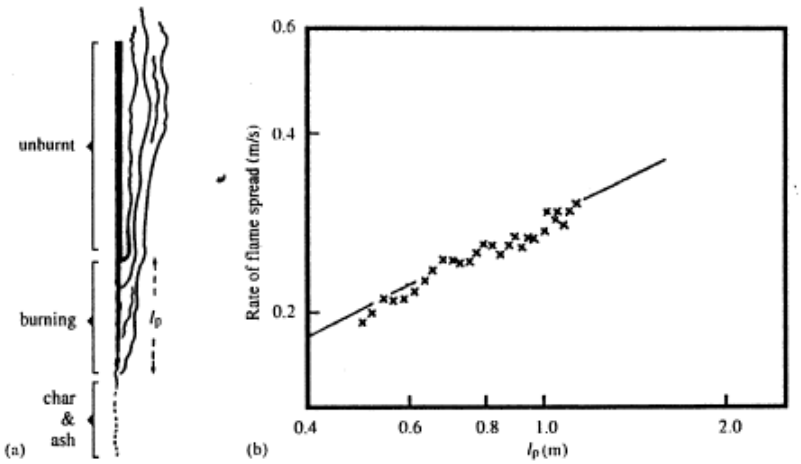

Figure 2.5: Upward spread of flame on a vertical strip of fabric (a) showing the burning (pyrolysis) zone of length l_p; (b) increase of rate of upward spread with increasing length of the pyrolysis zone. Cotton broadcloth (103 g/m^2) of width 0.457m and length 1.524m [5]

2.2.2 PROPERTIES OF THE FUEL

The depth of heating is given approximately by $(\alpha\, t)^{1/2}$, where α is the thermal diffusivity $(\frac{k}{\rho\, c})$ and t is the time in seconds during which the surface of the solid is exposed to a heat flux. For an advancing flame front, the exposure time for the unburnt fuel is $\frac{l}{V}$, where V is the rate of spread and l is the "heating length". The heating length is defined by the length of sample perpendicular to the advancing flame over which the temperature rises from ambient to the temperature corresponding to the firepoint.

A critical thickness, τ_{cr} for flame spread is then estimated from the expression:

$$\tau_{cr} = (\alpha\, l\, /V)^{0.5} \tag{2.9}$$

Thin fuels may be treated by the lumped thermal capacity model for which the time to achieve the firepoint (t_i) under a given heat flux is directly proportional to the product $\rho\, c\, \tau$. As the rate of spread will be inversely proportional to t_i, then:

$$V \;\propto\; (\rho\, c\, \tau)^{-1} \tag{2.10}$$

In order to determine how thermal properties of a thick fuel influence the rate of spread, τ must be replaced by an expression for depth of the heated layer at the surface of the material (δ):

$$\delta = (\alpha\, l\, /V)^{0.5} \;\;\rightarrow\;\; V \;\propto\; (\rho\, c\, \delta)^{-1} \;\;\rightarrow\;\; V \;\propto\; \frac{l}{k\, \rho\, c} \tag{2.11}$$

provided that l is constant. The thermal conductivity (k) of a solid is roughly proportional to its density (ρ). Equation 2.11 shows that the rate of flame spread is extremely sensitive to the density of the fuel bed; $V \;\propto\; \rho^{-2}$. This is why foamed plastics and other combustible materials of low density spread flame and develop fire so rapidly.

2.2.3 GEOMETRICAL FEATURES OF THE FUEL

Flame spreads much more rapidly along an edge or in a corner than over a flat surface. This has been studied using wedges and the findings are reported in the literature (Refer to Figure

2.6). The rate of downward propagation at the edge was measured as a function of the angle (θ), and the following dependence is found for $20° \leq \theta \leq 180°$:

$$V \propto \theta^{4/3} \tag{2.12}$$

The narrower the angle θ, the closer the edge of the solid approaches thin-fuel behavior, with flame spreading down both sides. The rate of downward spread is a minimum for $\theta = 180°$. If θ is greater than 180°, the rate of downward spread is enhanced by cross-radiation near the junction of the walls.

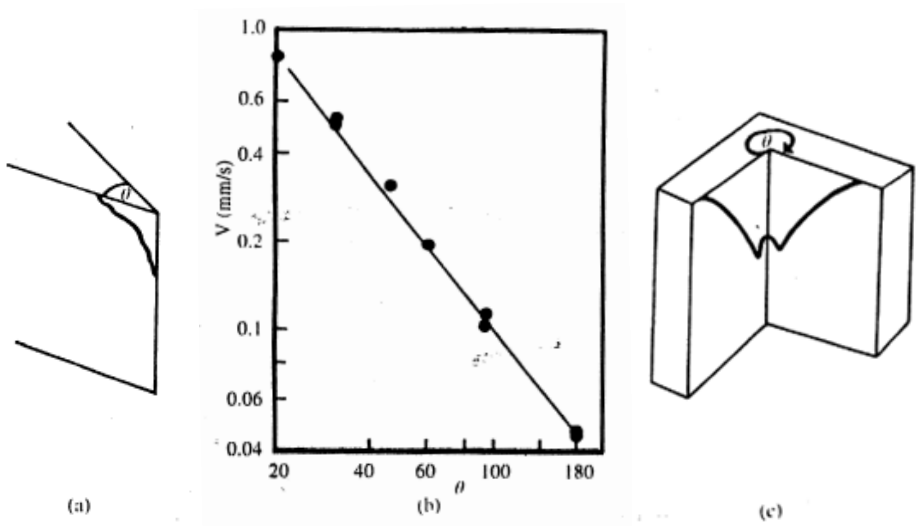

Figure 2.6: Rate of downward spread of flame on edges and in corners (a) Definition of the angle (θ) at an edge; (b) Variation of V for $20° \leq \theta \leq 180°$; (c) Definition of θ for a corner [5]

2.2.4 ENVIRONMENTAL CONDITIONS

Combustible materials will ignite more readily, spread flame more rapidly and burn more vigorously if the oxygen concentration is increased. Any increase in oxygen concentration in the air is accompanied by an increase in the rate of flame spread. This is because the flame is hotter and can lose more heat to the fuel. It will lie closer to the fuel surface, thus increasing the rate of heat transfer. It is reported in the literature [5] that the dependence of propagation rate (V) on oxygen concentration is greater for 'thick' fuels than for 'thin' fuels, at least for vertically downward spread.

Increasing the temperature of the fuel increases the rate of flame spread. This is to be expected as the higher the initial fuel temperature the less heat is required to raise the unaffected fuel to the firepoint ahead of the flame. The following relations are reported in the literature:

Thin fuels:

$$V \propto \frac{1}{T_P - T_0} \tag{2.13}$$

Thick fuels:

$$V \propto \frac{1}{(T_P - T_0)^2} \tag{2.14}$$

where T_P is the minimum temperature at which decomposition occurs and T_0 is the initial fuel temperature.

An imposed radiant heat flux will cause an increase in the rate of flame spread, primarily by preheating the fuel ahead of the flame front. However, the increased rate of burning behind the flame front will give stronger flames which will provide additional forward heat transfer and thus enhance the process. The effect of the radiant heat flux is significant during the early stages of a compartment fire when the levels of radiant heat flux from the compartment boundaries and the layer of hot smoky gases trapped below the ceiling are increasing. The response of a surface to the imposed flux is not instantaneous and the effect of transient heating must be considered if the flame begins to spread over the surface before thermal equilibrium has been reached.

In general, confluent air movement will enhance the rate of spread of flame over a combustible surface. It is reported that the rate will increase quasi-exponentially up to a critical level at which extinction will occur, but there has been no fundamental study of this dependence. The mechanism is understood to involve flame deflection which, combined with enhanced burning behind the flame front, will increase the rate of forward heat transfer. If the direction of air flow is opposed to the spread of flame, the net effect depends on the air velocity. Sufficiently large velocities will cause the rate of spread to decrease and ultimately the flame to extinguish, but low velocities promote flame spread.

2.3 BURNING OF LIQUIDS

In this thesis, the emphasis is given to the fires within the passenger compartment. Therefore, the focus is on flame spread over the solid surfaces. However, there might be incidents involving pool fires, such as during a terrorist attack petrol could have been brought to the passenger compartment and been ignited.

The rate of heat release in a pool fire from the combustion of the liquid fuel is calculated by:

$$\dot{Q} = \dot{m}\, \Delta H_{c,\,eff} \tag{2.15}$$

where $\dot{m}$ is the mass loss rate (kg/s), and $\Delta H_{c,\,eff}$ is the effective heat of combustion (kJ/kg).

For fire hazard analysis purposes, liquid pool fires will rarely be significantly dangerous if they are smaller than about 0.2m in diameter. Thus, it will often only be necessary to treat pools burning in the radiative regime. In the radiative regime, it is reported in the literature [5, 10] that data for most liquid fuels can be well correlated by:

$$\dot{Q} = \dot{m}''_{\infty}\,(1 - e^{-k\beta D}) \;\cdot\; A \;\cdot\; \Delta H_{c,\,eff} \tag{2.16}$$

where $\dot{m}''_{\infty}$ is the mass loss rate per unit area per unit time (kg/m^{2}s), D is the pool diameter (m), and $k\beta$ is the empirical constant (1/m), which is a fuel-specific value. The fuel-specific empirical constants and the values of heat of combustion for a number of common fuels are listed in 'The SFPE Handbook of Fire Protection Engineering' [10].

The burning rate of a given fuel is controlled by both its chemistry and its form. A particularly important form factor is the surface area to mass ratio of the fuel, which is defined as the surface area available to combust as compared to the total mass of the material.

The concept of burning duration is a way of characterizing the hazard of a compartment fire in terms of the length of time the fuel in the compartment could be expected to burn, which depends on the total amount of fuel available. A fire burning at a constant heat release rate consumes fuel mass at a constant rate. Thus, if the mass of material being burned per second and the amount of material available to be consumed are known, it is possible to estimate the total burning duration of a fuel.

In a pool fire, provided that sufficient amount of oxygen is available, the amount of surface area of the given liquid becomes the defining parameter. Liquid pool fires with a given amount of fuel can burn for long periods of time if they have a small surface area, or for short periods of time over a large spill area. For a fixed volume of combustible liquid, the burning duration for the pool fire is estimated using the following expression:

$$t = \frac{4\forall}{\pi D^2 v} \tag{2.17}$$

where $\forall$ is the volume of liquid, and v is the regression rate (m/s). The rate of burning, also called the regression rate (v), is defined as the volumetric loss of liquid per unit surface area of the pool per unit time, as illustrated by the following expression:

$$v = \frac{\dot{\forall}}{A} = \frac{\dot{m}''}{\rho} \tag{2.18}$$

where $\dot{m}''$ is the mass burning rate of fuel per unit area, and ρ is the liquid fuel density.

2.4 FLASHOVER PHENOMENON

In a fire incident after localized burning has established, one of three following events may happen:

1. the fire may burn itself out without involving other items of combustible material, particularly if the item first ignited is in an isolated position,
2. if there is inadequate ventilation, the fire may self-extinguish or continue to burn at a very slow rate dictated by the availability of oxygen, or
3. if there is sufficient fuel and ventilation, the fire may progress to full enclosure involvement in which all exposed combustible surfaces are burning.

Two important issues should be addressed for the latter scenario. These are the conditions associated with the onset of flashover, and the factors which determine the duration of the growth period. The latter is quite important as it has a major impact on life safety: if the time to flashover is short, the time available for escape may be inadequate.

The transition from localized burning to the fully developed fire is referred to as “flashover” and involves a rapid spread from the area of localized burning to all combustible surfaces

within the enclosure. The transition is normally short in comparison to the duration of the main stages of the fire and is sometimes considered to be a well-defined physical event, in the same way that ignition is considered as an event. The duration of flashover depends on a number of factors, including the nature and distribution of the combustible contents, as well as the size and shape of the compartment.

In case of a fire in a compartment, the generated heat is not totally lost from the environs of the fuel as fire gases will be deflected and trapped below the ceiling, which will be heated. If the size of the fire is such that the natural flame height is greater than the height of the enclosure, then the flame may extend as a ceiling jet and thus contribute significantly to the heat transfer to the ceiling. This in turn will provide an increasing radiant heat flux back to the fuel as the temperature of the ceiling rises. The effect on the burning fuel will be to increase the rate of burning. However, more significantly, it will promote flame spread over the item first ignited and to contiguous surfaces and adjacent items, thereby increasing the area of burning.

It has been discussed in the literature that the rate of increase in the area of burning is more important than the rate of increase of burning rate of the fuel in determining the rate of fire development to the flashover stage. It is reported that any scenario which leads to fast fire spread - and hence a rapidly increasing area of burning - will promote the onset of flashover [5].

Given that flashover marks the beginning of the fully developed fire, this term must be defined more precisely in order that the factors which determine the duration of the growth period can be examined. The most common definitions are:

1. the transition from a localized fire to the general conflagration within the compartment when all the fuel surfaces are burning,
2. the transition from a fuel controlled fire to a ventilation controlled fire, and
3. the sudden propagation of flame through the unburnt gases and vapors collected under the ceiling.

It is discussed in the literature that 2. is the result of 1. and is not a fundamental definition. The third definition is based partly on an observation that flames often emerge from the window or other ventilation openings at around the time full room involvement commences. Therefore the first definition is selected to be the most appropriate, although it may not apply to very

long or deep compartments in which it may be physically impossible for all the fuel to become involved at the same time.

The fuel and ventilation conditions necessary for flashover can be derived by analyzing the heat balance equation applied to the layer of hot gases below the ceiling.

$$\dot{Q}_c = (\dot{m}_a + \dot{m}_f)\, c_p\, (T - T_0) + h_k\, A_T\, (T - T_0) \tag{2.19}$$

where T and T_0 are the temperatures of the upper layer and the ambient atmosphere respectively. It is assumed that the layer is well mixed and its temperature is uniform. Writing

$$\dot{m}_g = \dot{m}_a + \dot{m}_f \tag{2.20}$$

and rearranging 2.19 gives

$$\frac{\Delta T}{T_0} = \frac{\dot{Q}_c/(c_p\, T_0\, \dot{m}_g)}{1 + h_k\, A_T/(c_p\, \dot{m}_g)} \tag{2.21}$$

The mass flow rate of gas leaving the compartment above the neutral plane can be approximated by the expression developed for flow of air induced by a small fire:

$$\dot{m}_g = \frac{2}{3}\, C_d\, A_w\, H^{1/2} \rho_0 \left(2g\frac{T_0}{T}\left(1 - \frac{T_0}{T}\right)\right)^{1/2} \left(1 - \frac{h_0}{H}\right)^{3/2} \tag{2.22}$$

where h_0 is the height of the neutral plane and C_d is the discharge coefficient. The equation can then be reduced to the following proportionality:

$$\dot{m}_g \propto g^{1/2}\, \rho_0\, A_w\, H^{1/2} \tag{2.23}$$

where $g = 9.81$ m/s^2 and ρ_0 is the density of ambient air. Using this relationship Equation 2.21 can be rewritten as a function of two dimensionless groups:

$$\frac{\Delta T}{T_0} = f\left(\frac{\dot{Q}_c}{g^{1/2}\, c_p\, \rho_0\, T_0\, A_w\, H^{1/2}}\ ,\ \frac{h_k\, A_T}{g^{1/2}\, c_p\, \rho_0\, A_w\, H^{1/2}}\right)$$

$$or \quad \frac{\Delta T}{T_0} = C\, {X_1}^N\, {X_2}^M \tag{2.24}$$

where X_1 and X_2 represent the two dimensionless groups, and the constant C and exponents N and M remain to be determined.

It is reported in the literature that the analysis of experimental fires show that the steady burning rates are achieved for the cases when the upper gas layer temperatures do not exceed 600°C. Above 600°C, flaming can occur intermittently within the layer and the assumptions in the model break down. Therefore, in order to fit the experimental data with Equation 2.24, it is necessary to obtain appropriate values for h_k which depend on the duration of the fire and the thermal characteristics of the compartment boundary. For a fire which burns with a characteristic time t_c greater than the thermal penetration time t_p of the boundary, h_k can be approximated by:

$$h_k = \frac{k}{\delta} \tag{2.25}$$

where k is the thermal conductivity of the material from which the compartment boundaries have been constructed. If, on the other hand, t_c is less than t_p, the boundary will be storing heat during the fire and little will be lost through the outer surface. Normally, this would require detailed solution of the transient heat conduction equations but a simplification can be achieved by replacing δ by $(\alpha\, t_c)^{1/2}$, the effective depth of the lining material which is heated significantly during the course of the fire. In these circumstances:

$$h_k = \frac{k}{(\alpha\, t_c)^{1/2}} = \left(\frac{k\,\rho\,c}{t_c}\right)^{1/2} \tag{2.26}$$

For a compartment bounded by different lining materials, the overall value of h_k must be weighted according to the areas; thus, if the walls and ceiling (W, C) are of a different material to the floor (F), then, if $t_c > t_p$:

$$h_k = \frac{A_{W,C}}{A_T}\,\frac{k_{W,C}}{\delta_{W,C}} + \frac{A_F}{A_T}\,\frac{k_F}{\delta_F} \tag{2.27}$$

But if $t_c < t_p$, then:

$$h_k = \frac{A_{W,C}}{A_T}\left(\frac{(k\,\rho\,c)_{W,C}}{t_c}\right)^{1/2} + \frac{A_F}{A_T}\left(\frac{(k\,\rho\,c)_F}{t_c}\right)^{1/2} \tag{2.28}$$

where A_T is the total internal surface area.

It is reported in the literature that the experimental results were found to fit satisfactorily to the form in Equation 2.24. Further analysis allowed constants C, N and M be evaluated to give:

$$\Delta T = 480\, {X_1}^{2/3}\, {X_2}^{-1/3} \tag{2.29}$$

in which T_0 is taken to be 295K.

Equation 2.29 can be used to estimate the size of fire necessary for flashover to occur. If a temperature rise of 500K is taken as a conservative criterion for the upper layer gas temperature at the onset of flashover then substitution for X_1 and X_2 in the equation gives:

$$\dot{Q}_c = \left(g^{1/2}\, c_p\, \rho_0\, {T_0}^2 \left(\frac{\Delta T}{480} \right)^3 \right)^{1/2} \left(h_k\, A_T\, A_w\, H^{1/2} \right)^{1/2} \tag{2.30}$$

with $\Delta T = 500K$ and appropriate values for g etc.:

$$\dot{Q}_{FO} = 610\, \left(h_k\, A_T\, A_w\, H^{1/2} \right)^{1/2} \tag{2.31}$$

where h_k is in kW/m^{2}K, A_T and A_w are in m^2 and H is in meters. $\dot{Q}_{FO}$ is the rate of heat output necessary to produce a hot layer at approximately 500°C beneath the ceiling.

The square root dependence indicates that if there is 100% increase in any of the parameters h_k, A_T or A_w, then the fire will have to increase in heat output by only 40% to achieve the flashover criterion as defined.

CHAPTER 3

LARGE EDDY SIMULATION (LES) APPROACH

3.1 INTRODUCTION

The most distinguishing feature of any Computational Fluid Dynamics (CFD) model is its treatment of turbulence. There are three main techniques of simulating turbulence; Direct Numerical Simulation (DNS), Reynolds-Averaged Navier-Stokes (RANS), and Large Eddy Simulation (LES).

Three simulation techniques are grouped in two families. LES and DNS are of the same category. While, both models compute directly the turbulent fluctuations in space and time, LES calculates them only above a certain length scale. Below that scale, called the sub-grid scale, the turbulence is modelled by semi-empirical laws. RANS model ignores the turbulent fluctuations and aims at calculating only the turbulent-averaged flow.

The phrase LES in fire and combustion modelling refers to the description of turbulent mixing of the gaseous fuel and combustion products with the local atmosphere surrounding the fire. This process, which determines the burning rate in most fires and controls the spread of smoke and hot gases, is extremely difficult to predict accurately. This is true not only in fire research but in almost all phenomena involving turbulent fluid motion.

The basic idea behind the LES technique is that the eddies that account for most of the mixing are large enough to be calculated with reasonable accuracy from the equations of fluid dynamics. The underlying idea, which must ultimately be justified by comparison to experiments, is that small-scale eddy motion can either be crudely accounted for or ignored. Therefore, LES is used to model the dissipative processes; viscosity, thermal conductivity, and material

diffusivity; that occur at length scales smaller than those that are explicitly resolved on the numerical grid. This means that the equations describing the transport of mass, momentum, and energy by the fire-induced flows cannot be used directly, but must be simplified so that they can be efficiently solved for the fire scenarios of interest.

In general, because it is more accurate, DNS is the preferred method whenever it is feasible. LES is the preferred method for flows in which the Reynolds number is high or the geometry is too complex to allow application of DNS.

LES requires less computational effort than DNS but more effort than those methods that solve RANS equations. The main advantage of LES over RANS approaches is the increased level of detail it can deliver. While RANS methods provide averaged results, LES is able to predict instantaneous flow characteristics and resolve turbulent flow structures. This is particularly important in simulations involving chemical reactions. A domain where LES is clearly coming close to practical industrial applications is the modelling of combustion phenomena.

It is proposed to use Fire Dynamics Simulator (FDS) software for the analysis of fire development and flame spread in the underground railway carriages. FDS uses LES technique in simulating turbulence. The brief explanation of the software, and the governing equations are given in Section 3.2.

3.2 FIRE DYNAMICS SIMULATOR (FDS) SOFTWARE

3.2.1 INTRODUCTION

The Fire Dynamics Simulator (FDS) was developed and is currently maintained by the Fire Research Division in the Building and Fire Research Laboratory (BFRL) at the National Institute of Standards and Technology (NIST).

The FDS is a Fortran 90 computer program that solves the governing equations of fluid dynamics. Smokeview is a companion program written in C/OpenGL programming language that produces images and animations of the FDS simulation results.

FDS is a Computational Fluid Dynamics (CFD) model of fire-driven fluid flow. The model

solves numerically a form of the Navier-Stokes equations appropriate for low-speed, thermally-driven flow with an emphasis on smoke and heat transport from fires. The partial derivatives of the conservation equations of mass, momentum and energy are approximated as finite differences, and the solution is updated in time on a three-dimensional, rectilinear grid. Thermal radiation is computed using a finite volume technique on the same grid as the flow solver. Lagrangian particles are used to simulate smoke movement and sprinkler discharge.

Throughout its development, FDS has been aimed at solving practical fire problems in fire protection engineering, while at the same time providing a tool to study fundamental fire dynamics and combustion. FDS can be used to model the following phenomena:

- Low speed transport of heat and combustion products from fire,
- Radiative and convective heat transfer between the gas and solid surfaces,
- Pyrolysis,
- Flame spread and fire growth,
- Sprinkler, heat detector, and smoke detector activation, and
- Sprinkler sprays and suppression by water.

Although FDS was designed specifically for fire simulations, it can be used for other low-speed fluid flow simulations that do not necessarily include fire or thermal effects. [24]

3.2.2 GOVERNING EQUATIONS IN FDS

3.2.2.1 FUNDAMENTAL CONSERVATION EQUATIONS

In fire modelling, similar to other studies which involve fluid flow, following conservation equations should be satisfied within the flow domain. It should be noted that $\vec{u}$ in the conservation equations represents the velocity vector $\vec{u} = (u, v, w)$ in three-dimensional domain.

Conservation of mass:

$$\frac{\partial \rho}{\partial t} + \nabla \cdot \rho \vec{u} = 0 \tag{3.1}$$

This equation is also known as the Continuity Equation, which is an expression of the overall mass conservation requirement and must be satisfied at every point in the flow. This equa-

tion applies for a single species fluid, as well as for mixtures in which species diffusion and chemical reactions may be occurring. The first term in Equation 3.1 describes the change in density with time and the second term defines the mass convection.

The mass conservation equation is often written in terms of the mass fractions of the individual gaseous species:

$$\frac{\partial(\rho Y_i)}{\partial t} + \nabla \cdot \rho Y_i \, \vec{u} = \nabla \cdot \rho D_i \nabla Y_i + \dot{m}_i''' \tag{3.2}$$

where Y_i represents the mass fractions. Summing these equations over all species yields the original mass conservation equation. This implies that the sum of the mass fractions $\sum Y_i = 1$, the sum of production/loss rates $\sum \dot{m}_i''' = 0$, and the sum of the diffusion terms $\sum \rho D_i \nabla Y_i = 0$.

Conservation of Momentum (Newton's Second Law):

The second conservation law relevant to the convection heat transfer problem is the Newton's second law of motion. For a differential control volume in a flow field, this requirement states that the sum of all forces acting on the control volume must be equal to the rate of increase of the fluid momentum within the control volume, plus the net rate at which momentum leaves the control volume (outflow-inflow).

$$\frac{\partial(\rho \vec{u})}{\partial t} + \nabla \cdot \rho \vec{u} \, \vec{u} + \nabla p = \rho f + \nabla \cdot \tau_{ij} \tag{3.3}$$

The forces acting on the fluid may be categorized into body forces, such as the gravitational force, and surface forces, such as the fluid static pressure and viscous stresses. Among the forces acting on the fluid, gravitational body force is the most important from the fire science point of view, since it represents the influence of buoyancy on the flow.

Conservation of Energy (First Law of Thermodynamics):

The conservation of energy equation is the first law of thermodynamics which states that increase in energy of the control volume is equal to the heat added minus the work done by expansion. In other words, the conservation of energy describes the balance between the net rate of energy accumulation in a control volume and the various energy gain and loss terms associated with the control volume that contribute to the net energy accumulation. The conservation of energy equation can be written in terms of sensible enthalpy, h, as follows:

$$\frac{\partial(\rho h)}{\partial t} + \nabla \cdot \rho h \, \vec{u} = \frac{Dp}{Dt} + \dot{q}''' - \nabla \cdot q + \Phi \tag{3.4}$$

The sensible enthalpy, h, is a function of temperature: $h = \int_{T_0}^{T} c_p(T')\, dT'$. In the energy equation, $\dot{q}'''$ is the heat release rate per unit volume from a chemical reaction, $\nabla \cdot q$ represents the conductive and radiative heat fluxes, and Φ, the dissipation function, is the rate at which kinetic energy is transferred to thermal energy due to the viscosity of the fluid. The term Φ is usually neglected because it is very small relative to the heat release rate of the fire.

Equation of State for a Perfect Gas:

The conservation equations are accompanied by the equation of state in fire modelling. One of the assumptions that has to be made is the fluid obeys the perfect gas law. In FDS, the equation of state for a perfect gas is given as:

$$p = \frac{\rho R T}{M} \tag{3.5}$$

3.2.2.2 COMBUSTION MODELLING EQUATIONS

There are two types of combustion models used in FDS. The choice depends on the resolution of the underlying grid. For a DNS calculation, a global one-step, finite rate chemical reaction is the most appropriate. However, in an LES calculation where the grid is not fine enough to resolve the diffusion of fuel and oxygen, a mixture fraction based combustion model is used.

The actual chemical rate processes that control the combustion energy release are often unknown in fire scenarios. Even if they were known, the spatial and temporal resolution limits imposed by both present and foreseeable computer resources places a detailed description of combustion processes beyond reach. Thus, the model adopted in FDS is based on the assumption that all species of interest can be described in terms of a mixture fraction $Z(x, t)$.

The mixture fraction combustion model is based on the assumption that large-scale convective and radiative transport phenomena can be simulated directly, but physical processes occurring at small length and time scales must be represented in an approximate manner. The nature of the approximations employed is necessarily a function of the spatial and temporal resolution limits of the computation, as well as the understanding of the phenomena involved.

The most general form of the combustion equation is:

$$\nu_F \; Fuel + \nu_O \; O_2 \rightarrow \sum_i \nu_{P,i} \; Products \tag{3.6}$$

The numbers ν_i are the stoichiometric coefficients for the overall combustion process that react fuel "F" with oxygen "O_2" to produce a number of products "P". The stoichiometric equation implies that the mass consumption rates for fuel and oxidizer are related as follows:

$$\frac{\dot{m}_F'''}{\nu_F \; M_F} = \frac{\dot{m}_O'''}{\nu_O \; M_O} \tag{3.7}$$

The mixture fraction Z is defined as:

$$Z = \frac{sY_F - (Y_O - Y_O^\infty)}{sY_F^I + Y_O^\infty} \quad where \quad s = \frac{\nu_O \; M_O}{\nu_F \; M_F} \tag{3.8}$$

The value of Z varies from 1, in a region containing only fuel, to 0 where the oxygen mass fraction takes on its undepleted ambient value, Y_O^∞. The term Y_F^I in Equation 3.8 is the fraction of fuel in the fuel stream. The quantities M_F and M_O are the fuel and oxygen molecular weights.

The mixture fraction satisfies the conservation law:

$$\rho \frac{DZ}{Dt} = \nabla \cdot \rho D \nabla Z \tag{3.9}$$

The reaction is assumed to proceed infinitely fast, meaning that all mixtures of oxygen and fuel react instantaneously, such that both fuel and oxygen cannot coexist. This will result in both fuel and oxygen vanishing at a certain instant where their mass fractions, Y_i, drop to zero. Therefore, Equation 3.8 can be simplified to obtain the flame mixture fraction, Z_f:

$$Z_f = \frac{Y_O^\infty}{sY_F^I + Y_O^\infty} \tag{3.10}$$

The flame mixture fraction, Z_f, defines the flame by prescribing a two-dimensional surface, commonly known as the flame surface, in a three dimensional space.

The assumption that fuel and oxidizer cannot coexist leads to the state relation between the oxygen mass fraction, Y_O and the mixture fraction, Z:

$$Y_O(Z) = \begin{cases} Y_O^{\infty}\,(1 - Z/Z_f) & Z < Z_f \\ 0 & Z > Z_f \end{cases} \tag{3.11}$$

State relations for both reactants and products can be derived by considering the following ideal reaction of a hydrocarbon fuel:

$$C_xH_y + \eta(x + y/4)(O_2 + 3.76N_2) \rightarrow max(0, 1 - \eta)\, C_xH_y + min(1, \eta)\, x\, CO_2$$

$$+ min(1, \eta)\, (y/2)H_2O + max(0, \eta - 1)\, (x + y/4)\, O_2 + \ \eta(x + y/4)\, 3.76N_2 \tag{3.12}$$

Here η is a parameter ranging from 0 (all fuel with no oxygen) to infinity (all oxygen with no fuel). A correspondence between η and Z is obtained by applying the definition of Z to the left hand side of Equation 3.12.

An expression for the local heat release rate can be derived from the conservation equations and the state relation for oxygen. The relationship for the heat release rate as a function of the oxygen consumption can be written as:

$$\dot{q}''' = \Delta H_O\, \dot{m}_O''' \tag{3.13}$$

where ΔH_O is the heat release rate per unit mass of oxygen consumed.

The oxygen mass conservation equation:

$$\rho\, \frac{DY_O}{Dt} = \nabla \cdot \rho D \nabla Y_O + \dot{m}_O''' \tag{3.14}$$

can be transformed into an expression for the local heat release rate using the conservation equation for the mixture fraction and the state relation for oxygen $Y_O(Z)$.

$$-\dot{m}_O''' = \nabla \cdot \left(\rho D \frac{dY_O}{dZ}\ \nabla Z\right) - \frac{dY_O}{dZ}\ \nabla \cdot \rho D \nabla Z = \rho D \frac{d^2Y_O}{dZ^2}\ |\nabla Z|^2 \tag{3.15}$$

An expression for the oxygen consumption rate per unit area of flame sheet can be derived from Equation 3.15 by integrating $\dot{m}_O'''$ over a small volume through which the flame sheet cuts. It should be noted that $\frac{dY_O}{dZ}$ is constant on one side of the flame sheet and zero on

the other, the volume integral can be rewritten as a surface integral over the flame sheet by applying the divergence theorem and seeing that the two terms cancel at the exterior boundary of the control volume. Therefore, it is more convenient to express the oxygen consumption rate in units of mass per unit time per unit area of flame sheet:

$$-\dot{m}_O'' = \left.\frac{dY_O}{dZ}\right|_{Z<Z_f} \rho D \nabla Z \cdot \vec{n} \tag{3.16}$$

In the numerical algorithm, the local heat release rate is computed by first locating the flame sheet, then computing the local heat release rate per unit area, and finally distributing this energy to the grid cells cut by the flame sheet.

3.2.2.3 THERMAL RADIATION MODELLING EQUATIONS

The Radiative Transport Equation (RTE) for an absorbing/emitting and scattering medium is:

$$s \cdot \nabla I_\lambda(x,s) = -[\kappa(x,\lambda) + \sigma_s(x,\lambda)]\, I(x,s) + B(x,\lambda) + \frac{\sigma_s(x,\lambda)}{4\pi} \int_{4\pi} \Phi(s,s')\, I_\lambda(x,s')\, d\Omega' \tag{3.17}$$

where $I_\lambda(x,s)$ is the radiation intensity at wavelength λ, s is the direction vector of the intensity, $\kappa(x,\lambda)$ and $\sigma_s(x,\lambda)$ are the local absorption and scattering coefficients, respectively. $B(x,\lambda)$ is the emission source term.

In FDS, the radiative heat flux is computed using a Finite Volume approach in solving the Radiative Transport Equation (RTE) for a non-scattering gas. In the case of a non-scattering gas the RTE becomes:

$$s \cdot \nabla I_\lambda(x,s) = \kappa(x,\lambda)[I_b(x) - I_\lambda(x,s)] \tag{3.18}$$

where $I_b(x)$ is the source term given by the Planck function.

In practical simulations the spectral dependence cannot be solved accurately. Instead, the radiation spectrum is divided into a relatively small number of bands, and a separate RTE is derived for each band. The limits of the bands are selected to give an accurate representation of the most important radiation bands of CO_2 and water.

The source term for each band can be written as a fraction of the blackbody radiation:

$$I_{b,n} = F_n(\lambda_{min}, \lambda_{max})\, \sigma T^4/\pi \tag{3.19}$$

where σ is the Stefan-Boltzmann constant. The references for the calculation of factors F_n are given by McGrattan [24]. When the intensities corresponding to the bands are known, the total intensity is calculated by summing over all the bands. It is reported that from a series of numerical experiments it has been found that six bands are usually enough.

In most large-scale fire scenarios soot is the most important combustion product controlling the thermal radiation from the fire and hot smoke. As the radiation spectrum of soot is continuous, it is possible to assume that the gas behaves as a gray medium. The spectral dependence is lumped into one absorption coefficient ($N = 1$) and the source term is given by the black-body radiation intensity.

$$I_b(x) = \sigma T(x)^4/\pi \tag{3.20}$$

In calculations of limited spatial resolution, the source term, I_b, in the RTE requires special treatment in the neighborhood of the flame sheet because the temperatures are spread out over a grid cell and are thus considerably lower than one would expect in a diffusion flame. Because of its dependence on the temperature raised to the fourth power, the source term must be modelled in those grid cells cut by the flame sheet. Elsewhere, there is greater confidence in the computed temperature, and the source term can assume its ideal value there.

$$\kappa I_b = \begin{cases} \kappa\sigma T^4/\pi & Outside\ flame\ zone \\ max(\chi_r\, \dot{q}'''/4\pi\ ,\ \kappa\sigma T^4/\pi) & Inside\ flame\ zone \end{cases} \tag{3.21}$$

where $\dot{q}'''$ is the chemical heat release rate per unit volume, and χ_r is an empirical estimate of the local fraction of that energy emitted as thermal radiation.

In FDS, the radiative transport equation, Equation 3.18, is solved using techniques similar to those for convective transport in finite volume methods for fluid flow, thus the name given to it is the Finite Volume Method (FVM).

The radiant heat flux vector, $\vec{q}_r$ is defined by:

$$\vec{q}_r(x) = \int_{4\pi} s\, I(x, s)\, d\Omega \tag{3.22}$$

The radiative loss term in the energy equation is:

$$-\nabla \cdot \vec{q}_r(x) = \kappa(x)\,[U(x) - 4\pi\, I_b(x)] \quad where \quad U(x) = \int_{4\pi} I(x,s)\, d\Omega \tag{3.23}$$

In words, the net radiant energy gained by a grid cell is the difference between that which is absorbed and that which is emitted.

3.2.2.4 CONVECTION MODELLING EQUATIONS

The calculation of the convective heat flux depends on whether one is performing a Direct Numerical Simulation (DNS) or a Large Eddy Simulation (LES). In a DNS calculation, the convective heat flux to a solid surface $\dot{q}_c''$ is obtained directly from the gas temperature gradient at the boundary:

$$\dot{q}_c'' = -k\frac{\partial T}{\partial n} \tag{3.24}$$

where n is the spatial coordinate pointing into the solid.

In an LES calculation, the convective heat flux to the surface is obtained from a combination of natural and forced convection correlations:

$$\dot{q}_c'' = h\,\Delta T \;\; W/m^2 \quad ; \quad h = max\,[C\,|\Delta T|^{1/3}\,,\; \frac{k}{L}0.037\,Re^{4/5}Pr^{1/3}] \;\; W/m^2K \tag{3.25}$$

where ΔT is the difference between the wall and the gas temperature, C is the coefficient for natural convection (1.52 for a horizontal surface and 1.31 for a vertical surface), L is the characteristic length related to the size of the physical obstruction, k is the thermal conductivity of the gas, and Re and Pr are the Reynolds and Prandtl numbers based on the gas flowing past the obstruction.

3.2.2.5 PYROLYSIS MODELLING EQUATIONS

A simple model for ignition and surface-flame spread, in which an ignition temperature is assigned to the combustible surface, can be implemented in numerical calculations. The rate

of pyrolysis being governed by a user prescribed constant which is either a rate of heat release per unit of the surface area HRRPUA or a heat of vaporization (gasification) ΔH_v.

If HRRPUA is prescribed, the surface will burn like a burner when it has reached its ignition temperature. If heat of vaporization is prescribed, the burning rate of the fuel will depend on the net heat feedback to the surface from the fire. For thermoplastic fuel, the calculation of net heat feedback will depend on whether the surface material is thermally-thick or thermally-thin.

If the surface material is assumed to be thermally thick, one-dimensional heat conduction equation for the material temperature $T_s(x,t)$ is applied in the direction x pointing into the solid (the point $x = 0$ represents the surface). The equation is given by:

$$\rho_s\, c_s\, \frac{\partial T_s}{\partial t} = \frac{\partial}{\partial x}\left(k_s \frac{\partial T_s}{\partial x}\right) \quad ; \quad -k_s \frac{\partial T_s}{\partial x}(0,t) = \dot{q}''_c + \dot{q}''_r - \dot{m}''\, \Delta H_v \tag{3.26}$$

where ρ_s , c_s and k_s are the temperature dependent density, specific heat and conductivity of the material respectively; $\dot{q}''_c$ is the convective and $\dot{q}''_r$ is the net radiative heat flux at the surface, $\dot{m}''$ is the mass loss rate of fuel and ΔH_v is the heat of vaporization.

Fuel pyrolysis is assumed to take place at the surface thus the heat required to vaporize the fuel is extracted from the incoming energy flux. The pyrolysis rate is estimated using a single-step Arrhenius rate law of the first order, written as:

$$\dot{m}'' = A\, \rho_s\, e^{-E_A/RT} \tag{3.27}$$

where R is the universal gas constant. The value of the pre-exponential factor A and the activation energy E_A are chosen such that the burning takes place very close to a given ignition temperature. These parameters are often difficult to obtain most of the fuels. The intent of using the given expression for the mass loss rate is to mimic the behavior of burning objects when details of their pyrolysis mechanisms are unknown. As referenced by Chiam [20], the values found in the literature are not consistent with each other and an differ by one order of magnitude or more. If A and E_A are not known, which is usually the case, user can prescribe the critical mass flux rate and the ignition temperature. This will direct the code to choose A and E_A so that the fuel burns at the critical mass flux rate when its surface temperature reaches ignition temperature. [25]

The latter method is used in the simulations reported in this thesis. Besides prescribing the critical mass flux rate and the ignition temperature, the maximum burning rate of the fuel will also be prescribed to prevent excess pyrolysis. The intent is to limit the burning rate of the fuel to its measured maximum.

If the surface material is assumed to be thermally-thin, then its temperature is assumed uniform across its width, $T_s(t)$ is affected by gains and losses due to convection, radiation and pyrolysis. The thermal lag of the material is a function of the product of its density, specific heat and thickness δ. The heat transfer equation is given by:

$$\frac{dT_s}{dt} = \frac{\dot{q}_c'' + \dot{q}_r'' - \dot{m}'' \, \Delta H_v}{\rho_s \, c_s \, \delta} \tag{3.28}$$

The convective and radiative fluxes are summed over the front and back surfaces of the thin fuel. The back surface is assumed to face an ambient temperature void by default in FDS [24]. The pyrolysis rate for a thermally-thin fuel is the same as for a thermally-thick fuel and estimated using Equation 3.27.

The heat transfer and pyrolysis for the charring fuels e.g. wood and liquid fuels e.g. methanol are different from the thermoplastic fuels. They are not covered here since these fuels are not likely to be involved in an underground train fire. However, the details of how these fuels are handled in FDS can be found in FDS Technical Reference Guide [24].

3.2.3 ASSUMPTIONS AND INPUTS IN FDS FIRE MODELLING

There are few assumptions due to the limitations of the fire modelling equations or the computational techniques, which one shall define and accept before simulating the fire development and flame spread behavior using numerical techniques. The main assumptions can be listed as follows:

- The thermal properties such as the thermal conductivity and the specific heat are constant during the course of the fire.
- The heat release rate properties for fuels such as the heat of combustion and the heat of vaporization are constant. The time-averaged values can be used in simulations if they are available.

- Only one fuel combustion reaction can be defined in the input file. Even though there might be more than one combustible material and accompanying combustion reaction, the most suitable reaction shall be selected for the analysis.
- The following shall be defined in the input file:
  - The heat release rate and burning duration of the ignition source
  - The status of the openings, e.g. windows and doors, and any accompanying criteria for failure or time-based status changes
  - Material properties of each item within the enclosure, including density, specific heat, and thermal conductivity if the surface is assumed to be thick
  - The identification of combustible and non-combustible surfaces. For combustible surfaces, the burning characteristics including ignition temperature, maximum burning rate, and effective heat of combustion have to be defined.
- Additional assumptions specific for train fires can be listed as:
  - The floor is fire-rated, therefore it would prevent an onboard fire from spreading to under-carriage, and any fire in the under-carriage spreading to the passenger compartment.
  - Flame spread over the floor between adjacent carriages are not allowed for a train made up of physically separated carriages. However, flame spread between adjacent carriages is possible for an open train, i.e. a train incorporating open wide gangways.

3.2.4 VALIDATION OF FDS SOFTWARE

The validation of the algorithms within FDS program has been studied in depth and reported widely in literature. [18, 24, 27, 29]

US Nuclear Regulatory Commission (NUREG) has conducted an extensive validation study, in which the FDS predictions are compared with measurements collected from six sets of large-scale fire experiments. They compared the predictions of FDS with the experimental measurements of 13 quantities, presented under 9 groups of items. The findings from the validation studies can be summarized as follows:

- Hot Gas Layer Temperature and Height
  - The FDS predictions of the hot gas layer temperature and height are, with few exceptions, found to be within experimental uncertainty. NUREG concludes that FDS is suitable for predicting hot gas layer temperature and height, with no specific cautions, in both the room of origin and adjacent rooms.
- Ceiling Jet Temperature
  - It is reported that FDS is slightly less accurate in its prediction of the near-ceiling temperature than of the overall hot gas layer temperature. However, inaccuracies in its prediction tend to be averaged out when examining the bulk hot gas layer temperature. Consequently, predictions of FDS is reported to be found within the experimental uncertainty.
- Plume Temperature
  - It is reported that FDS users should approach with caution to the predictions of the plume temperature. It is stated that a fairly fine numerical grid near the plume is required, which makes considerable computation time necessary to well-resolve temperatures within the fire plume. Even with a relatively fine grid, it might still be challenging to accurately predict plume temperatures, especially in the fire itself or just above the flame tip.
- Flame Height
  - It is noted that the flame height could only be measured through visible observations during experiments. Consequently, there is considerable uncertainty in interpreting the photographs and videos, as there is in the definition of 'flame height'. It concluded that there is not enough information about flame heights to reach any definite conclusions about FDS predictions of flame height, so the predictions should be treated with caution.
- Oxygen and Carbon-dioxide Concentration
  - The FDS mixture fraction model is capable of making predictions of major gas species concentrations, assuming that the basic stoichiometry of the combustion reaction is known and that the fire is well-ventilated. It is reported that with a few exceptions, the FDS predictions of major gas species concentrations are within experimental uncertainty.

- Smoke Concentration
  - FDS is capable of transporting smoke throughout a compartment, assuming that the production rate is known and that its transport properties are comparable to gaseous exhaust products. However, FDS does not have the ability to adjust the production rate or the optical properties of smoke, and it has been found to over-predict the smoke concentration, when compared against experimental results, in a number of validation studies.
- Compartment Pressure
  - The basic mass and energy conservation equations solved by FDS ensure reliable predictions of compartment pressure. It is reported that compartment pressure predictions are extremely sensitive to the leakage area and forced ventilation. The predictions have generally been found to be within experimental uncertainty, with an exceptional case related to the behavior of a ventilation fan.
- Radiation Heat Flux, Total Heat Flux, and Target Temperature
  - FDS has the appropriate radiation and solid phase models for predicting the radiative and convective heat flux to targets, and capable of predicting the surface temperature of a target, assuming the targets are relatively simple in shape and have uniform composition. Although, it is reported that FDS predictions of heat flux and surface temperature are generally within experimental uncertainty, the accuracy of the predictions generally decreases as the targets move closer to, or go inside of, the fire.
- Wall Heat Flux and Surface Temperature
  - FDS has the necessary radiation and solid phase sub-models for predicting the radiative and convective heat flux to walls, and the subsequent temperature rise within the walls, assuming the composition of the wall liner is uniform. Although, it is reported that FDS predictions of heat flux and surface temperature are generally within experimental uncertainty, the accuracy of the predictions, as is for targets, typically decreases closer to the fire or plume impingement region.

The validation studies conducted by NUREG [27] show that for a fire whose heat release rate is known, FDS can reliably predict gas temperatures, major gas species concentrations, and compartment pressures to within about 15%, and heat fluxes and surface temperatures to

within about 25%. It is also stated that in the predictions of heat flux and surface temperature FDS is noticeably better than the two-zone models, such as CFAST software, that are also evaluated. It is also mentioned that FDS is overly time-consuming in comparison to the other models.

The NUREG research team summarized their findings during the validation studies in a table, where they assigned green, yellow, or red colors to the simulation softwares, based on their capability and accuracy in predicting the desired quantities. Figure 3.1, acquired from NUREG research report [26], shows the evaluation of FDS program. In Figure 3.1 the color Green indicates that the research team has concluded that the model physics accurately represent the experimental conditions, and that the differences between model prediction and experimental measurement are less than the combined experimental uncertainty. The color Yellow suggests that one exercise caution when using the model to evaluate this quantity consider carefully the assumptions made by the model, how the model has been applied, and the accuracy of its results.

Parameter		Fire Model		
		CFAST	MAGIC	FDS
Hot gas layer temperature ("Upper Layer Temperature")	Room of Origin	GREEN	GREEN	GREEN
	Adjacent Room	YELLOW	YELLOW	GREEN
Hot gas layer height ("Layer interface height")		GREEN	GREEN	GREEN
Ceiling jet temperature ("Target/Gas temperature")			YELLOW	YELLOW
Plume temperature			GREEN	GREEN
Flame height		GREEN	GREEN	YELLOW
Oxygen concentration		GREEN	GREEN	GREEN
Smoke concentration		YELLOW	YELLOW	YELLOW
Room pressure		GREEN	GREEN	GREEN
Target temperature		YELLOW	YELLOW	YELLOW
Radiant heat flux		YELLOW	YELLOW	YELLOW
Total heat flux		YELLOW	YELLOW	YELLOW
Wall temperature		YELLOW	YELLOW	YELLOW
Total heat flux to walls		YELLOW	YELLOW	YELLOW

Figure 3.1: Results of the Validation & Verification of the Selected Fire Models by NUREG [26]

Wen et al. [29] simulated a medium-scale methanol pool fire using FDS program and compared their predictions against the published experimental results by Weckman and Strong [4]. The simulation used predominantly the existing features in FDS except that an additional sub-grid scale combustion model based on the laminar flamelet approach was used alongside the default mixture fraction combustion model for comparison. They reported that FDS with its existing features can deliver accurate predictions for the most important parameters of pool fires, including mean values of temperature and axial velocity distributions, and the air entrainment ratios, that are of significance in the fire safety context. They concluded that the predictions of the two different combustion models were in reasonably good agreement with each other and the experimental data. The overall agreement between the predictions demonstrates the robustness of the existing mixture fraction combustion model for medium-scale pool fire predictions.

Hietaniemi et al. [18] performed a set of case studies where they compared predictions of FDS with the data obtained from three experimental setups; Cone Calorimeter setup, SBI test setup, and room corner test setup. They conducted experiments using upholstered furniture and three construction materials; spruce timber, MDF board, and PVC wall carpet on gypsum plasterboard, where they recorded the burning characteristics of these items in individual test setups. The FDS simulations replicating experimental conditions show that the simulation results and experimental predictions are in good agreement overall. They also noted some discrepancies in the predictions of FDS program and the measured results. They suggested that in order to achieve better agreement in comparison between FDS and test results, a model to calculate heat transfer on layered products should be implemented in FDS, which would make simulation of multi-layered products, such as building materials, more accurate.

FDS has been validated widely in the industry against controlled experiments, although some of the works only provide a qualitative assessment of the model, concluding that the model agreement with a particular experiment as ‘good’ or ‘reasonable’. In addition to the validation studies reported herein, many others can be found in the literature.

CHAPTER 4

FIRE DYNAMICS SIMULATOR (FDS) SIMULATIONS

4.1 INTRODUCTION

The Fire Dynamics Simulator (FDS) program is a Computational Fluid Dynamics (CFD) model of fire-driven fluid flow, and was designed specifically for fire simulations. Therefore, the FDS program is used as the main simulation program in this thesis.

In an FDS simulation, the initial and boundary conditions are defined in the computational domain, and then the fire development in the carriage is solved naturally rather than being specified in advance. During a fire incident, once the specified ignition criteria for the combustible materials are reached, they become involved in the fire development. The flames spread to adjacent items as the combustible surfaces are ignited in the computational domain, yielding a gradual increase in the total heat release rate from the fire. If the intensity of the ignition source is not sufficient to ignite the combustible items adjacent to the source, then the fire could decay and suppress itself without any growth.

A typical rolling stock is modelled in FDS and the in-car fire development is analyzed under various ventilation and evacuation conditions, and with different ignition sources.

The details of the CFD modelling including the dimensions of the tunnel and train geometries, computational grid, material properties, and ventilation and evacuation conditions are explained in Section 4.2.

The predictions from the simulations are discussed in detail and the effects of various parameters such as the tunnel length, number of open doors, location of the ignition source, the forced ventilation and the material properties are summarized in Section 4.3.

4.2 MODELLING APPROACH

4.2.1 ROLLING STOCK GEOMETRY

The FDS modelling has been carried out to examine heat and smoke spread in a Bombardier Class-378 rolling stock, and to predict design heat release rate for an in-car fire incident. The dimensions of the items that are believed to affect the fire development in the interior of rolling stock, such as combustible surfaces, windows, and passenger and end doors, are modelled accurately within the limits of the CFD program. However, it should be noted that some simplification has been done during modelling of the items that have insignificant effect on the fire development within the rolling stock.

The layout and sectional views of the rolling stock modelled are given in Appendix A.

The width of the rolling stock is 2.8m, which gives an internal width of 2.5m for the passenger area. The height of the rolling stock is 2.75m with 2.2m of clear height inside the carriage. The rolling stock is made up of four 20m long carriages, giving a total length of the rolling stock as 80m.

The proposed layout includes open wide gangways between the adjacent carriages to form a single vestibule. The gangways allow 1.5m wide and 2.0m high openings between the two adjacent carriages. Each carriage has two pairs of side doors on each side, making four pairs of doors per car. Each pair of side doors are 1.5m wide and 2.0m high.

In the event of a fire when the train is stopped in the twin-track tunnel, where a side walkway for evacuation of the passengers is available, two pairs of side doors facing the walkway in each carriage will be opened for ventilation and evacuation. The other pairs of side doors remain closed for operational safety purposes. The rolling stock also includes end doors, which will be used for evacuation of passengers in the event of a fire in the single-track tunnel, where side walkway is not present. The end doors are 0.75m wide and 2.0m high.

The Bombardier Class-378 rolling stock incorporates open wide gangways. Consequently, a train made up of four carriages form a single combined volume for fire development and smoke spread. However, most of the traditional rolling stock models are made up of physically separated individual carriages. In this configuration, the flames are unlikely to spread to

the adjacent carriages within the first 30 minutes from the ignition, due to physical separation between the individual carriages. Therefore, in this thesis, the fire development and flame spread in two different train models are investigated; a train made up of four carriages incorporating open wide gangways, and a single car representing a train model with physically separated carriages.

The views of the single car model built in FDS are given in Figure 4.1.

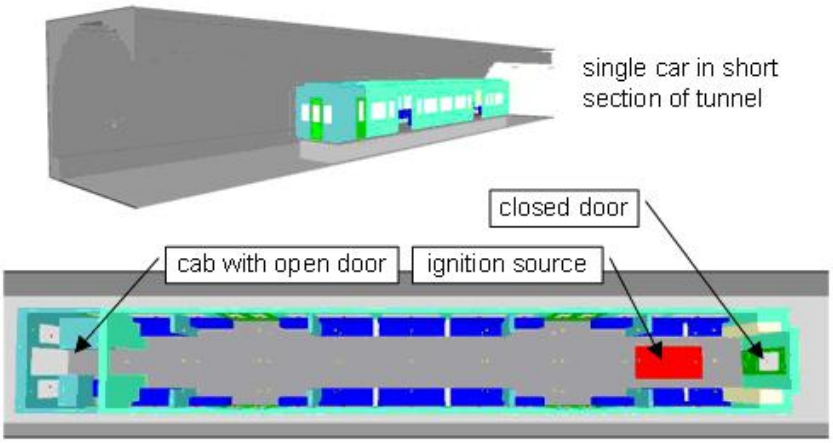

Figure 4.1: Views of the single car FDS model

4.2.2 TUNNEL GEOMETRY

The CFD simulations have been performed at two different tunnel cross-sections; a single-track tunnel and a twin-track tunnel. The tunnel cross-sections at which the train is stopped are selected in accordance with the presumed evacuation scenarios.

The evacuation in case of an incident in the single-track tunnel will be by means of the end doors, since there is no side walkway provided in this section of the running tunnel. The evacuation during an incident at the twin-track tunnel section will be by means of the side passenger doors. Therefore, the two types of the tunnel construction would provide and help investigating different ventilation conditions over the developing fire within the rolling stock.

In the CFD simulations only a section of the tunnel is modelled rather than the full length of the running tunnel in order to save computational time. In addition, it has been predicted

that the length of the tunnel has insignificant effect on the in-car fire development. However, the effect of the tunnel length on flame spread within the rolling stock has been investigated through the sensitivity simulations, results of which are discussed further in this chapter.

The length of the computational domain, i.e. the tunnel length in FDS simulations, is initially defined to be 120m for both simulation models involving the single car and the 4-car train model with open wide gangways. The length of the domain is then reduced to 40m for the simulations involving single car through the sensitivity simulations. The length of the domain allows a 10m long tunnel from the edge of the single car on each side. The length of the computational domain remains 120m where 4-car open train model is simulated.

The single-track tunnel is 4.0m high and has a cross-sectional area of 12.7m^2. The twin-track tunnel is 6.0m high with a cross-sectional area of 37.7m^2. The tunnel geometries are defined to be level, i.e. with 0% gradient for simplicity. The tunnel cross-sectional views are given in Figure 4.2.

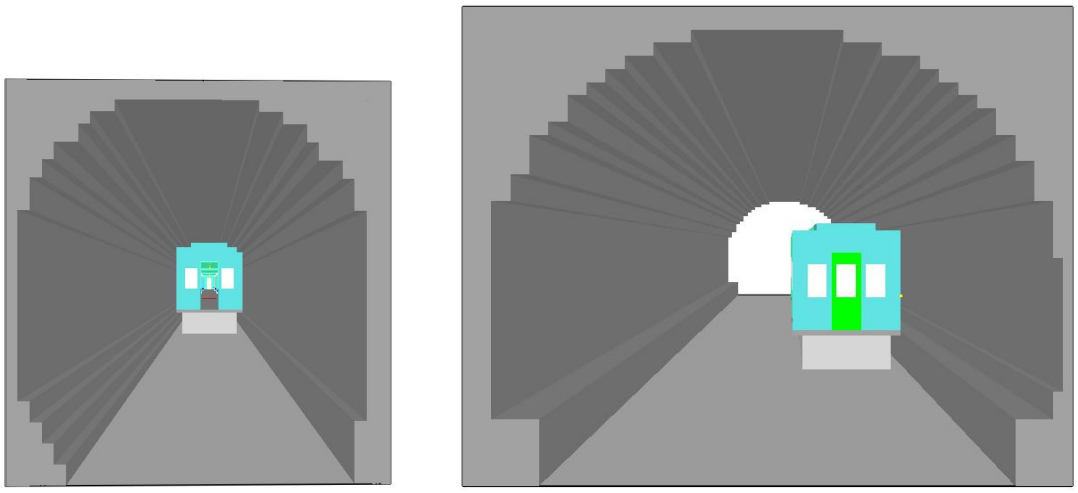

Figure 4.2: Cross-sections for single and twin-track tunnels

4.2.3 IGNITION SOURCES

In the FDS modelling, mainly two different types of ignition sources have been simulated; arson fire, and baggage fire.

The arson fire is defined to start on a seat and release 80kW of heat to its surroundings for 30 minutes. The heat release rate from the ignition source is defined to be constant during this time interval. This ignition source is compliant to the British Standard BS 6853, and referred to as the design condition by the rolling stock manufacturers.

The baggage fire is defined to start on the floor and grow according to a 'fast' fire growth rate to reach a peak heat release rate of 1.5MW. The peak heat release rate of ignition source is reached within 3 minutes and maintained for 5 minutes. The ignition source is then defined to decay exponentially. The fire development curve for the baggage fire source is given in Figure 4.3. The baggage fire ignition source releases 1.6GJ of energy, calculated from the area under the heat release rate curve using the Trapezoidal Rule, over the 30 minutes burning duration. The baggage fire source represents a particularly severe scenario for fire development within the rolling stock and for the evacuation of passengers.

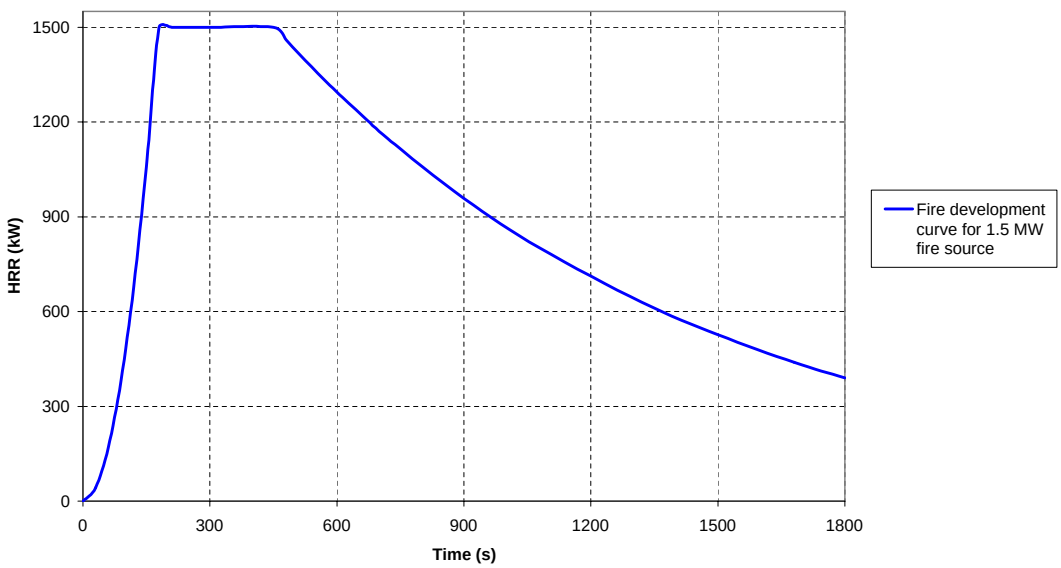

Figure 4.3: Fire development curve for baggage fire source

The ignition source areas are defined to give a heat flux value between 550 kW/m^2; arson fire; and 750 kW/m^2; baggage fire; at the ignition location. The fire size per unit area for baggage fire is given to be slightly high compared to the typical range of values recommended by the British Standard PD 7974-1 [14]. However, this value corresponds to a high stack of luggage, and is considered acceptable for practical purposes when the ignition source area is considered.

In addition to the described arson and baggage fire ignition sources, a set of simulations has been performed with modified baggage fire source and with liquid fuel source, as a part of the sensitivity studies. The details of the ignition sources are explained further, along with the cases simulated, in Section 6.4 in Chapter 6.

4.2.4 VENTILATION

In the FDS simulations, a stationary train on fire is simulated in a single-track and in a twin-track section of the running tunnel. The fire development is defined to be under natural ventilation conditions, i.e. without any mechanical ventilation, and the residual airflows due to the train movements in the tunnels are not considered. The tunnel boundaries at both ends are defined to be open to atmosphere during natural ventilation conditions.

The ventilation of the fire, i.e. airflow within the rolling stock, depends on the individual scenario simulated. As mentioned earlier in Sub-section 4.2.2, the evacuation of passengers and ventilation of an incident in a single-track tunnel are through the open end doors in the absence of side walkways in the running tunnel. The fire is ventilated and the passengers evacuate using the side doors in an incident in the twin-track tunnel section. These two distinct cases help to investigate the effects of ventilation on the fire development.

In the simulations, the doors are defined to be open at the beginning of the simulation, i.e. when the fire starts at time is equal to zero. It is assumed that when the fire is noticed inside the rolling stock, passengers will inform the driver, and be able to open the doors as fire starts to develop.

The windows are modelled as laminated safety glass which fails when the temperature at the face of the window reaches 675°C. The temperature at which the windows fail depends highly on the quality of the glass and the seal that holds the glass. The temperature value defined in the simulations is taken from the research work done by Chiam [20] on a similar subject for practical purposes.

The window failure is simulated through monitoring the temperature at the center of the glass surfaces facing the interior of the carriage. The windows are removed when the predefined temperature limit is reached. In some cases, the windows are predicted to fail altering the in-car ventilation conditions which assist extracting smoke and removing heat from the incident

carriage.

The rolling stock is modelled as a sealed non-leaky enclosure. No leakage paths around windows and doors are represented. The windows and doors are defined to be airtight, i.e. they do not permit any airflow in to or out of the rolling stock unless they are open or failed due to high temperature.

The Class-378 rolling stock is equipped with in-car air-conditioning systems, which include smoke detectors. The air-conditioning units will be deactivated in the event of a fire in the rolling stock. These units are not designed to extract smoke, and therefore have not been represented in the FDS model.

In addition to the base cases, a set of sensitivity simulations incorporating different ventilation conditions are performed. These investigate the effects of:

- the number of open doors in the incident carriage,
- the limited window failure in the incident carriage, and
- the mechanical ventilation

on fire development. The details of the sensitivity simulations are given in Chapter 6.

4.2.5 MATERIALS

The fire rating of the materials play an important role in fire development in the interior of the rolling stock. The combustible materials in a typical rolling stock are classified based on their flame resistance characteristics into three categories; 1a, 1b, and 2; in British Standard BS 6853 [6]. It is proposed by the rolling stock manufacturers that the materials which will be used in Class-378 rolling stock are highly fire retardant and classified as category 1a with respect to British Standard BS 6853.

In the FDS simulations, the specific material properties for the rolling stock model are defined for the body of the car, including walls and the ceiling, for the floor, for seats, and for the electrical equipment inside the passenger compartment. The materials and equipments under the carriage are not modelled in this study.

Once the materials in the rolling stock model are defined, they are further classified to be either combustible or non-combustible. It is proposed by the rolling stock manufacturer, and also

noted in the design specification of Class-378 rolling stock that the electrical equipment boxes located at the ends of the carriages are fire-rated. Consequently, the electrical equipment boxes are defined to be non-combustible in the FDS simulations.

It has been discussed and shown in previously published research and project reports that the wall and ceiling materials of a typical rolling stock require very high heat flux levels to be ignited. In addition, it has been shown that when these materials are ignited, their contribution in the overall fire development is insignificant [11, 20, 35]. Consequently, the wall and ceiling materials are modelled to be non-combustible in the FDS simulations.

In the simulation model, the non-combustible surfaces are defined to be thermally-thick. The following physical properties, in addition to the thickness of the linings, are required for the non-combustible materials:

- density,
- thermal conductivity, and
- the specific heat of the lining material.

The one-dimensional heat transfer equation is solved, using the parameters listed, across the thickness of the material for the non-combustible surfaces.

The seats and the floor are defined to be the combustible surfaces in the simulations. It has also been reported in the previous publications [11, 20, 35] that the highest contribution to the development of fire are from these two surfaces in a typical rolling stock model.

For the combustible materials, in addition to the properties listed for the non-combustible materials above, the parameters that affect the ignition and combustion have to be defined. These properties include:

- ignition temperature,
- heat of vaporization,
- effective heat of combustion,
- maximum burning rate, and
- critical mass flux.

The parameters listed for combustible materials and the materials' response while burning are often acquired from Cone Calorimeter experiments. However, the burning characteristics of the combustible materials change with the heat flux levels that they are exposed to.

Therefore, for a combustible material, experiments are performed for a range of surface heat flux levels during the Cone Calorimeter testing. In addition, the Cone Calorimeter experiments should comply with the guidance and procedure given in ISO 5660-1:2002 standard. Consequently, it is usually difficult to obtain a full set of experimental results for the required materials due to lengthy and expensive testing methods.

The FDS simulations presented in this thesis can be divided into two groups in terms of the combustible material properties used in the simulations. In the early stages of the research, the burning characteristics of the materials used in Class-378 rolling stock were unavailable.

In the absence of Cone Calorimeter test results of the materials proposed for Class-378 rolling stock, the material properties for Singapore Circle Line stock are used in the initial set of FDS simulations. The burning characteristics of the materials used in Singapore Circle Line stock are obtained from a published research study in the similar field of interest [20]. In the final set of simulations, the burning characteristics of the materials proposed for Class-378 rolling stock are used.

During the course of a fire incident in the rolling stock, the combustible materials are exposed to different heat flux levels. However, the FDS simulation program allows only one characteristic to be input to the code to reflect the behavior of combustible materials during the fire development.

One accepted practice is to test the behavior of the materials under different heat flux levels, and select a representative characteristic for each of the combustible materials. Chiam [20] in his research performed a set of FDS cone calorimeter simulations for different levels of heat flux, and calibrated the results with his predictions from the experiments. He has performed simulations for 25, 35, 50, and 65kW/m^2 heat flux levels, and selected the results for 35kW/m^2 to be used as the representative characteristic.

Conversely, British Standard BS 6853 [6] specifies the surface heat flux levels that the combustible materials should be tested according to their orientation. The standard states the following values for the fire performance characteristics of the combustibles:

- 50kW/m^2 for ceiling-like downward facing surfaces,
- 35kW/m^2 for wall-like vertical surfaces, and
- 25kW/m^2 for floor-like upward facing surfaces.

It should be noted that if a single representative characteristic for a combustible material, predicted under a certain surface heat flux value, is used in the simulations, then the heat release rate values could be under-predicted at lower heat flux levels and over-predicted at higher heat flux levels. Therefore, a limiting value of maximum burning rate for the combustible materials should be specified to control and prevent excessively high values of heat release rates during combustion. The single representative characteristic could also predict earlier ignition at lower heat flux levels, and delayed ignition at higher heat flux levels. Consequently, the representative characteristic should be selected wisely and the parameters that affect the burning behavior of the combustibles should be calibrated in order to obtain a typical characteristic that covers the entire range of surface heat flux levels.

Chiam [20] used a set of material properties calibrated at a surface heat flux of 35kW/m^2 for the combustibles in his research. The seats in the Singapore Circle Line stock are made of FRP Polyester, and the floor material is a type of rubber, namely Styrene Butadiene. It should be noted that these materials are not classified as category 1a according to BS 6853. However, as mentioned earlier, in the initial set of simulations and in the sensitivity studies, the material properties calibrated by Chiam are used since the experimental results for Class-378 rolling stock materials were not available.

The material properties used in the initial and sensitivity simulations are given in Table 4.1.

Table 4.1: Material properties used in the initial and sensitivity simulations

	Combustible Materials		Non-combustible Materials				
Location	Seats	Floor	Tunnel Walls	Train Walls	Train Ceiling	Doors	Windows
Material	FRP Polyester	Styrene Butadiene	Concrete	Glass wool sandwich between aluminum panels			Laminated safety glass
Density, ρ (kg/m^3)	1795	1478	2100	119	176	276	1380
Thermal conductivity (W/mK)	0.295	0.19	1.1	0.038	0.038	0.038	0.049
Specific heat, c (kJ/kgK)	1.393	5.805	0.88	0.68	0.68	0.68	0.84
Thickness, δ (m)	0.00216	0.00162	0.7	0.1	0.06	0.035	0.023
Ignition temperature (°C)	448	419	-	-	-	-	-
Heat of vaporization (kJ/kg)	3700	6250	-	-	-	-	-
Effective heat of combustion (kJ/kg)	13670	14570	-	-	-	-	-
Maximum burning rate (kg/m^{2}s)	0.0161	0.0079	-	-	-	-	-
Critical mass flux (kg/m^{2}s)	0.0044	0.0024	-	-	-	-	-
ρ c δ (kJ/m^{2}K)	5.4	13.9	-	-	-	-	-

In an FDS simulation, the amount of heat released from the surface is calculated by multiplying the density, thickness, surface area and effective heat of combustion, i.e. $\rho \cdot \delta \cdot A \cdot \Delta H_{c,eff}$. Therefore, in order to reflect the correct amount of heat release from the combustible surfaces, the lining thicknesses are adjusted based on the average amount of mass loss during the cone calorimeter experiments. Consequently, the thicknesses given in Table 4.1 do not represent the physical thickness of the surfaces, but the calibrated values to be used in simulations.

4.2.6 COMPUTATIONAL DOMAIN

The mesh in the computational domain in an FDS simulation is defined by the number of cells on each of the three dimensional coordinates; x, y, and z. The number of cells and the dimensions of the computational domain define the cell sizes, namely the edge length of an element in the computational domain. In defining the mesh for the computational domain, a uniform distribution along the length, height and width of the domain is sought. However, this may not be possible if the geometry is complex.

In the rolling stock model, the mesh is defined to match the location of obstacles defining the positions and dimensions of the openings such as doors and windows, and combustible materials such as seats and floor. Once the critical cell edge lengths are decided, the mesh is stretched or shrunk to represent the correct lengths of the critical items in the rolling stock.

The nominal cell edge lengths, used in the simulations, are selected as follows:

- x = 0.25m
- y = 0.125m
- z = 0.175m

The cell edge length in x-direction, i.e. in the longitudinal direction, varies between 0.125m and 0.25m inside the rolling stock model. However, in order to make up for the total number of cells, the cells are slightly expanding towards the tunnel boundaries from the edge of the rolling stock model. The cell edge length never exceeds 0.25m in the interior of rolling stock in any direction.

In assessing the accuracy of the predictions of FDS, it is important to keep in mind that the software has the potential of producing ever-more accurate results as the numerical grid is refined. However, FDS calculations require hours or days to complete, depending on the

size of the numerical grid and the desired level of accuracy. Based on the requirement of FDS program producing results in a reasonable amount of time, the following procedure is recommended on what size grid to use for a given application that will produce good results in a timely manner.

Therefore, the nominal cell size in x-direction is selected based on the calculated characteristic fire diameter, D^*, using the following equation:

$$D^* = \left(\frac{\dot{Q}}{\rho_\infty c_p T_\infty \sqrt{g}} \right)^{\frac{2}{5}} \tag{4.1}$$

For a typical underground train, the value of the design heat release rate, $\dot{Q}$, varies between 8MW and 15MW depending on the quality of the materials used. If a nominal design heat release rate of 10MW is substituted in Equation (4.1) along with the appropriate values for density, specific heat, and temperature then the characteristic fire diameter can be calculated to be about 2.4m.

The quality of mesh in the computational domain for simulations involving buoyant plumes is given by the non-dimensional expression $D^*/\delta x$. The greater the ratio $D^*/\delta x$, the more the fire dynamics are resolved directly, and the more accurate the simulation. In the literature, the values between 8.0 and 12.5 are used and recommended for similar type of simulations [20, 27, 31]. It has been reported in NUREG's research publications [27] that a ratio of 5 to 10 produces favorable results at a moderate computational cost, noted based on their past experience. Consequently, the cell edge length in x-direction is selected to be 0.25m for practical purposes, which also fall within the recommended range of $D^*/\delta x$.

The cell edge lengths given above are used in all simulations, unless otherwise specified. Typical grid distributions in three planes are given in Figure 4.4.

A set of sensitivity simulations have been performed to investigate the effects of element size in the computational domain on the predicted simulation results of fire spread simulations. The predictions and results of these simulations are given in Chapter 6.

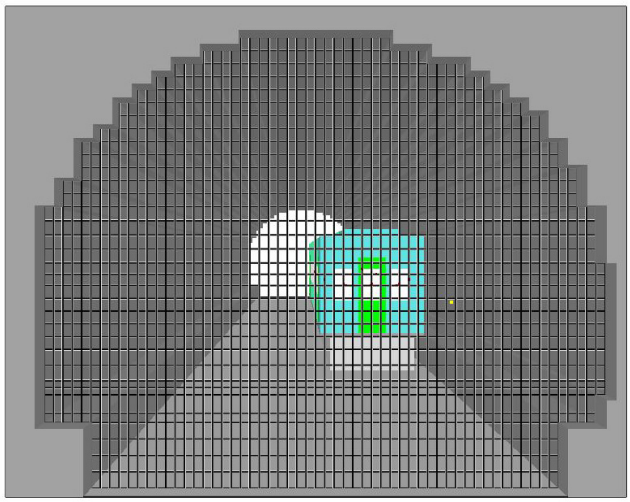

a. Grid distribution on y-z plane

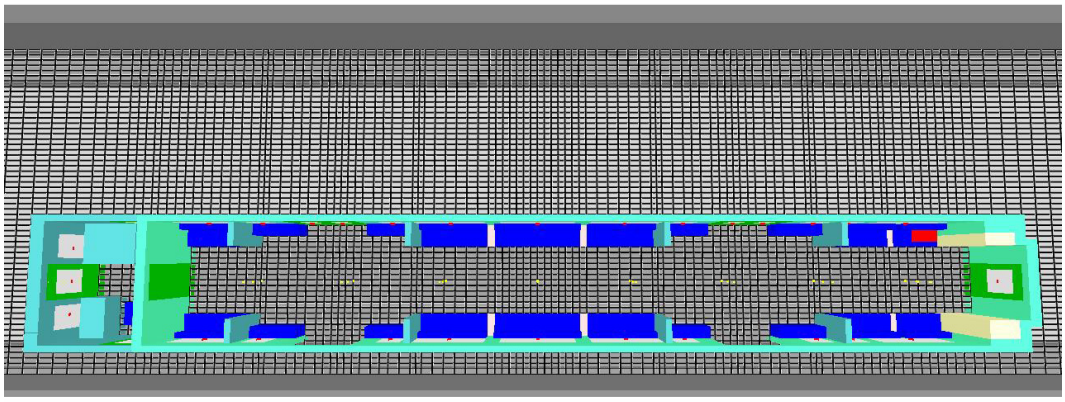

b. Grid distribution on x-y plane

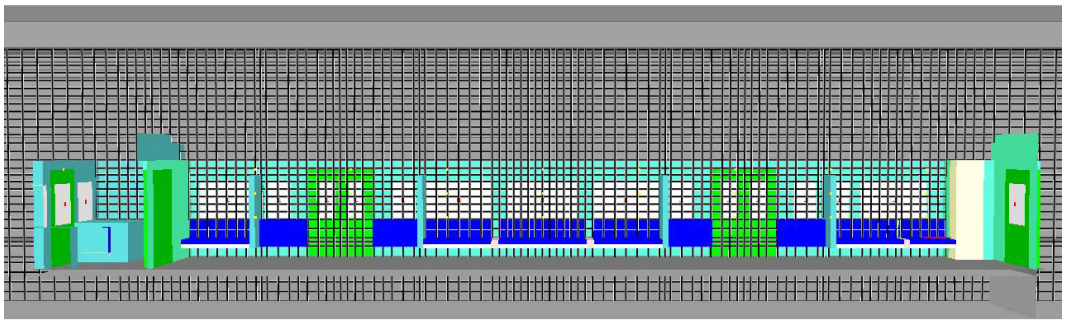

c. Grid distribution on x-z plane

Figure 4.4: Grid distribution for single-car model in twin-track tunnel

4.3 SIMULATIONS

The Fire Dynamics Simulator (FDS) program is used to perform a set of simulations to investigate the fire development and flame spread within the typical rolling stock models. The simulations are classified and discussed in three groups:

- Initial Simulations,
- Parametric Sensitivity Studies, and
- Final Simulations.

In the initial simulations, two separate ignition sources are simulated in two different rolling stock models immobilized in either a single-track or a twin-track tunnel. These cases constitute the possible basic fire scenarios in a running tunnel. The purpose of the initial set of simulations, in addition to gain a better understanding of the FDS program and fire development phenomena, is to distinguish the developing fires from the localized fire incidents.

The results of the initial set of simulations are analyzed:

- to predict onboard conditions for the evacuating passengers, and
- to predict the peak heat release rate from the incident.

The onboard conditions are evaluated against the tenability limits given by the standards [16, 28] in terms of three variables; temperature, visibility, and carbon-monoxide concentration.

The published standards [16, 28] state that thermal burns to the respiratory tract can occur upon inhalation of air above 60°C when saturated with water vapor, which can occur when water is used for fire extinguishment. The thermal tolerance data for unprotected skin of humans suggest a limit of about 120°C for convected heat. The NFPA 130 Standard [28] gives the maximum exposure times, which lead incapacitation of passengers, for a range of temperature values that the passengers could be exposed to during fire incidents. These limits are given in Table 4.2. However, for the purposes of this study, the temperature limit for tenability is taken to be 60°C, as accepted and widely used in the industry.

Table 4.2: Exposure temperature limits for tenability given by NFPA 130

Exposure Temperature (°C)	Maximum Exposure Time Without Incapacitation (min)
80	3.8
70	6.0
60	10.1
50	18.8
40	40.2

Ability to escape through smoke depends upon the effects of irritancy and visual obscuration on ability to move through enclosed spaces and ability to locate escape routes and exits. The tenability criterion that defines the ability to locate the escape routes is defined by the visibility term. The British Standards [16] suggest that people move as if in darkness at a visibility of five meters in irritant smoke in small enclosures and for short travel distances. The standard suggests a visibility of 10m as the tenability limit for large enclosures and longer travel distances. For the purposes of this study, a visibility of 5m is taken as the tenability limit for onboard conditions. A visibility of 10m is widely used in industry in fire simulations at underground stations and atriums. Although the visibility does not directly cause fatalities, it would hinder the evacuating passengers. The parameter can also be used as an indication of timescales for smoke filling of the enclosure.

In a fire calculation using the mixture fraction approach, the smoke is tracked along with all other major products of combustion. The visibility in a space is assessed by the light extinction coefficient, K. The intensity of monochromatic light passing a distance L through smoke is attenuated according to:

$$\frac{I}{I_o} = e^{-KL} \tag{4.2}$$

The light extinction coefficient, K, is a product of the density of smoke particulate, ρY_s , and a mass specific extinction coefficient that is fuel dependent.

$$K = K_m \, \rho \, Y_s \tag{4.3}$$

Estimates of visibility through smoke can be made by using the equation:

$$S = \frac{C}{K} \tag{4.4}$$

where C is a non-dimensional constant characteristic of the type of object being viewed through the smoke, i.e. $C = 8$ for a light-emitting sign and $C = 3$ for a light-reflecting sign. Since K varies from point to point in the domain, the visibility S does as well.

Three parameters control smoke production and visibility. They are:

- Soot Yield, which is the fraction of fuel mass that is converted to soot,
- Mass Extinction Coefficient, K_m in Equation 4.3 above, has a default value of 7600m^2/kg in FDS program, and
- Visibility Factor, C in Equation 4.4 above, has a default value of 3 in FDS program.

One of the asphyxiant gases important with respect to incapacitation and death in fires is carbon-monoxide. Asphyxiant gases have little or no immediate effect on exposed passengers, but when a sufficient exposure dose has been inhaled during the course of a fire, then incapacitation occurs due to collapse and loss of consciousness. If the passengers are not rescued immediately after incapacitation occurs, death is likely within a few minutes. The NFPA 130 Standard [28] gives the maximum exposure times, which lead incapacitation of passengers, for a range of carbon-monoxide concentration in air that the passengers could be inhaling during fire incidents. These limits are given in Table 4.3.

Table 4.3: Exposure air carbon-monoxide content limits for tenability given by NFPA 130

Tenability Limit Exposure Concentration of Air Carbon-monoxide Content	Maximum Exposure Time Without Incapacitation
Maximum 2000 ppm	few seconds
Averaging 1150 ppm	first 6 min
Averaging 450 ppm	first 15 min
Averaging 225 ppm	first 30 min
Averaging 50 ppm	remainder of exposure

The fire development and flame spread in the rolling stock are illustrated with the burning rate, also referred as the mass loss rate per unit area, of the combustible surfaces. The scale is set to be between 0.0, shown in dark blue representing surfaces that have not yet ignited or already been burnt out, and 1.0 g/m^{2}s, shown in red representing actively burning surfaces. The com-

ments on fire development within the incident rolling stock are based on and supplemented with the fire spread images in each case discussed.

The sensitivity simulations focus on the development of fire and flame spread within the underground rolling stock under various initial and boundary conditions. The effects of ignition source characteristics and ventilation conditions on the fire development are investigated in the cases simulated. In addition, a set of simulations has been performed to assess the accuracy of predictions through changes in the computational parameters, such as the domain length and grid size.

The final simulations include re-running the selected cases from the initial and sensitivity simulations with the revised material properties. The cases that will be simulated are selected based on the importance of their predictions with the initial material properties. The revised material properties of the combustibles should be used in FDS simulations only after their combustion characteristics are calibrated against the experimental results. Consequently, final simulations include cone calorimeter modelling for the calibration of new materials.

The details of the initial, sensitivity, and the final simulations are given in the subsequent chapters. It should be noted that the same tenability criteria, listed above, are applied in all sets of simulations. In addition, where fire development and flame spread discussions are supplemented by the images of burning rates of the combustible surfaces, the same scale as noted above is used in the figures.

CHAPTER 5

INITIAL SIMULATIONS

5.1 INTRODUCTION

This chapter gives brief information on the initial cases simulated. The purpose of the initial set of simulations is:

- to explore the capabilities of FDS program,
- to gain insight into fire modelling,
- to identify localized or developing fire incidents, and
- to predict heat release rate variations and onboard conditions for typical rolling stock and running tunnel models.

The simulations have been performed for two different possible rolling stock models; physically separated carriages and single vestibule with open wide gangways. The model incorporating physically separated carriages is represented by only one carriage based on the assumption that it is unlikely for fire to spread to adjacent carriages in the case of physical separation.

The simulations incorporate two different sections of running tunnel. These are selected specifically to create various evacuation and ventilation scenarios. The open or closed doors are defined in accordance with the tunnel geometry modelled in each specific case simulated.

In the initial set of simulations, the material properties derived and published by Chiam [20] are used.

The simulations have been performed for 30 minutes, with the ignition defined at 0 seconds. In all simulations, the initial temperature is taken to be 25°C, and the maximum visibility is

defined to be 30m for smoke-free conditions.

5.2 CASE-01: 1-CAR, 80kW SOURCE, SINGLE-TRACK TUNNEL

The first case of the initial set of simulations incorporates an arson ignition source, which releases a constant heat of 80kW for the entire duration of the incident. The ignition source is placed on the seat at opposite end of the carriage from the cab.

For an arson fire incident in the single-track tunnel, it is assumed that the end door close to the ignition source is inaccessible due to the high temperature and smoke produced by the fire in the vicinity of the ignition source. Therefore, in this case only the driver cab door is assumed to be open for evacuation of passengers and ventilation of fire.

5.2.1 FIRE DEVELOPMENT

The simulation shows that for the 80kW arson fire incident, the heat flux from the ignition source and the temperature around the ignition location are not sufficient to ignite the adjacent combustibles in the incident carriage.

Therefore, once the ignition source is placed on the seat, it is predicted that only the adjacent seats are involved in the fire development. The floor or the other combustible items at the far end of the carriage are not ignited and therefore not contributed to the fire development.

The fire development for this incident, illustrated with the burning rate of the combustible surfaces is given in Figure 5.1.

The peak heat release rate is predicted to be 125kW for this incident. The heat release rate variation during the course of the incident is shown in Figure 5.2. Since the fire burns locally on the seat, this case cannot be used to assess the design heat release rate of the railway carriages. However, this case can be used to assess the onboard conditions to comment on the safety of the passengers in the rolling stock.

Ignition

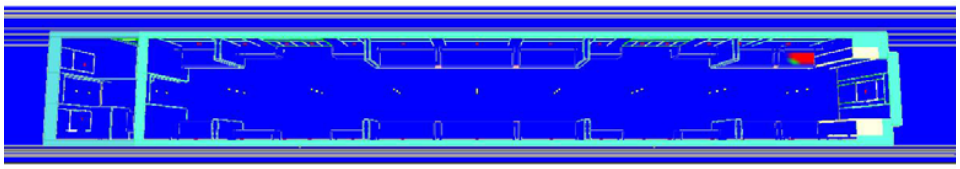

5 minutes

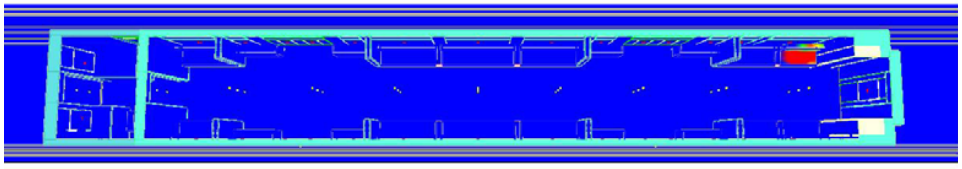

10 minutes

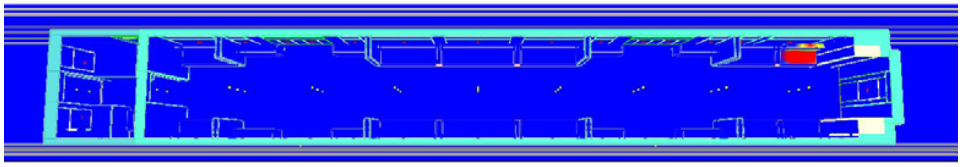

15 minutes

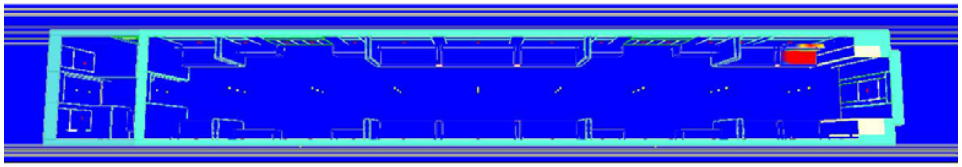

20 minutes

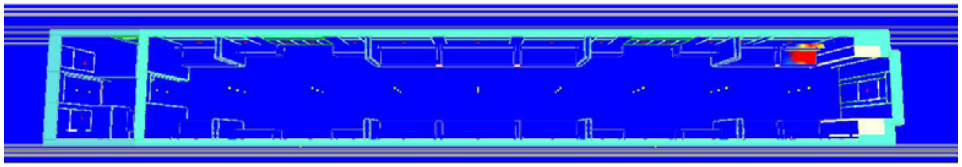

30 minutes

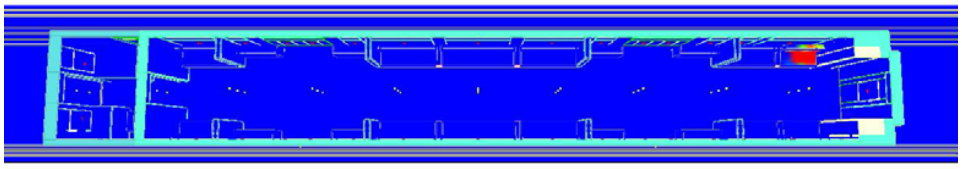

Figure 5.1: Fire spread, 1-car, 80kW source, single-track tunnel

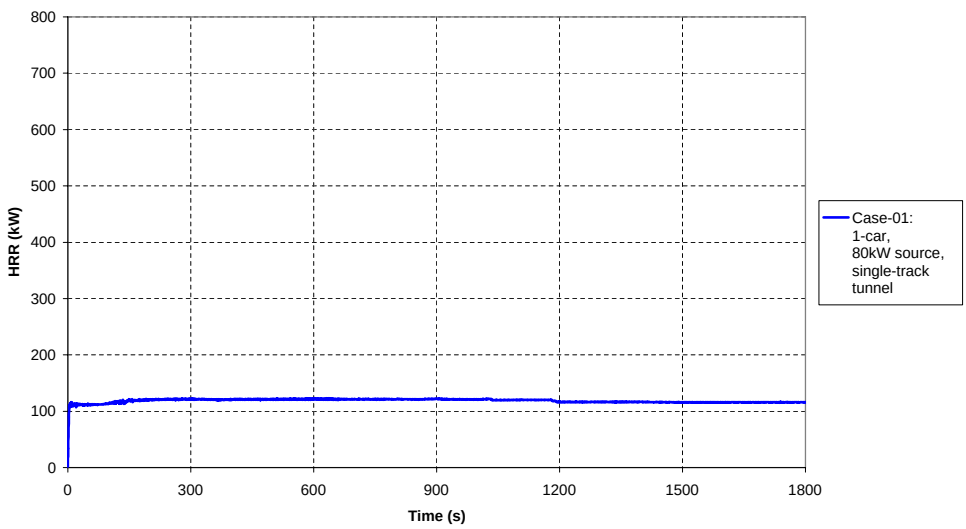

Figure 5.2: Heat release rate, 1-car, 80kW source, single-track tunnel

5.2.2 ONBOARD CONDITIONS

As mentioned earlier, for an incident in the single-track tunnel, only the driver cab door is open for ventilation of heat and smoke from the fire.

It is predicted from the simulation that even though the power of the ignition source is small, temperature increases and visibility drops quickly within the enclosed railway carriage. The results show that the temperature at the center of the carriage exceeds the 60°C limit within the first minute at 1.5m above the floor, and within four minutes at seat level. The maximum temperatures at the center of the carriage are predicted to be about 140°C at 1.5m above the floor, and about 100°C at seat level. The temperatures within the carriage do not reach the limiting temperature for window failure, therefore the simulation does not predict any window failure within 30 minutes from the ignition. The temperature variations at three points along the carriage are given in Figures 5.3 and 5.4, at 1.5m and 1.0m above the floor level, respectively.

The simulation shows that visibility drops below 5m within the first minute at the center of the carriage at 1.5m above the floor level and at the seat level. The loss of visibility is caused by smoke produced by the fire. The loss of visibility does not directly cause fatalities, but hinder the evacuating passengers.

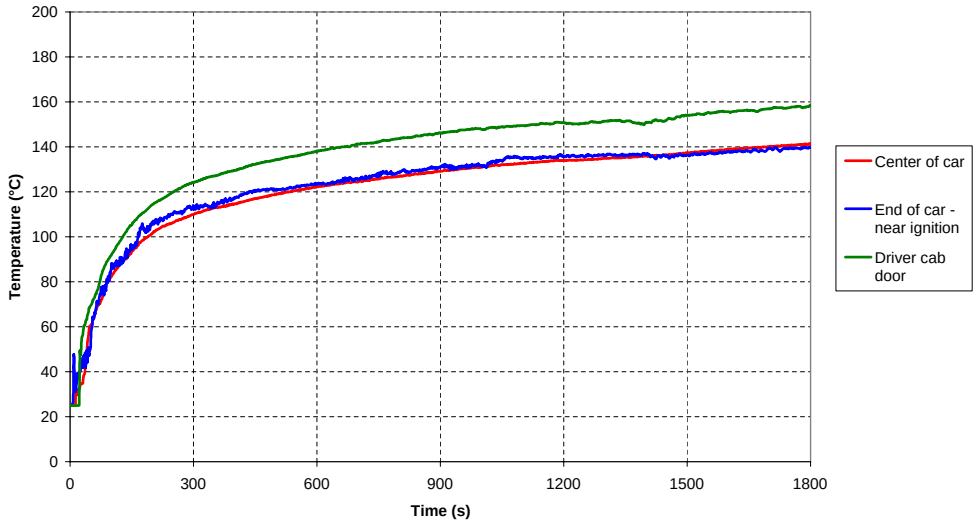

Figure 5.3: Case-01: Temperature variation at 1.5m above the floor level

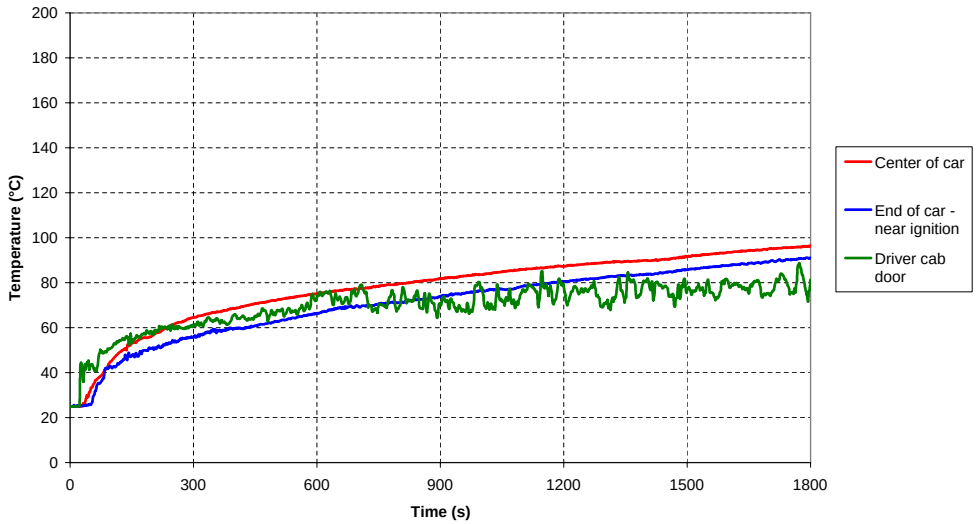

Figure 5.4: Case-01: Temperature variation at 1.0m above the floor level

In an arson fire case, the ignition source is placed on the seat, and the smoke is predicted to accumulate at ceiling level due to the buoyancy forces. Therefore, although the visibility is predicted to drop below 5m within the first minute at the center of the carriage at 1m and above, the results show that better visibility could be maintained at levels below 1m in the incident carriage. The variations of visibility at 1.5m and 1.0m above the floor level are given in Figures 5.5 and 5.6, respectively. The figures are given only for five minutes from the ignition since once the visibility is vanished in the incident carriage, it has not been recovered.

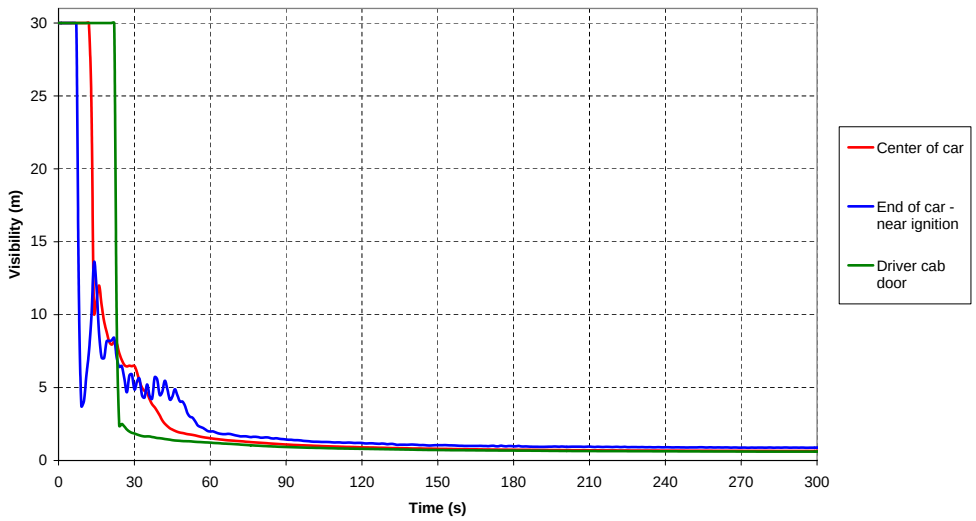

Figure 5.5: Case-01: Visibility variation at 1.5m above the floor level

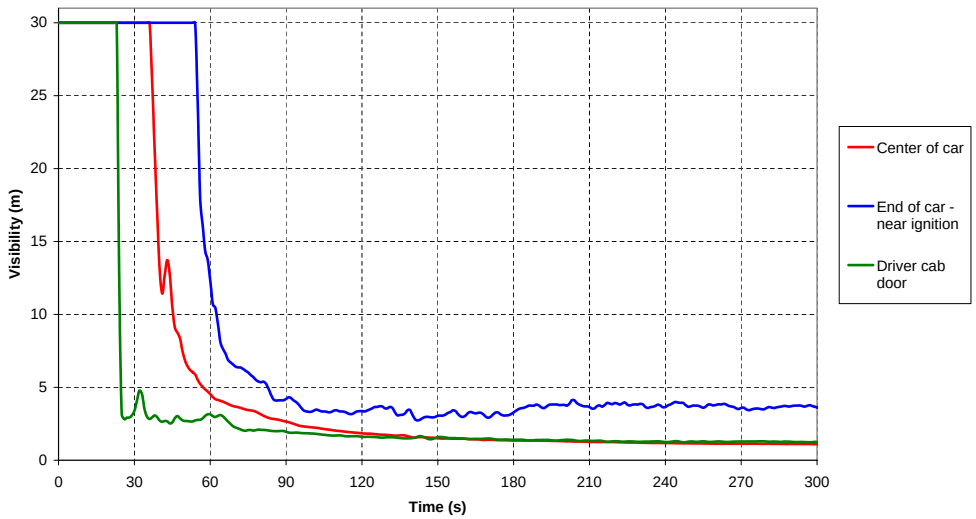

Figure 5.6: Case-01: Visibility variation at 1.0m above the floor level

It is predicted from the simulation that the average carbon-monoxide concentration in the incident carriage at 1.5m above the floor level is about 685ppm over a 30 minute exposure time. The average carbon-monoxide concentration at seat level is predicted to be about 300ppm within the first 30 minutes from the ignition. The variations of carbon-monoxide concentration at 1.5m and 1.0m above the floor level are given in Figures 5.7 and 5.8, respectively.

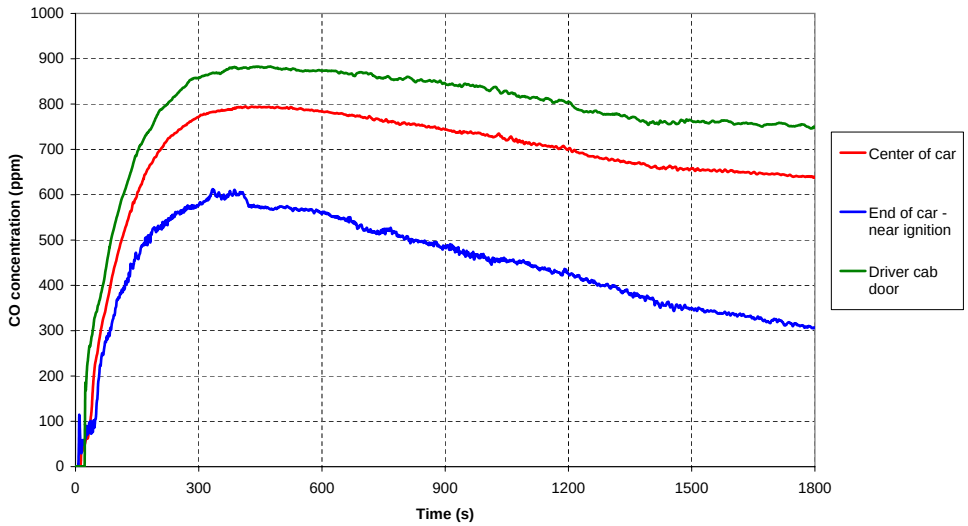

Figure 5.7: Case-01: Carbon-monoxide concentration at 1.5m above the floor level

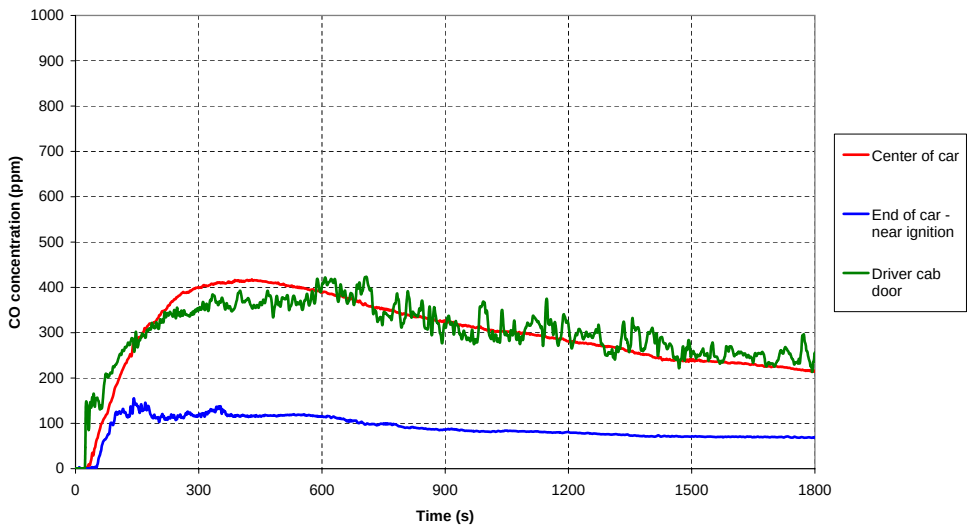

Figure 5.8: Case-01: Carbon-monoxide concentration at 1.0m above the floor level

The carbon-monoxide concentration predicted at seat level is slightly above the limiting value of 225ppm for 30 minutes exposure, recommended by the NFPA standards [28]. Once the predictions of carbon-monoxide concentration and temperature are combined, it can be concluded that the conditions are tenable in the incident carriage at seat level and above.

The temperature, visibility and carbon-monoxide slices on a longitudinal section through the center of the carriage are given in Figures B.1 to B.3 in Appendix B.

5.3 CASE-02: 1-CAR, 80kW SOURCE, TWIN-TRACK TUNNEL

The fire incident from an 80kW ignition source is also simulated using the 1-car model in the twin-track tunnel section. For an incident in the twin-track tunnel, the evacuation of passengers and ventilation of smoke from the incident are through the open side doors.

5.3.1 FIRE DEVELOPMENT

The fire development and flame spread simulation within the incident carriage shows that the fire is localized around the ignition source and does not ignite any other combustible items in the carriage, except the seats adjacent to the ignition source. The peak heat release rate for this incident is predicted to be 135kW.

The predicted heat release rate variation for this incident is shown in Figure 5.9.

The fire development for this incident, illustrated with the burning rate of the combustible surfaces, involving an 80kW ignition source in the 1-car model in a twin-track tunnel is given in Figure 5.10.

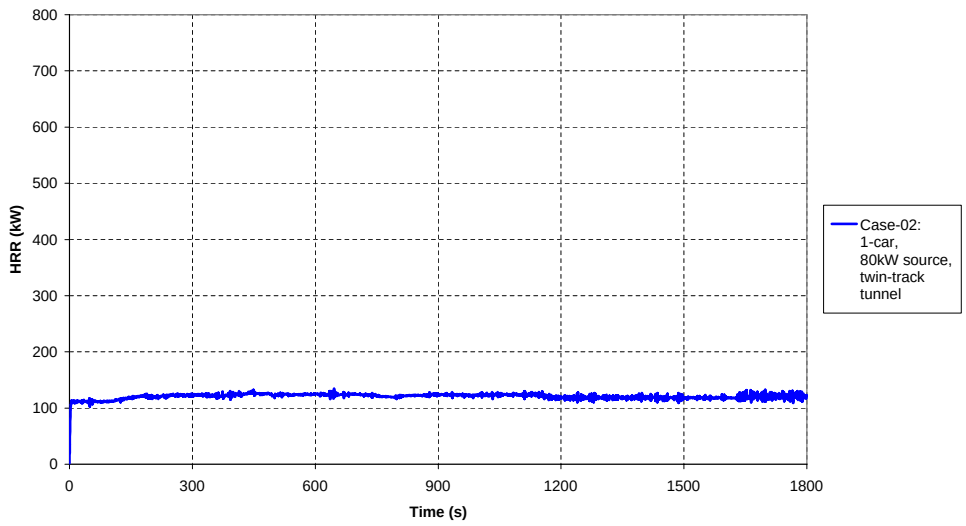

Figure 5.9: Heat release rate, 1-car, 80kW source, twin-track tunnel

Ignition

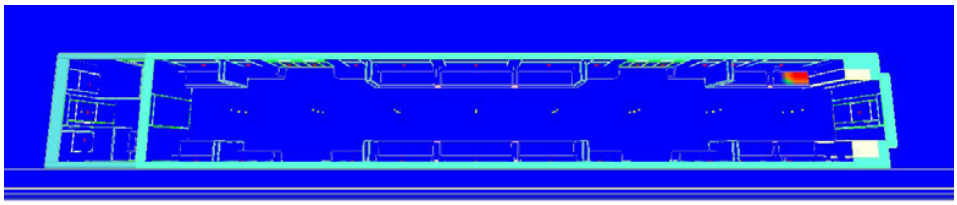

5 minutes

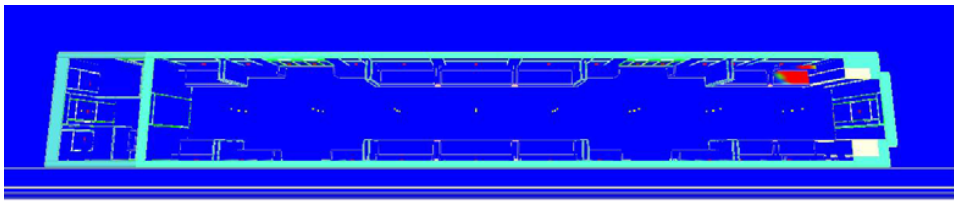

10 minutes

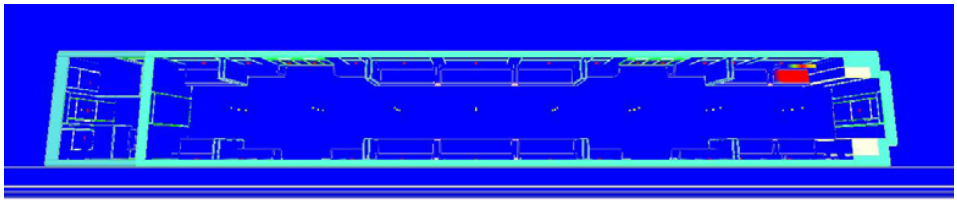

15 minutes

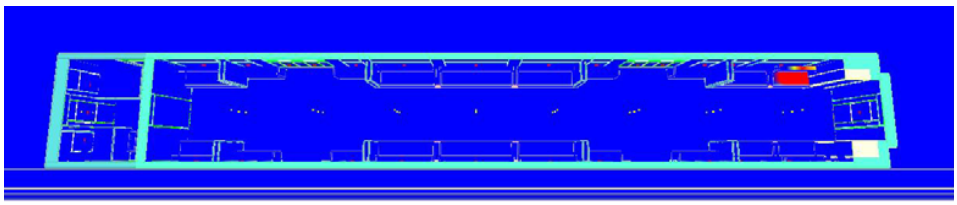

20 minutes

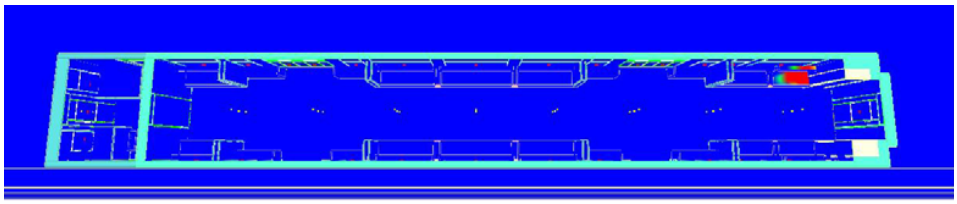

30 minutes

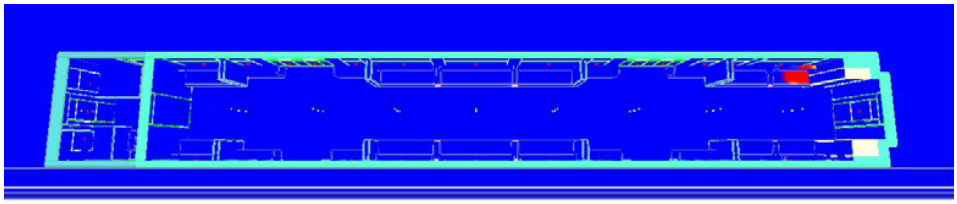

Figure 5.10: Fire spread, 1-car, 80kW source, twin-track tunnel

5.3.2 ONBOARD CONDITIONS

The results of the simulation of an incident, involving an 80kW ignition source, in a rolling stock in a twin-track tunnel show that the temperatures at 1.5m above the floor level exceed the 60°C limit within two minutes at the center of the incident carriage. The temperatures at the center of the carriage at 1.5m increases to 73°C during the course of the incident.

The smoke and hot gases, generated at incident location, tend to move upstream in the incident carriage away from the ignition source due to buoyancy forces and residual airflows. Although most of the smoke is ventilated effectively through the open side doors, a plume of smoke moves upstream and builds up a smoke layer between the driver's cab and the first set of side doors, until the steady state conditions are reached within the incident carriage. This smoke layer causes temperatures to increase to 86°C at 1.5m above the floor at that section of the carriage. The temperatures exceed the 60°C limit at 1.5m just after the first minute of the ignition, at a section between the driver's cab and the first set of side doors.

The predicted temperature variations at three points along the incident carriage at 1.5m above the floor level are given in Figure 5.11.

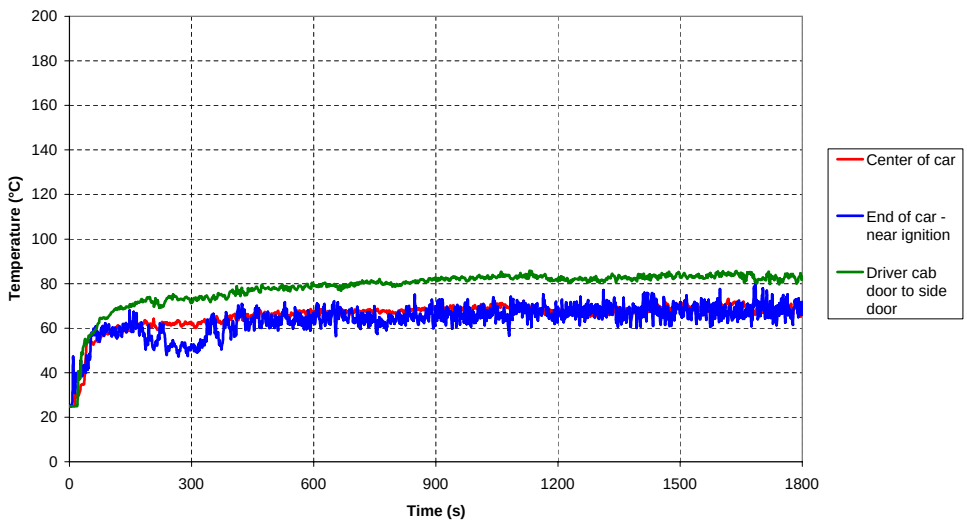

Figure 5.11: Case-02: Temperature variation at 1.5m above the floor level

The temperatures at seat level are predicted to be within the acceptability limit of 60°C in the entire carriage for this incident. The temperatures at 1.0m above the floor level are predicted to increase to 48°C, near the ignition source. An instantaneous increase of temperature at 1.0m is predicted at the section of incident carriage between the driver's cab and the first set of side doors, due to the plume of smoke moving upstream in the carriage, as discussed above. The predicted temperature variations in the incident carriage at 1.0m above the floor are given in Figure 5.12.

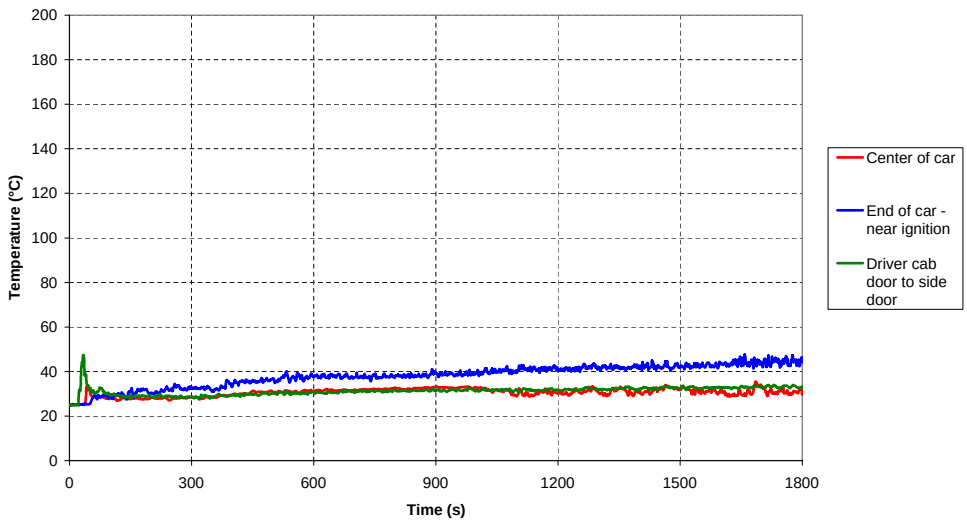

Figure 5.12: Case-02: Temperature variation at 1.0m above the floor level

The visibility levels at 1.5m in the incident carriage are predicted to drop below the acceptability level of 5m within the first minute from the ignition. During the course of the incident, an increase in the visibility at 1.5m near the ignition source is predicted. The change in visibility is due to the unsettled movement of smoke between the 4th and the 6th minute from the ignition. The effects of smoke movement within this interval is also apparent in the temperature variation. However, once the steady state conditions are reached, temperature and visibility levels remain constant for the rest of the incident.

The predicted visibility levels at 1.5m are given in Figure 5.13. It should be noted that the visibility levels are given only for 10 minutes of the incident, since the visibility levels drop below the acceptability level within this interval and remain constant for the rest of the incident.

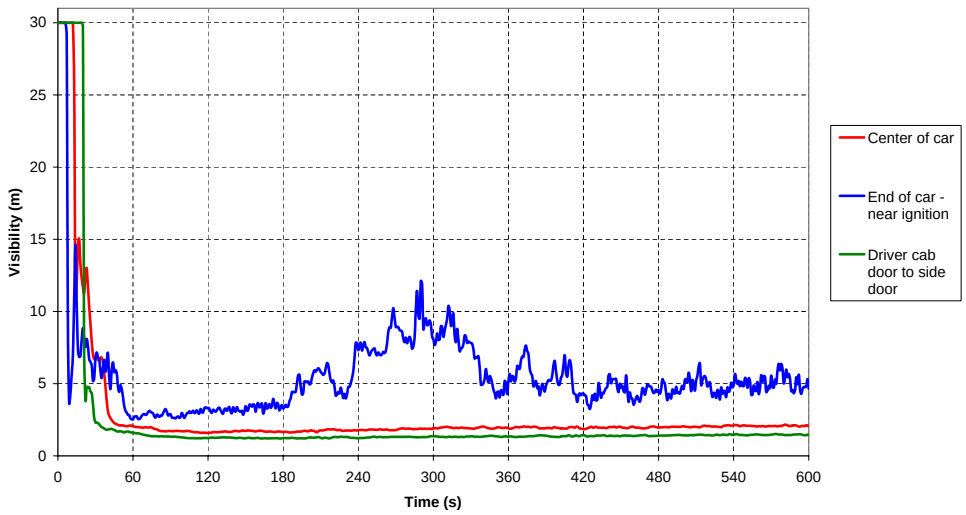

Figure 5.13: Case-02: Visibility variation at 1.5m above the floor level

The visibility at 1.0m above the floor level is predicted to be greater than 5m in the entire carriage for this incident. The simulation shows an exception within the first minute, where the visibility drops below 5m locally. However, the visibility levels remain above 11.5m from the 4th minute and onwards, as conditions converge towards the steady state. The predicted variation of visibility at 1.0m in the incident carriage is given in Figure 5.14. In Figure 5.14, variations for only the first 10 minutes of the incident are given, since the visibility levels remain above 5m for the rest of the incident.

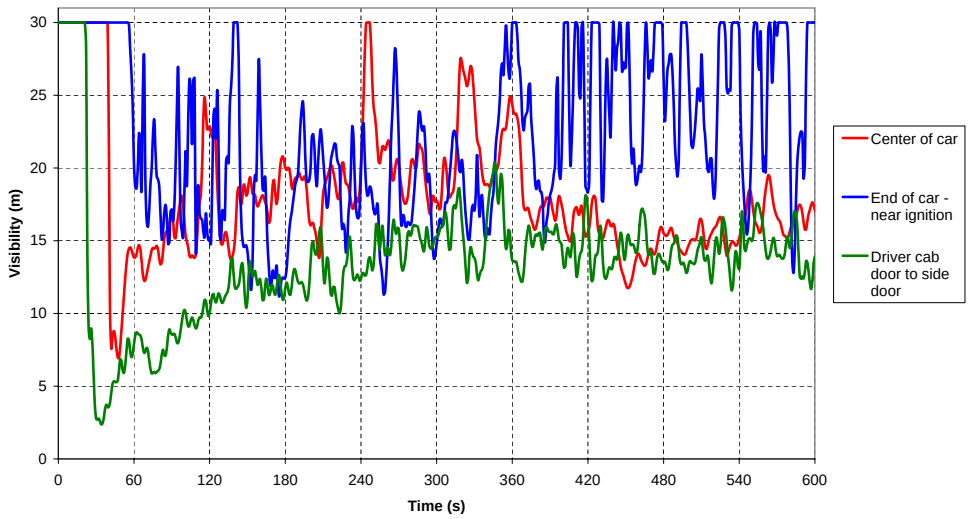

Figure 5.14: Case-02: Visibility variation at 1.0m above the floor level

The simulation shows that the instantaneous carbon-monoxide concentrations within the incident carriage at 1.5m above the floor level increase to about 175ppm near the ignition source, 280ppm at the center of the carriage, and about 380ppm at the section between the driver's cab and the first set of side doors. The average carbon-monoxide concentrations over the first 30 minutes are predicted to be 95ppm, 200ppm, and 305ppm at respective locations given above. The predicted carbon-monoxide concentrations are within the tenability limits at most of the incident carriage for the first 30 minutes.

The exception is predicted adjacent to the driver's cab door. However, the carbon-monoxide concentrations are within the tenability criterion when averaged over the first 15 minutes. The predicted variation of carbon-monoxide concentrations at 1.5m in the incident carriage is given in Figure 5.15.

The simulation shows that the carbon-monoxide concentration at 1.5m above the floor level at the section of incident carriage close to the driver's cab door is higher than the values predicted closer to the ignition source at the same height. This is predicted since the buoyancy forces and residual airflows move the smoke and toxic gases away from the ignition location. This causes thicker smoke layer being built up closer to the driver's cab door, due to relatively stagnant airflows in that section. This is also observed in the slice of carbon-monoxide distribution at a longitudinal section through the center of the carriage, as shown in Figure B.6 in Appendix B.

The carbon-monoxide concentration at higher levels, i.e. at heights closer to the ceiling level, are predicted to be higher near the ignition source, as expected.

It should be noted that although the carbon-monoxide concentrations at 1.5m above the floor level could be judged as within the tenability limits, the final decision on the tenability should be made in conjunction with the temperature predictions.

The carbon-monoxide concentrations at seat level are predicted to be within the acceptability criterion for the entire carriage. The predicted variations of carbon-monoxide concentrations at 1.0m above the floor level are given in Figure 5.16.

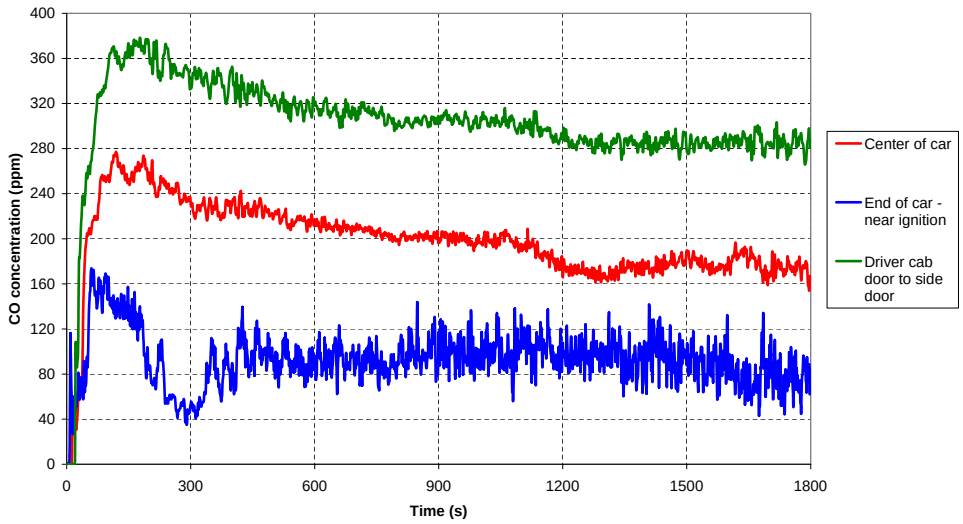

Figure 5.15: Case-02: Carbon-monoxide concentration at 1.5m above the floor level

The temperature, visibility and carbon-monoxide slices on a longitudinal section through the center of the carriage are given in Figures B.4 to B.6 in Appendix B.

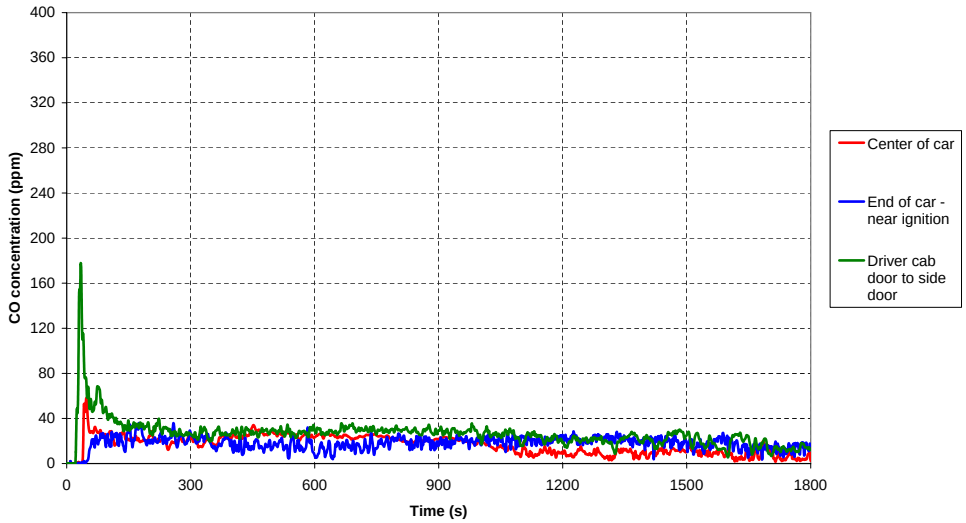

Figure 5.16: Case-02: Carbon-monoxide concentration at 1.0m above the floor level

5.4 CASE-03: 4-CAR, 80kW SOURCE, SINGLE-TRACK TUNNEL

The fire incident due to 80kW arson ignition source is also simulated in the 4-car train, incorporating open wide gangways, in the single-track tunnel. In this case, open wide gangways allow smoke to be exchanged between the incident carriage and the adjacent carriages. In this particular case, the ventilation of smoke and evacuation of passengers will be through the end doors at both front and the back of the train.

5.4.1 FIRE DEVELOPMENT

The simulation shows that the fire is localized around the ignition source, and would not spread to the incident carriage or to the adjacent carriages. It is predicted that fire only spreads to the adjacent seat in the premises of the initial ignition location.

The peak heat release rate for this incident is predicted to be 125kW. The predicted heat release rate variation for this incident is shown in Figure 5.17.

The fire development for this incident, illustrated with the burning rate of the combustible surfaces, involving an 80kW ignition source in the 4-car model in the single-track tunnel is given in Figure 5.18.

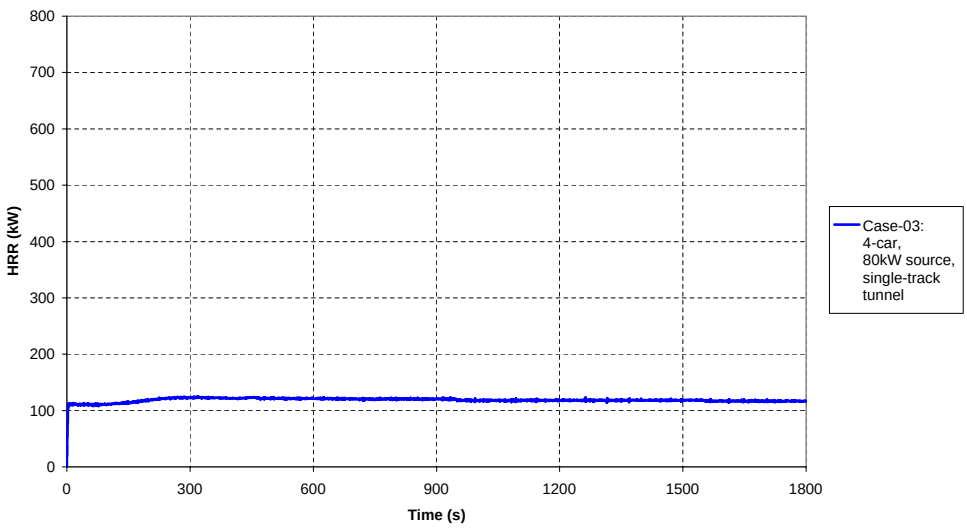

Figure 5.17: Heat release rate, 4-car, 80kW source, single-track tunnel

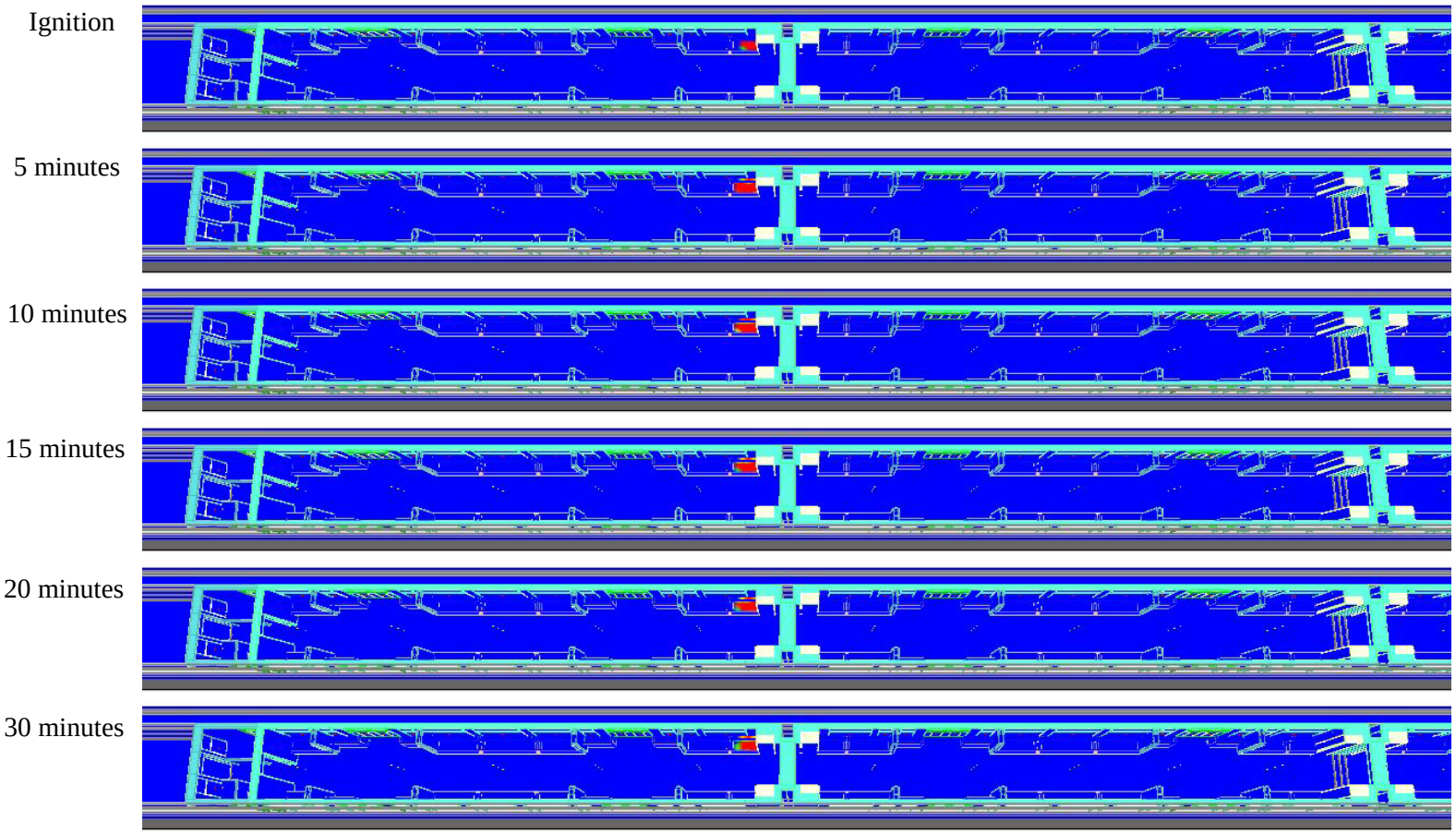

Figure 5.18: Fire spread, 4-car, 80kW source, single-track tunnel

5.4.2 ONBOARD CONDITIONS

The simulation, incorporating an 80kW ignition source in the 4-car rolling stock in a single-track tunnel, shows that the temperature at the center of the incident carriage at 1.5m above the floor level exceeds the 60°C limit within the first minute from the ignition. In this incident, the smoke is ventilated through the end door of the incident carriage. However, the amount of smoke generated is greater than the amount extracted from the end door. Consequently, a plume of smoke moves to the adjacent carriages through open wide gangways.

The dispersion of smoke changes the onboard conditions in the adjacent carriage and in the rest of the rolling stock. The temperature at 1.5m above the floor level at the center of the carriage, adjacent to the incident, is predicted to exceed 60°C at 8 minutes. The temperature at the same height at the center of third carriage exceeds the acceptability criterion at 27 minutes from the ignition. The temperature is predicted to remain below 60°C at the center of last carriage, which is the farthest away from the incident, within the simulated time interval.

The predicted temperature variations at the center of each carriage at 1.5m above the floor level are given in Figure 5.19.

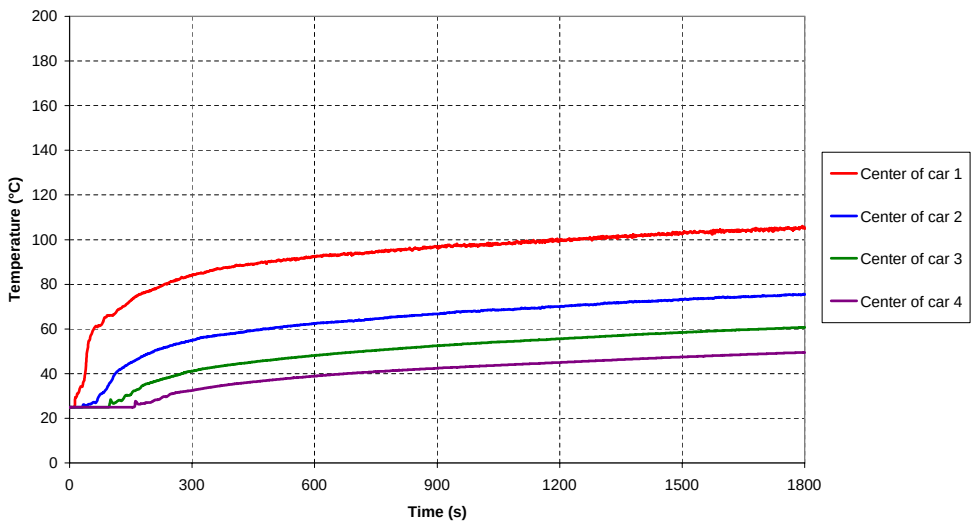

Figure 5.19: Case-03: Temperature variation at 1.5m above the floor level

The temperature at seat level in the incident carriage is predicted to exceed 60°C at the 21st minute from the ignition. The simulation shows that temperatures remain below the acceptability criterion at 1.0m in the rest of the rolling stock within the first 30 minutes. The temperatures increase to 52°C at the center of the carriage, adjacent to the incident, measured at 1.0m above the floor level. The variations of temperature at 1.0m above the floor level at the center of each carriage are given in Figure 5.20.

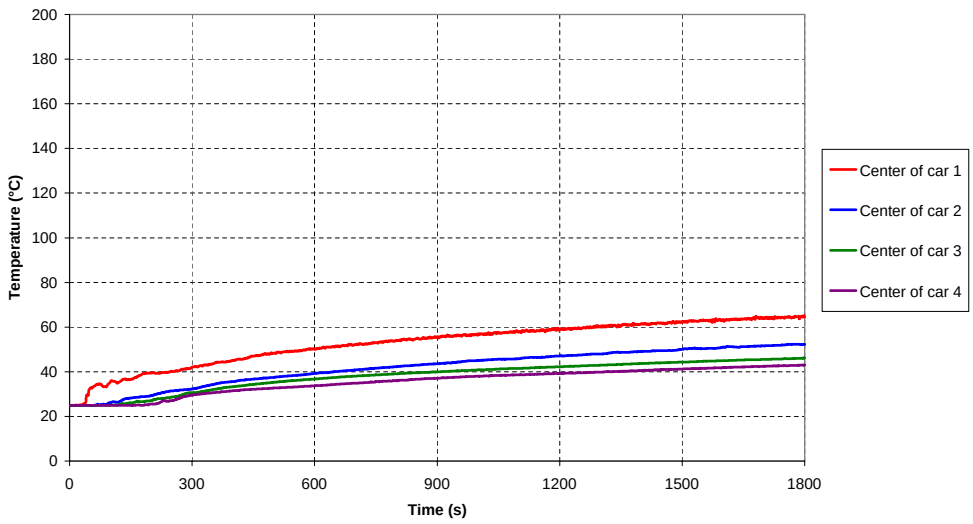

Figure 5.20: Case-03: Temperature variation at 1.0m above the floor level

The simulation shows that the visibility level at 1.5m above the floor level at the center of the incident carriage drops below the recommended value of 5m within the first minute from the ignition. It is predicted that the visibility levels at 1.5m at the center of the carriages in the rest of the rolling stock drop gradually as the smoke disperses and builds up layers in each carriage.

The visibility levels are predicted to drop below 5m within one minute intervals between the successive carriages. Consequently, the visibility at the specified height at the center of the carriage, adjacent to the incident, drops below 5m within two minutes. The visibility drops below the acceptability criterion within the third and the fourth minutes at the center of the third and the fourth carriages, respectively.

The predicted visibility levels at 1.5m are given in Figure 5.21. It should be noted that the visibility levels are given only for 10 minutes of the incident, since they drop below the acceptability level within this interval and remain constant for the rest of the incident.

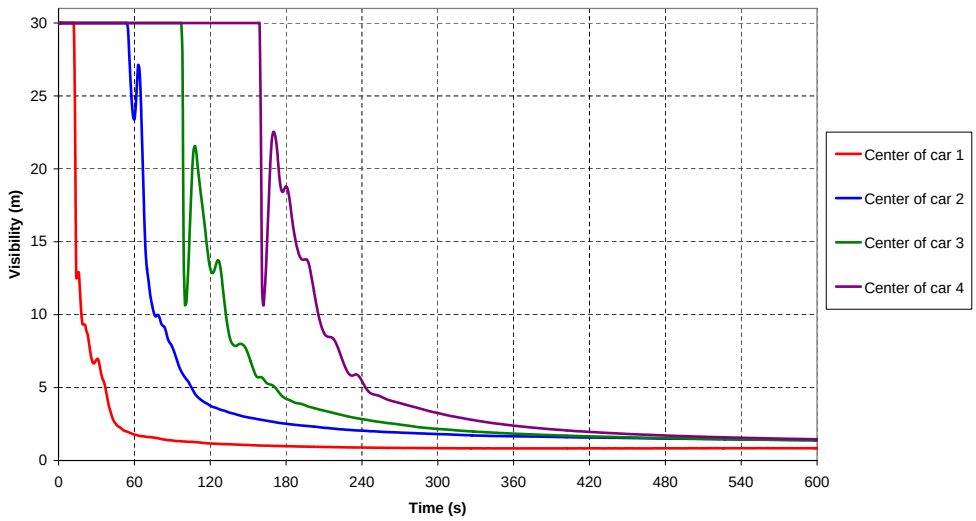

Figure 5.21: Case-03: Visibility variation at 1.5m above the floor level

The simulation shows that the visibility drops below 5m just after the first minute from the ignition at 1.0m above the floor level at the center of the incident carriage. The dispersion of smoke causes visibility to drop within the entire rolling stock. The visibility is predicted to drop below 5m in the rest of rolling stock within the first 5 minutes from the ignition. The predicted variations of visibility at 1.0m at the center of the carriages are given in Figure 5.22.

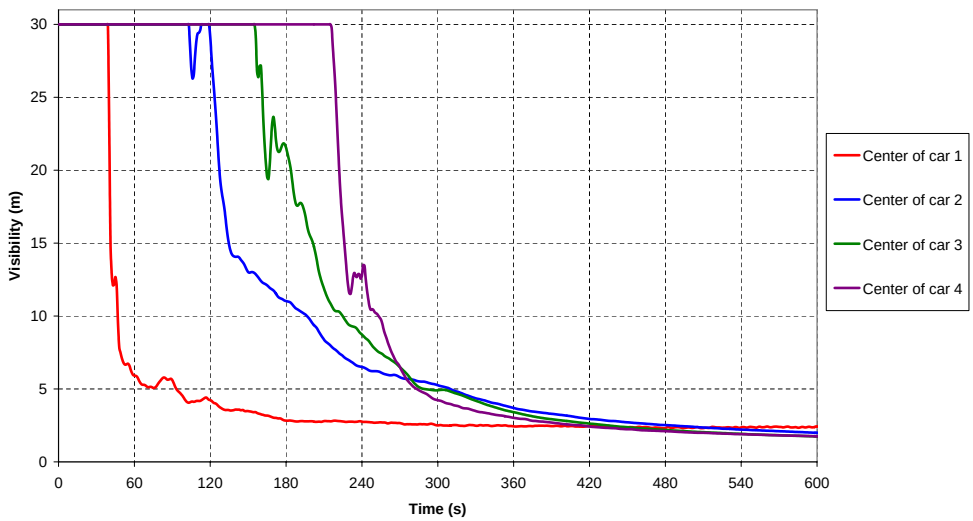

Figure 5.22: Case-03: Visibility variation at 1.0m above the floor level

It is predicted from the simulation that the carbon-monoxide concentration at 1.5m above the floor level at the center of the incident carriage increases to 595ppm during this incident. Although the carbon-monoxide level at the specified height is found to be well below the fatality limit, when the concentration is averaged over the 15 minute and 30 minute intervals, the values exceed the incapacitation limits defined by the standards [28]. The carbon-monoxide concentration at 1.5m above the floor level at the center of the incident carriage is predicted to be 510ppm and 540ppm, when averaged over 15 minutes and 30 minutes, respectively.

The carbon-monoxide concentrations at 1.5m above the floor level at the center of the remaining carriages are predicted to increase to about 365ppm during the incident. The concentrations averaged over the 30 minutes vary between 275ppm to 295ppm, lowest being in the farthest carriage. Although these values exceed marginally the defined acceptability limit for 30 minutes, once they averaged over the 15 minute interval they indicate tenable conditions.

The carbon-monoxide concentrations predicted at 1.5m at the center of the carriages are given in Figure 5.23.

The carbon-monoxide concentration at 1.0m above the floor level at the center of the incident carriage is predicted to increase to about 190ppm. The open end door assists ventilation of smoke in the incident carriage, and keeps carbon-monoxide concentrations within the acceptability limits at 1.0m height, measured from the floor level.

The simulation shows that the maximum carbon-monoxide concentration levels in the rest of the rolling stock at 1.0m above the floor level vary between 300ppm to 325ppm. Once averaged over the 30 minute interval, carbon-monoxide concentrations at the center of the carriages are predicted to change between 215ppm and 235ppm. It can be stated that some of the predicted average concentrations marginally exceed the acceptability criterion of 225ppm for a period of 30 minutes. However, one can also conclude that the conditions are within the tenability limits just below the 1.0m height, measured from the floor level, in terms of carbon-monoxide concentrations.

The carbon-monoxide concentrations predicted at 1.0m at the center of the carriages are given in Figure 5.24.

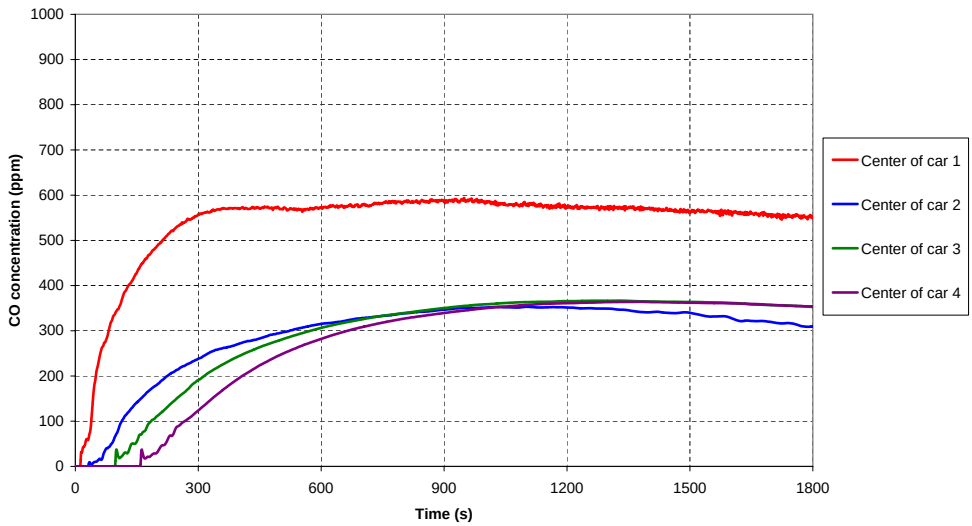

Figure 5.23: Case-03: Carbon-monoxide concentration at 1.5m above the floor level

The temperature, visibility and carbon-monoxide slices on a longitudinal section through the center of the rolling stock are given in Figures B.7 to B.9 in Appendix B.

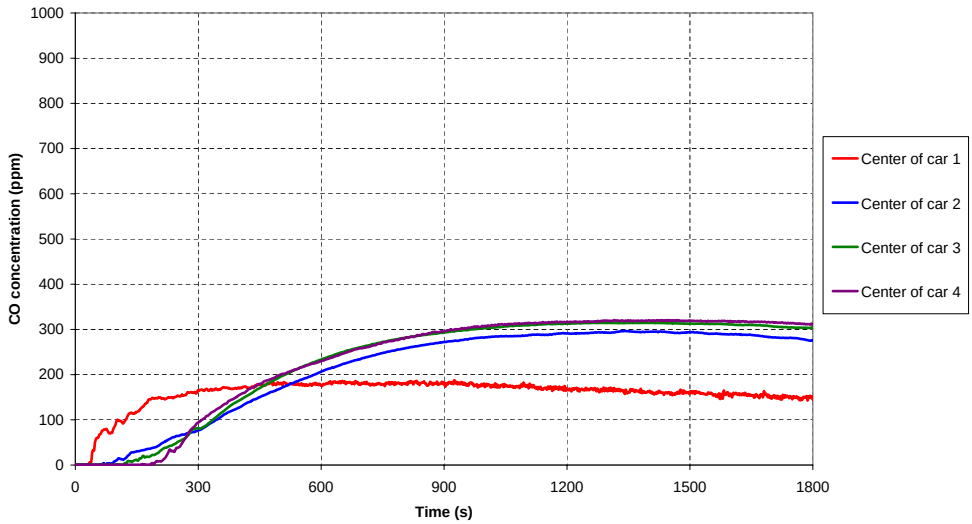

Figure 5.24: Case-03: Carbon-monoxide concentration at 1.0m above the floor level

5.5 CASE-04: 4-CAR, 80kW SOURCE, TWIN-TRACK TUNNEL

The arson fire ignition source, releasing 80kW of heat to its surroundings for 30 minutes, is also simulated using the 4-car model, incorporating open wide gangways, in the twin-track tunnel section. As mentioned previously, for an incident in the twin-track tunnel, side doors are defined to be open for smoke ventilation and passenger evacuation. This case is labelled as Case-04 in this thesis.

5.5.1 FIRE DEVELOPMENT

The simulation of fire development and flame spread shows that only the combustible seats adjacent to the ignition location are involved in the fire. It is predicted that burning takes place locally over few seats, and the floor would not be involved in the fire. The peak heat release rate for this incident is predicted to be 135kW.

The predicted heat release rate variation for this incident is shown in Figure 5.25.

The fire development for this incident, illustrated with the burning rate of the combustible surfaces, involving an 80kW ignition source in the 4-car model in the twin-track tunnel is given in Figure 5.26.

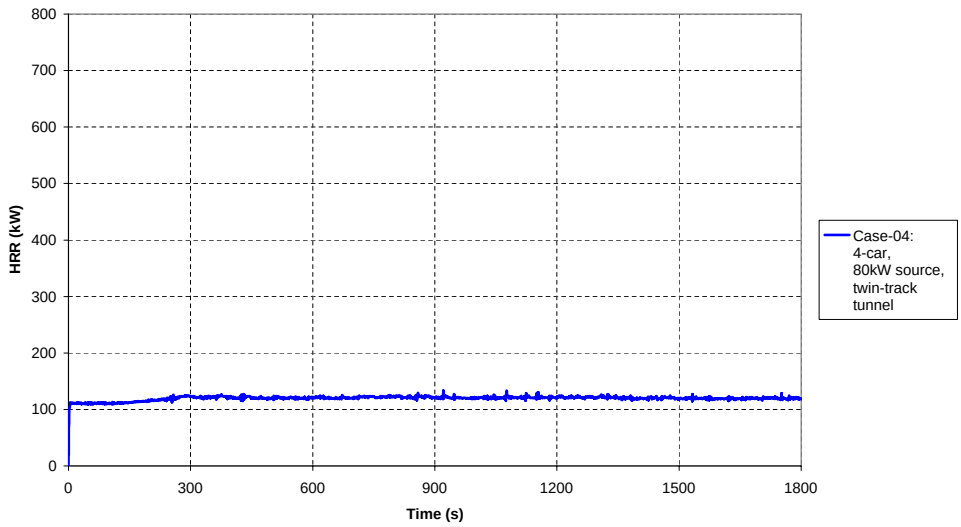

Figure 5.25: Heat release rate, 4-car, 80kW source, twin-track tunnel

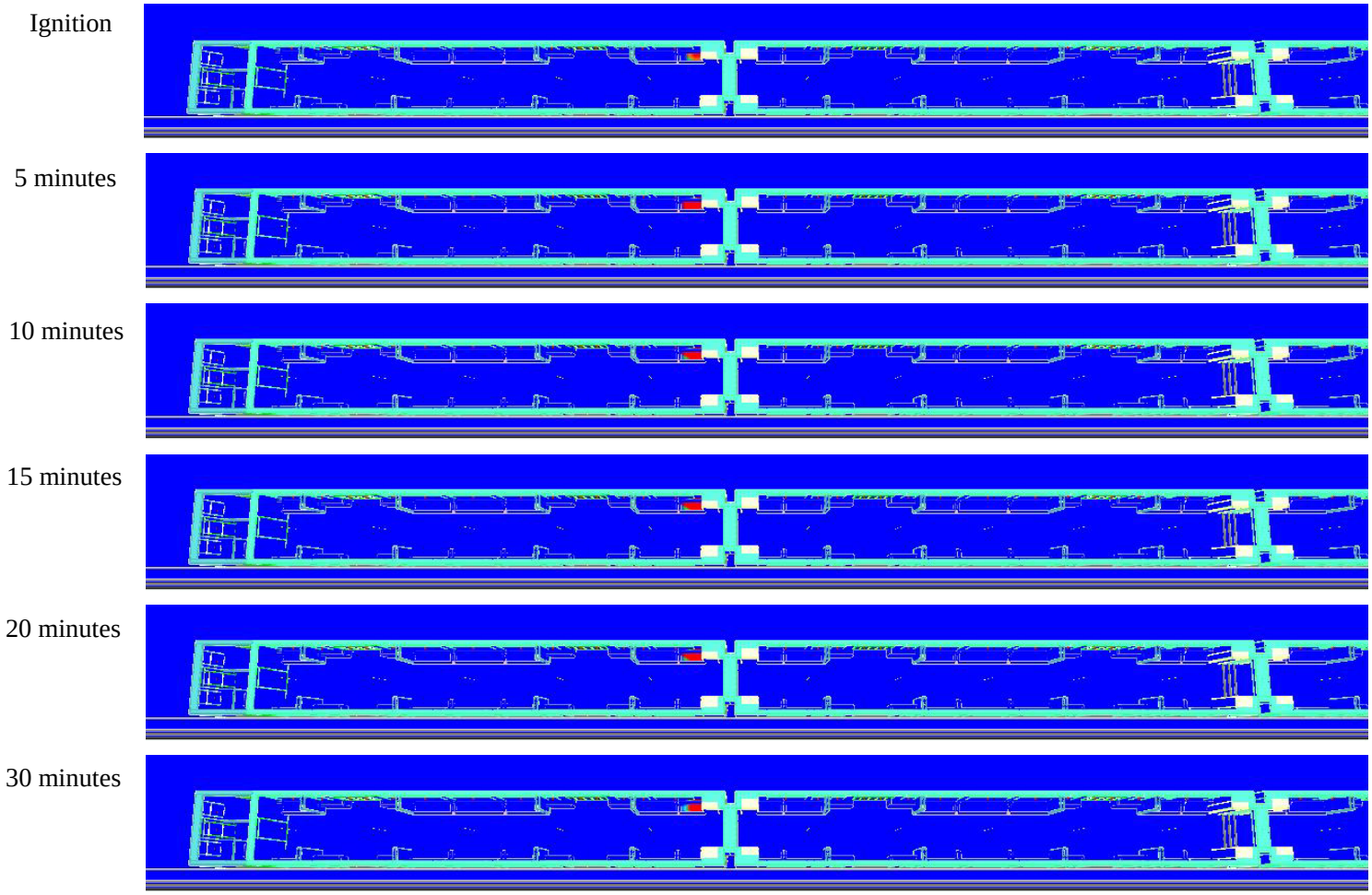

Figure 5.26: Fire spread, 4-car, 80kW source, twin-track tunnel

5.5.2 ONBOARD CONDITIONS

The simulation incorporating an 80kW ignition source in the 4-car rolling stock with open wide gangways and open side doors shows that the smoke and hot gases generated during the fire incident are very well ventilated. The temperature at 1.5m at the center of the incident carriage is predicted to increase to 62°C, marginally exceeding the acceptability criterion of 60°C. The temperatures at the same height at the center of the remaining carriages are found to be less than 35°C, which corresponds to 10°C above the initial air temperature defined within the rolling stock.

The peak temperature at 1.0m above the floor level at the center of the incident carriage is predicted to be about 38°C within the first 30 minutes from the ignition. Temperatures at 1.0m at the center of the remaining carriages are predicted to increase only slightly from the defined initial air temperature. The temperatures at the center of the remaining carriages are found to be less than 28°C.

The predicted variations of temperature at the center of the carriages at 1.5m and 1.0m above the floor level are given in Figures 5.27 and 5.28, respectively.

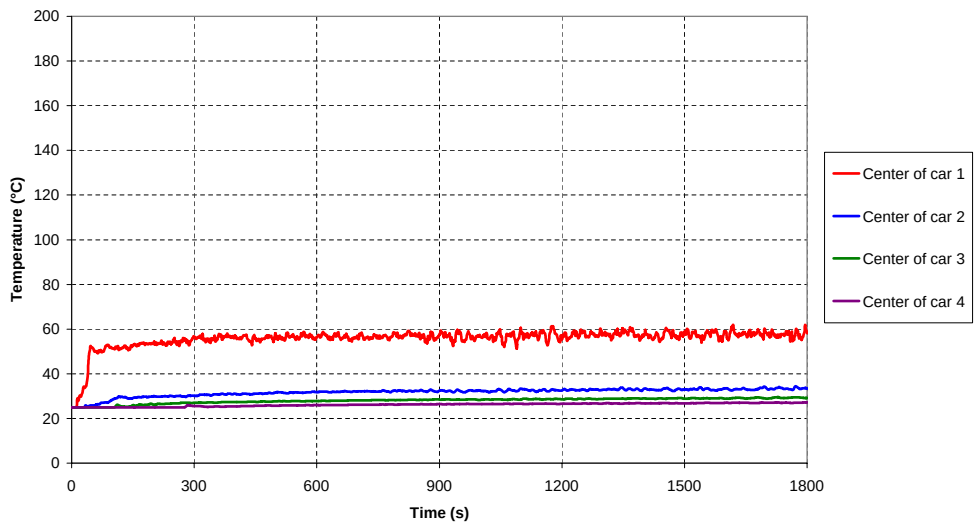

Figure 5.27: Case-04: Temperature variation at 1.5m above the floor level

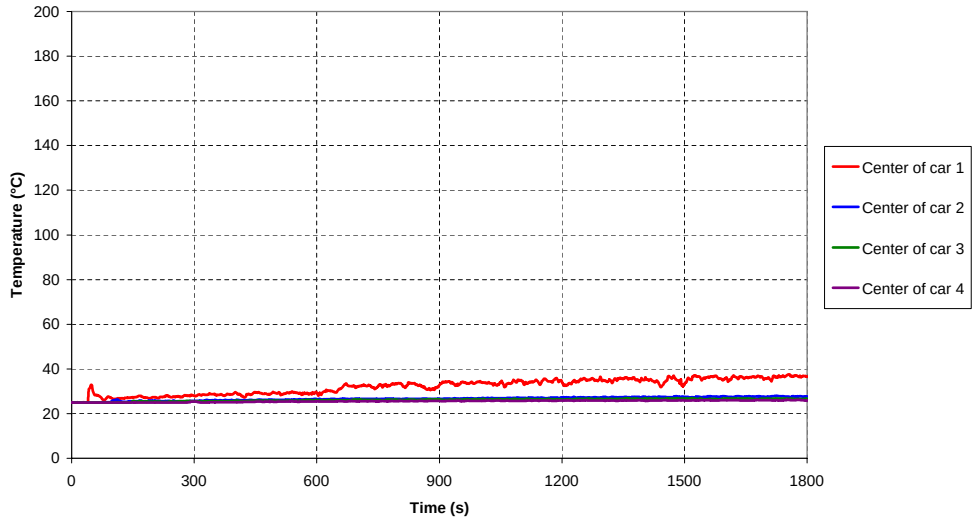

Figure 5.28: Case-04: Temperature variation at 1.0m above the floor level

The simulation shows that the visibility at 1.5m at the center of the incident carriage drops below the recommended value of 5m within the first minute from the ignition. The visibility levels at the same height at the center of the remaining carriages are found to remain above 6.1m during the first 30 minutes of the incident. The minimum visibility is predicted at the 26th minute, as the thickness of the smoke layer marginally increases after the 20th minute from the ignition.

It is predicted from the simulation results that the visibility at 1.0m above the floor level at the center of the carriages remains above 5m during the first 30 minutes of the incident. A drop of visibility is predicted within the first minute at the center of the incident carriage. However, higher visibility levels are restored, once the airflow distribution within the rolling stock is stabilized. A minimum visibility level of 10.3m is predicted at the center of the fourth carriage at the 29th minute of this incident.

The predicted variations of visibility at the center of the carriages at 1.5m and 1.0m above the floor level are given in Figures 5.29 and 5.30, respectively. It should be noted that only the first 10 minutes are shown in the figures, since they reflect the general trend of the variations.

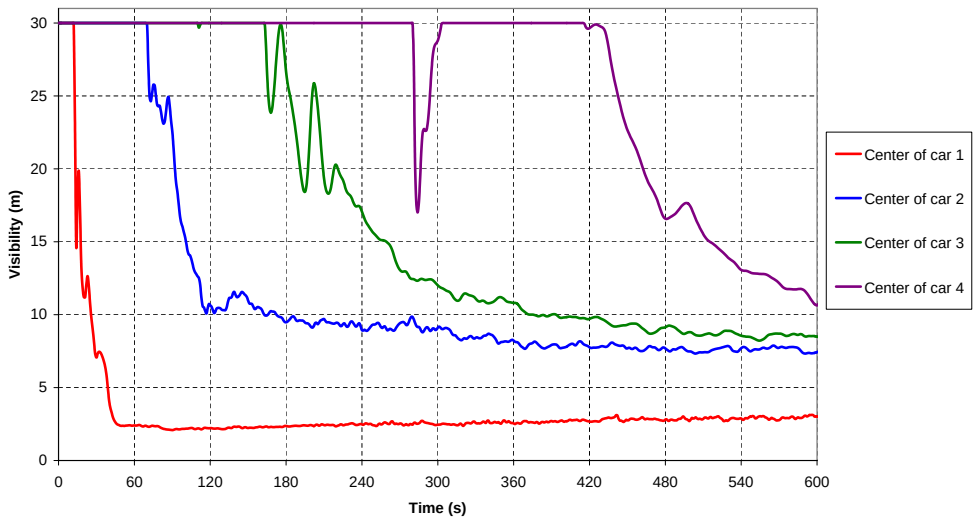

Figure 5.29: Case-04: Visibility variation at 1.5m above the floor level

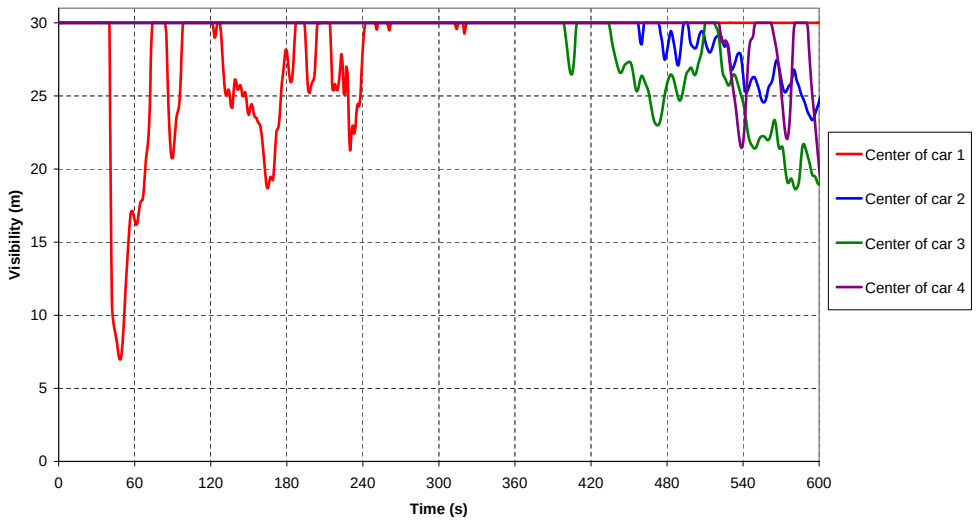

Figure 5.30: Case-04: Visibility variation at 1.0m above the floor level

The simulation results show that the carbon-monoxide concentration at 1.5m above the floor level at the center of the incident carriage increases to 210ppm during this incident. The carbon-monoxide concentration is found to be 140ppm when averaged over the 30 minute interval. It can be concluded that the predicted carbon-monoxide concentrations are well below the acceptability criterion of 225ppm over the first 30 minutes of the incident at 1.5m height, measured from the floor level.

The carbon-monoxide concentrations at 1.0m at the center of the carriages are predicted to remain below 40ppm. The exception is predicted at the center of the incident carriage within the first minute, where the concentration increases to 60ppm. The concentrations are very well below the incapacitation limits given by the standards [28].

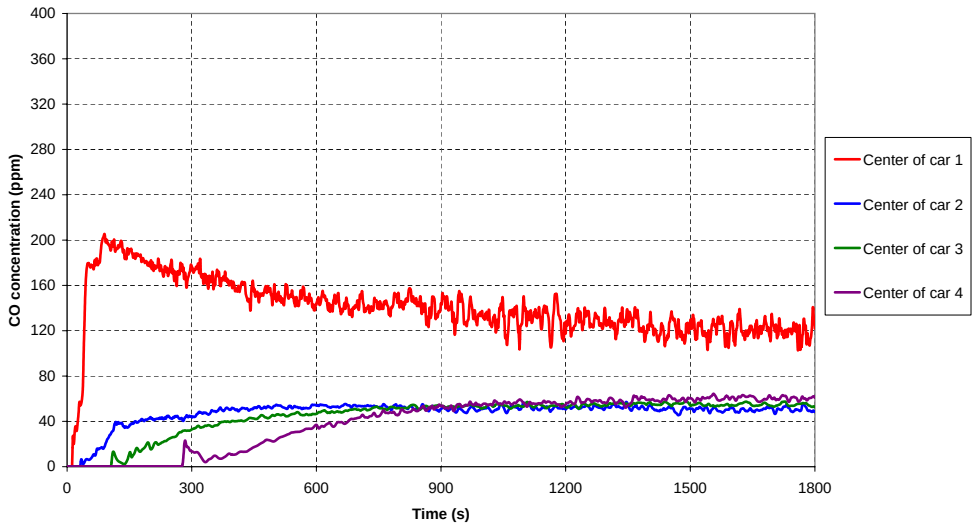

Figure 5.31: Case-04: Carbon-monoxide concentration at 1.5m above the floor level

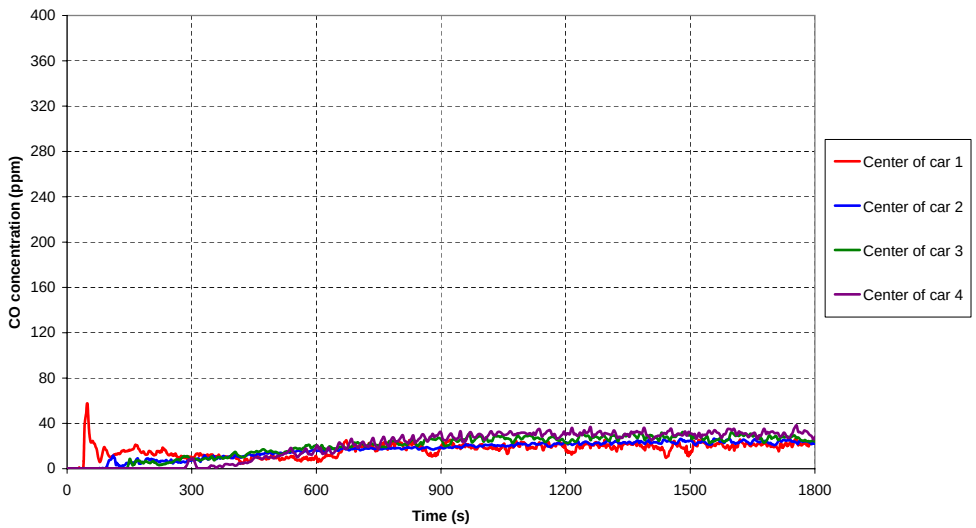

Figure 5.32: Case-04: Carbon-monoxide concentration at 1.0m above the floor level

The temperature, visibility and carbon-monoxide slices on a longitudinal section through the center of the rolling stock are given in Figures B.10 to B.12 in Appendix B.

5.6 CASE-05: 1-CAR, 1.5MW SOURCE, SINGLE-TRACK TUNNEL

The first of the baggage fire incidents is simulated with 1-car model in a single-track tunnel. The ignition source is placed on floor opposite end of the carriage from the driver cab. As in the case of arson fire incident, it is assumed that the end door close to the ignition source is inaccessible, therefore defined to be closed during the entire duration of the simulation. Consequently, this case assumes only the driver cab door is open for evacuation of passengers and ventilation of fire.

5.6.1 FIRE DEVELOPMENT

5mins: The fire starts to develop in the carriage and the seats adjacent to the ignition source are involved in fire.

The high temperature smoke and gases from the fire accumulated at ceiling level within the carriage could not be ventilated effectively due to the limited opening area. Therefore, the hot layer develops and starts to ignite the rest of the seats in the incident carriage.

8mins: It has been predicted from the results that between 7th and 8th minute, the pairs of windows, on both sides of the carriage, closest to the ignition source fail due to high temperature inside the incident carriage.

10mins: All the seats in the incident carriage are involved in the fire development, and the fire has started to propagate on the floor.

15mins: The window of the detrainment door, close to the ignition source, fails just before the 15th minute from the ignition. At 15 minutes and shortly after, the entire floor is involved in the fire development.

16mins: At 16th minute, the conditions for flashover are achieved and it has been predicted from the simulation that all the combustible surfaces in the incident carriage, except a pair of burnt-out seats, are involved in fire. This results in a rapid increase in the predicted heat release rate. (See Figure 5.33)

The peak heat release rate for this case is predicted to be 6.0MW. The peak heat release rate is predicted to remain constant for about 2 minutes.

It has been predicted from the results that between 16th and 17th minute, three pairs of windows at the central section of the incident carriage fail as the predefined temperature criterion has reached.

In the following minute, the windows adjacent to the side doors and the windows of the side doors close to the ignition source fail due to high temperature within the incident carriage. This introduces additional openings for heat and smoke extract.

18mins: After 18th minute, the fire loses its intensity as all the combustible items start to burn-out. The simulation shows that in the following two minutes, most of the seats are burnt-out, and the fire on floor reduces to a localized area between the side doors close to the ignition source. In conjunction with these occurrences, a steep decrease in heat release rate is predicted after the 18th minute from the ignition.

The fire development in the incident carriage, illustrated with the burning rate of the combustible surfaces, is given in Figure 5.34.

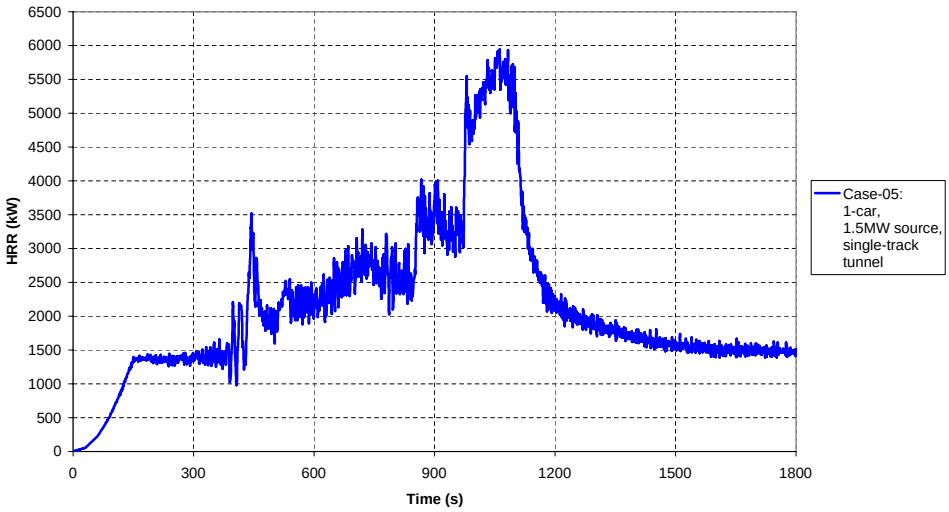

Figure 5.33: Heat release rate, 1-car, 1.5MW source, single-track tunnel

Ignition

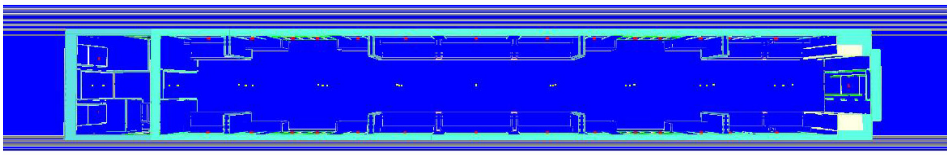

5 minutes

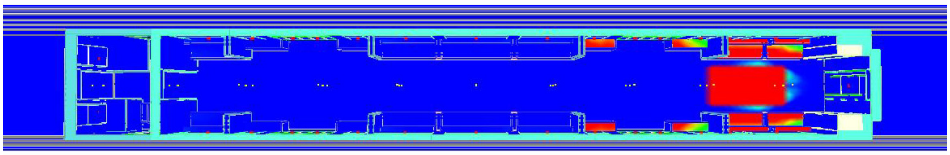

10 minutes

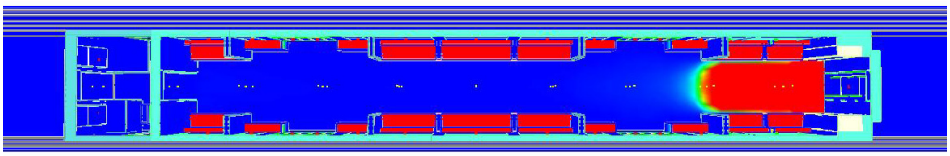

15 minutes

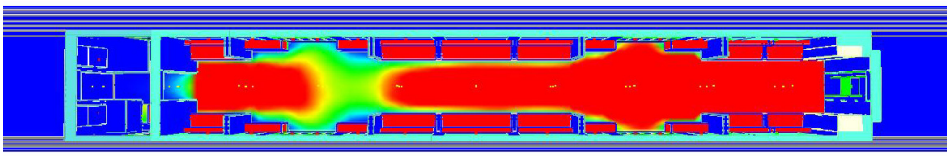

20 minutes

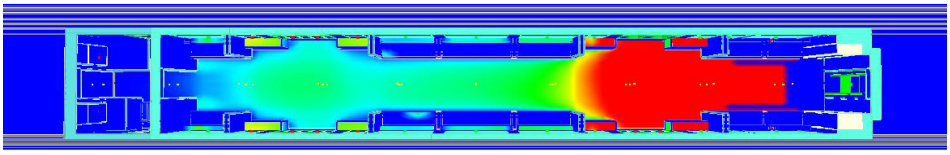

30 minutes

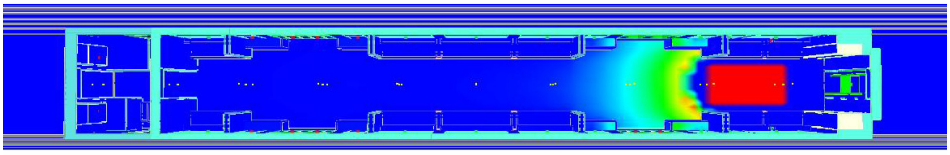

Figure 5.34: Fire spread, 1-car, 1.5MW source, single-track tunnel

The fire development during this incident and prediction of flashover conditions are further discussed in Sub-section 5.10.

The energy released during this incident is estimated through the calculation of area under the time history curve of heat release rate using the Trapezoidal Rule with 1.0s intervals. The energy released during this incident is calculated to be 3.9GJ.

5.6.2 ONBOARD CONDITIONS

For an incident in the single-track tunnel, the heat and smoke from the fire is ventilated through the open end door. The limited smoke extract area with rapidly growing ignition source results in untenable conditions in the incident carriage fairly quickly.

It is predicted from the simulation that the temperature at the center of the carriage exceeds the 60°C limit just after the first minute at 1.5m above the floor, and within 1.5 minutes at seat level. The temperatures in the incident carriage are predicted to exceed 600°C at the onset of flashover. The peak temperatures increase to about 1100°C above the ignition source during flashover period. Then the temperatures in the carriage decrease as the fire loses its intensity. The temperature variations at three points along the carriage are given in Figures 5.35 and 5.36, at 1.5m and 1.0m above the floor level, respectively.

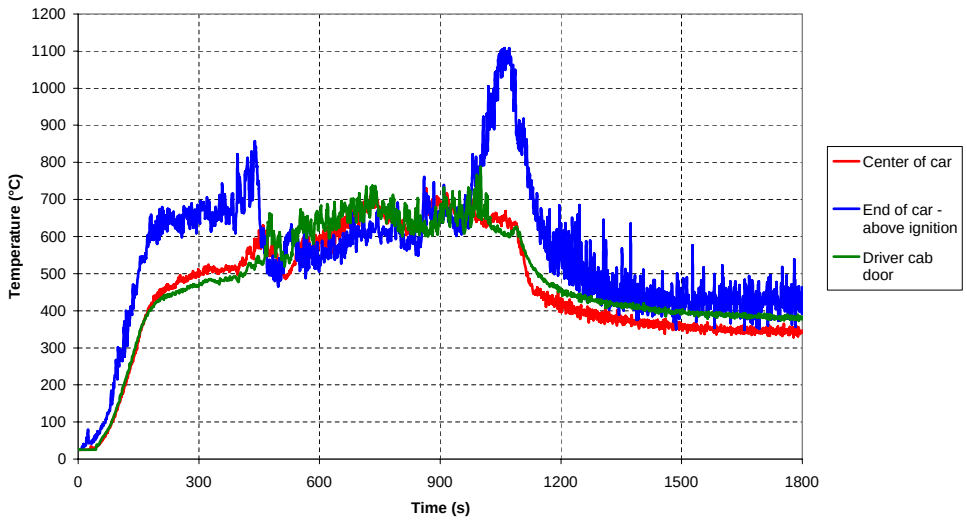

Figure 5.35: Case-05: Temperature variation at 1.5m above the floor level

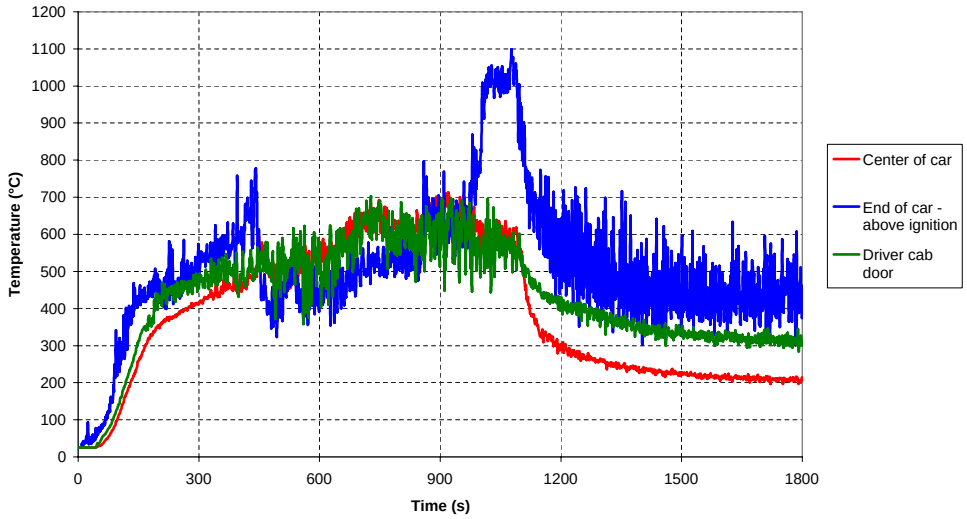

Figure 5.36: Case-05: Temperature variation at 1.0m above the floor level

The simulation shows that the visibility drops below 5m within the first minute at 1.5m above the floor level at the center of the carriage. The visibility at seat level is predicted to drop to 5m just after the first minute from the ignition. Although the loss of visibility does not directly cause fatalities, the parameter can be used as an indication of how quickly the carriage is filled with smoke produced from the fire. The variations of visibility at 1.5m and 1.0m above the floor level are given in Figures 5.37 and 5.38, respectively. The figures are given only for five minutes from the ignition since once the visibility is vanished in the incident carriage, it has not been recovered even though some of the windows fail during the course of the incident.

It is predicted from the simulation that the carbon-monoxide concentration in the incident carriage exceeds the limiting value of 2000ppm between 2 and 2.5 minutes from the ignition. This concentration of carbon-monoxide is reported to be the fatality limit for passengers, even for few seconds of exposure, in the published standards [28].

The variations of carbon-monoxide concentration at 1.5m and 1.0m above the floor level are given in Figures 5.39 and 5.40, respectively. The figures are given only for five minutes from the ignition since the limiting value for the passengers' life safety has been reached within this time interval.

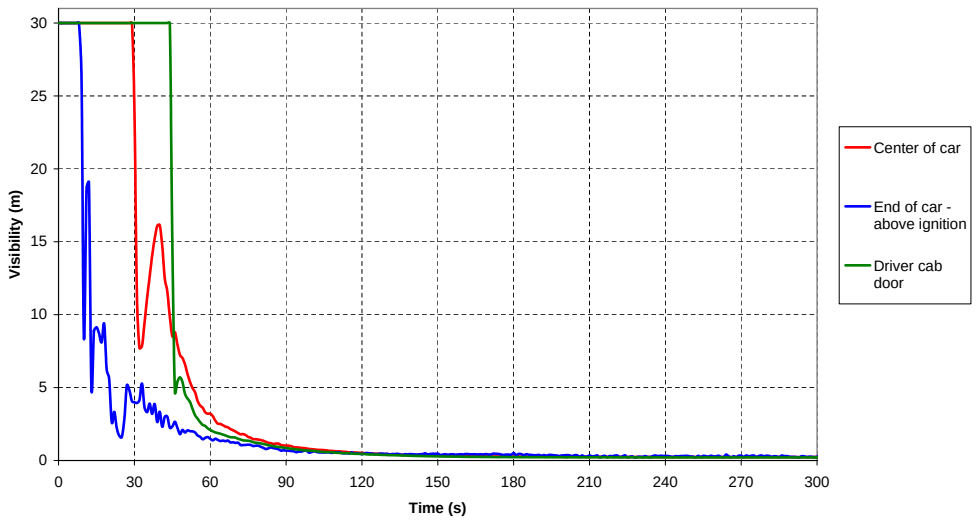

Figure 5.37: Case-05: Visibility variation at 1.5m above the floor level

The reported values of temperature and carbon-monoxide concentration within the incident carriage confirm that the 1.5MW ignition source is too severe for assessing the onboard conditions for passenger life safety.

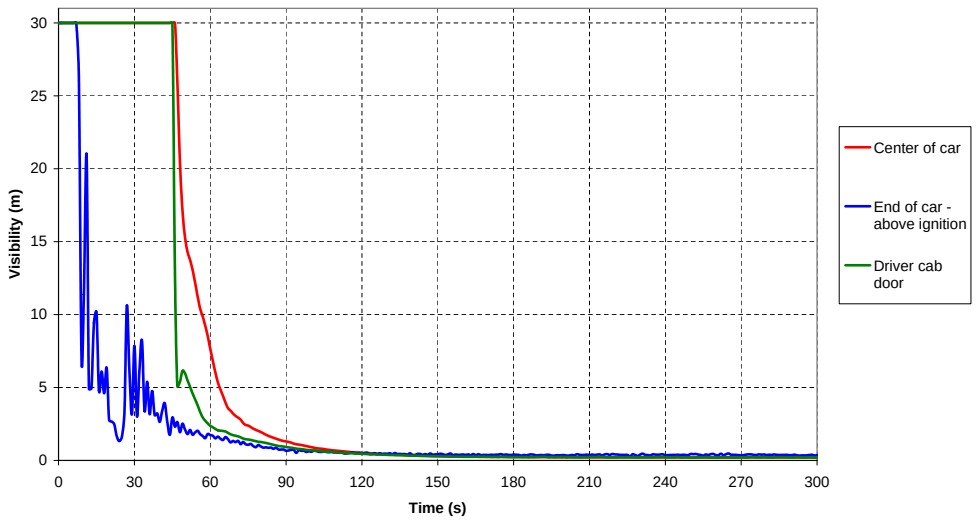

Figure 5.38: Case-05: Visibility variation at 1.0m above the floor level

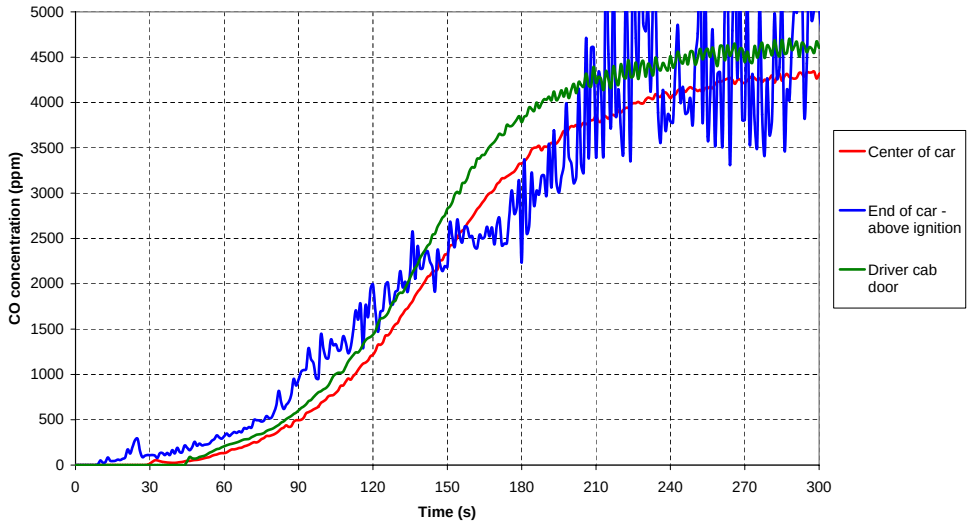

Figure 5.39: Case-05: Carbon-monoxide concentration at 1.5m above the floor level

The temperature, visibility and carbon-monoxide slices on a longitudinal section through the center of the carriage are given in Figures B.13 to B.15 in Appendix B.

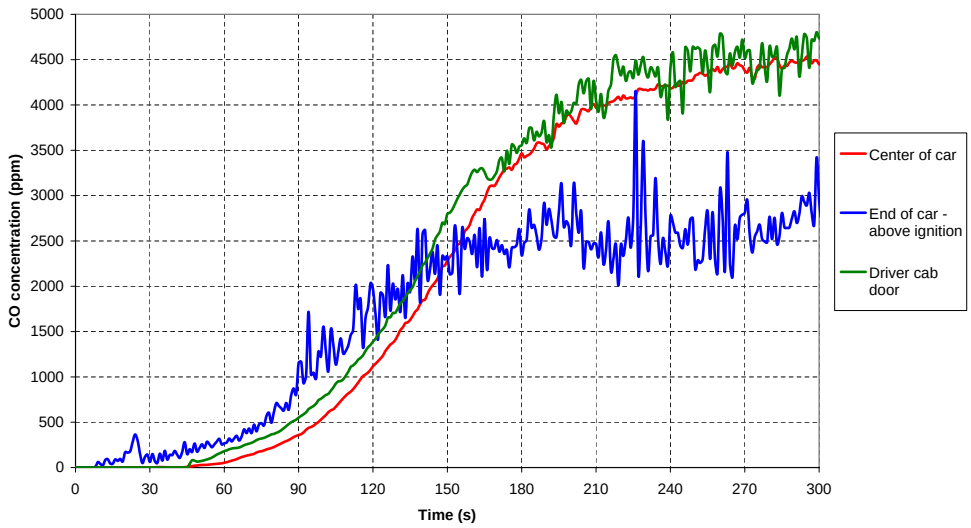

Figure 5.40: Case-05: Carbon-monoxide concentration at 1.0m above the floor level

5.7 CASE-06: 1-CAR, 1.5MW SOURCE, TWIN-TRACK TUNNEL

The baggage fire incident has also been simulated in a twin-track tunnel using the 1-car model. The location of the ignition source remains the same as explained in Case-05. In this case, the side doors facing the walkway are assumed to be open during the course of the incident.

The doors are assumed to be open at time is equal to zero, i.e. when the fire starts, in this particular case. However, effects of a delay in opening the side doors are investigated as a part of the sensitivity studies.

5.7.1 FIRE DEVELOPMENT

5mins: The fire starts to develop in the carriage and the seats adjacent to the ignition source are involved in fire.

In contrast to an incident in the single-track tunnel, the smoke and high temperature gases can be ventilated more effectively through the open side doors. This prevents earlier ignition of the seats at the far end in the incident carriage away from the ignition location.

8mins: The simulation shows that the fire spread to the folded seats located next to the doors on both sides of the carriage between the 6th and 8th minute from the start of the fire.

It has been predicted from the results that two large windows, on both sides of the incident carriage, and a smaller window on one side, closest to the ignition source fail due to high temperature just after the 8th minute from the ignition.

Further investigation shows that the temperature at the face of the smaller window that remains intact increases to 600°C, and the temperature increases to 611°C at the center of the back end door window at 8th minute. Since the failure criterion is defined to be 675°C, both windows remain undamaged.

The peak heat release rate for this case is predicted to be 2.5MW, reached after 8 minutes from the ignition. The peak heat release rate remains constant about one minute. The fire is predicted to spread farthest, until it involves the folded seats closer to the ignition location, within this interval.

10mins: At 10 minutes from the ignition, the fire is predicted to be contained around the ignition location. The smoke and hot gases are ventilated through the open side doors and through the broken windows. Therefore, the fire loses its intensity and has not propagated since the ignition temperature of the adjacent combustible items is not reached.

15mins: After 11 minutes from the ignition, the seats close to the ignition location start to burn-out. At 15 minutes, most of the seats have completely consumed, and the floor starts to be exhausted.

20mins: At 20 minutes and onwards, the fire is localized on floor around the ignition source, and the heat release rate from the fire decreases gradually as the ignited combustible items are consumed.

The simulation shows that less than half of the carriage is involved in fire during this incident. In addition, there is no sudden increase in the predicted heat release rate during the course of the incident. Therefore, flashover is not predicted for this case.

The fire development in the incident carriage, illustrated with the burning rate of the combustible surfaces, is given in Figure 5.42.

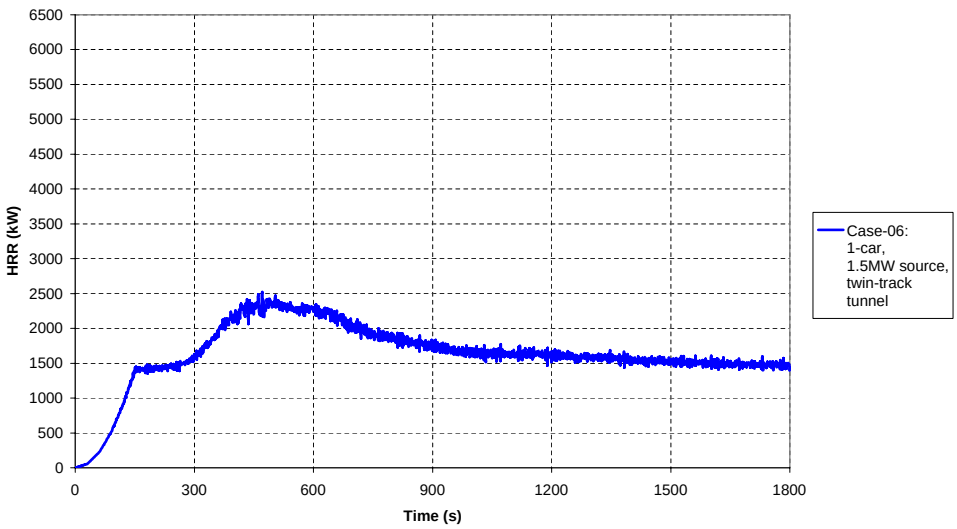

Figure 5.41: Heat release rate, 1-car, 1.5MW source, twin-track tunnel

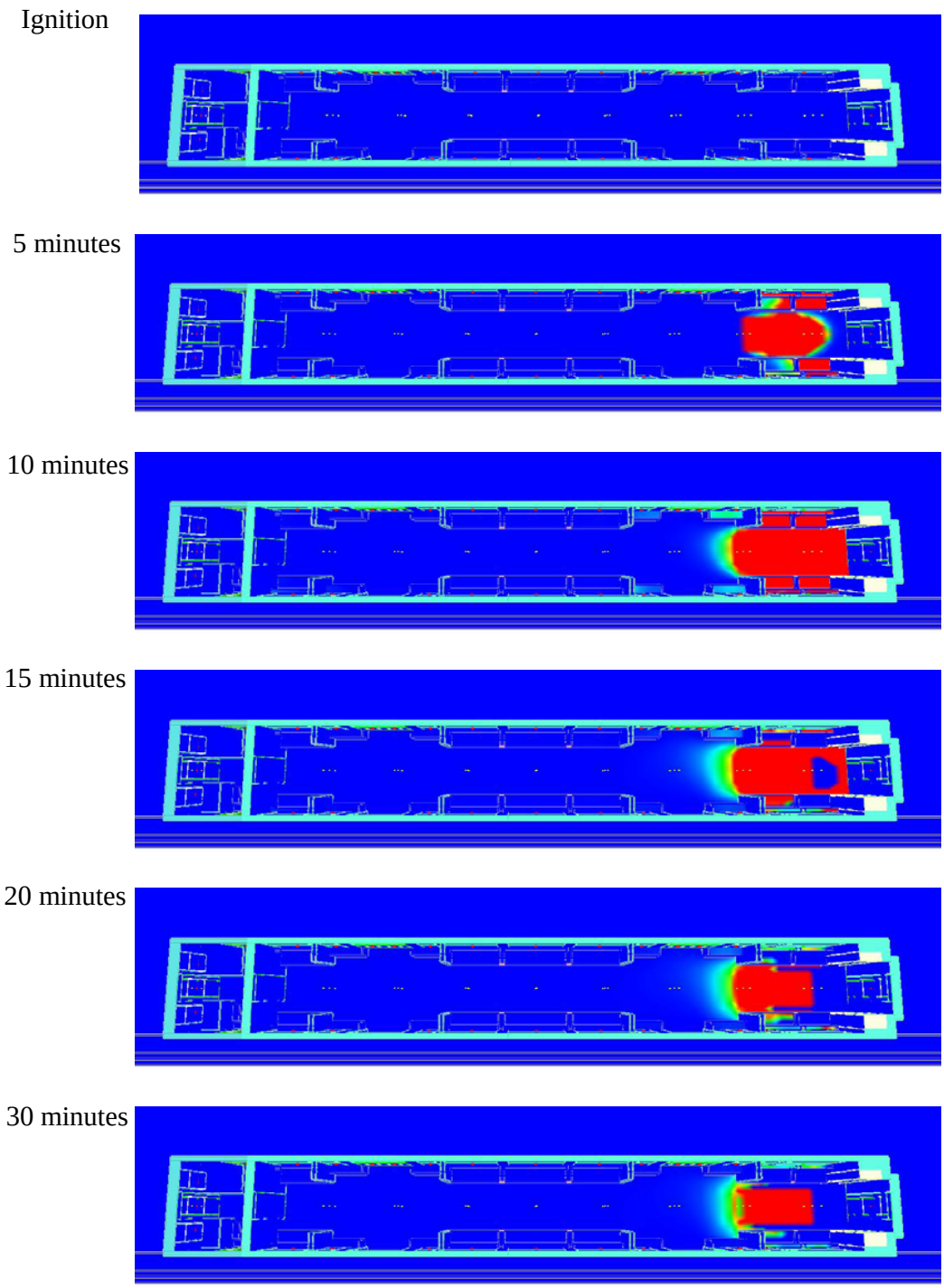

Figure 5.42: Fire spread, 1-car, 1.5MW source, twin-track tunnel

The energy released during this incident is estimated to be 2.9GJ through calculation of area under the heat release rate curve using the Trapezoidal Rule.

5.7.2 ONBOARD CONDITIONS

The heat and smoke from an incident in the twin-track tunnel are ventilated more effectively through the open side doors compared to an incident in the single-track tunnel. However, the rapidly growing ignition source, once again, results in untenable conditions in the incident carriage.

It is predicted from the simulation that the temperature at the center of the carriage exceeds the 60°C limit within 1.5 minutes at 1.5m above the floor, and within 2 minutes at seat level. The temperatures in the incident carriage increase to about 730°C above the ignition source at 1.5m above the floor level. The temperatures in the carriage then decrease as some of the windows fail and the fire starts to lose its intensity. The temperature variations at three points along the carriage are given in Figures 5.43 and 5.44, at 1.5m and 1.0m above the floor level, respectively.

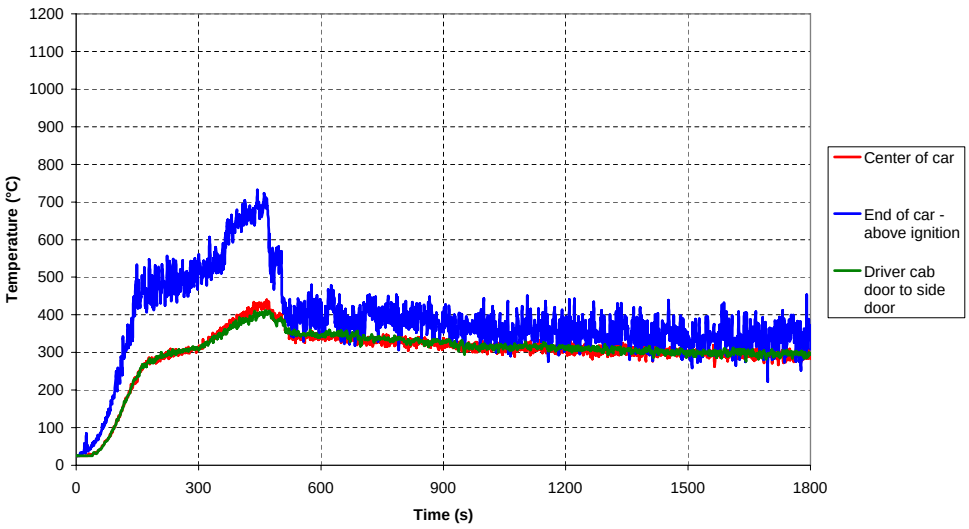

Figure 5.43: Case-06: Temperature variation at 1.5m above the floor level

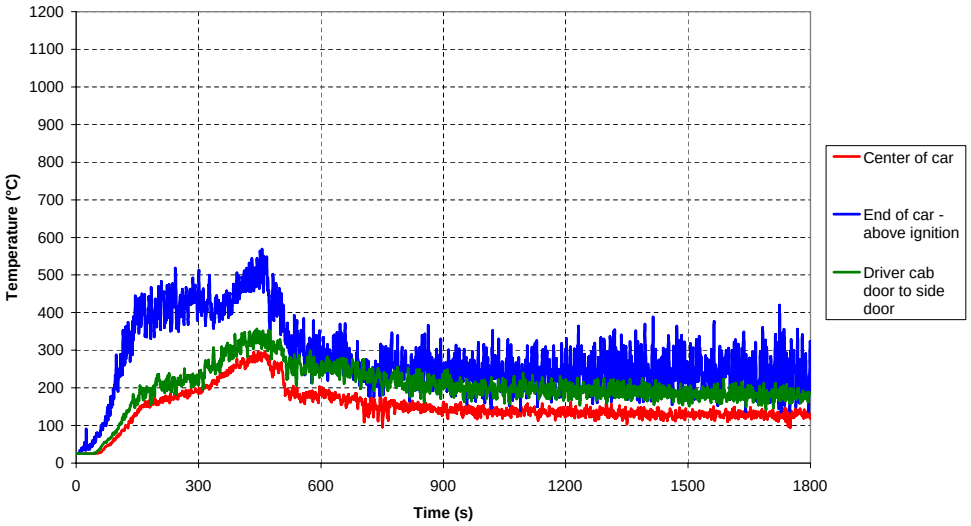

Figure 5.44: Case-06: Temperature variation at 1.0m above the floor level

The visibility is predicted to drop to 5m within the first minute at 1.5m above the floor level, and within 1.5 minutes at seat level at the center of the carriage. The variations of visibility at 1.5m and 1.0m above the floor level are given in Figures 5.45 and 5.46, respectively. The figures are given only for five minutes from the ignition since once the visibility is vanished in the incident carriage, it has not been recovered even though some of the windows fail during the course of the incident.

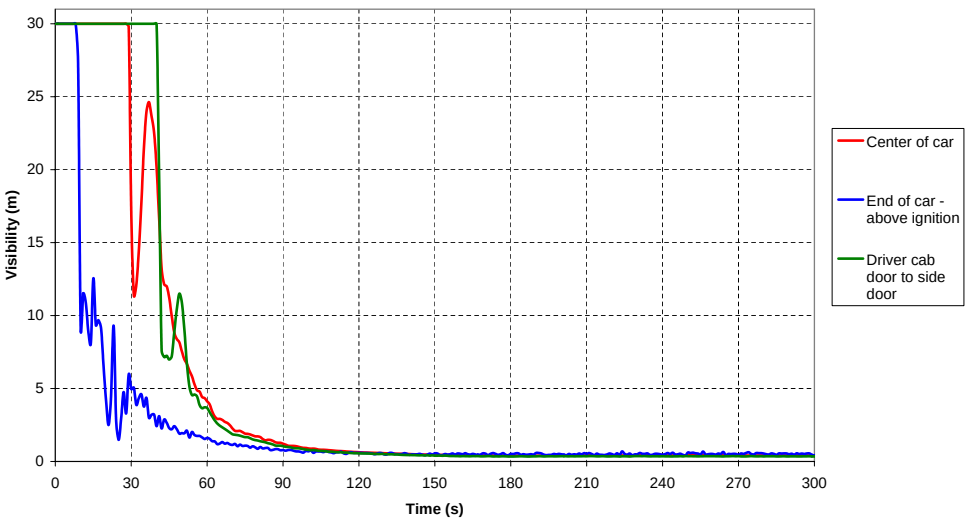

Figure 5.45: Case-06: Visibility variation at 1.5m above the floor level

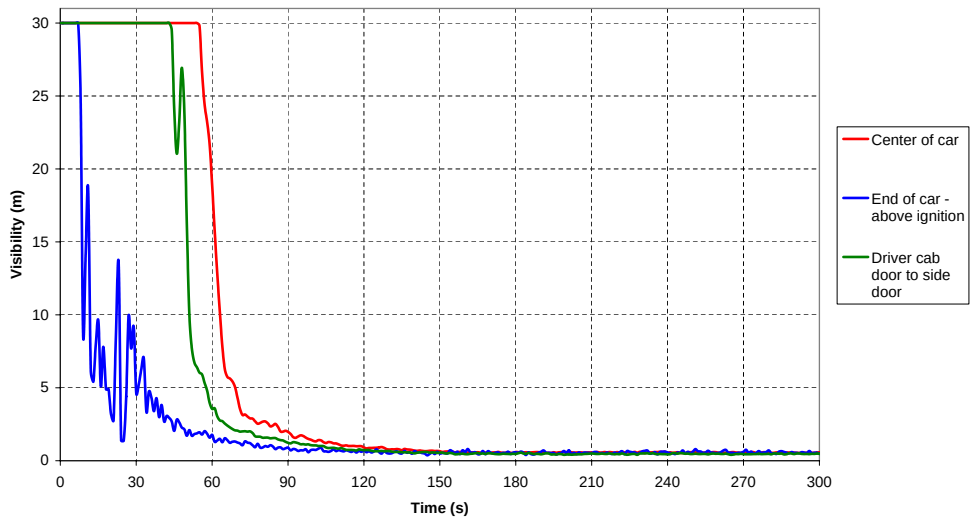

Figure 5.46: Case-06: Visibility variation at 1.0m above the floor level

It is predicted from the simulation that the carbon-monoxide concentration at the center of the incident carriage exceeds 1500ppm in 2.5 minutes at 1.5m above the floor level, and reaches the limiting value of 2000ppm just after 5 minutes from the ignition.

The carbon-monoxide level at the center of the carriage at seat level remains below 1150ppm for about 5 minutes, and increases to 1800ppm when the fire reaches at its peak heat release rate.

The simulation shows that the carbon-monoxide concentrations at each end of the incident carriage are higher than the predicted values at the center of the carriage. This is expected since the center of the carriage is ventilated better by means of open side doors compared to the relatively stagnant air movements at both ends of the carriage.

The reported values of carbon-monoxide concentrations will cause fatalities in such an incident. However, the critical timescale in terms of passenger life safety is defined by the time that the temperature in the carriage exceeds the limiting value of 60°C as reported above in this Sub-section.

The variations of carbon-monoxide concentration at 1.5m and 1.0m above the floor level are given in Figures 5.47 and 5.48, respectively. The figures are given only for ten minutes from the ignition since the limiting value for the passengers' life safety has been reached within this time interval.

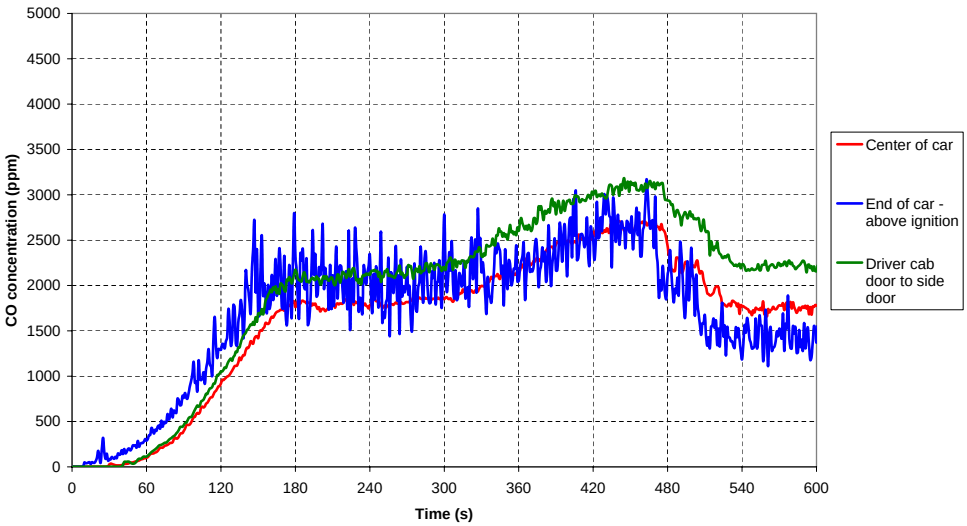

Figure 5.47: Case-06: Carbon-monoxide concentration at 1.5m above the floor level

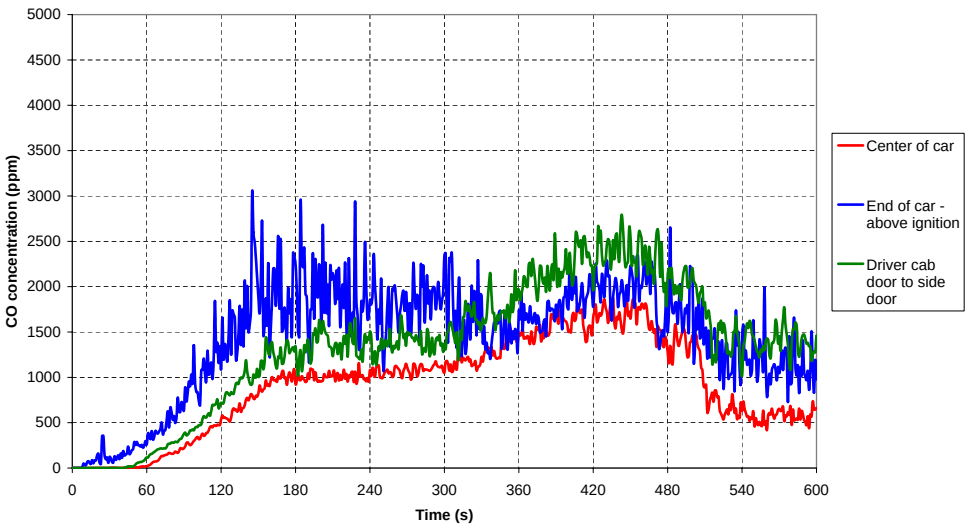

Figure 5.48: Case-06: Carbon-monoxide concentration at 1.0m above the floor level

The reported values of temperature and carbon-monoxide concentration within the incident carriage once again confirm that the 1.5MW ignition source is too severe for assessing the onboard conditions for passenger life safety. In addition, the timescales indicate that for a rolling stock made up of physically separated carriages, a severe ignition source would cause fatalities irrespective of the side doors or the end door left open for ventilation.

The temperature, visibility and carbon-monoxide slices on a longitudinal section through the center of the carriage are given in Figures B.16 to B.18 in Appendix B.

5.8 CASE-07: 4-CAR, 1.5MW SOURCE, SINGLE-TRACK TUNNEL

The baggage fire incident has also been simulated in a 4-car rolling stock with open wide gangways. The first of the two incident cases, incorporating the single vestibule rolling stock model, has been simulated in the single-track tunnel. The location of the ignition source remains the same as explained in Cases-05 and 06.

In this particular case, two end doors, at the front and back of the rolling stock, are defined to be open for evacuation of passengers and ventilation of fire.

5.8.1 FIRE DEVELOPMENT

The simulation results show that at the initial stages of the fire development, heat and smoke from the fire dissipates into the non-incident carriages fairly quickly. While this heat and smoke dissipation affects the onboard conditions in all carriages, it reduces the intensity of the fire in the incident carriage. Therefore, slightly delayed ignition of combustibles is predicted in the open rolling stock model compared to a model made up of physically separated carriages.

5mins: The fire initially starts to develop in the carriage on the floor at five minutes from the ignition. The seats adjacent to the ignition source are predicted to be ignited at 5th minute. However, it takes two additional minutes for all the surfaces of these seats be involved in the fire development.

10mins: It has been predicted from the results that at 10 minutes from the ignition, the top surfaces of the folded seats, closest to the ignition location, are involved in fire. The fire also spread along the floor in both upstream and downstream directions. However, the fire is still localized around the ignition location. The simulation shows that the large windows, on both sides of the incident carriage, closest to the ignition source fail just after the 10th minute due to high temperature around the ignition source.

12mins: At 12 minutes from the ignition, the back of the seats and top of the folded seats in the incident carriage start to burn. However, the temperatures at slightly lower height, such as at the base of the seats, do not reach ignition temperatures of the combustibles.

The peak heat release rate for this incident is predicted, just after the 12th minute, to be 2.7MW. At that instant, the base of the seat closest to the driver cab is involved in fire development. The fire on the floor spread towards the folded seats in the upstream direction, and towards the adjacent carriage via open wide gangway in the downstream direction. The peak heat release rate is maintained for about two minutes.

14mins: The simulation shows that the smaller windows, on both sides of the incident carriage, closest to ignition location fail at 14 minutes. In addition, the seats closest to the ignition source start to burn-out. The fire starts to lose its intensity from this point onwards.

18mins: The seats adjacent to the ignition source are consumed between 17 and 18 minutes. At 18th minute, combustibles on floor around the ignition source start to burn-out. However, the fire on floor slowly continue to progress in both directions, and reach the adjacent carriage at the downstream end.

It is predicted from the simulation that in the later stages of this incident, the flames on the seat bases in the incident carriage could not be maintained. In addition, the spread of fire along the floor is not intense enough to involve the adjacent carriage in fire development. The heat release rate from the fire is predicted to decrease as the ignited floor in the incident carriage burns-out gradually in time, and the contribution of the recently ignited items is not sufficient to increase the rate of heat release within the first 30 minutes from the ignition.

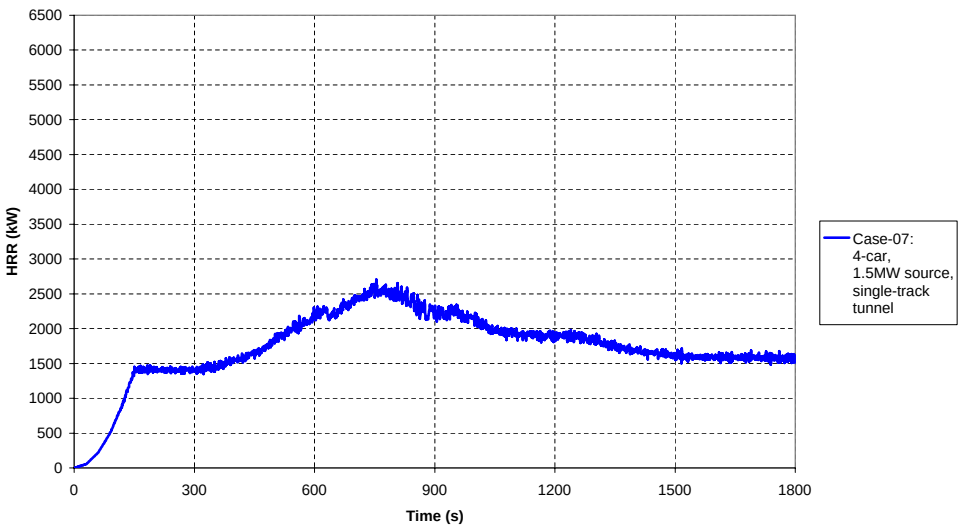

Figure 5.49: Heat release rate, 4-car, 1.5MW source, single-track tunnel

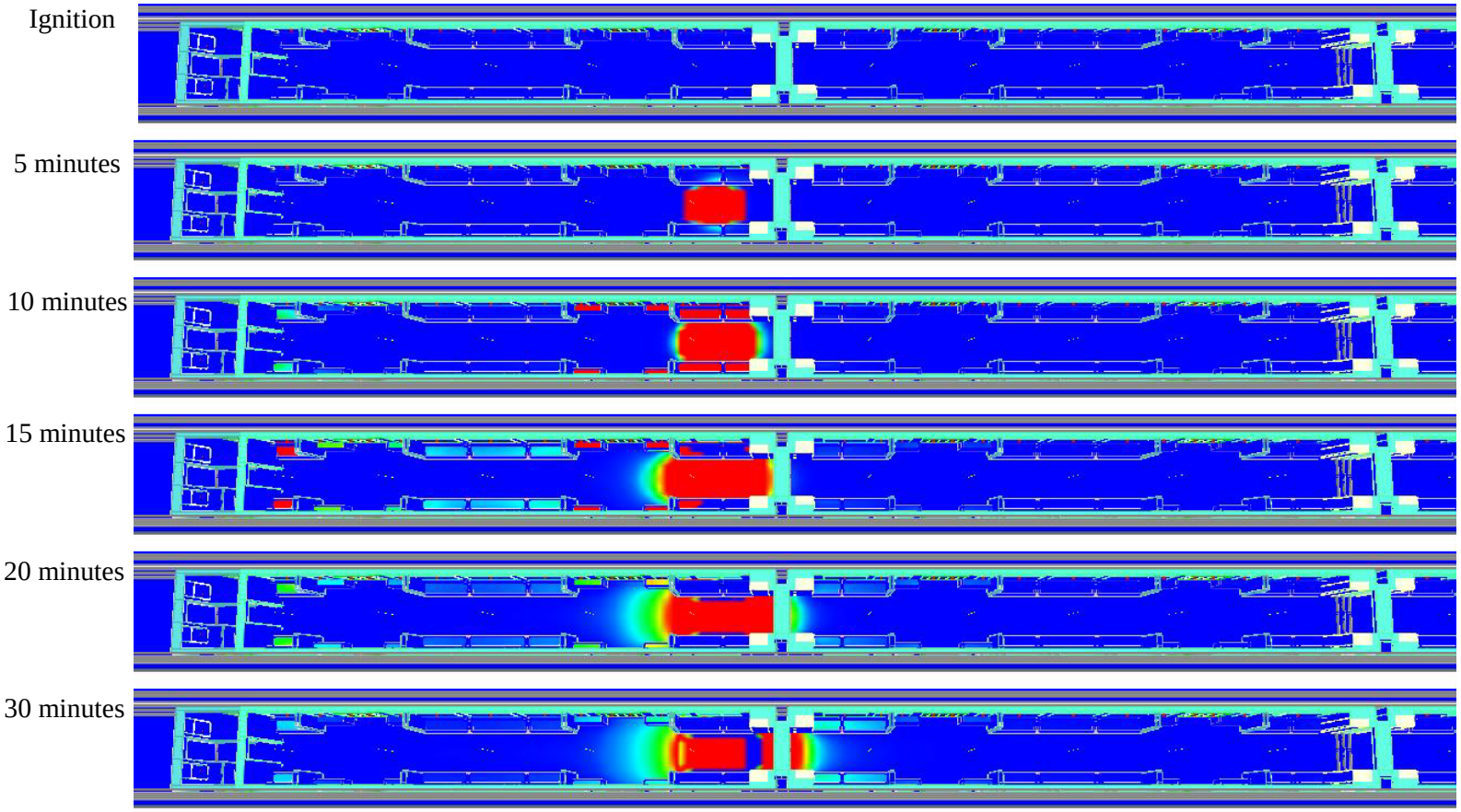

Figure 5.50: Fire spread, 4-car, 1.5MW source, single-track tunnel

The energy released during this incident is estimated to be 3.1GJ through calculation of area under the heat release rate curve using the Trapezoidal Rule.

5.8.2 ONBOARD CONDITIONS

As mentioned earlier in the text, the open wide gangways allow smoke and hot gases to spread from incident carriage to the adjacent carriages, which causes onboard conditions deteriorate from the initial tenable conditions. In the event of a severe baggage fire incident, the rapid production of heat and smoke at the incident carriage results in untenable conditions in the entire rolling stock fairly quickly.

The simulation of the baggage fire incident in the 4-car rolling stock in the single-track tunnel shows that the temperature at the center of the incident carriage at 1.5m above the floor level increases to about 495°C. The temperature at the center of the incident carriage at the given height is predicted to exceed the 60°C limit just after the first minute of the incident. It is predicted that the temperatures at 1.5m at the center of the remaining carriages exceed the acceptability limit within the first 3 minutes from the ignition, including the carriage farthest to the incident.

The temperature at 1.0m above the floor level at the center of the incident carriage is predicted to increase to about 425°C. In this incident, since the rate of smoke produced is greater than the rate of smoke extracted from the rolling stock, the conditions at 1.0m above the floor level are not significantly different from the conditions at 1.5m. The temperature tenability limit at 1.0m is reached at the center of the carriages approximately half a minute later than the predicted times for points at 1.5m above the floor level. The temperature at the center of the incident carriage at 1.0m above the floor level is predicted to exceed the acceptability limit at 1.5 minutes from the ignition. The temperatures at the same height in the remaining carriages are predicted to exceed the 60°C limit within 3.5 minutes of the incident.

The predicted variations of temperature at the center of the carriages at 1.5m and 1.0m above the floor level are given in Figures 5.51 and 5.52, respectively.

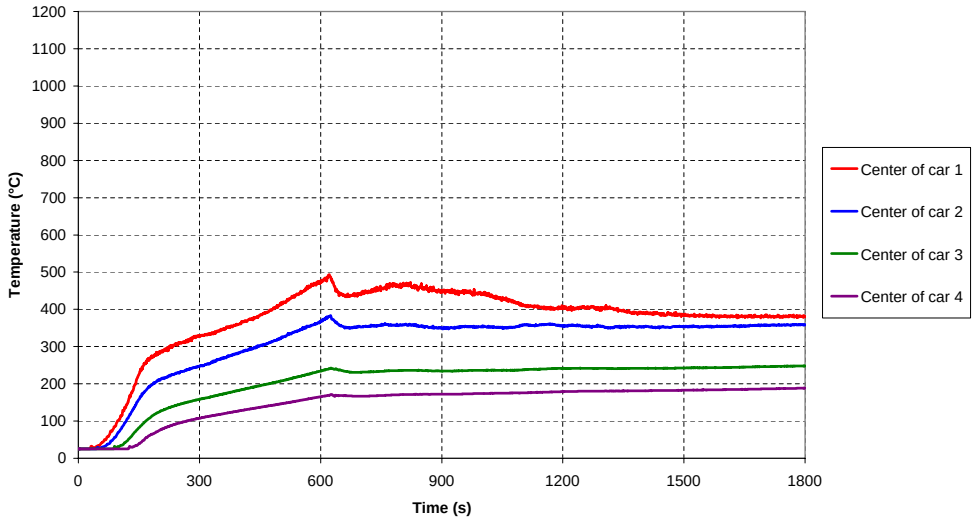

Figure 5.51: Case-07: Temperature variation at 1.5m above the floor level

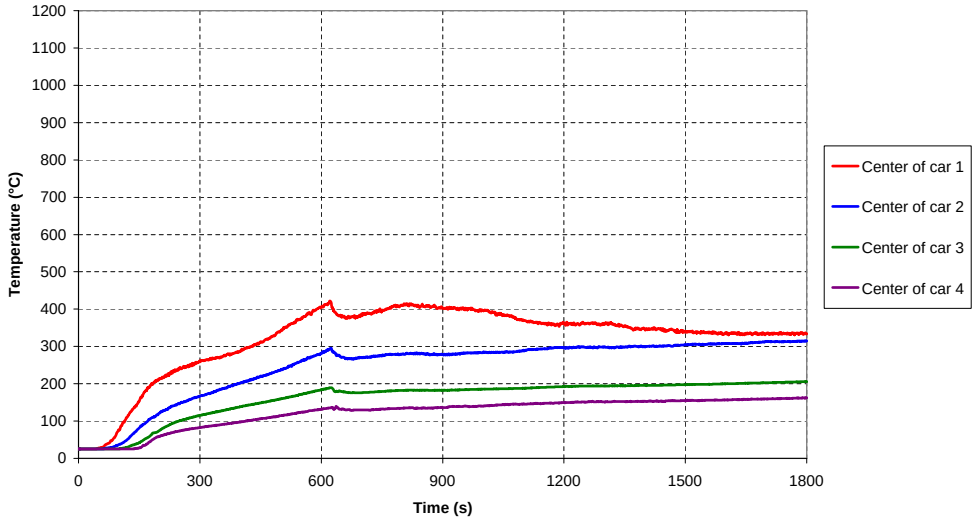

Figure 5.52: Case-07: Temperature variation at 1.0m above the floor level

The visibility level at 1.5m at the center of the incident carriage is predicted to drop below 5m within the first minute from the ignition. At the center of the remaining carriages, it takes less than 2.5 minutes for visibility to drop below the recommended value, at targets points 1.5m above the floor level.

The visibility at 1.0m at the center of the incident carriage drops below 5m limit just after the first minute of the incident. The visibility at the same height in the remaining carriages are

predicted to fall below the recommended value within the first 3 minutes from the ignition.

The variations of the visibility at the center of the carriages at 1.5m and 1.0m above the floor level are given in Figures 5.53 and 5.54, respectively. It should be noted that only the first five minutes of the incident is given in the figures, since the visibility levels remain constant for the rest of the simulation.

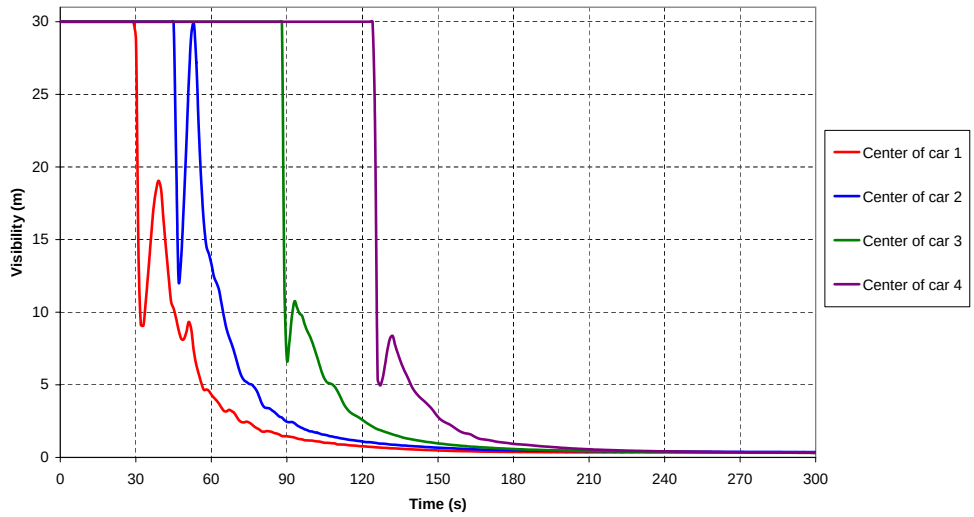

Figure 5.53: Case-07: Visibility variation at 1.5m above the floor level

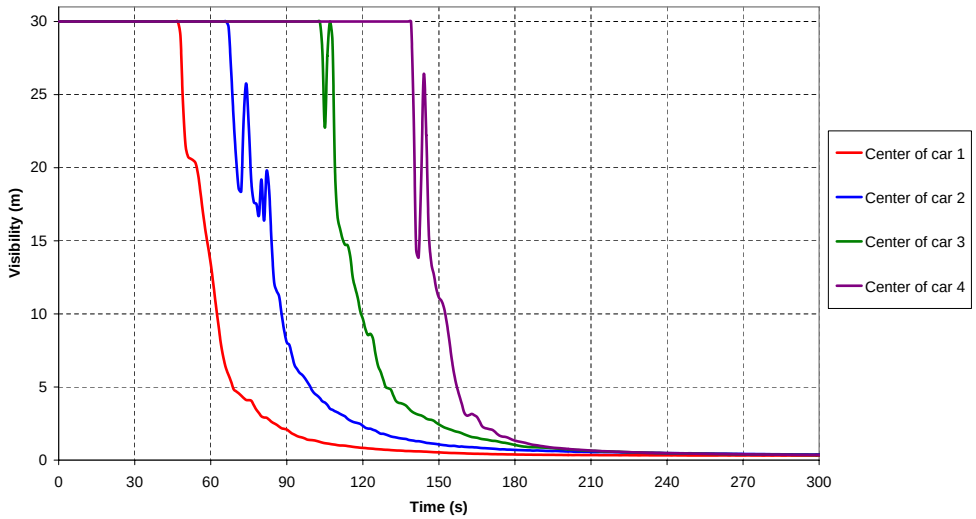

Figure 5.54: Case-07: Visibility variation at 1.0m above the floor level

The simulation of a severe baggage fire incident in the 4-car rolling stock in the single-track tunnel shows that the carbon-monoxide concentration levels exceed the fatality limit of 2000ppm just after the 3rd minute from the ignition at the center of the incident carriage at 1.5m above the floor level. The maximum allowable carbon-monoxide concentration limit is reached within 6.5 minutes at the center of the remaining carriages at the same height.

The predictions of carbon-monoxide concentration show that the fatality limit is also exceeded at 1.0m above the floor level within the rolling stock. The concentration levels exceed 2000ppm within 4 minutes at the center of the incident carriage and within 8 minutes at the center of the remaining carriages at 1.0m, measured from the floor level.

The predicted variations of carbon-monoxide concentrations at 1.5m and 1.0m above the floor level are given in Figures 5.55 and 5.56, respectively. It should be noted that only the first 10 minutes of the incident is given in the figures, since the fatality limit for the carbon-monoxide concentration is reached and exceeded within this interval.

The temperature, visibility and carbon-monoxide slices on a longitudinal section through the center of the carriage are given in Figures B.19 to B.21 in Appendix B.

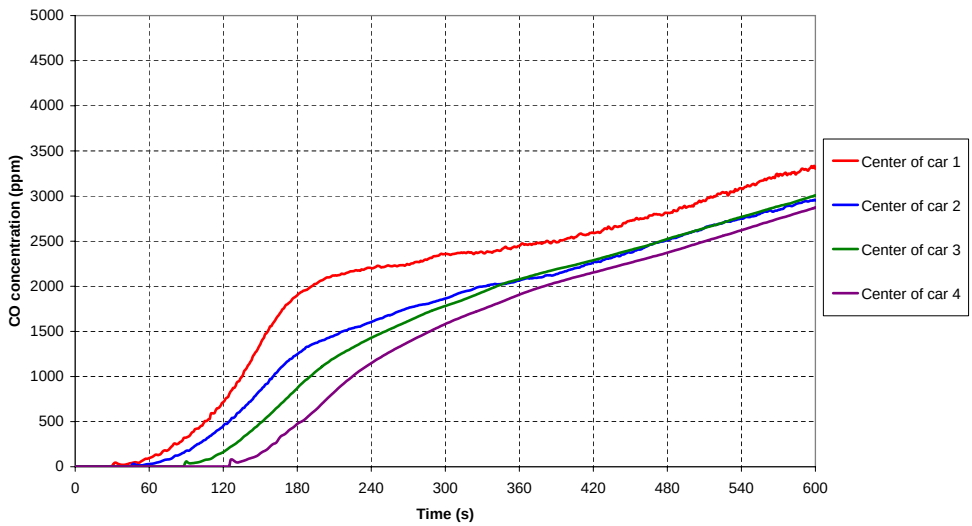

Figure 5.55: Case-07: Carbon-monoxide concentration at 1.5m above the floor level

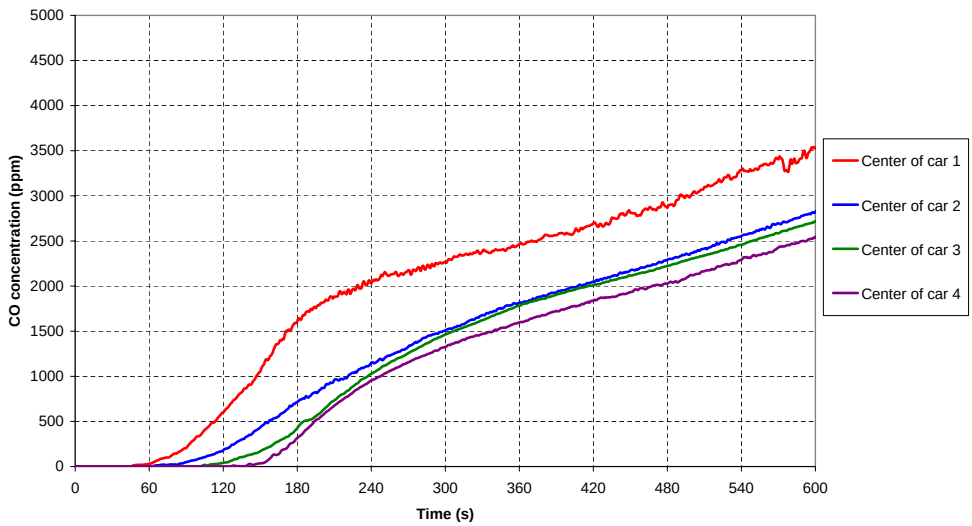

Figure 5.56: Case-07: Carbon-monoxide concentration at 1.0m above the floor level

5.9 CASE-08: 4-CAR, 1.5MW SOURCE, TWIN-TRACK TUNNEL

The last case of the initial simulations includes a baggage fire incident in the 4-car rolling stock incorporating open wide gangways. The rolling stock is defined to come to a rest in the twin-track tunnel, and all doors on one side of the train is defined for ventilation of smoke and evacuation of passengers.

The location, physical size, and the power of the ignition source in this case are kept as simulated in Cases 05 to 07. This incident is labelled as Case-08 in this thesis.

5.9.1 FIRE DEVELOPMENT

As predicted and explained in Case-07, the open wide gangways in the 4-car rolling stock allow heat and smoke produced by the fire to be carried from the incident carriage and be dispersed to the adjacent non-incident carriages. It is predicted from the simulation that this dissipation of heat and smoke alters the intensity of fire and the associated flame spread characteristic within the rolling stock.

5mins: In this incident, fire initially starts to develop on the floor, then spreads to the seat adjacent to the ignition location on the same side with the open doors at 4 minutes from the ignition. At the 5th minute, flames cover the base of the ignited seat.

10mins: The simulation shows that fire develops further on floor between the 5th and the 10th minutes, and cover the section bounded by the pair of seats at the end of the incident carriage. The pair of seats on both sides of the incident carriage, which are in the premises of ignition source, are also found to be involved in fire within this interval. However, flames have not yet spread to the folded seats, located just adjacent to the side doors, or have not spread to the adjacent non-incident carriage over the floor.

It is predicted that the small window, located on the same with open doors above the burning seats, fails at the 10th minute.

13mins: The predictions of flame spread show that fire on the floor propagates further in both directions from the 10th minute and onwards. It is predicted that just after 12 minutes from the ignition, flames cover a region between the center of the folded seats, at upstream end, and the center of the gangway, at downstream end, on the floor. The sides of the folded seats are also ignited between the 12th and the 13th minutes. However, the seats that ignited first in this incident are completely burnt out by 13 minutes.

The peak heat release rate for this incident is predicted, between the 12th and the 13th minutes from the ignition, to be 3.2MW.

The simulation shows that at 13 minutes, the pair of windows at the opposite side of the open doors, located above the burning seats, fail due to high temperature.

15mins: At 15 minutes, the flames on floor is predicted to move further upstream to the edge of the open side doors. The flames continue to burn the sides of the folded seats within this interval. However, simulation shows that the bases of the seats, adjacent to the ignition source, are mostly burnt out by 15 minutes.

The predicted and reported failure of windows reduce the intensity of the fire within the rolling stock. The simulation shows that starting from the 13th minute and onwards, the heat release rate decreases as the areas of the combustibles that are burning out are greater than the areas of the combustibles being introduced in fire.

20mins: At 20 minutes, some of the floor material around the ignition source is completely burnt out. However, burning is predicted to continue on floor around the folded seats and around the gangway area at the end of the incident carriage.

For the rest of the simulation, a localized fire between the edge of the open side door and the center of the gangway, between the incident carriage and the adjacent carriage, is predicted.

The predicted variation of the heat release rate for this incident is shown in Figure 5.57. The fire development in the rolling stock, illustrated with the burning rate of the combustible surfaces, is given in Figure 5.58 for this incident.

The energy released during this incident is estimated to be 3.0GJ through calculation of area under the heat release rate curve using the Trapezoidal Rule.

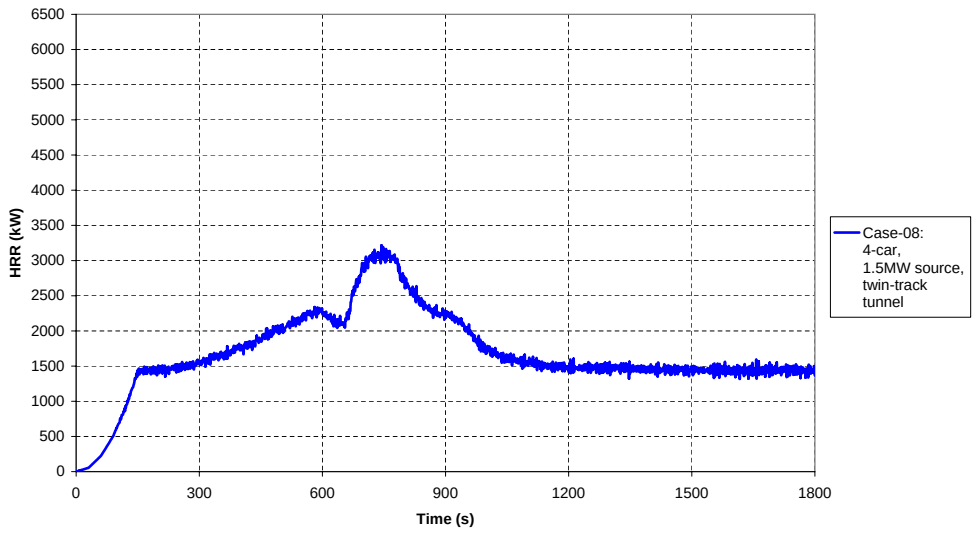

Figure 5.57: Heat release rate, 4-car, 1.5MW source, twin-track tunnel

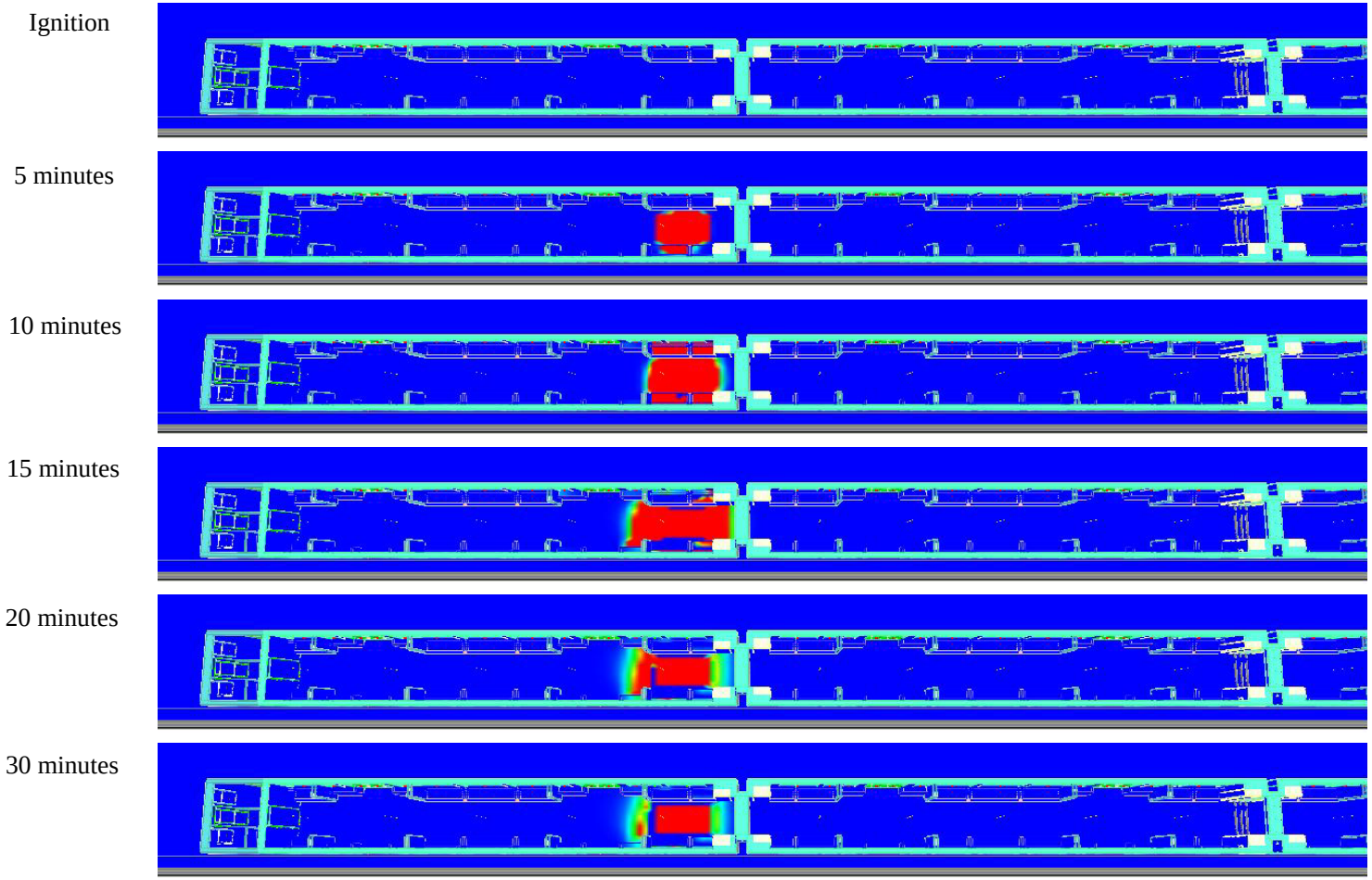

Figure 5.58: Fire spread, 4-car, 1.5MW source, twin-track tunnel

5.9.2 ONBOARD CONDITIONS

The simulation of a severe baggage fire incident in the 4-car open train in the twin-track tunnel shows that the smoke and hot gases produced at the incident carriage spreads to the adjacent carriages and alters the onboard conditions in the entire rolling stock. It is predicted that even though the smoke is dispersed into relatively large enclosure compared to 1-car model and is ventilated through a pair of side doors per carriage, the tenability limits are exceeded fairly quickly in the incident carriage and in the adjacent carriage to incident.

The simulation shows that the temperatures at 1.5m above the floor level at the center of the incident carriage and the adjacent carriage exceed the acceptability limit of 60°C within the first two minutes from the ignition. The effective ventilation of smoke through the side doors keeps the temperatures below 60°C at the same height at the center of the third and the fourth carriages for 3 and 8 minutes, respectively, where the reported durations are taken from the ignition. The temperatures are predicted to increase to 390°C at 1.5m at the center of the incident carriage during this incident.

It is predicted that the temperatures at 1.0m above the floor level at the center of the incident carriage exceeds 60°C within the first two minutes from the ignition. In this incident, temperature at the same height at the center of carriage adjacent to the incident exceeds the acceptability limit at the 9th minute. The temperatures at 1.0m at the center of the third and the fourth carriages remain below 60°C for the simulated duration of this incident.

The predicted variations of temperature at the center of the carriages at 1.5m and 1.0m above the floor level are given in Figures 5.59 and 5.60, respectively.

The results of the simulation show that the visibility at 1.5m above the floor level at the center of the incident carriage drops below the recommended value of 5m just after the first minute from the ignition. The visibility at the same height at the center of the adjacent and the third carriages is predicted to fall below the acceptability limit within the following minute. The visibility level drops below 5m at the center of the fourth carriage, which is the farthest away from the incident, at the height of 1.5m within the 3rd minute of the incident.

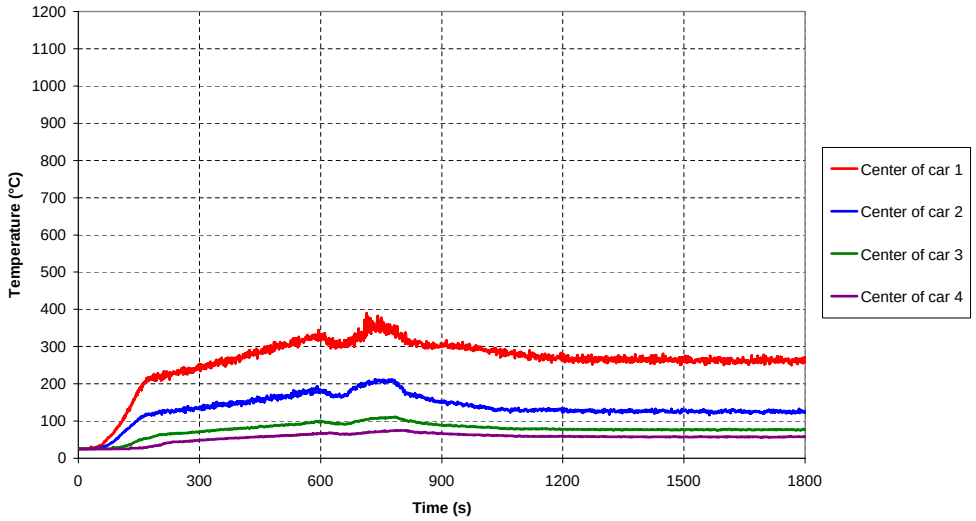

Figure 5.59: Case-08: Temperature variation at 1.5m above the floor level

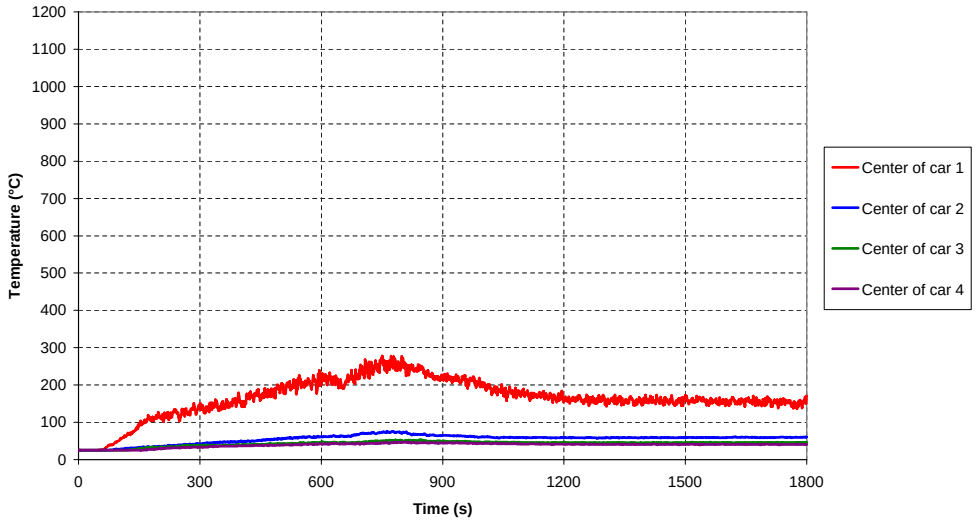

Figure 5.60: Case-08: Temperature variation at 1.0m above the floor level

In this case, even though the fire is ventilated more effectively, compared to other cases simulated, by means of the open side doors, the simulation shows that the smoke fills the rolling stock rapidly. This is also reflected in the predicted values of visibility at 1.0m above the floor level.

The visibility level at 1.0m at the center of the incident carriage is predicted to drop below 5m just after the first minute of the incident. The visibility levels at the same height at the center of the remaining carriages are predicted to drop below the recommended value between the 3rd and the 4th minutes from the ignition.

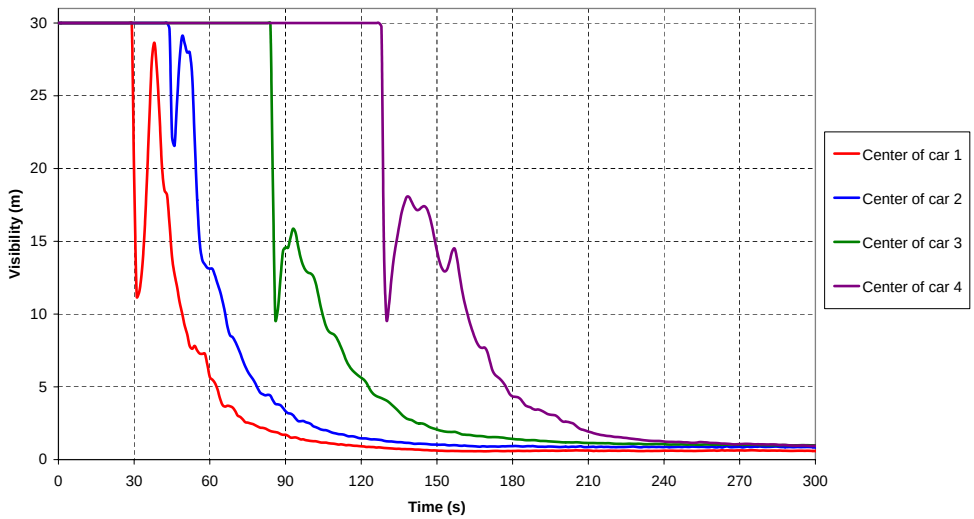

Figure 5.61: Case-08: Visibility variation at 1.5m above the floor level

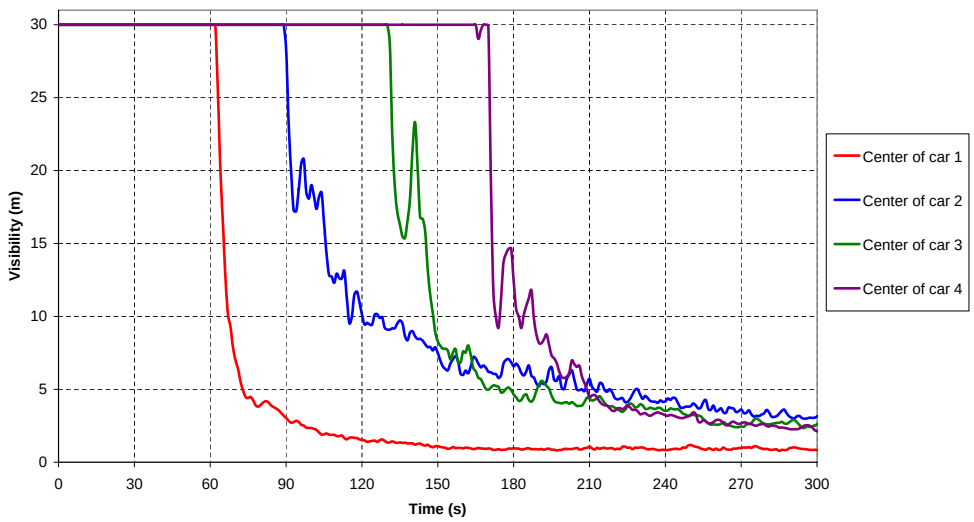

Figure 5.62: Case-08: Visibility variation at 1.0m above the floor level

The predicted variations of visibility levels at the center of the carriages at 1.5m and 1.0m above the floor level are given in Figures 5.61 and 5.62, respectively. It should be noted that only the first five minutes of the incident is given in the figures showing visibility, since the visibility levels do not change significantly over the rest of the simulation.

The simulation results show that the carbon-monoxide concentration at 1.5m above the floor level at the center of the incident carriage increases to a peak value of 2240ppm, predicted between the 12th and the 13th minutes from the ignition. It is predicted that at the same height the average values of carbon-monoxide concentrations at the center of the carriages, including the incident carriage, are within the acceptability criterion of 1150ppm for the first 6 minutes, but exceed the acceptability limit of 450ppm when values averaged over the first 15 minutes. The average values of concentration vary between 185ppm and 760ppm over the first 6 minutes, and between 480ppm and 1240ppm over the first 15 minutes at 1.5m above the floor level.

The carbon-monoxide concentration at 1.0m above the floor level at the center of the incident carriage is predicted to remain within the acceptability criterion when averaged over the first 6 minutes. However, the carbon-monoxide concentration exceeds the defined criterion when averaged over the first 15 minutes. The average values are predicted to be 390ppm and 780ppm, for 6 and 15 minute intervals, respectively. The carbon-monoxide concentrations at 1.0m above the floor at the center of the remaining carriages are predicted to vary between 145ppm and 200ppm, when averaged over the first 30 minutes, which leaves them within the acceptability criterion of 225ppm.

The predicted variations of carbon-monoxide concentrations at the center of the carriages at 1.5m and 1.0m above the floor level are given in Figures 5.63 and 5.64, respectively. It should be noted that only the first 10 minutes of the incident is given in the figures showing carbon-monoxide concentrations, since the concentration levels reflect the general trend of the variations.

The temperature, visibility and carbon-monoxide slices on a longitudinal section through the center of the carriage are given in Figures B.22 to B.24 in Appendix B.

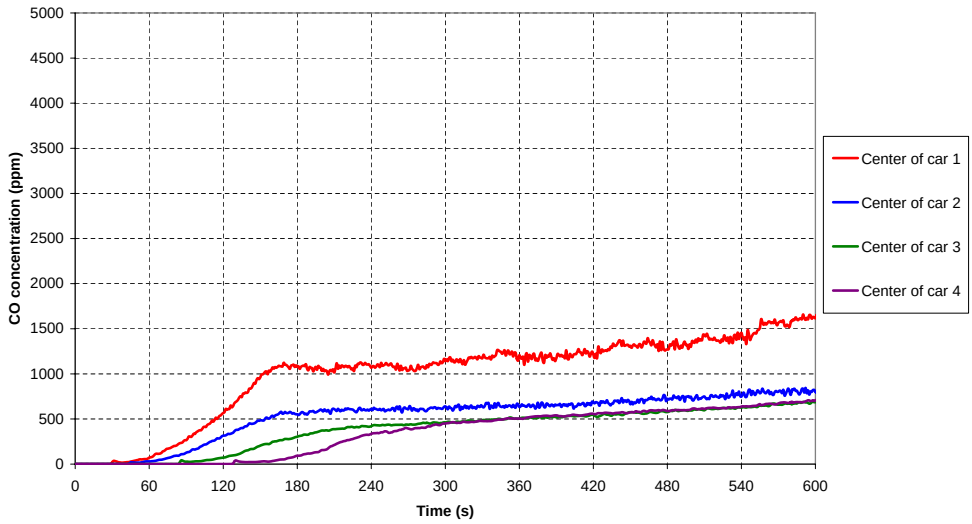

Figure 5.63: Case-08: Carbon-monoxide concentration at 1.5m above the floor level

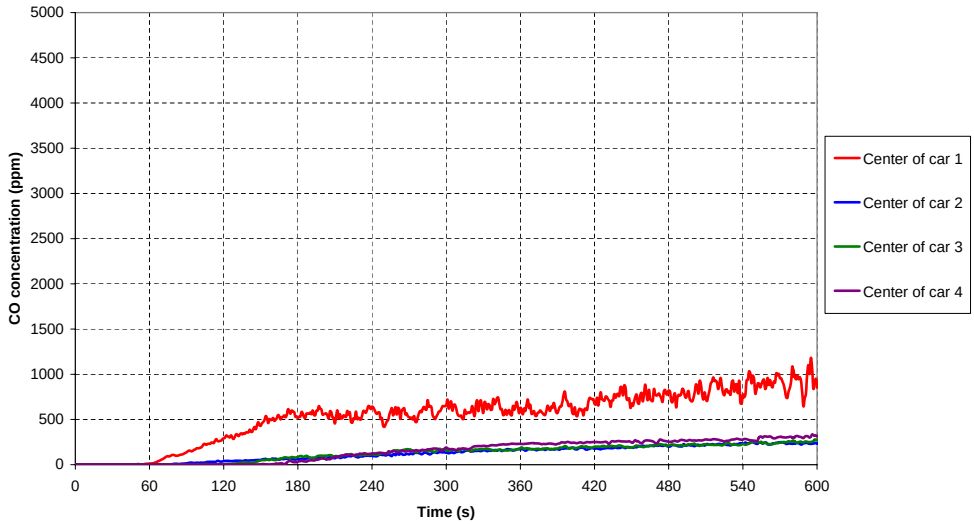

Figure 5.64: Case-08: Carbon-monoxide concentration at 1.0m above the floor level

5.10 DISCUSSION ON PREDICTIONS OF INITIAL SIMULATIONS

A set of simulations has been performed using the FDS program to predict fire development and flame spread in the underground trains in the event of an arson fire incident and a more severe baggage fire incident. The cases have been simulated using two rolling stock models, 1-car model representing a train made up of physically separated carriages and a 4-car rolling stock incorporating open wide gangways.

The simulations incorporating an 80kW ignition source show that regardless of the position or number of doors defined open, or the configuration of the rolling stock being set either to incorporate physically separated carriages or to incorporate open wide gangways, fire would be localized and would not spread to involve the entire carriage or rolling stock. In all 4 cases simulated, fire is predicted to remain in the premises of the initial ignition location. The peak heat release rate in the simulated cases is found to be about 135kW.

The simulations incorporating a severe baggage fire ignition source, releasing 1.5MW heat at its peak, show that the fire development and flame spread characteristics vary with the ventilation strategies, i.e. areas and the positions of open doors, and with the configuration of the rolling stock. The peak heat release rate, amongst the cases simulated, is predicted to be 6.0MW in the 1-car model, when the train is defined to be immobilized in the single-track tunnel section, where ventilation of smoke is through the single open end door. This case was labelled as Case-05 in this thesis.

In Case-05, the fire starts to develop at the end of the carriage, farthest away from the driver's cab. During the initial stages of the incident, fire is under-ventilated as the smoke is extracted only through the single open door. As the fire develops, the temperatures near the windows reached the predefined target values, and therefore window failures are predicted. The failure of windows increased smoke extract and caused fresh air entrainment to the incident carriage, which altered the conditions from under-ventilated to well-ventilated fire. The fire has also changed characteristics from fuel-controlled to ventilation-controlled during this phase. The predictions of sudden increase in the heat release rate through involvement of all surfaces in the carriage in fire development, and temperatures exceeding 600°C confirmed the occurrence of flashover phenomenon.

A set of calculations is performed to find the values of required heat release rates at the onset

of flashover conditions for the selected cases from the initial simulations. The calculations would support the discussion on observation of the flashover phenomenon.

In the calculations of flashover onset conditions, the material properties and the surface areas associated with these materials are taken as defined in the initial FDS simulations. The first calculation is performed for Case-05, where the only opening is defined to be one end door, having a cross-sectional area of 1.5m^2. The areas of the floor, the seats, and the walls and ceiling are calculated for the DMOS type carriage, as this type is modelled in Case-05. The layouts of the carriages are given in Appendix A.

$$k_{floor} = 0.19\ W/m.K \qquad k_{seats} = 0.295\ W/m.K \qquad k_{walls-ceil} = 0.038\ W/m.K$$

$$\delta_{floor} = 0.00162\ m \qquad \delta_{seats} = 0.00216\ m \qquad \delta_{walls-ceil} = 0.1\ m$$

$$A_{floor} = 39.6\ m^2 \qquad A_{seats} = 22.7\ m^2 \qquad A_{walls-ceil} = 58.8 + 37.0\ m^2$$

$$A_{total} = A_{floor} + A_{seats} + A_{walls-ceil}$$

$$A_{total} = 158.1\ m^2$$

$$\text{Using Equation 2.27: } h_{k-ave} = \frac{A_{floor}}{A_{total}}\frac{k_{floor}}{\delta_{floor}} + \frac{A_{seats}}{A_{total}}\frac{k_{seats}}{\delta_{seats}} + \frac{A_{walls-ceil}}{A_{total}}\frac{k_{walls-ceil}}{\delta_{walls-ceil}}$$

$$h_{k-ave} = 49.216\ W/m^2.K$$

$$H_{open} = 2.0\ m \quad ; \quad A_{open} = 1.5\ m^2$$

$$\text{Using Equation 2.31: } Q_{FO} = 610\,(h_{k-ave} \cdot A_{total} \cdot A_{open} \cdot {H_{open}}^{1/2})^{1/2}$$

$$Q_{FO} \approx 2480\ kW$$

It should be noted that the window failures are defined in the simulations. Therefore, the area of the opening changes during the course of the incident simulated in Case-05. Since the value of heat release rate at the onset of flashover condition depends on the area of the openings, this occurrence should be taken into account in the calculations. The results of Case-05 show

that within 15 minutes from the ignition, a total of 5 windows including the window of the back end door fail due to high temperatures within the carriage. At that instant, the total open area for smoke ventilation becomes:

$$\begin{aligned} A_{open} &= \underbrace{1.5}_{\text{front door}} + \underbrace{2 \cdot 0.5 \cdot 0.85}_{\text{small windows}} + \underbrace{2 \cdot 1.5 \cdot 0.85}_{\text{large windows}} + \underbrace{0.5 \cdot 0.85}_{\text{back-end window}} \\ A_{open} &= 5.325\, m^2 \end{aligned}$$

If all the parameters are assumed to be identical, and the opening area is revised in the calculation of heat release rate, then:

$$H_{open} = 2.0\, m \quad ; \quad A_{open} = 5.325\, m^2$$

$$\begin{aligned} \text{Using Equation 2.31: } Q_{FO} &= 610\, (h_{k-ave} \cdot A_{total} \cdot A_{open} \cdot {H_{open}}^{1/2})^{1/2} \\ Q_{FO} &\approx 4670\, kW \end{aligned}$$

The heat release rate at the onset of flashover is calculated to be about 4.7MW. This value matches with the predictions in Case-05, as shown in Figure 5.33. Consequently, the observation of flashover phenomenon is confirmed.

On the contrary, if Case-06 is considered, where the same ignition source and the same carriage is modelled but two side doors are defined open for smoke ventilation, it can be concluded that the fire in the incident carriage is localized and burns steadily. Although the extent of the fire spread is limited and therefore much less window failures are predicted in Case-06 compared to Case-05, the initial openings were much larger in Case-06. The incident in this case can be classified as well-ventilated, and therefore is fuel-controlled for the entire duration of fire. The effective ventilation of the incident decreased the temperatures onboard, which slowed down the flame spread and therefore limited the amount of fuel brought into the region of influence of fire.

Therefore, flashover conditions are not predicted for the incident simulated in Case-06. This can also be confirmed through the calculation of heat release rate at the onset of flashover for

this case. If the areas and properties of the materials within the carriage are kept constant, the heat release rate for an incident in the twin-track tunnel, where two side doors each having an area of 3.0m^2 defined open, can be calculated as follows:

$$H_{open} = 2.0\,m \quad ; \quad A_{open} = 6.0\,m^2$$

$$\text{Using Equation 2.31: } Q_{FO} = 610\,(h_{k-ave} \cdot A_{total} \cdot A_{open} \cdot {H_{open}}^{1/2})^{1/2}$$

$$Q_{FO} \approx 4960\,kW$$

The predicted variation of heat release rate during the incident in Case-06, given in Figure 5.41, shows that the peak value never reaches to the calculated value of heat release rate required for the flashover condition. The calculated value of about 5.0MW at the onset of flashover is much greater than the predicted peak value of 2.5MW. Consequently, the statement of localized and steady burning, or flashover conditions' not being achieved, can be confirmed with this analysis.

It should be kept in mind that the empirical equation to predict the heat release rate at the onset of flashover assumes the conditions are available for fire to flashover. However, in long compartments like railway rolling stock, it may not be possible for all the materials be involved in fire at the same time. The fire development and flame spread predictions for Cases 07 and 08 show that flashover conditions are not achieved in the rolling stock incorporating open wide gangways. The increase in the enclosed space, and relatively more effective ventilation of smoke compared to Case-05 resulted in slightly lower onboard temperatures and limited flame spread within the rolling stock.

It has been shown that ventilation plays an important role in the predicted fire development and flame spread characteristics, and therefore the value of peak heat release rate, in the event of a fire within the underground trains. A number of sensitivity cases has also been simulated and reported in Chapter 6, including cases with limited window failure and mechanical ventilation.

Table 5.1 summarizes the cases simulated and the predicted peak values of heat release rate in each case.

Table 5.1: Summary of the initial simulations with predicted peak heat release rates

Case ID	Ignition Source Characteristics	Tunnel Section	Rolling Stock Model	Ventilation Openings*	Predicted Peak HRR
Case-01	Arson fire, releasing constant 80kW heat, located on a passenger seat	Single-track tunnel	1-car representing a train made up of physically separated carriages	1-end door on the driver's cab end	< 0.2MW
Case-02	Arson fire, releasing constant 80kW heat, located on a passenger seat	Twin-track tunnel	1-car representing a train made up of physically separated carriages	2-side doors, on one side of carriage	< 0.2MW
Case-03	Arson fire, releasing constant 80kW heat, located on a passenger seat	Single-track tunnel	4-car rolling stock, incorporating open wide gangways	2-end doors at each end of the rolling stock	< 0.2MW
Case-04	Arson fire, releasing constant 80kW heat, located on a passenger seat	Twin-track tunnel	4-car rolling stock, incorporating open wide gangways	2-side doors per carriage, 8 doors in total on one side	< 0.2MW
Case-05	Baggage fire on floor, releasing peak heat of 1.5MW following fast-growth curve	Single-track tunnel	1-car representing a train made up of physically separated carriages	1-end door on the driver's cab end	6.0MW
Case-06	Baggage fire on floor, releasing peak heat of 1.5MW following fast-growth curve	Twin-track tunnel	1-car representing a train made up of physically separated carriages	2-side doors, on one side of carriage	2.5MW
Case-07	Baggage fire on floor, releasing peak heat of 1.5MW following fast-growth curve	Single-track tunnel	4-car rolling stock, incorporating open wide gangways	2-end doors at each end of the rolling stock	2.7MW
Case-08	Baggage fire on floor, releasing peak heat of 1.5MW following fast-growth curve	Twin-track tunnel	4-car rolling stock, incorporating open wide gangways	2-side doors per carriage, 8 doors in total on one side	3.2MW

* This column shows only the initial ventilation openings defined in the input files. The window failures are defined implicitly in all cases, in some of which failures are predicted as reported in the text above.

The initial simulations show that for an 80kW arson fire incident in an underground train, the number and size of the ventilation openings are crucial in assessing the onboard conditions. The incident simulated using the 1-car model in a single-track tunnel resulted in untenable conditions due to high temperature and high level of carbon-monoxide concentration. However, the simulation of an 80kW ignition source in the 4-car open train in the twin-track tunnel shows that onboard conditions are tenable for the first 30 minutes from the ignition. A number of open doors effectively ventilate the smoke produced, and a larger enclosure assisted dilution of smoke within the rolling stock.

The initial simulations incorporating a severe baggage fire incident show that the conditions become untenable within the incident carriage, and in the rest of the rolling stock where open wide gangways are implemented, within few minutes from the ignition. The temperatures within the incident carriage are found to exceed the acceptability criterion within the first two minutes, whichever the rolling stock model is used or ventilation strategy is implemented.

It has been predicted that for the 4-car open train, a severe baggage fire incident would result in loss of tenability in the entire rolling stock within the first 4 minutes of the incident, when the fire is ventilated through the open end doors. The simulations show that the conditions can be maintained tenable for 9 minutes in the adjacent carriage to incident, and for 30 minutes in the carriages farthest away from the incident, if the side doors are opened in the 4-car open train.

Consequently, in order to maintain the onboard conditions tenable longer, and to reduce the risk of flashover, a fire should be suppressed as soon as possible within the rolling stock before it gains intensity and starts to spread. In addition, if it is reasonably safe to open the side doors in the event of fire in a rolling stock, the risk of flashover would be reduced and the smoke from fire would be ventilated more effectively. It can be concluded that increasing the ventilation areas, by opening doors or breaking windows, at the early stages of fire would slow down the development of fire within the rolling stock. However, increasing ventilation areas during a developing fire with intense power could lead to flashover conditions.

CHAPTER 6

PARAMETRIC SENSITIVITY STUDIES

6.1 INTRODUCTION

The initial set of simulations helped distinguishing a localized fire from a developing one, shed light on the conditions required for an incident to develop, and gave the extent of flame spread along with an indicative set of design fire sizes for the selected base cases.

The initial simulations also showed that the intensity of the selected arson ignition source is not sufficient for the fire to develop or to be sustained within the rolling stock. However, flame spread and fire development were predicted in the simulations with the baggage fire ignition source.

The initial simulations incorporated only a fixed length of tunnel with the described grid size, and had been undertaken under natural ventilation conditions where the ignition source location was defined to be the same in each subset of cases. Consequently, a set of simulations has been performed to check the sensitivity of the results to computational aspects; such as the tunnel length and the grid size; to ignition source; such as the location of the source and the ignition source characteristics; and to ventilation; such as the window failure, the number of open doors, and the activation of mechanical ventilation. The findings and the results of the simulations are summarized in the following Sections. In the sensitivity simulations only the baggage fire ignition source is used, except in Section 6.4 where the effects of the ignition source characteristics are investigated.

6.2 THE TUNNEL LENGTH

The length of domain in the base case simulations involving 1-car model, representing a train made up of physically separated carriages, is defined to be 40m. Two simulations have been undertaken to investigate the effects of the length of the computational domain on the fire development within the incident carriage. Since the main aim is to examine the effects on the fire development and flame spread, the baggage fire ignition source is used in the simulations. In the sensitivity simulations, the length of the computational domain is increased from 40m to 120m.

The first of the two cases involves an incident in the twin-track tunnel, in which the side doors are open for smoke ventilation and passenger evacuation. This incident is labelled as Case-09a in this thesis. The simulation shows that the fire development and flame spread within the incident carriage is almost identical to the case simulated in the 40m long domain. Consequently, it is predicted that the length of the domain does not have significant effect on the fire development for this incident.

The variations of heat release rate predicted from an incident in the 40m long and in the 120m long domains are given in Figure 6.1 for comparison.

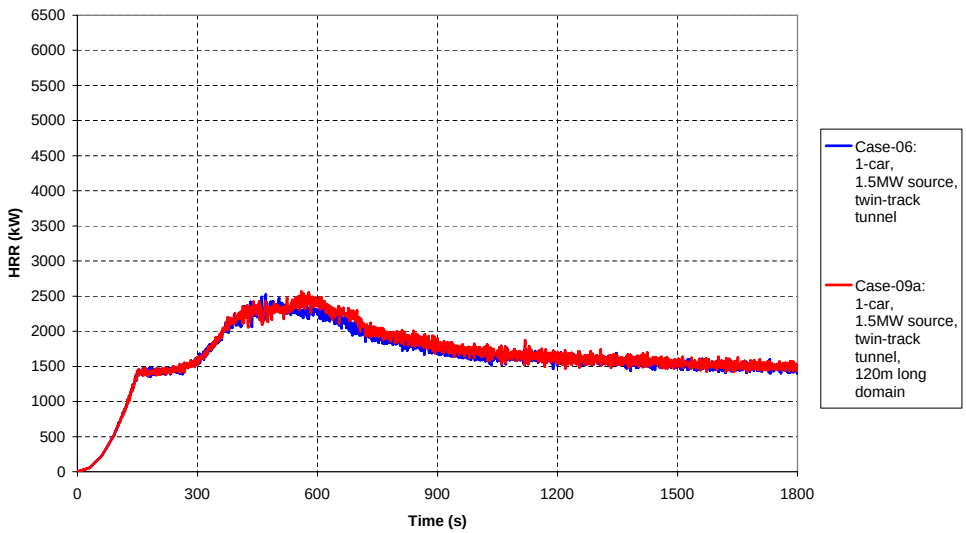

Figure 6.1: Heat release rate, 1-car, 1.5MW source, twin-track tunnel, 120m long domain

The sensitivity of fire development and flame spread predictions to the length of the computational domain has also been investigated through an incident in the single-track tunnel. This case is labelled as Case-09b in this thesis. The single-track tunnel has much smaller cross-sectional area compared to the twin-track tunnel modelled in the simulations. Consequently, for a certain length of tunnel, single-track cross-section could hold much less smoke than a twin-track section. In other words, smoke is ventilated better over a fixed length of tunnel for an incident in the single-track tunnel.

It is predicted from the simulation that the fire development and flame spread follow the same trend as predicted for the case with shorter tunnel. However, the simulation shows that when the tunnel length is increased, the peak heat release rate is achieved slightly earlier and with slightly greater magnitude. The peak heat release is predicted to be 6.4MW, achieved at 15 minutes from the ignition. The peak heat release rate and flashover onset conditions for the incident in longer tunnel are predicted about 2.5 minutes earlier than the values predicted for shorter tunnel.

The variations of heat release rate predicted from an incident in the 40m long and in the 120m long single-track tunnels are given in Figure 6.2 for comparison.

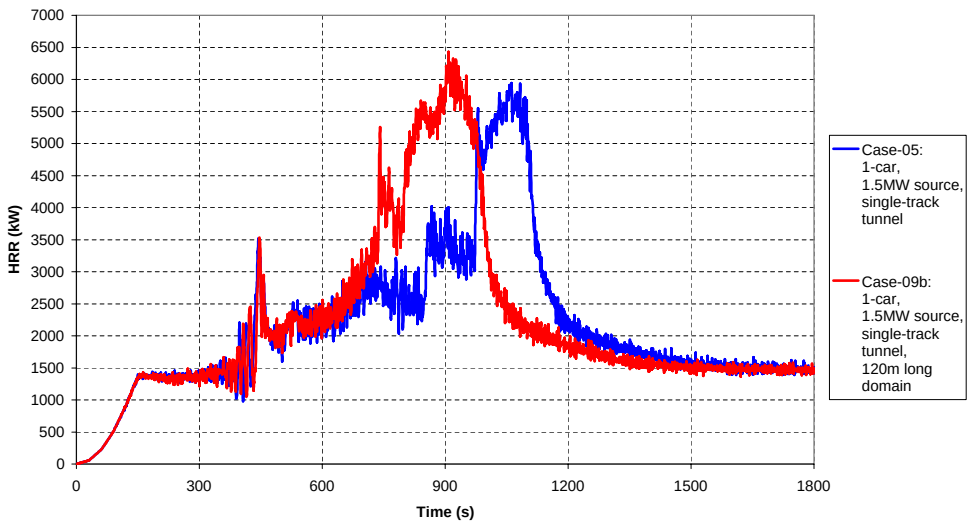

Figure 6.2: Heat release rate, 1-car, 1.5MW source, single-track tunnel, 120m long domain

The fire development in the incident carriage, illustrated with the burning rate of the combustible surfaces, in a 120m long single-track tunnel is given in Figure 6.3.

The differences in the predictions of simulations incorporating single-track tunnel are due to the heat feedback from smoke stored in the tunnel. For the shorter tunnel, smoke is ventilated through the portals, which reduces effects of smoke layer being built up in the tunnel. However, when the tunnel length is increased, it takes longer to ventilate the smoke from the portals which promotes additional heat feedback from the smoke layer accumulated within the tunnel. However, this effect has not been observed in the twin-track tunnel cases, since the tunnel cross-section is large enough to moderate the additional heat feedback from smoke.

The sensitivity simulations of increased tunnel length show that:

- fire development and flame spread patterns are almost identical for the incidents in the twin-track tunnel, irrespective of the length of the computational domain.
- the peak heat release rate and flashover onset conditions are achieved slightly earlier for an incident in the single-track tunnel, compared to an incident in the shorter tunnel.
- there are no significant differences in flame spread patterns or overall burning behavior within the incident carriage in a single-track tunnel, when the tunnel length is increased.
- increasing the tunnel length three-fold adds 92 hours of additional computational time for an incident in the twin-track tunnel, and adds 28 hours for an incident in the single-track tunnel.

It can be concluded that increased domain length does not affect the predicted fire development and flame spread patterns significantly. The peak heat release rate is predicted to be only 7% higher with increased tunnel length, even in an incident where flashover is observed. In addition, increasing domain length, increases the computational time by 133%, for an incident in single-track tunnel, and by 177%, for an incident in the twin-track tunnel. Consequently, by the reasons listed, it has been decided to undertake simulations involving an incident in the 1-car model using the shorter domain length.

Ignition

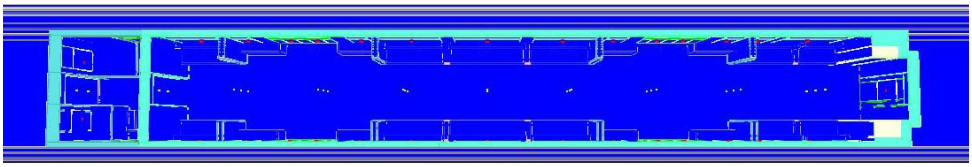

5 minutes

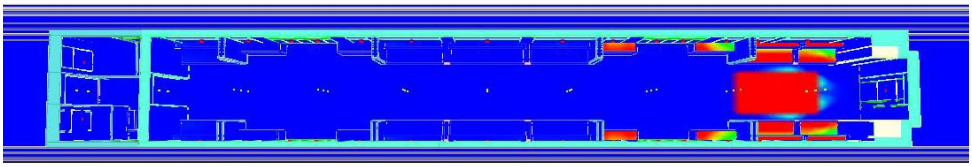

10 minutes

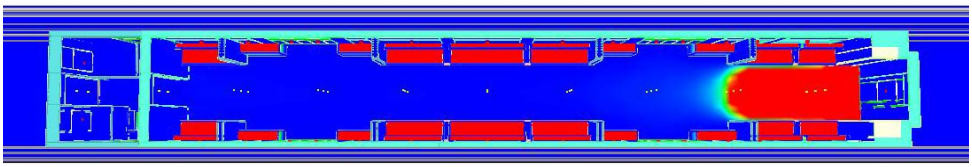

15 minutes

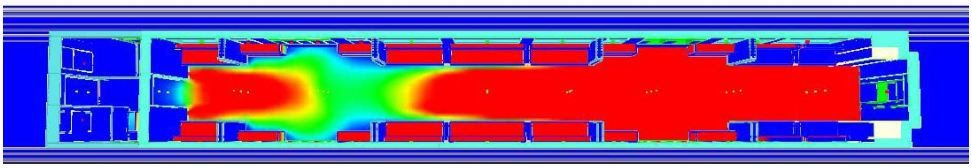

20 minutes

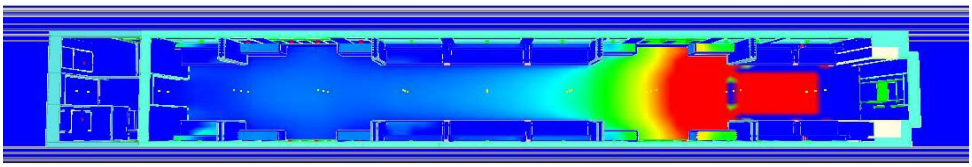

30 minutes

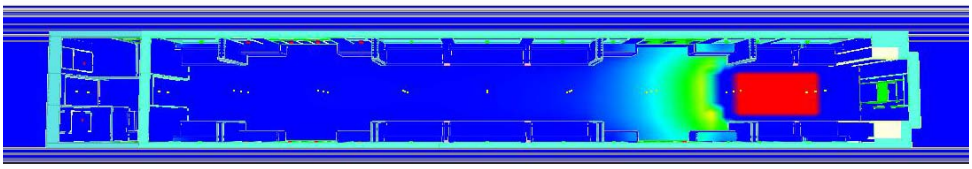

Figure 6.3: Fire spread, 1-car, 1.5MW source, 120m long single-track tunnel

6.3 THE LOCATION OF IGNITION SOURCE

A case has been simulated with the 4-car rolling stock with open wide gangways where the ignition source is moved to the second car. This case has been simulated to investigate the sensitivity of the results to the location of ignition source. This case will be referred as Case-10 in this thesis.

In this case, the baggage fire ignition source is placed at the center of the second car of a 4-car rolling stock with open wide gangways. The ignition source is moved from the end of the carriage to the center, since there are more combustible items, in the form of seats around the ignition source, at the center of the carriage. In addition, fire spread to adjacent carriages would be delayed in the case where the ignition source is moved to the center of the carriage.

The predicted heat release rate variation shows that there are two peaks during the course of this incident. The flames spread and the fire develops gradually within the first 13 minutes from the ignition. At the 13th minute, all the seats in the incident carriage are involved in fire, and the flames spread in both directions on the floor. The first window failure is also predicted in this minute. One of the windows at the center of the incident carriage fails at the 13th minute. This is followed by the failure of three other windows within the next minute, leaving two broken windows on each side of the incident carriage. The peak heat release rate is predicted to be 4.5MW in this interval.

At the 15th minute from the ignition, the remaining pair of windows at the center of the incident carriage and the pair of windows above the folded seats fail due to high temperature. The failure of windows assists ventilation of heat and smoke from the incident which reduces the intensity of the fire. From the 15th minute and onwards, the fire on the floor starts to spread in the downstream direction towards the third carriage. However, the seats at the center of the incident carriage starts to burn-out, which prevents a significant variation in the heat release rate.

It is predicted from the simulation that just after the 16th minute from the ignition, the pair of large windows at the downstream end of the incident carriage fail. From the 16th minute, the flames on the floor do not propagate further in downstream direction, however, continue to burn steadily until the 19th minute. From the 19th minute to the 23rd minute, the fire on the floor in the downstream direction dies out gradually.

The simulation shows that from the 23rd minute and onwards, the flames on the floor start to spread in the upstream direction towards the first carriage. The flames reach to the first carriage and the pair of seats closest to the incident carriage are involved in the fire at the 25th minute. The second peak in the heat release rate is predicted at the 27th minute, at which the flames cover the half of the incident carriage in the upstream direction and spread to the seats of the first car at its downstream end. The simulation shows that all the windows in the upstream half of the incident carriage fail between the 26th minute and the 27th minute. Once again, multiple window failure reduces the intensity of the fire and the rate of heat release. The peak heat release rate is predicted to be 5.5MW for this incident.

The variation of heat release rate for this incident and its comparison to the initial case simulated are given in Figure 6.4.

The fire development in the rolling stock, illustrated with the burning rate of the combustible surfaces, is given in Figure 6.5.

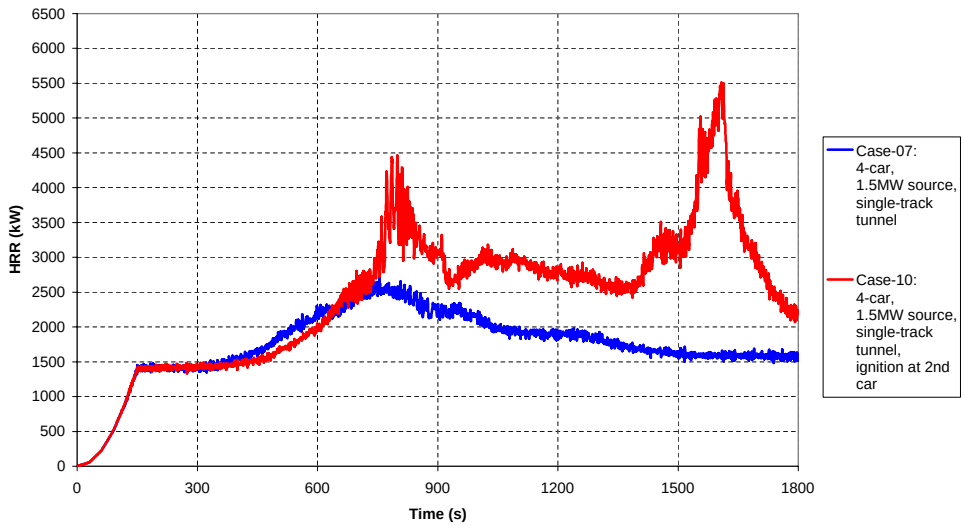

Figure 6.4: Heat release rate, 4-car, 1.5MW source, single-track tunnel, different ignition locations

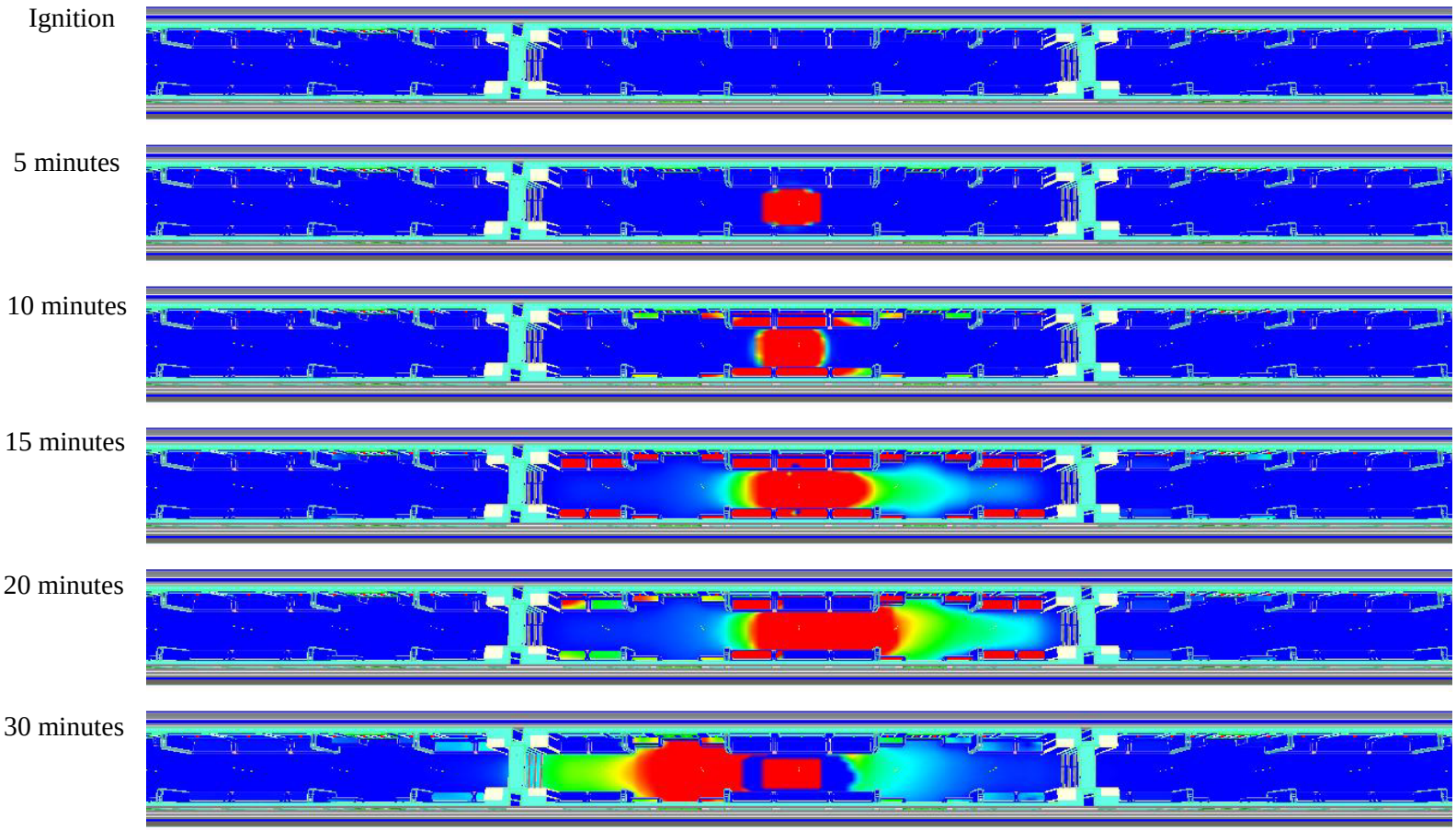

Figure 6.5: Fire spread, 4-car, 1.5MW source, single-track tunnel, ignition at second car

6.4 THE IGNITION SOURCE CHARACTERISTIC

It has been predicted from the simulations that for the fire to develop within the rolling stock, a powerful ignition source that is intense enough to ignite combustibles in the premises of ignition location is required. However, the selected baggage fire ignition source, reaching a peak heat release rate of 1.5MW in three minutes, could be considered as severe by some authorities. Consequently, a sensitivity case is simulated using a slightly relaxed ignition source.

The new ignition source follows a fast growth rate as the baggage fire source, however the peak heat release rate is defined to be 1.0MW, reached at 2.5 minutes from the ignition. The peak heat release rate of the ignition source remains constant at 1.0MW for 4.5 minutes. The source is then set to decay exponentially from 7 minutes and onwards. The heat release rate variations of the 1.0MW and 1.5MW ignition sources are given in Figure 6.6 for comparison.

A fire incident incorporating the new ignition source is simulated using the 1-car model in the single-track tunnel. This case is selected since the highest peak heat release rate is predicted for this particular case and conditions for flashover were achieved with the 1.5MW baggage fire ignition source. This case is labelled as Case-11a.

In the simulation, all the parameters including the ignition source area are set identical to the values defined in Case-05, except the growth curve of the ignition source. Consequently, the peak value of heat flux per unit area is 500 kW/m^2, when the ignition source reaches its peak heat release rate.

It is predicted from the simulations incorporating 1-car model in a single-track tunnel that the fire development and flame spread within the carriage result in similar patterns for both of the ignition sources. Figure 6.7 shows the variations of heat release rate for both cases, incorporating an ignition source with a peak heat release rate of 1.0MW and 1.5MW, for comparison.

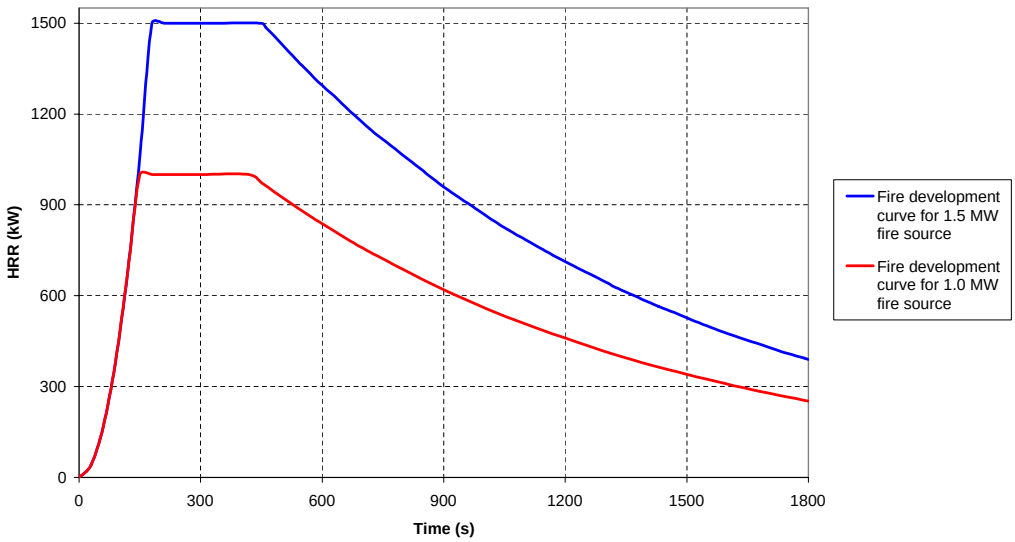

Figure 6.6: Comparison of fire development curves for ignition sources reaching 1.0MW and 1.5MW

Consequently, the new ignition source, reaching a peak heat release rate of 1.0MW, delivers almost the same conclusions derived from the simulations incorporating the 1.5MW ignition source. It can be concluded that the severity of the assumed baggage fire ignition source is comparable to the new source with peak heat release rate of 1.0MW, which is more readily accepted by the authorities.

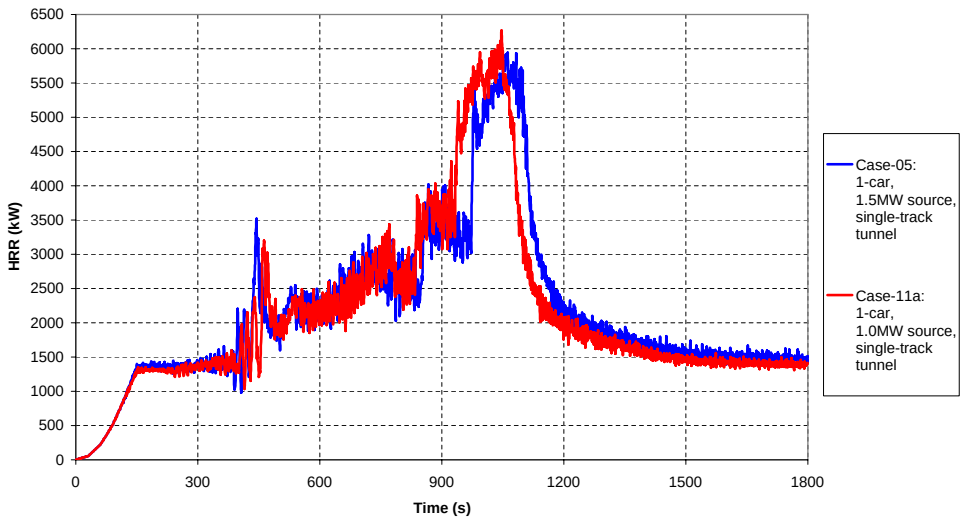

Figure 6.7: Heat release rate, 1-car, single-track tunnel, 1.0MW and 1.5MW sources

In the event of a fire incident in an underground train, there could be high number casualties and even fatalities. The vulnerability of the underground railway systems made those possible targets for terrorists as much as arsonists. In order to represent a terrorist attack to the underground train, a set of simulations has been performed during which an amount of liquid fuel is assumed to be brought into the rolling stock.

In the cases simulated, the liquid fuel is selected to be gasoline, and the amount of fuel is defined to be between 2.0 and 10.0 liters. The governing equations for liquid fuel, or pool fires, are given in Chapter 2. As noted by the equations, apart from the volume of the liquid fuel, the fuel spill area has a significant effect on the burning duration and the peak heat release rate. A sample calculation with a set of values assumed for volume of fuel and spill area is given below.

$$\rho_{Gasoline} = 740 \ kg/m^3 \quad [10]$$

$$\Delta H_{c,\,Gasoline} = 43.7 \ MJ/kg \quad [10]$$

$$\dot{m}''_{max} = 0.055 \ kg/m^2 s \quad [10]$$

$$\forall = 2.0 \ lt \ ; \ A = 2.0 \ m^2 \quad [Assumed]$$

Mass of fuel:	$\rho_{Gasoline} \cdot \forall = 740 \cdot 0.002$	$= 1.48 \ kg$
Energy of fuel:	$\Delta H_{c,\,Gasoline} \cdot m_{fuel} = 43.7 \cdot 1.48$	$= 64.68 \ MJ$
Mass burning rate:	$\dot{m}''_{max} \cdot A = 0.055 \cdot 2.0$	$= 0.11 \ kg/s$
Heat release rate (HRR):	$\Delta H_{c,\,Gasoline} \cdot \dot{m}_{fuel} = 43.7 \cdot 0.11$	$= 4.8 \ MW$
Burning duration:	$E_{fuel} \ / \ \dot{Q}_{fire} = 64.68 \ / \ 4.8$	$= 13 \ s$

Table 6.1 shows the data set defined in the respective simulations performed. It should be noted that for a fixed volume of liquid fuel, the energy content remains constant. Consequently, the burning duration and the intensity of the fire solely depend on the fuel spill area assumed, provided that the mass loss rate flux ($\dot{m}''$) is constant.

It should also be noted that the free spill of fuel is not allowed and the spill area is limited between 0.5 and 2.0m^2. This is done since, when the area is increased the intensity of the fire increases, which causes the duration of the burning to decrease significantly. Consequently, a range of values are selected in the simulations to represent a reasonable set of parameters for the analysis.

Table 6.1: Data set for incident cases involving liquid fuel

	Case-11b	Case-11c	Case-11d	Case-11e	Case-11f
$\forall$ (lt)	2.0	2.0	2.0	10.0	10.0
A (m^2)	1.0	2.0	0.5	1.0	0.5
m_{fuel} (kg)	1.48	1.48	1.48	7.4	7.4
E_{fuel} (MJ)	64.68	64.68	64.68	323.4	323.4
$\dot{m}_{fuel}$ (kg/s)	0.055	0.11	0.0275	0.055	0.0275
HRR (MW)	2.4	4.8	1.2	2.4	1.2
$t_{burning}$ (s)	27	13	54	135	270

The cases are simulated using the 1-car model in a single-track tunnel, since this case was shown to be the most critical. All the parameters are set to remain as they are defined for Case-05 in the simulations. However, the reaction has changed from the burning of the seat material to the chemical reaction of benzene. This is done to correctly represent the effective heat of combustion and the production of soot and carbon-monoxide from the combustion of the liquid fuel.

The simulations show that a very short duration of burning is not sufficient to ignite combustible items and to sustain burning in the rolling stock, even though the intensity of the fire is high. The variations of the heat release rates for the cases simulated are given in Figure 6.8. It should be noted that since the durations of incidents are short, the timescale in Figure 6.8 is set to be 600s. The predictions of peak heat release rate and the actual burning durations are given in Table 6.2.

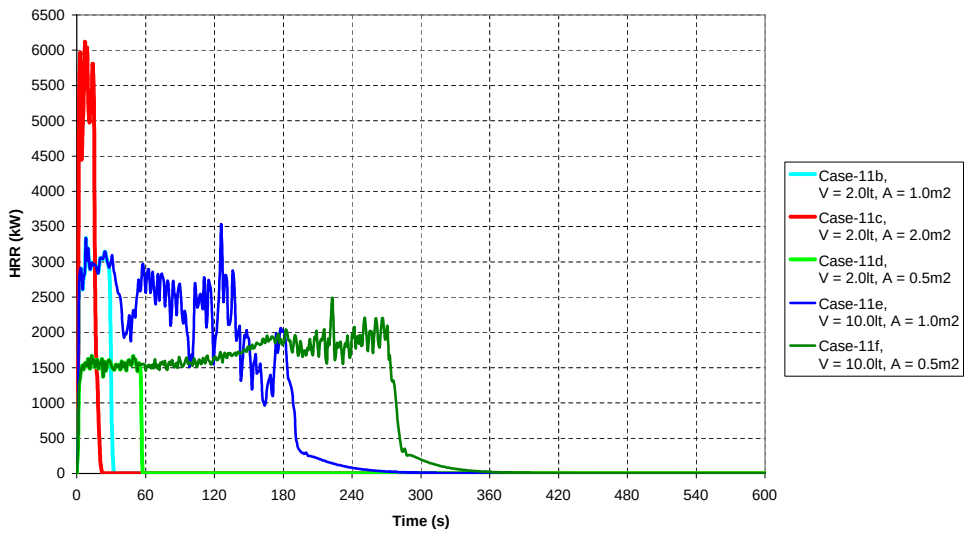

Figure 6.8: Heat release rate, 1-car, single-track tunnel, incidents involving liquid fuel

Table 6.2: Predicted peak heat release rate and duration of fire incidents for cases involving liquid fuel

	Case-11b	Case-11c	Case-11d	Case-11e	Case-11f
Peak HRR (MW)	3.3	6.1	1.7	3.5	2.5
t_{fire} (s)	32	22	58	310	390

The simulations show that the duration of the fire within the incident carriage depends largely on the burning duration of the liquid fuel. This is predicted since the liquid fuel ignition source either is not intense enough to ignite the floor material, or burns for a short period so that the fire on the floor is not sustained.

The fire development, illustrated with the burning rate of the combustible surfaces for Case-11f is given in Figure 6.9. This case is selected since the burning is sustained longer compared to the other cases involving liquid fuel. It should be noted that the fire development is given only for 8 minutes, since the fire dies out within this interval in Case-11f.

Ignition

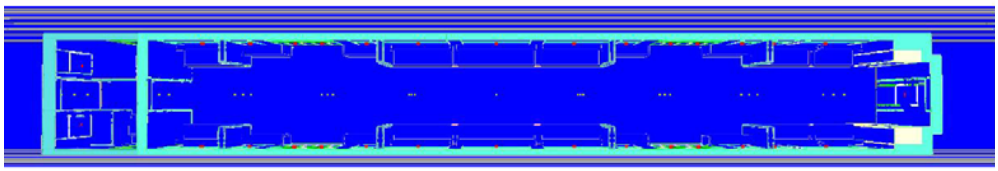

3 minutes

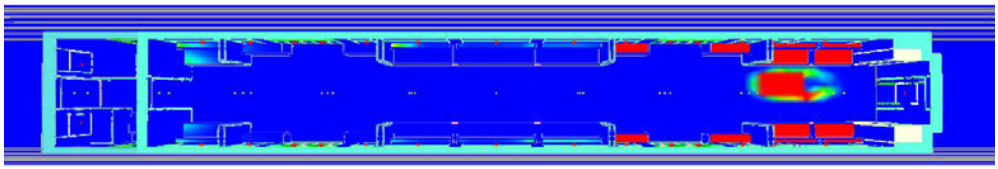

5 minutes

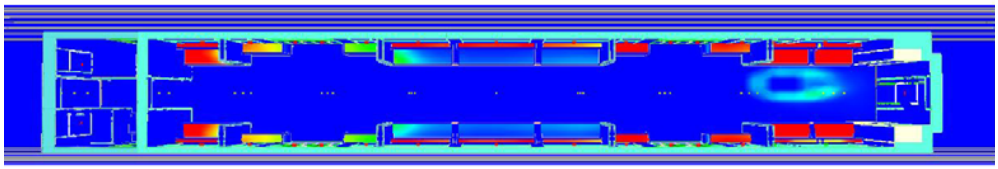

8 minutes

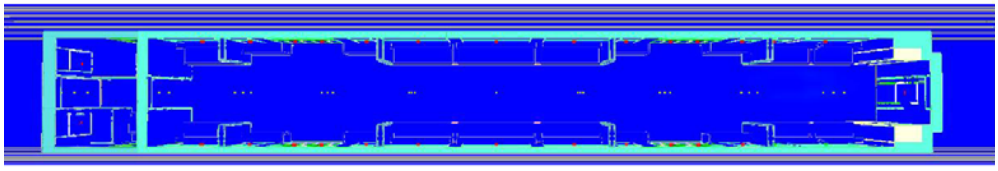

Figure 6.9: Fire spread, 1-car, single-track tunnel, 10lt gasoline fuel spilled to 0.5m^2 area

6.5 THE WINDOW FAILURE

The simulations show that the development of fire within the rolling stock depends strongly on the ventilation of heat and smoke from the incident. It has been found that ventilation could promote the fire development, as discussed in Case-05, or could reduce the intensity of the fire if multiple window failures happen, as discussed in Case-10.

Therefore, two cases have been simulated to investigate the sensitivity of the results to the failure of windows in the rolling stock. The fire development in the 1-car model with only one end door open, and in the 4-car rolling stock with both end doors open are investigated in separate cases.

The 1-car model with limited window failure will be referred as Case-12a. In this case, the heat detectors that measure the temperatures at the center of the inner surfaces of the windows located on the right hand side of the carriage with respect to its direction of travel, and of the window of closed end door are displaced into the windows by 1.0cm.

The FDS simulation results show that the windows with misplaced heat detectors do not fail, since the predefined temperature criterion for failure has not been reached. Consequently, it is found that while the windows on one side of the incident carriage fail, the windows on the other side and the end door window remain intact during the course of the incident. This case could be considered as hypothetical, however, yields different ventilation conditions that would affect the fire development within the rolling stock.

The results show that the fire development and flame spread within the carriage follow the similar trend as in the original case, where windows fail normally, for the first 10 minutes from the ignition.

As the fire starts to develop in the carriage, the seats adjacent to the ignition location are involved in fire within five minutes. In ten minutes all the seats are involved in the fire development, and the fire has started to grow on the floor. Since the high temperature gases are collected at high level within the carriage, all the seats are ignited before all the floor is involved in the fire. After 15 minutes from the ignition, more than half of the floor is involved in the fire. However, the seats adjacent to the ignition location are burnt completely within this interval.

At the 20th minute, the entire floor is involved in the fire development. At that instant, most of the seats located along the midway of the carriage have burnt out in addition to the section of floor next to the ignition location. After 30 minutes from the ignition, it is predicted that all the seats have burnt completely. However, most of the floor has still been burning when the simulation is terminated. The peak heat release rate is predicted to be 3.3MW for this incident.

It is predicted for this incident that before the entire floor has been involved in the fire development, most of the seats have been burnt completely. Consequently, flashover is not predicted for this case.

The results of the simulation show significant differences in the predicted peak heat release rates and the flame spread characteristics compared to the original case with normal window failures. In the case with limited window failure, Case-12a, the rate of increase in the ventilation opening areas, in other words the failure of the windows, is such that the seats burn out faster due to higher temperatures within the carriage and surface heat flux levels that the seats are exposed to. In Case-12a, the rate of burning of the seats does not coincide with the progress of fire spread over the floor. Consequently, lower peak heat release rate and almost steady burning characteristics are predicted. In the case with normal window failure, Case-05, the burning of seats are sustained longer due to lower surface heat flux levels. This results in a rapid increase in the heat release rate, when simultaneous burning of seats and increasing flame spread over the floor are achieved. The window failures in Case-05 assist effective ventilation of the smoke generated by the fire, and promote flame spread within the carriage.

The comparison of the predicted heat release rates for Case-05 and Case-12a are given in Figure 6.10.

The fire development, illustrated with the burning rate of the combustible surfaces, in 1-car model with limited window failure is given in Figure 6.11.

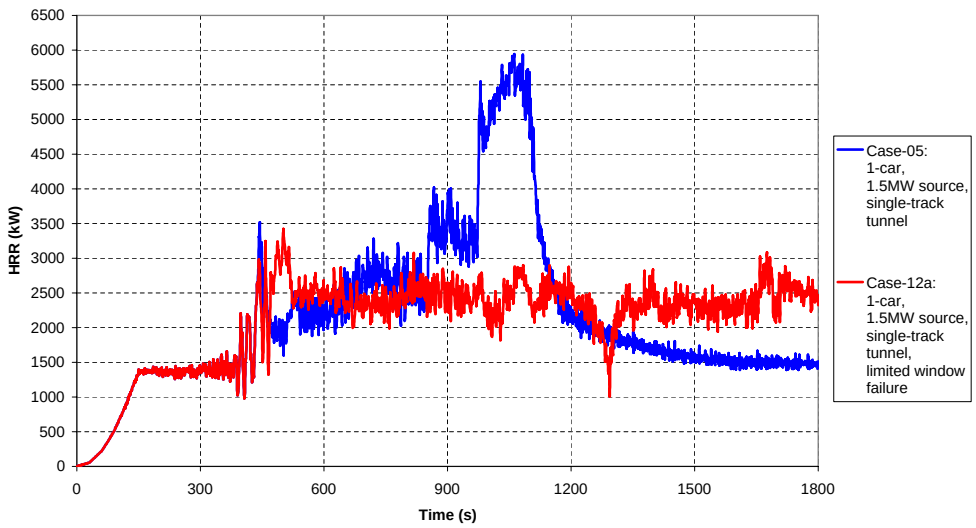

Figure 6.10: Heat release rate, 1-car, 1.5MW source, single-track tunnel, limited window failure

Ignition

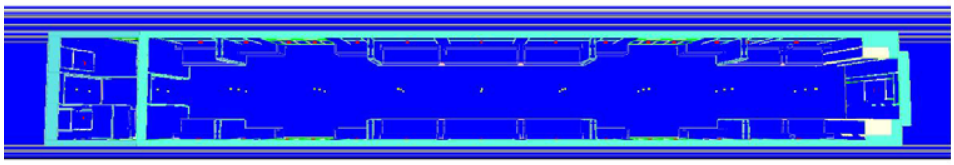

5 minutes

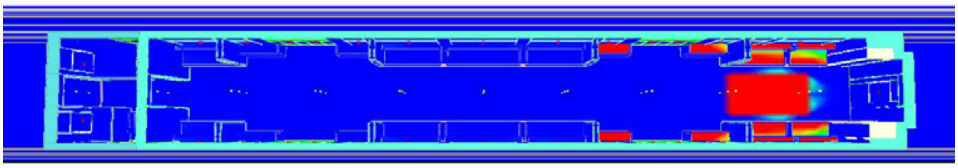

10 minutes

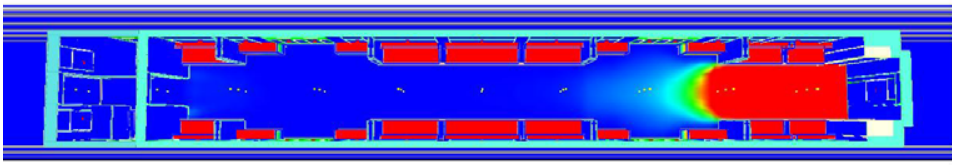

15 minutes

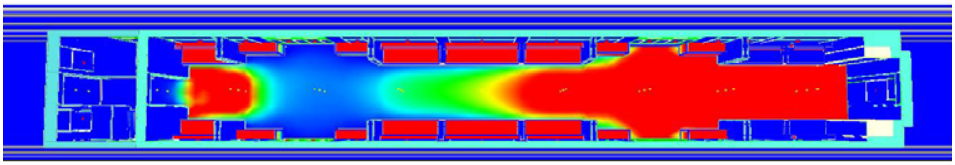

20 minutes

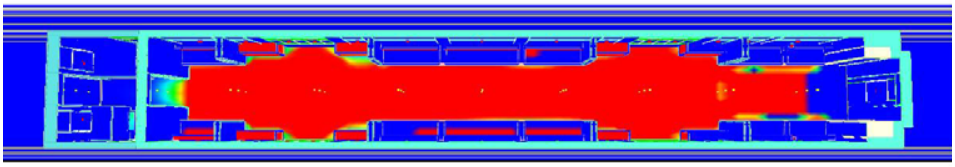

30 minutes

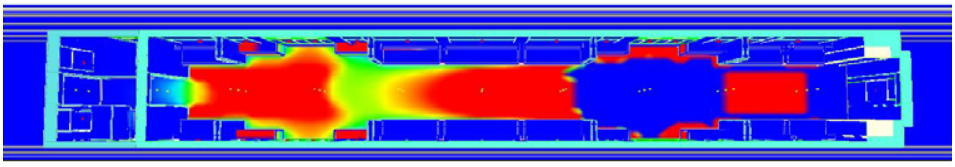

Figure 6.11: Fire spread, 1-car, 1.5MW source, single-track tunnel, limited window failure

The baggage fire incident, i.e. an ignition source following a fast growth curve with a peak heat release rate of 1.5MW, is also simulated in the 4-car rolling stock with limited window failure. The train is defined to stop in a single-track tunnel, therefore the end doors are open for ventilation of smoke and evacuation of passengers. This incident simulation will be referred as Case-12b. In this case, as it was mentioned in Case-12a, the heat detectors on the windows are displaced into the windows by 10cm on one side of the train. Consequently, a group of windows on one side of the rolling stock do not fail since the predefined temperature criterion for failure is not achieved.

The simulations show almost identical fire development and flame spread characteristics for the incidents with limited window failure and with normal window failure for the first 15 minutes from the ignition.

At the 15th minute a pair of large windows and a pair of small windows adjacent to the ignition location fail in the case with normal window failures. No further window failures are predicted for this case.

However, in the case with limited window failure, one large window and a small window adjacent to the ignition source fail within the first 15 minutes from the ignition. This created a slightly different environment within the rolling stock, especially in the incident carriage. It is predicted from the simulation that three more windows, adjacent to the broken ones, in the incident carriage fail at the 19th minute. The simulation shows that additional four windows fail within the following five minutes. The windows fail one by one, approximately at a rate of one window per minute, along the incident carriage towards the driver's cab. From the 24th minute and onwards, no more window failures are predicted for the incident carriage. However, two more windows, closest to the incident location, in the adjacent carriage are predicted to fail between the 28th and the 29th minutes. The sequence of window failures assisted ventilation of smoke and provided fresh air entrainment to the incident carriage, which promoted the fire development and flame spread in the rolling stock.

The largest extent of flame spread in the rolling stock is predicted for this case. At 20 minutes from the ignition and onwards, the seats and the floor in the adjacent carriage are involved in the fire development. As the fire develops further in the rolling stock, higher peak heat release rate is predicted in this case compared to the case with normal window failure, where localized burning was observed. With the flame spread over the floor of incident carriage

and the involvement of the adjacent carriage, a smooth increase in the heat release rate is predicted. However, the conditions are in favor of steady burning characteristics rather than the flashover conditions. The peak heat release rate is predicted to be 4.8MW for this incident, and the fire develops to an extent of about one and a half carriage in terms of the surface area involvement.

The comparison of the predicted heat release rates for Case-07 and Case-12b are given in Figure 6.12.

The fire development, illustrated with the burning rate of the combustible surfaces, in 4-car model with limited window failure is given in Figure 6.13.

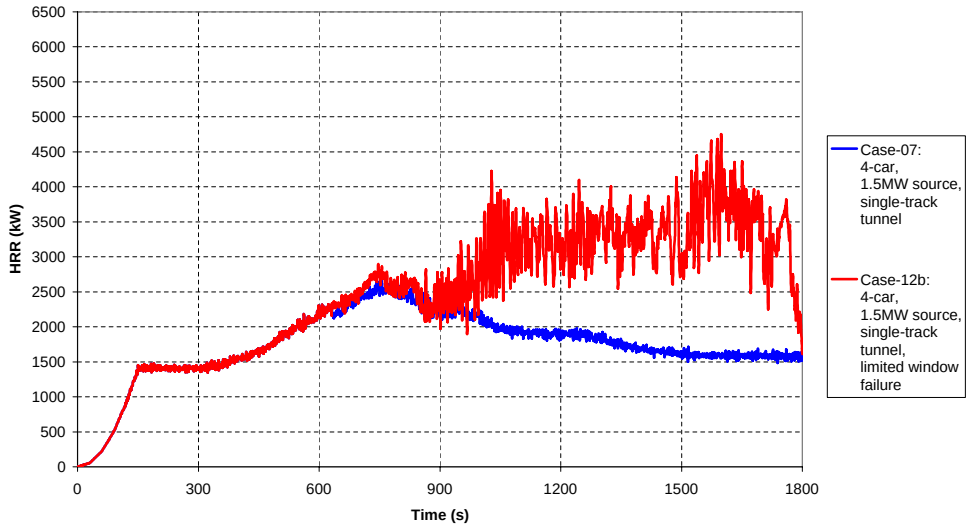

Figure 6.12: Heat release rate, 4-car, 1.5MW source, single-track tunnel, limited window failure

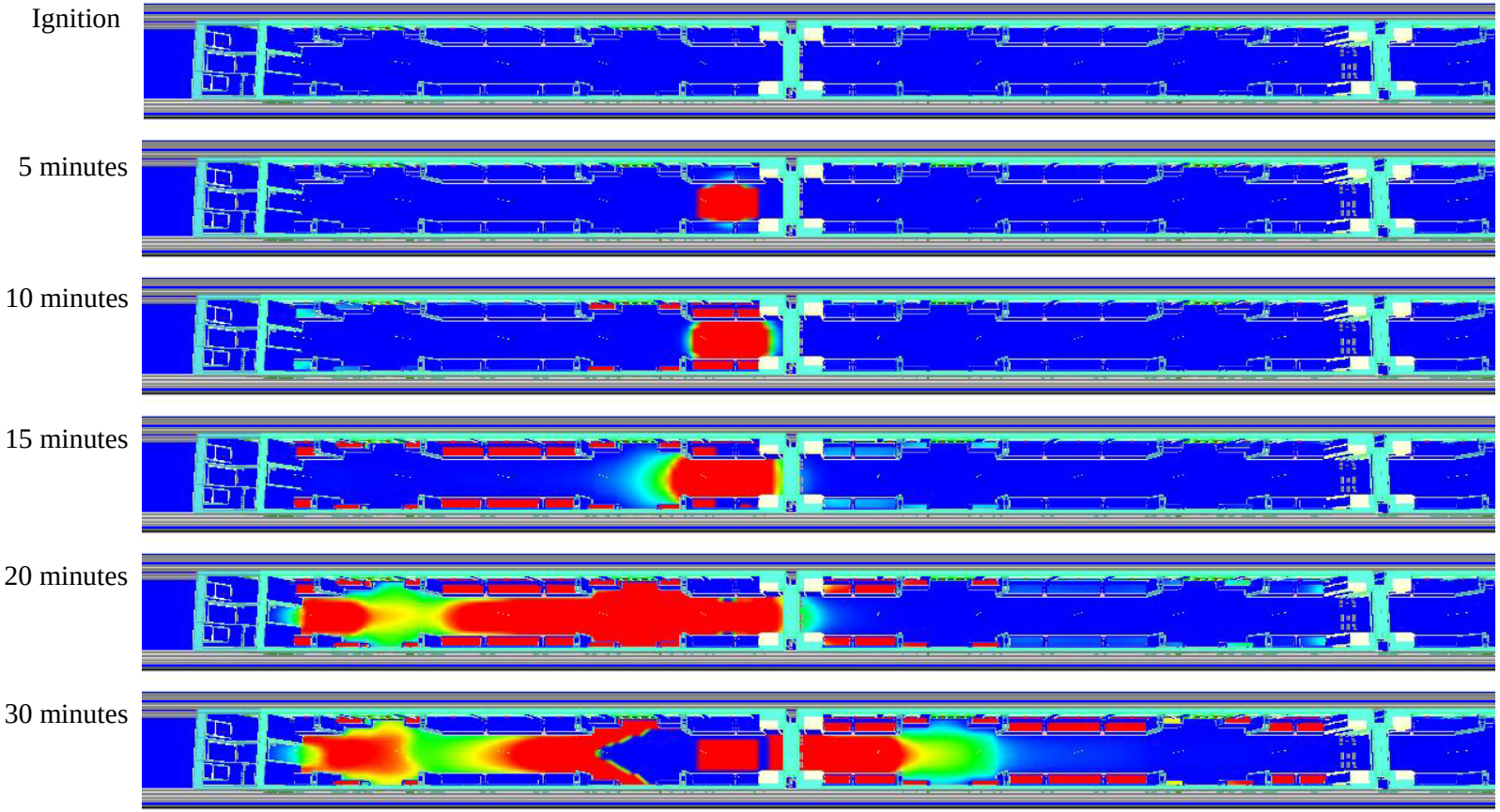

Figure 6.13: Fire spread, 4-car, 1.5MW source, single-track tunnel, limited window failure

6.6 THE NUMBER OF OPEN DOORS

The effects of ventilation on the fire development within the rolling stock have also been investigated through simulations incorporating different conditions at the passenger doors.

The first case is the baggage fire incident in the 1-car model, simulated in the twin-track tunnel section, with all four doors of the carriage defined open. In this case, the end doors are defined to be closed, two of the doors facing the walkway are open for passenger evacuation, and the other two doors are defined to be open to assist the ventilation of smoke generated by the fire. This case is labelled as Case-13a in this thesis.

The fire development and flame spread in the carriage are predicted to be similar to the case in which only two side doors are open (Case-06). The results show that when all four side doors are open, the fire development is slightly delayed. Since the smoke is ventilated more effectively, it takes slightly longer to reach the ignition temperatures of the combustibles within the rolling stock, which results in a slight delay in achieving the peak heat release rate.

The peak heat release rate is predicted to be 2.6MW, which is quite close to the predicted peak heat release rate value of 2.5MW for the case with only two side doors open. However, it takes two additional minutes for the fire to reach its peak size. The peak heat release rate is achieved at 10 minutes from the ignition for Case-13a. The simulations also show that the extent of flame spread for Case-06 and Case-13a are quite similar.

The comparison of the predicted heat release rates for Case-06 and Case-13a are given in Figure 6.14.

It should be noted that opening all four doors in the incident carriage requires additional safety and operational procedures for the evacuating passengers, and is therefore not preferred by the railway operators. Since opening all doors does not provide significant improvement on the predicted design fire size and on the predicted onboard conditions for such an incident, it is not recommended. Figure 6.15 shows the temperature predictions for Case-06 and Case-13a at the center of the carriage at 1.0m and 1.5m above the floor level.

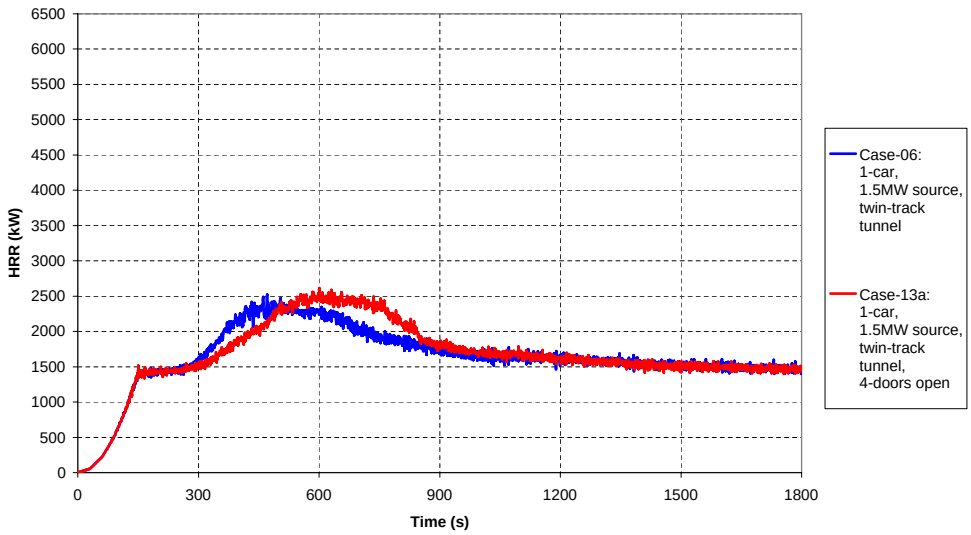

Figure 6.14: Heat release rate, 1-car, 1.5MW source, twin-track tunnel, 4-doors open

The fire development, illustrated with the burning rate of the combustible surfaces, in 1-car model with all four doors open is given in Figure 6.16.

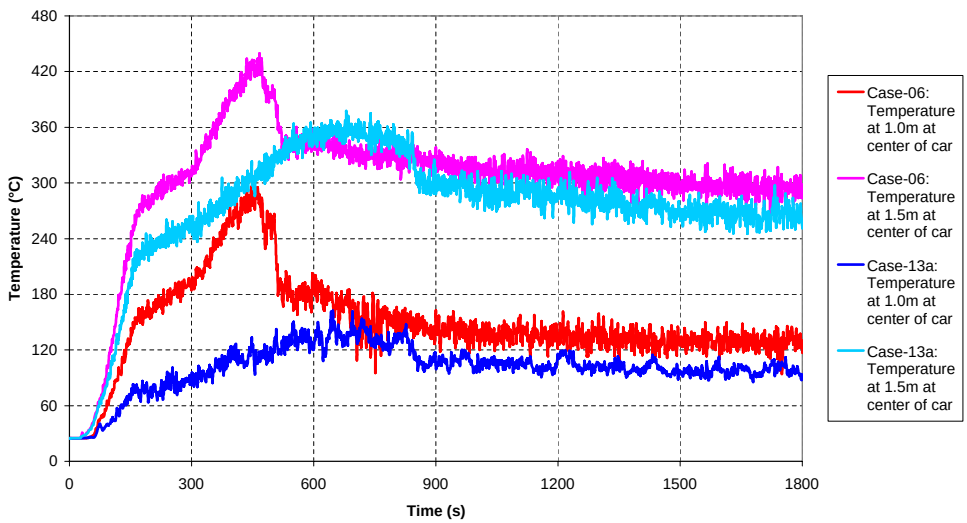

Figure 6.15: Temperature predictions for Case-06 and Case-13a at the center of the carriage

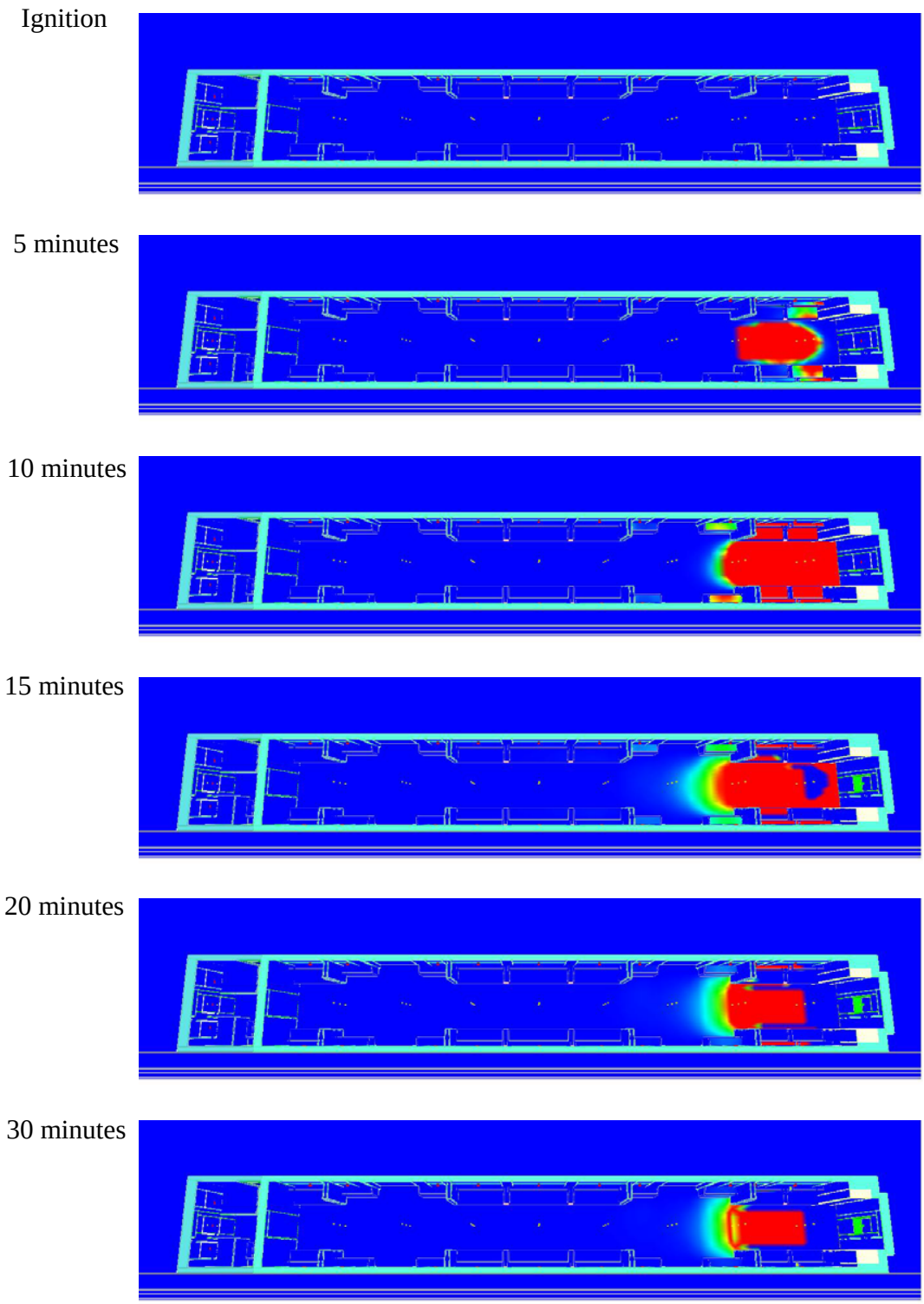

Figure 6.16: Fire spread, 1-car, 1.5MW source, twin-track tunnel, 4-doors open

The results of the simulations reported in this thesis until now show that the fire development and flame spread within the railway carriages strongly depend on the imposed ventilation conditions. Another case has been simulated with all doors of the rolling stock defined closed for the entire duration of the incident. This case has been investigated to predict the fire development within the trains, which would either yield to a developing fire incident due to air entrainment through gradually breaking windows, or die out before spreading due to lack of oxygen within the rolling stock. This case is labelled as Case-13b in this thesis.

In Case-13b, no leakage through the windows or doors is defined, as per the other cases simulated and reported herein. This could be considered as a hypothetical case, however would show how long the fire can survive under limited oxygen levels in the rolling stock during such an incident. In this case, the baggage fire ignition source is placed at the center of second carriage, as described in Case-10.

It is predicted that the fire follows the ignition source heat release rate curve up to 5 minutes. However, the fire starts to decay just after 5 minutes from the ignition. The simulation shows that during the entire course of this incident none of the windows fail since the predefined failure criterion for windows has not been reached. The peak temperature at the windows is predicted to be 405°C, just after the 6th minute from the ignition. The fire is predicted to die out in 13 minutes.

The comparison of the predicted heat release rates for Case-10 and Case-13b are given in Figure 6.17.

In such an incident, since there is no means of smoke extract through doors or windows, smoke fills the entire rolling stock fairly quickly. This obviously results in fatal conditions for the passengers onboard. The simulation shows that the carbon-monoxide concentration levels reach the critical limit of 2000ppm in two minutes in the incident carriage, and within four and a half minutes in the entire rolling stock. The predicted carbon-monoxide concentrations at 1.5m above the floor level at the center of the carriages are given in Figure 6.18. The figure is given only for eight minutes from the ignition since the limiting value for the passengers' life safety has been reached within this time interval.

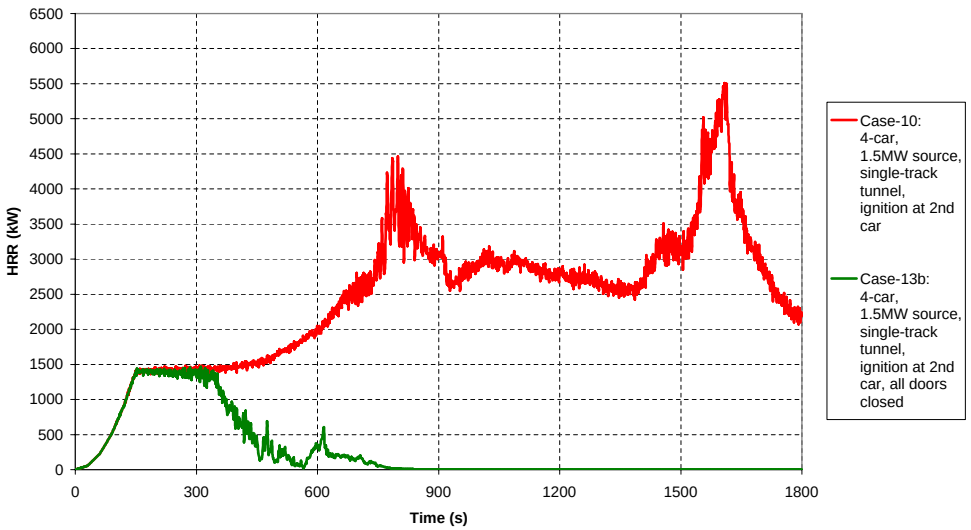

Figure 6.17: Heat release rate, 4-car, 1.5MW source, single-track tunnel, all doors closed

Consequently, closing doors is not recommended when there are passengers onboard. Eventually, during such an incident, even though the doors fail at closed position, human instinct would compel passengers to force open the doors or break windows for smoke extract. On the contrary, this case could represent an incident in the rolling stock parked in an underground depot.

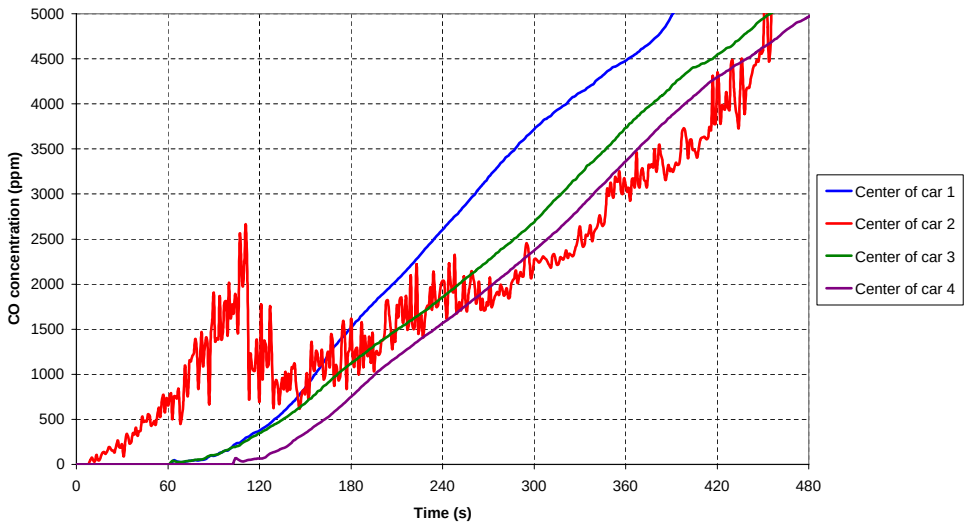

Figure 6.18: Case-13b: Carbon-monoxide concentration at 1.5m above the floor level

In all cases reported herein, except Case-13b, the doors are defined to be open at the start of the simulations, i.e. at time is equal to zero, which is the accepted approach in the industry for similar type of analysis. In principle, once the fire has been spotted in the rolling stock, it should immediately be reported to the driver and to the central control room, who are responsible to stop the rolling stock at the safest possible location and open doors for passenger evacuation, as soon as possible.

However, there might be a short delay in opening the doors in real life situations. Cases 13c and 13d investigate the effects of a delay in opening the doors on fire development and flame spread within the rolling stock.

In Case-13c, the side doors are assumed to be opened at 3 minutes from the ignition. The simulation shows that the fire develops based on the predefined ignition source heat release rate curve for 2.5 minutes. Thereafter, the fire starts to decay due to lack of oxygen within the incident carriage. However, once the doors are opened at the 3rd minute, fire gains intensity as smoke is ventilated and fresh air is brought into the carriage. At the moment the doors open, a sudden peak in the heat release rate is observed. The peak heat release rate is predicted to be 3.5MW, however it lasts only for about 15 seconds. Opening doors causes sudden exchange of heat and mass between the tunnel and the incident carriage, which results in numerical instability for a very short duration. This sudden increase in heat release rate does not affect flame spread, or is not a consequence of flame spread within the incident carriage. The simulation shows that at 3.5 minutes and thereafter the fire development and flame spread are quite similar to the predictions of Case-06, where the side doors are defined to be open at the start of the ignition. The peak heat release rate is predicted to be 2.5MW for this incident, if the sudden increase in heat release rate due to numerical instability is ignored.

The variation of heat release rate for Case-06 and Case-13c are given in Figure 6.19 for comparison.

Another case has been simulated in which the passenger doors are assumed to be opened at 6 minutes from the ignition. This case can be considered as extreme, however could be possible if the communication between the driver and the incident carriage is lost and the doors fail at closed position. This case is labelled as Case-13d in this thesis.

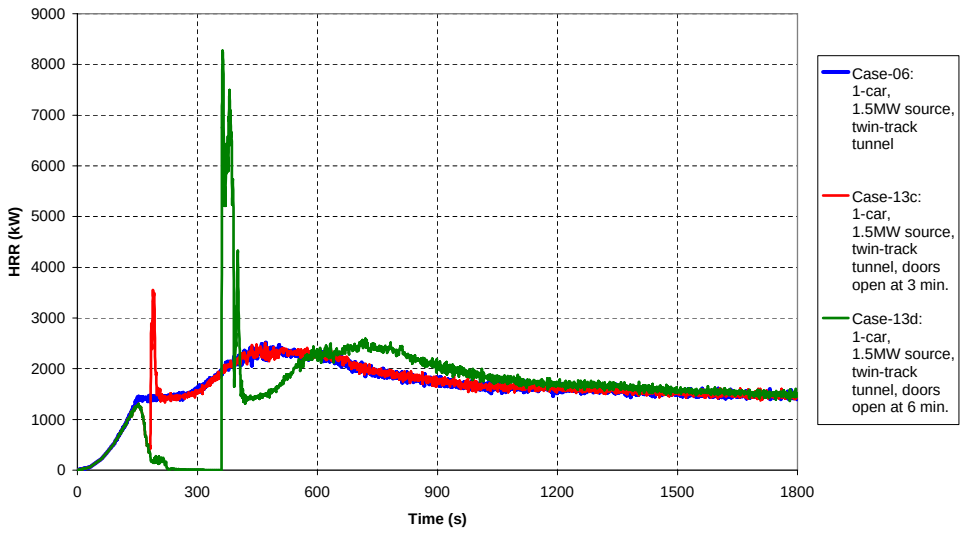

Figure 6.19: Heat release rate, 1-car, 1.5MW source, twin-track tunnel, doors opening at 3 min. or 6 min.

The simulation shows that fire follows the ignition source heat release rate curve for 2.5 minutes, as predicted for Case-13c, after which it starts to decay as the oxygen level in the carriage starts to drop. The fire is predicted to decay within the first four minutes from the ignition. However, within this interval incident carriage is filled with smoke and hot gases generated by the fire. The temperature increases to 412°C at the center of the carriage at 1.5m above the floor level within the first 4 minutes.

The simulation shows that once the doors open, heat release rate suddenly increases to about 8.3MW. However, this peak heat release rate lasts only for few seconds. As discussed in Case-13c, this sudden increase in the heat release rate is due to an instantaneous exchange of the compressed hot gases and smoke between the incident carriage and the relatively fresh air in the running tunnel. The entrainment of fresh air ramps up the fire once again, as instability in the heat release rate is predicted during the very next minute the doors open. The temperature at 1.5m above the floor level at the center of the carriage is predicted to increase to 621°C, just after the doors are opened.

It is predicted from the simulation that the heat release rate from the fire becomes stable after the 7th minute from the ignition, in other words a minute after the doors are opened. Thereafter, the heat release rate is predicted to follow the same trend as predicted for Cases 06 and 13c, with a delay of approximately four minutes. The heat release rate for design

purposes is predicted to be 2.6MW for this incident, if the instability in the heat release rate is ignored. The design heat release rate is predicted to be quite similar to the values in Cases 06 and 13c. However, in Case-13d the design fire size is achieved at the 12th minutes, whereas in Cases 06 and 13c it was achieved around 8 minutes from the ignition.

The variation of heat release rate for Case-13d along with Cases 06 and 13c are given in Figure 6.19 for comparison.

The fire development, illustrated with the burning rate of the combustible surfaces, in 1-car model with doors opening at 6 minutes is given in Figure 6.20. As it can be judged from the fire spread predictions, the sudden increase in heat release rate does not affect flame spread, or is not a consequence of flame spread within the incident carriage.

The simulations show that:

- Opening passenger doors at 3 minutes from the ignition does not have significant effect on the predicted flame spread within the carriage. Once the conditions are restored in the carriage, within 30 seconds of opening the doors, the heat release rate and flame spread are predicted to be quite similar to the case in which the doors are defined open at time is equal to zero.
- Opening passenger doors at 6 minutes from the ignition slightly affects the predicted heat release rate. Once the conditions are restored in the carriage, which takes about one minute after the doors open, the heat release rate follows the same trend as predicted for the case in which the doors are defined open at time is equal to zero. A delay of about four minutes is predicted in achieving the design heat release rate for Case-13d, after the conditions stabilize in the incident carriage.
- In both cases, a sudden increase in the heat release rate is predicted once the passenger doors are opened. This is due to instantaneous exchange of smoke and relatively fresh air between the incident carriage and running tunnel. The conditions are predicted to be restored within a short time in both cases.
- In both cases, the severe baggage fire ignition source causes fatal conditions within the incident carriage. However, the conditions were also predicted to be untenable for the case in which the doors are defined open at time is equal to zero.

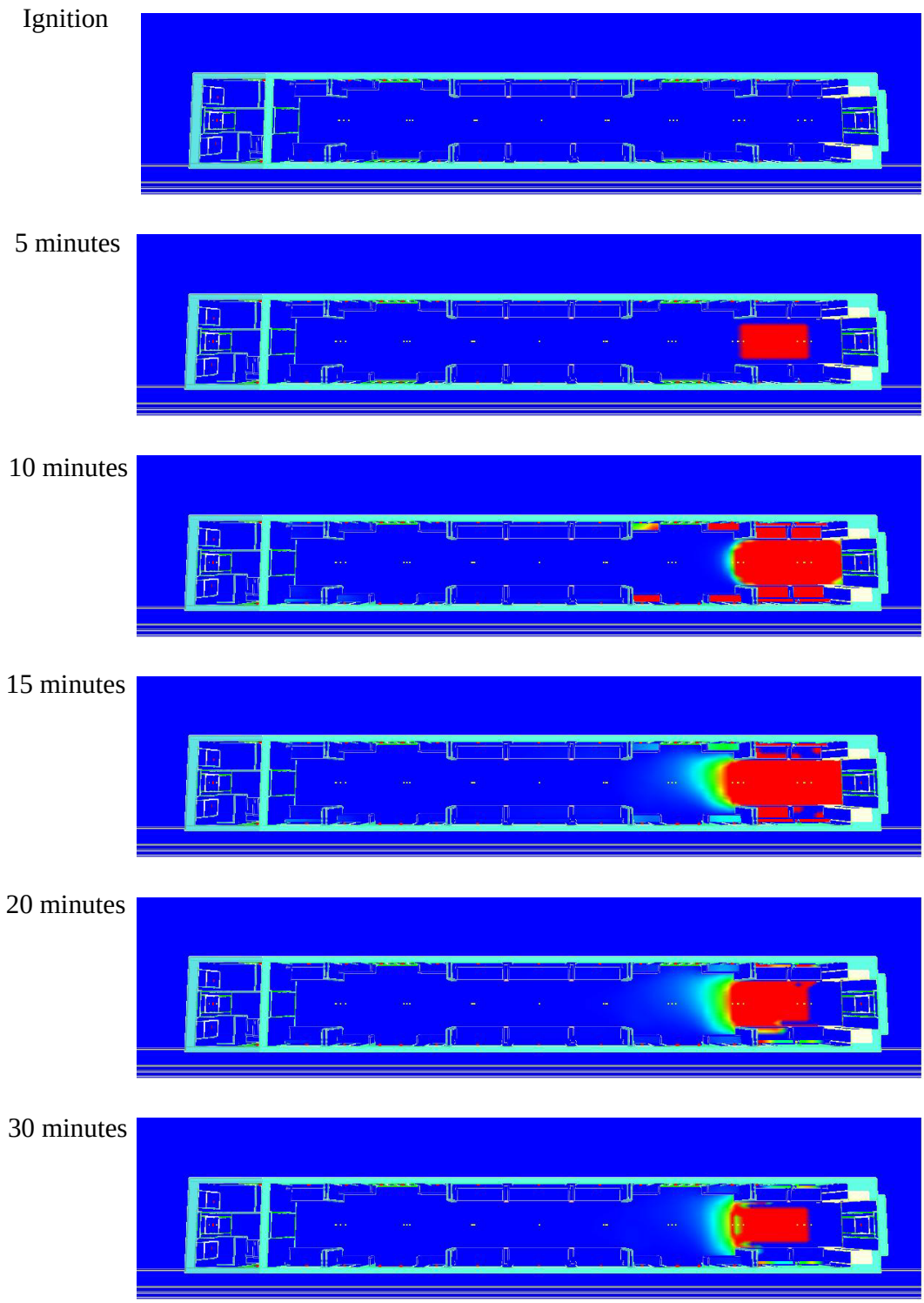

Figure 6.20: Fire spread, 1-car, 1.5MW source, twin-track tunnel, doors open at 6 minutes

6.7 THE MECHANICAL VENTILATION

Another case has been simulated using the 1-car model in the twin-track tunnel with the mechanical ventilation applied at the tunnel end.

It is common practice to provide longitudinal ventilation in the event of fire in the running tunnels. The purpose of the longitudinal ventilation is to push the smoke and hot gases in the downstream direction and to provide smoke-free evacuation path for the passengers in the upstream direction. The direction of ventilation is selected based on the location of fire along the rolling stock, and is applied so that the smoke is ventilated over the shorter length of the train.

The magnitude of the required minimum ventilation velocity to push the smoke only in the downstream direction, also referred as the critical velocity, depends on various parameters including the cross-sectional areas of the tunnel and the train, the height of the tunnel, the gradient of the tunnel, the temperature of the fire site gases, and the design fire size. The relevant equations and the calculation methodology can be found in the paper by Kennedy et al. [2] and in Annex D of NFPA 502 Standard [33].

In the first case simulated, the ventilation direction is defined to be towards the driver cab, since the DMOS type carriage is modelled. The ignition source is selected to be the baggage fire, and the location of the source is kept as defined in Case-06. In the absence of the design peak heat release rate, the critical airflow velocity cannot be calculated. Consequently, an airflow velocity of 2.5m/s is applied at the tunnel boundary as recommended by NFPA 130 Standard.

It is predicted that the fire development and flame spread are quite similar to the case simulated with natural ventilation conditions, Case-06. The smoke is extracted and ventilation is provided through the open side doors, therefore the mechanical ventilation has only an influence on the fire development when the fire spread beyond the side doors area. Consequently, the flame spread in the carriage within the first 10 minutes is almost identical to the case with natural ventilation conditions.

The simulation shows that the large windows at each side of the carriage closest to the ignition source failed at the 6th and the 8th minute from the ignition. The failure of windows increased the amount of smoke extracted from the carriage, but has insignificant effect on the fire development. It is predicted from the results of the simulation that the back end door window fails just before the 10th minute. The failure of the window at back end allows additional smoke extract from the incident carriage. It also allows some fresh air entrainment into the carriage. The longitudinal airflow velocity predictions just before and after the window failures are shown in Figure 6.21. It should be noted that the scale of the longitudinal velocities are defined to be between -2.0 and +2.0m/s in Figure 6.21 in order to clearly indicate the exchange of air and smoke through the back end door window.

The fresh air entrainment through the broken end window could be slightly lower in the actual model of a rolling stock incorporating physically separated carriages, since the adjacent carriage is not modelled and its blockage effect is overlooked in the simulation. However, the results are within the acceptable margin since they predict smoke extract through the end door window, which also confirms that the assumed magnitude of the airflow velocity at the tunnel boundary is reasonable. The smoke extract from the end door window is expected, as is the fresh air entrainment through the same window, in this simulation.

The simulation results show that with the additional fresh air entrainment through the broken end window, the flames propagate further towards the open side doors, compared to the case under natural ventilation conditions. However, the airflow ventilates the smoke effectively so that the overall effect on the peak heat release rate is insignificant. The peak heat release rate for this case is predicted to be 2.7MW. The simulation also shows that the assumed boundary condition of 2.5m/s airflow velocity is sufficient to push all the smoke downstream to create smoke-free evacuation path in the upstream direction.

The variation of heat release rate for this incident and the identical case under natural ventilation conditions are given in Figure 6.22 for comparison.

The fire development in the rolling stock, illustrated with the burning rate of the combustible surfaces, is given in Figure 6.23.

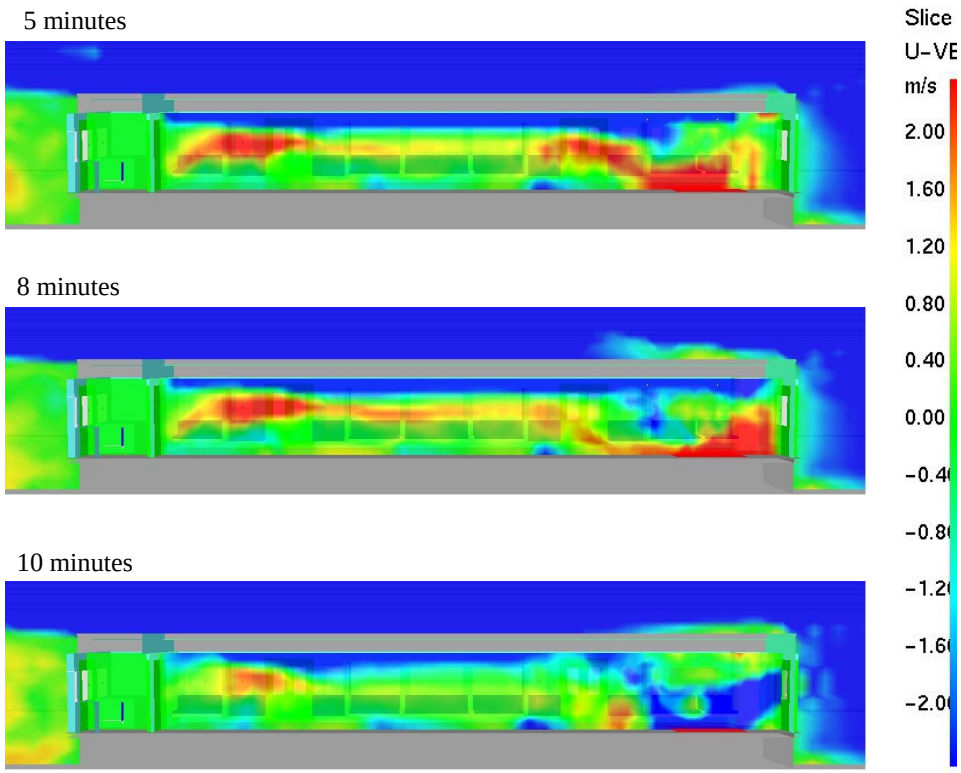

Figure 6.21: Airflow velocity predictions at a longitudinal plane through the center of the incident carriage, 1-car, mechanical ventilation

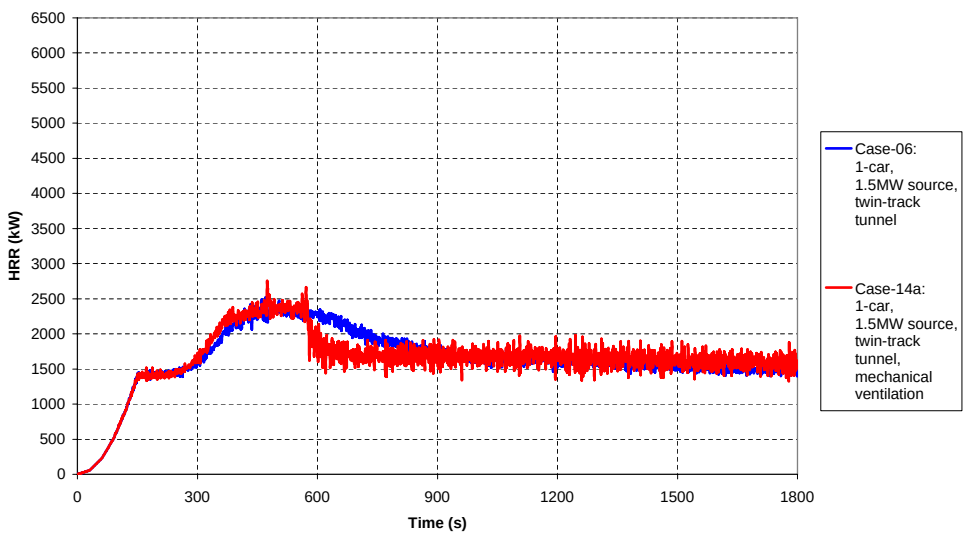

Figure 6.22: Heat release rate, 1-car, 1.5MW source, twin-track tunnel, mechanical ventilation

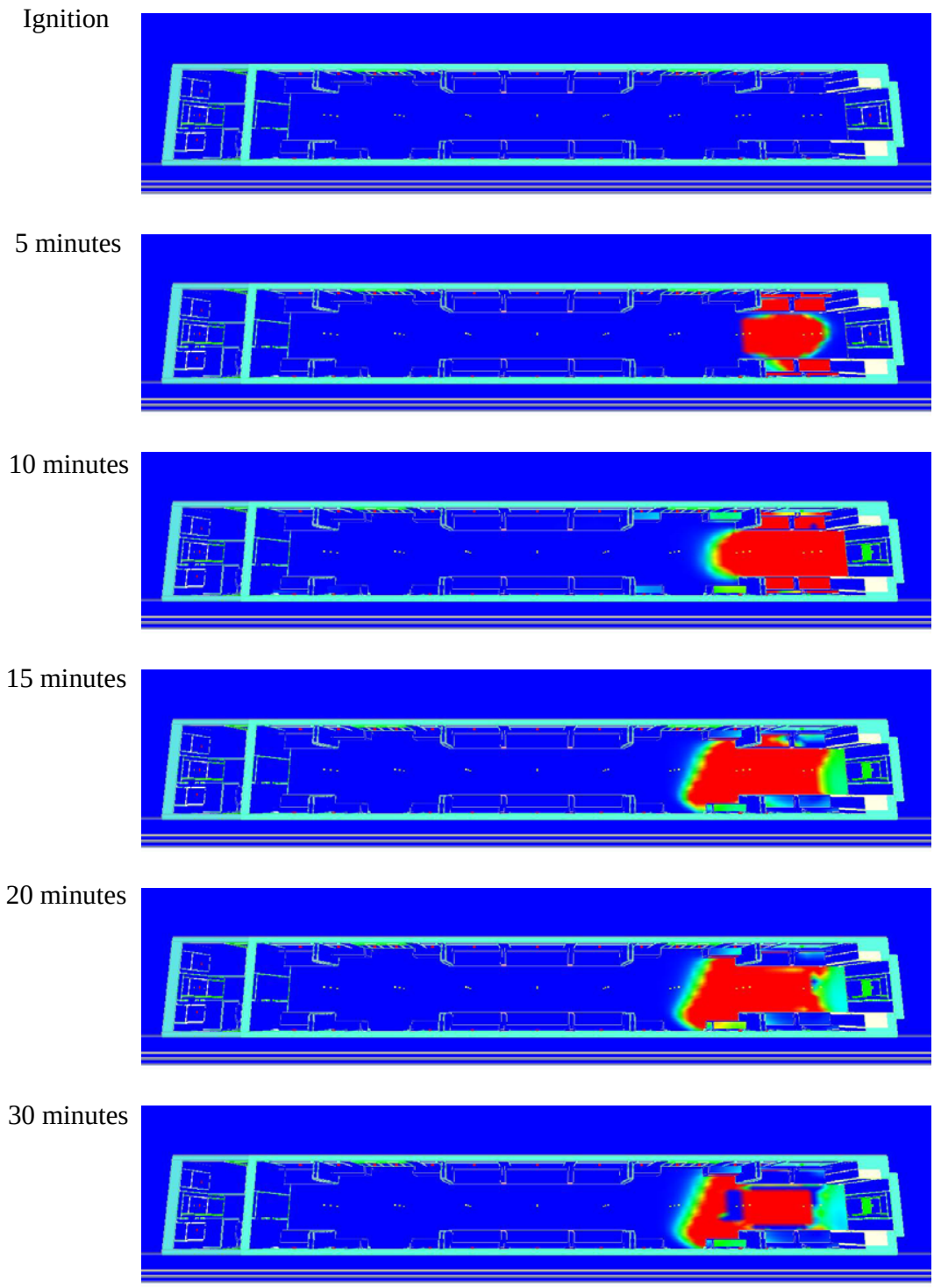

Figure 6.23: Fire spread, 1-car, 1.5MW source, twin-track tunnel, mechanical ventilation

The effects of mechanical ventilation on the fire development have also been investigated using the 4-car rolling stock with open wide gangways. In this case, the incident is simulated in the single-track tunnel, therefore the end doors are defined to be open for smoke ventilation and passenger evacuation. This case is labelled as Case-14b in this thesis.

In Case-14b, open end doors allow airflow to pass through the entire rolling stock from one end to the other. The simulation shows that unlike the other cases simulated, seats adjacent to the ignition source are not involved in the fire development in the initial stages of the incident. The bases of the seats adjacent to the ignition source do not contribute to the fire development within the first 15 minutes from the ignition, therefore the fire development is governed mainly by flame spread over the floor.

The flame spread within the rolling stock is predicted to be only in the imposed airflow direction. The mechanical ventilation, while keeping the temperatures in the incident carriage low enough to delay ignition of the seats, promotes flame spread over the floor in the ventilation direction. However, the fire spread is predicted to be localized due to reduced temperatures and effective ventilation of smoke. The simulation predicts a steady burning behavior with a peak heat release rate of about 2.0MW, reached after 17 minutes from the ignition. The variation of heat release rate for this incident and the identical case under natural ventilation conditions are given in Figure 6.24 for comparison.

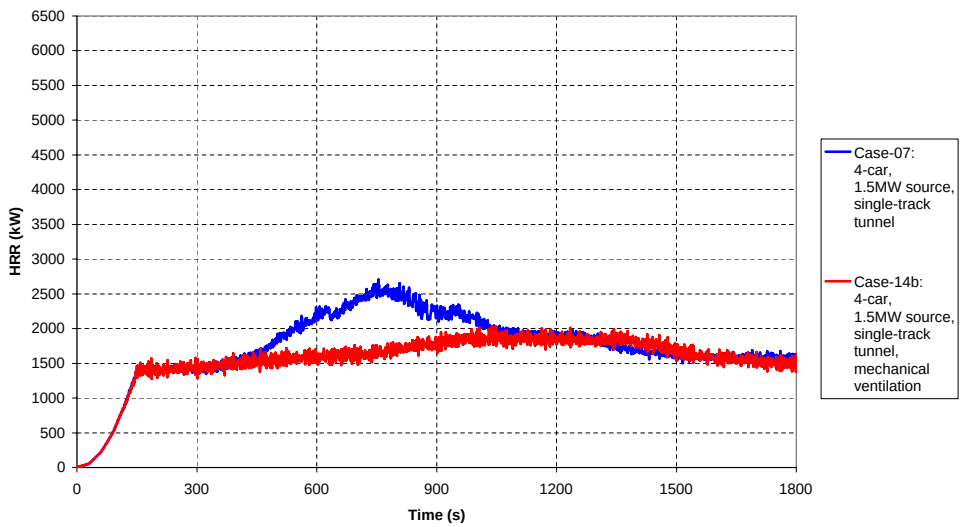

Figure 6.24: Heat release rate, 4-car, 1.5MW source, single-track tunnel, mechanical ventilation

The fire development in the rolling stock, illustrated with the burning rate of the combustible surfaces, is given in Figure 6.26.

The mechanical ventilation has a significant impact on the onboard conditions in the event of a fire incident, especially if the airflow is allowed to pass through the rolling stock. If the ventilation velocity is greater than the critical velocity required to push smoke and hot gases in the downstream direction, passengers would be safe in the upstream direction, not only in the running tunnel but also in the rolling stock. The predictions of temperature and visibility in the rolling stock is given in Figures 6.25 and 6.27, for the selected minutes during the course of the incident. Simulation shows that the predefined velocity at the tunnel boundary is sufficient to maintain tenable conditions in most of the rolling stock.

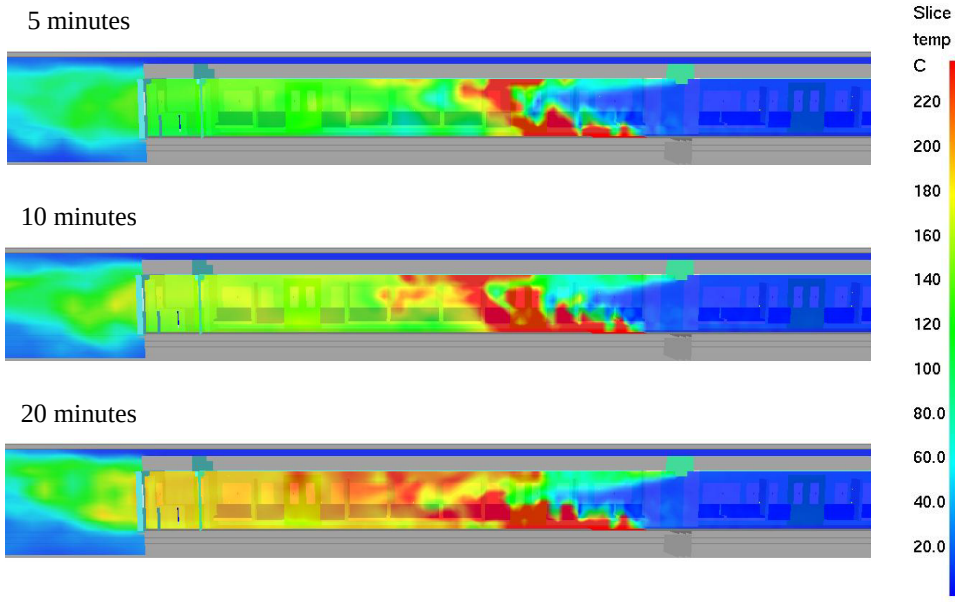

Figure 6.25: Temperature predictions at a longitudinal plane through the center of the rolling stock, 4-car, mechanical ventilation

In Cases 14a and 14b, the mechanical ventilation is activated at time is equal to zero, i.e. at the beginning of the simulation. It is assumed that the train has stopped in the tunnel prior to the fire incident, due to possible congestion or signalling failure, during which the ventilation is provided to cool down the heat released from the brakes of the train to the tunnel.

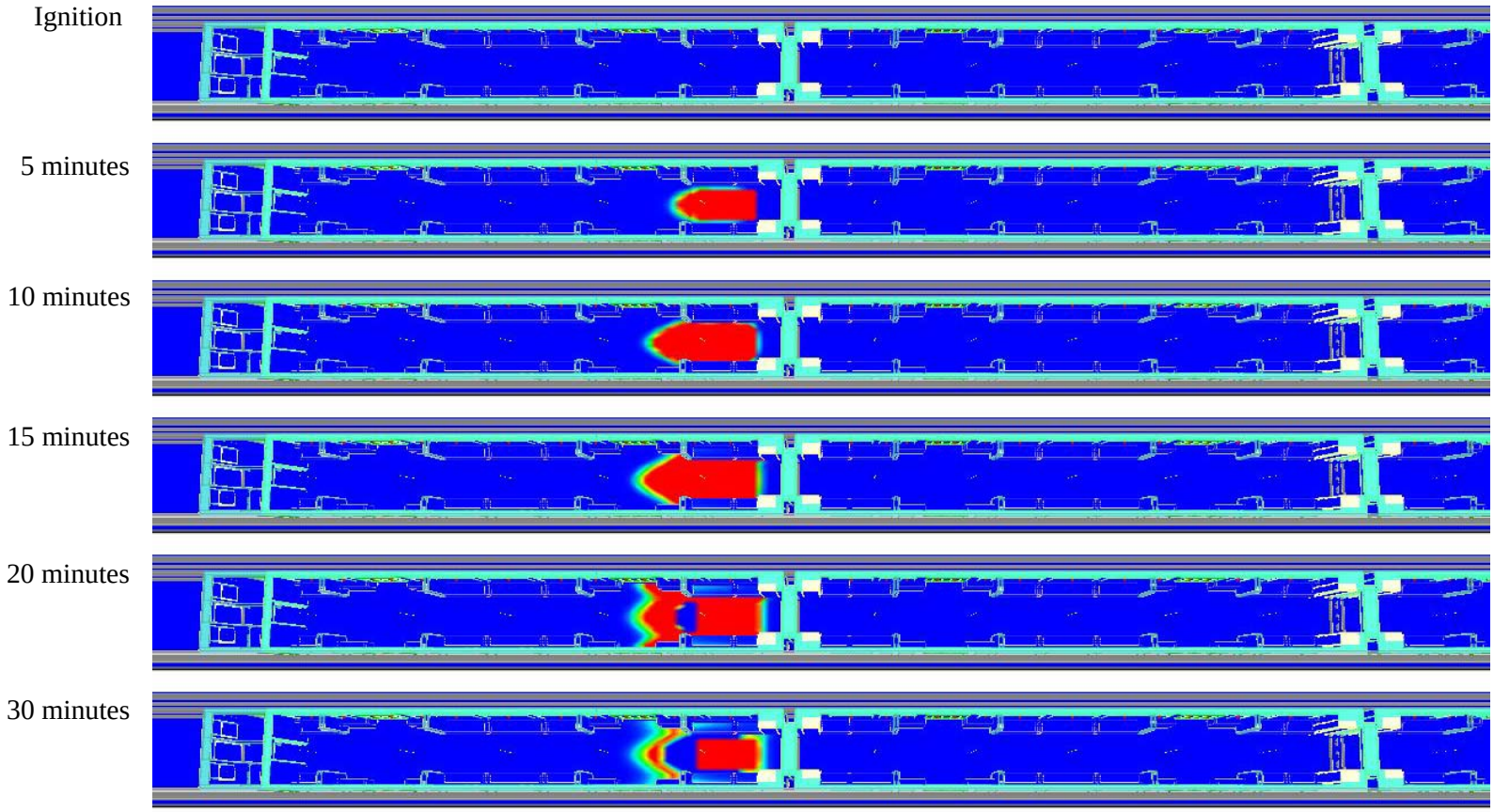

Figure 6.26: Fire spread, 4-car, 1.5MW source, single-track tunnel, mechanical ventilation

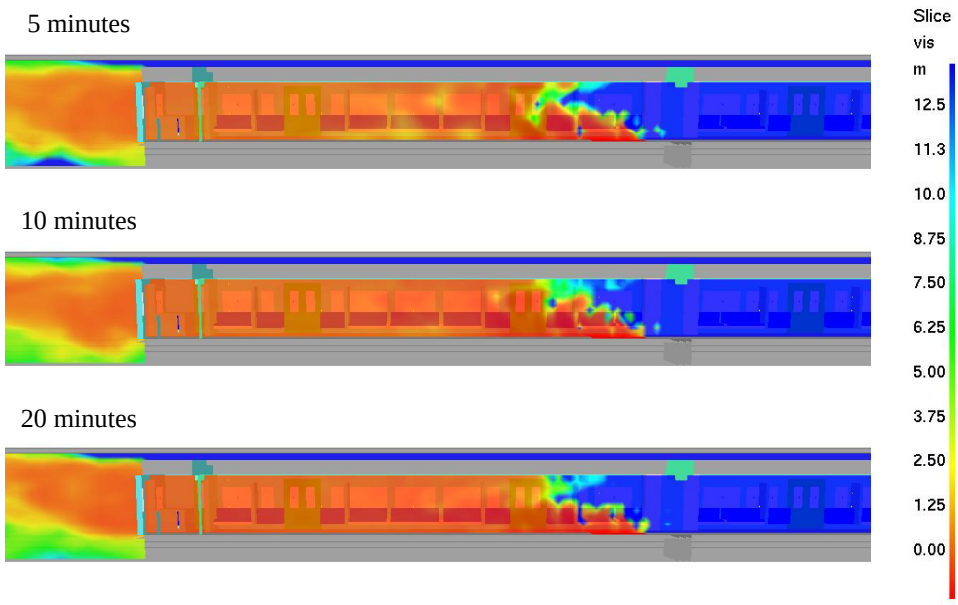

Figure 6.27: Visibility predictions at a longitudinal plane through the center of the rolling stock, 4-car, mechanical ventilation

However, there could be cases where the fire starts on the train, and then the authorities at the control center is informed of the fire, who are responsible for activating the tunnel ventilation system. In such an incident, there would be delay in achieving the required airflow rates in the running tunnel. Although a case has not been simulated to reflect this occurrence, the fire development can be estimated using the predictions of the other cases simulated. In such an incident in the 4-car rolling stock in a single-track tunnel:

- The conditions would be identical to that predicted in Case-13b until the doors are opened.
- Once the doors are opened, fire development and onboard conditions slightly diverge from the predictions of Case-13b and converge towards the predictions of Case-07. In Case-07, both end doors were defined to be open, in agreement with an incident in the single-track tunnel. In addition, natural ventilation conditions were simulated, which could reflect a stage in the incident where the doors are opened for evacuation but ventilation has yet to be activated.
- Once the tunnel ventilation fans are energized, conditions diverge from the predictions of Case-07 and converge towards the predictions of Case-14b, provided that the assumed ventilation velocity matches for both cases.

6.8 MESH SENSITIVITY

The grid cell size is an important numerical parameter in FDS. CFD models solve an approximate form of the conservation equations of mass, momentum and energy on a numerical grid. The error associated with the discretization of the partial derivatives is a function of the size of the grid cells and the type of differencing used.

FDS uses second-order accurate approximations of both the temporal and spatial derivatives of the Navier-Stokes equations, meaning that the discretization error is proportional to the square of the cell size. In theory, reducing the grid cell size by a factor of 2 reduces the discretization error by a factor of 4. However, it also increases the computing time by a factor of 16; a factor of 2 for the temporal and each spatial dimension. Clearly, there is a point of diminishing returns as one refines the numerical mesh.

Two cases have been simulated to investigate the effects of reducing the grid size on the predicted fire development and flame spread patterns during an incident within the underground rolling stock. In the mesh sensitivity analysis, only the cases involving the single carriage model are simulated in order to optimize the time and effort spent on the studies.

The sensitivity simulations showed that ventilation plays an important role on the fire development and flame spread within the rolling stock. Consequently, in the mesh sensitivity studies two extreme cases are simulated. These are:

- An incident in the single-track tunnel with only one end door open for ventilation and evacuation, and no window failure is allowed.
- An incident in the twin-track tunnel with two side doors open for ventilation and evacuation, and window failures are allowed as defined in the initial simulations.

The first of the two cases represents an under-ventilated fire, analysis of which would confirm the peak heat release rate predicted from the simulation with the original grid size. It would also show the extent of flame spread, which would be used to confirm that the progress of flame spread is not under-or-over-predicted when the original grid size is implemented in the simulations.

The second case of the mesh sensitivity analysis involves re-running of Case-06 of the initial simulations with the revised grid size. The initial simulations predicted localized burning

around the ignition location, since the incident was shown to be well ventilated. The initial simulations also predicted window failures that assisted ventilation of smoke. The second case of the mesh sensitivity analysis would confirm the predictions of localized burning and window failures.

Table 6.3 shows the nominal edge lengths in the computational domain in each of the cases simulated during the mesh sensitivity analysis. It should be noted that Case-15a and Case-06 incorporate the original element size that has been used in the initial and sensitivity simulations. Cases-15b and 15c incorporate the refined computational domain, with reduced grid size.

Table 6.3: Labels and nominal edge lengths of the mesh sensitivity cases

	Single-car, one end door open window failures not allowed		Single-car, two side doors open window failures allowed as usual	
Label	Case-15a	Case-15b	Case-06	Case-15c
Longitudinal (x)	0.25m	0.125m	0.25m	0.125m
Across (y)	0.125m	0.125m	0.125m	0.125m
Vertical (z)	0.175m	0.0875m	0.175m	0.0875m

The simulations, incorporating the original grid and the refined grid, of the baggage fire incident in a single carriage with only one end door open show that both simulations predict similar peak heat release rate values and flame spread patterns. However, few differences are predicted in the variation of heat release rate during the course of the incident along with few localized differences in the burning characteristics of combustibles.

The simulation with the refined grid, Case-15b, shows slightly earlier ignition of the combustibles compared to the results of simulation with the original grid size, Case-15a. However, earlier ignition along with predicted slightly faster burning causes combustibles being burnt out quicker than it is found from the simulation of Case-15a. The first difference between the two simulations is predicted between the 4th and the 7th minutes of the incident. Case-15b predicts slightly earlier ignition of some of the seats and a small area of floor adjacent to the ignition location in the downstream direction. This occurrence becomes apparent in the flame spread predictions for two incidents, given in Figure 6.28. However, it should be noted that the overall trend of flame spread predicted for both cases agree reasonably well.

The faster flame spread, predicted by Case-15b, in the initial stages of the fire results in higher heat release rates compared to predictions of Case-15a. The peak heat release rate for Case-15b is predicted to be 2.5MW at 5 minutes from the ignition. The heat release rate decreases between the 5th and the 10th minutes, although the flames continue to progress within carriage in the upstream direction. This is due to the combustibles', which are ignited at the very early stages of fire development, being burnt out within this interval. The heat release rate is found to remain constant at about 1.5MW for the rest of the simulation.

The simulation with original grid size shows slightly smoother transition and slightly longer burning of the combustibles. This results in peak heat release rate being predicted just after the 7th minute from the ignition. When two cases are compared, the flame spread predictions agree very well within the first 10 minutes, with minor exceptions such as a pair of burnt out seats in Case-15b observed at 10 minutes. Slight differences are predicted by 15 minutes and onwards, with slightly larger area of combustibles being involved in fire in Case-15a. However, the trend and the key ignition parameters, such as the ignition of floor near the driver's cab door, the extent of flame spread on floor, and the number of seats involved in fire, largely match between the two cases.

Differences are predicted in the form of burning rates between two cases at and after 20 minutes from the ignition. The burning rates of the surfaces show that in Case-15a a larger area of combustibles is involved in fire, burning at a slower rate, compared to the predictions of Case-15b. The results show that as the mesh is refined a sharper and clearer distinction between the burning items and the burnt out combustibles can be observed. However, with the original element size, the burning rate of combustibles seems to be averaged over the ignited surfaces.

It should be noted that both cases incorporate identical material properties, which were calibrated using a single cone calorimeter model with a fixed grid size that matches with the original grid size used in the simulations. Therefore, in order to get exact results between two simulations of mesh sensitivity analysis material properties, in Case-15b, would have to be re-calibrated using a cone calorimeter with refined grid size. Consequently, the findings are only to be used to assess the robustness of the material properties and the simulation model in predicting the peak heat release rate and flame spread patterns.

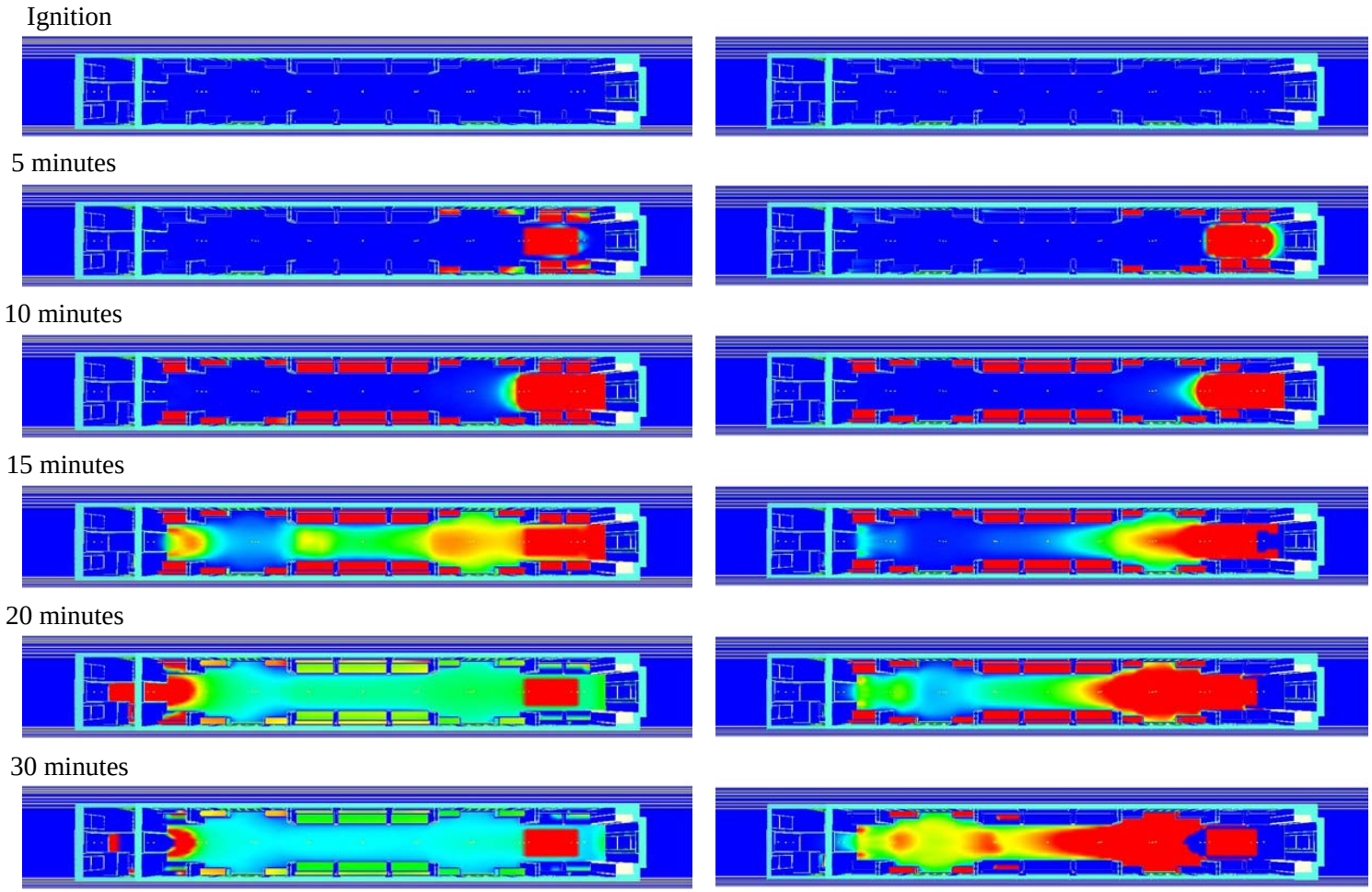

Figure 6.28: Fire spread, 1-car, single-track tunnel, mesh sensitivity analysis, Case-15a (left) and Case-15b (right)

The predicted variations of heat release rate for Case-15a and Case-15b are given in Figure 6.29.

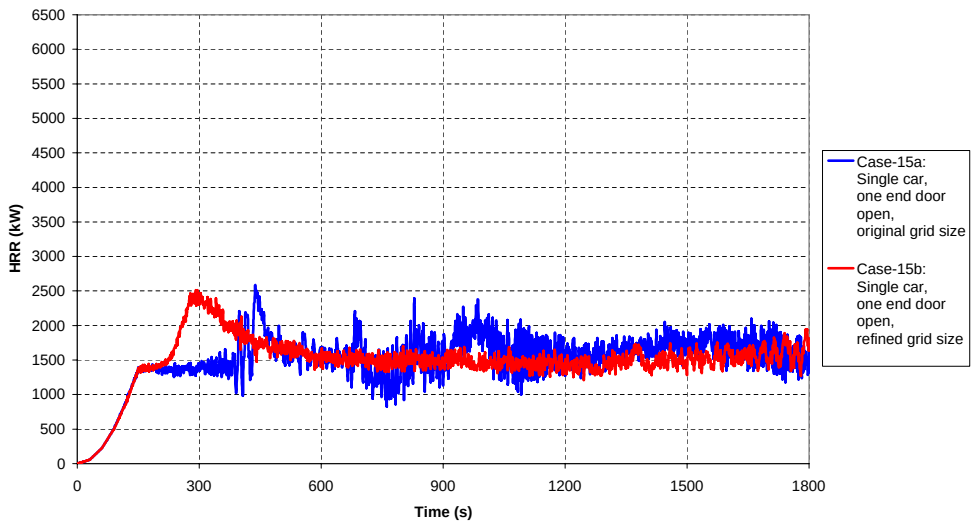

Figure 6.29: Heat release rate, 1-car, single-track tunnel, mesh sensitivity analysis

In the refined grid used in Case-15b, the element sizes have been halved in longitudinal (x) and vertical (z) directions. Therefore, the number of elements in the computational domain is quadrupled. The simulations incorporating the single-track tunnel show that the CPU requirement for Case-15a is about 0.76s/iteration, whereas in Case-15b the requirement increases to 2.53s/iteration. They also show that it takes twice as many number of iterations required in Case-15b to achieve a solution for 1800s. Consequently, it takes about 6.7 times longer to achieve a solution if one uses the refined grid in the simulation involving single-track tunnel.

The second of the two cases of mesh sensitivity analysis involves an incident in the twin-track tunnel. The results of the simulation incorporating the initial grid size are discussed under Case-06, in Section 5.7. The case incorporating the refined grid size is labelled as Case-15c in this thesis.

The simulations show that the trend of the heat release rate curves and the flame spread patterns match well between Case-06 and Case-15c. However, as predicted for the incident in the single-track tunnel, the simulation incorporating the refined grid reacts faster in spreading the flames over the floor and in igniting the passenger seats in the premises of the ignition source. Consequently, in the early stages of the fire development, Case-15c produces greater

heat release rate than Case-06, where original grid size was used. The peak heat release rates are predicted to be 3.0MW and 2.5MW for Case-15c and Case-06, respectively. Although in Case-15c the rate of increase in heat release rate is higher compared to Case-06, the peak heat release rate for both cases are reached within 8 minutes from the ignition.

The simulation incorporating the refined grid size also shows that the decay curve for the heat release rate, just after it reaches the peak value, is sharper than the predictions of the same incident with the original grid size. The slope of heat release rate during the decay period has been affected by the predicted window failures in Case-15c. The results of simulation show that the pair of large windows closest to the ignition source fail around 6 minutes from the ignition, slightly earlier than the predictions of Case-06. Additionally, in Case-15c the window of back end door is also predicted to fail at the 8th minute. The failure of this window increases the effectiveness of smoke ventilation and prevents any further increase in the heat release rate. The temperatures at the face of back end door window were predicted and reported to be just below the failure criterion for the same incident with the original grid size.

Contrary, failure of a small window on one side of the carriage was predicted in Case-06. This failure is not predicted in the simulation with refined grid size due to relatively reduced temperatures around that window caused by the failure of back end door window. Overall, the ventilation opening areas for both cases are predicted to be same.

The predicted variation of heat release rate and flame spread patterns within the incident carriage show quite similar results with minor differences. Despite the differences in the predicted peak heat release rate values and burning behavior of some of the seats, both simulations resulted in localized burning around the ignition source, between the end door and the first pair of side doors.

Figure 6.30 shows the fire development in the incident carriage, illustrated with the burning rate of the combustible surfaces, for both cases. The predicted variations of heat release rates for Case-06 and Case-15c are given in Figure 6.31 for comparison.

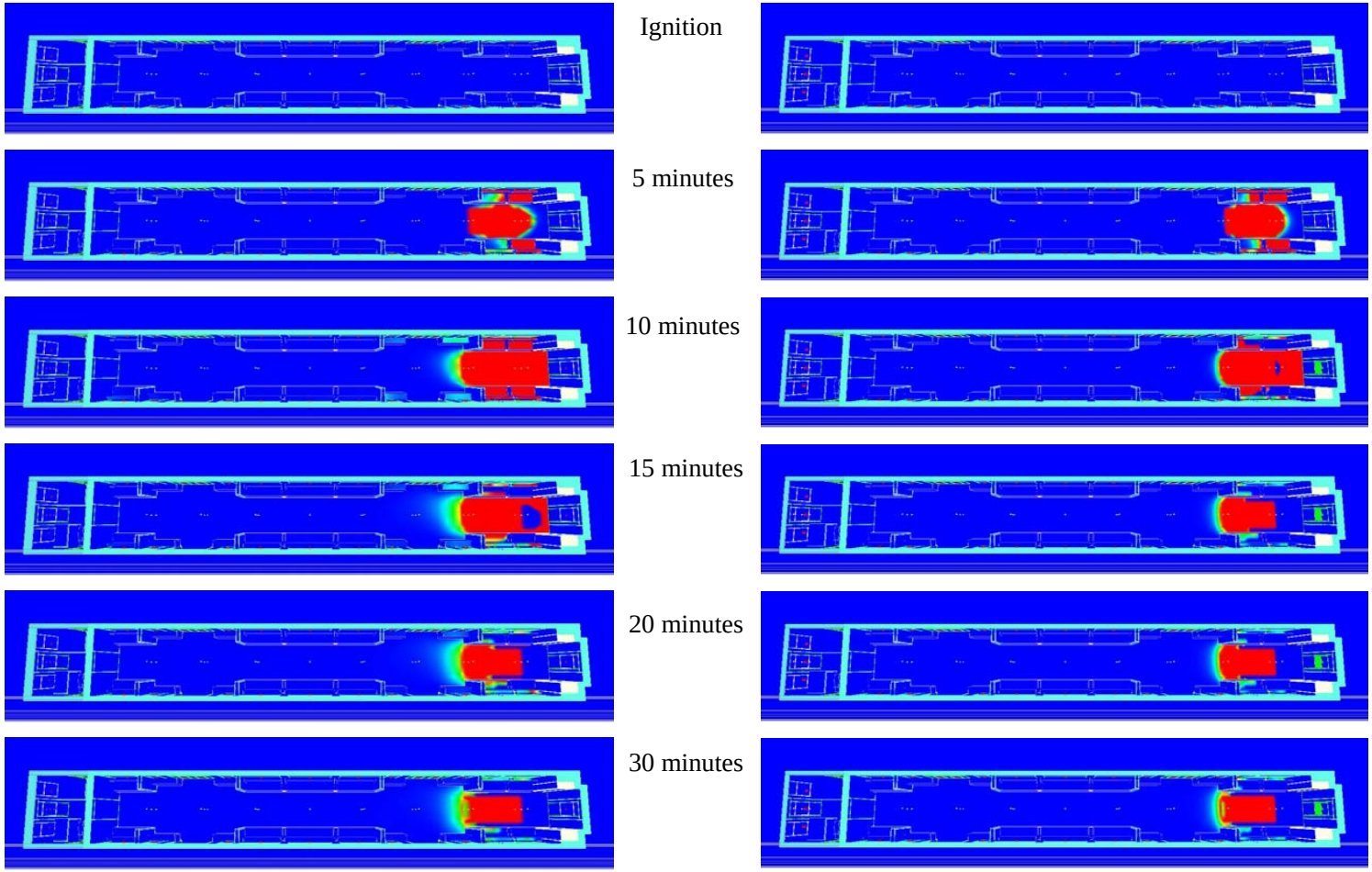

Figure 6.30: Fire spread, 1-car, twin-track tunnel, mesh sensitivity analysis, Case-06 (left) and Case-15c (right)

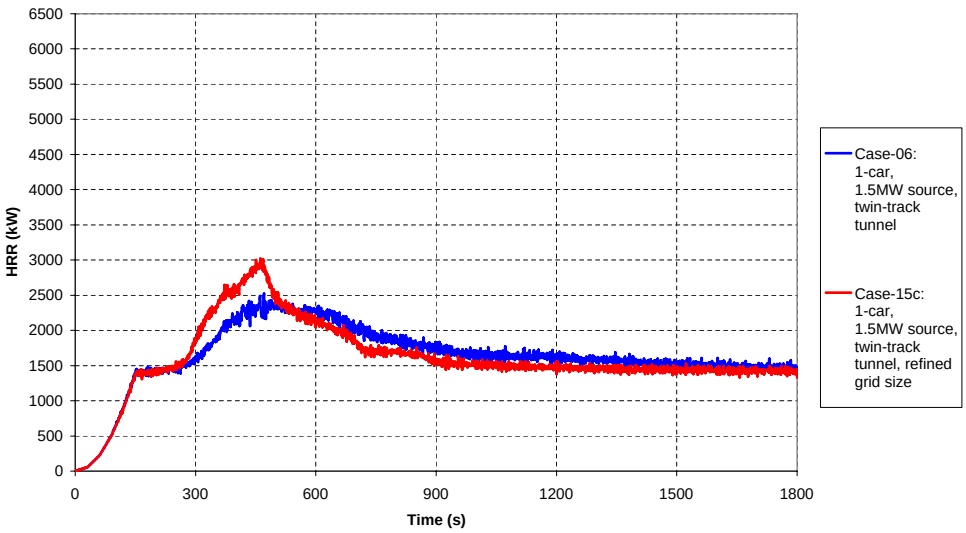

Figure 6.31: Heat release rate, 1-car, twin-track tunnel, mesh sensitivity analysis

The simulations incorporating the twin-track tunnel show that the CPU requirement for Case-06 is about 2.11s/iteration, whereas in Case-15c the requirement increases to 12.10s/iteration. They also show that it takes about 2.3 times the number of iterations of Case-06 to achieve a solution in Case-15c for 1800s simulation time. Consequently, it takes about 13 times longer to achieve a solution if one uses the refined grid in the simulation involving twin-track tunnel.

Once again, the combustible materials used in Case-15c were calibrated through cone calorimeter simulations for the computational cell sizes that are suitable for the grid size selected in the initial simulations. Consequently, there is a slight difference in burning behavior of these materials once the grid size is refined. Additionally, the change in ventilation conditions due to altered instances and locations of the window failures affected the overall flame spread patterns in the case with refined grid. However, the differences predicted between the two cases are within acceptable levels.

It can be concluded that although simulations incorporating refined grid sizes result in slightly altered variations of heat release rate and flame spread patterns, they produce identical trend and similar peak heat release rate values in the expense of significantly increased computational time and effort to achieve the desired solution. Consequently, the results produced by the proposed grid size, which has been used in the initial and sensitivity simulations, are reliable and acceptable.

6.9 CONCLUDING REMARKS FROM SENSITIVITY SIMULATIONS

The initial simulations provided the basic insight on the fire development and flame spread within the two types of rolling stock; incorporating individual carriages, and incorporating a single vestibule with open wide gangways. A further set of simulations has been performed, hereby labelled as sensitivity simulations, to investigate the effects of individual parameters on fire development and flame spread patterns in the underground trains. The parameters include computational variations such as the tunnel length and the grid size, and variations on the boundary and initial conditions such as ignition source characteristics, location of ignition source, and activation of mechanical ventilation.

TUNNEL LENGTH

The simulations incorporating two different tunnel lengths; 40m and 120m, show that increasing the tunnel length has an insignificant effect on the predicted peak heat release rate and flame spread patterns in the event of a fire incident in an underground train. It can be concluded from the results that the predicted variation of heat release rates are almost identical for the incident in the twin-track tunnel, since the smoke extracted from the incident carriage is collected in the tunnel at high level, and the tunnel cross-section is large enough to accommodate the amount of smoke produced during this incident.

However, minor differences are predicted for an incident in the single-track tunnel. Increasing the tunnel length in the simulations, increased the predicted peak heat release rate from 6.0MW to 6.4MW, which corresponds to a 7% increase in value, and shortened the duration to reach the peak heat release rate by 2.5 minutes, from 17.5 to 15 minutes. This is predicted since the cross-sectional area of the single-track tunnel is not large enough to accommodate all the smoke produced by the incident. Therefore in a short tunnel, the smoke is ventilated better through the portals compared to a longer tunnel. The main reason behind the prediction of an increase in the peak heat release rate is the heat feedback from the smoke that is kept longer in the longer tunnel.

Increasing the tunnel length three-fold in the flame spread simulations adds 92 hours of additional computational time for an incident in the twin-track tunnel, and adds 28 hours for an incident in the single-track tunnel. The CPU requirement for the simulations is also predicted

to increase from 0.94s/iteration to 2.19s/iteration, for an incident in the single-track tunnel, and from 2.11s/iteration to 5.85s/iteration, for an incident in the twin-track tunnel. The values correspond to an increase in the computational time by a factor between 2.3 and 2.8 of the initial computational time.

LOCATION OF IGNITION SOURCE

The results of the simulation incorporating an ignition source at the center of the second carriage in a 4-car rolling stock with open wide gangways show that the location of the ignition source has an influence on the predicted variation of the heat release rate. An ignition source located adjacent to an increased amount of combustibles, i.e. at the center of carriage rather than closer to one end, resulted in an increased peak heat release rate value. The instantaneous peak heat release rate is predicted to increase from 2.7MW to 4.5MW, when the source is moved to the center. In addition, the rise in the heat release rate is predicted to continue an additional minute, until the first drop in heat release rate is predicted at the 13th minute, compared to the predicted duration of 12 minutes with ignition source located at one end. The simulation shows that although the heat release rate increases to a greater value, the failure of windows in the premises of the ignition source reduces the intensity of fire. The simulation also shows that the flame spread patterns change direction in parallel with the predictions of window failure. As windows fail, smoke and hot gases are ventilated better in particular sections of the rolling stock, and fire tends to sustain burning through spreading in the other direction where local temperatures are high, until the windows fail in that section as well.

IGNITION SOURCE CHARACTERISTICS

The simulation incorporating a modified baggage fire ignition source, which releases 1.0MW heat at its peak, shows that the fire development and flame spread predictions are almost identical to the ones obtained from the same incident case simulated with the original baggage fire ignition source increasing to 1.5MW at its peak. Therefore, it can be concluded that once the ignition source is powerful enough for the flames to spread and sustain burning, then there are minor variations in the predicted peak heat release rate and flame spread patterns.

The simulations involving up to 10 liters of liquid fuel show that the peak heat release rate and the duration of the fire depend on the intensity of the ignition source, calculated through

volume and spillage area of the fuel. Incident cases with large spill areas resulted in shorter burning durations but higher peak heat release rates, and cases with smaller spillage areas tend to yield smaller peak heat release rates but longer burning durations. This is predicted since a constant volume of fuel is assumed in the simulations, while the effects of the variation in the spill areas on fire development are investigated. The peak heat release rates are predicted to be in the range between 1.7MW and 6.1MW, with burning durations changing from 22s to 390s.

WINDOW FAILURE

The simulations of fire development and flame spread showed that the ventilation openings play an important role on the development of fire and rate of heat released during an incident. It is predicted from the simulation of an incident in the 1-car model, where a set of windows is assumed to be fail-safe, the change in ventilation conditions alter the fire development significantly. While the case incorporating window failures in a normal manner predicting flashover conditions with a peak heat release rate of 6.0MW, the case with limited window failure predicted a steady burning behavior and a peak heat release of 3.3MW. This is predicted due to the change in onboard conditions, which are inevitably affected by the change in smoke extract rate from the incident carriage. The onboard temperatures caused rapid burning of seats in the limited window case, whereas the burning of seats was slower and longer in the case with normal window failure, in which a state of simultaneous burning of seats and floor is achieved resulting in observation of flashover.

Another case simulated using the 4-car rolling stock with open wide gangways showed that the fire is localized around the ignition source when windows are defined to fail in a normal manner. However, for the same incident when a set of windows is set to be fail-safe, fire is predicted to spread to the entire incident carriage and also spread through the open wide gangway to involve about half of the adjacent carriage. Once again, failure of windows alters the onboard temperatures, either decreasing them to a value where flames get weaker and cannot spread, or keeping temperatures at a value sufficient for the flames to sustain burning and spread over the floor in the rolling stock. In the simulations latter is predicted with limited window failure, which resulted in a peak heat release rate of 4.8MW, compared to the value of 2.7MW predicted for the localized incident.

NUMBER OF OPEN DOORS

The simulation of a baggage fire incident within the twin-track tunnel with all four doors defined open shows that the development of fire and flame spread patterns are almost identical to the same incident with only two side doors open. The peak heat release rate for the incident with all four doors open is predicted to be 2.6MW, which is marginally greater than the value of 2.5MW predicted for the case with two doors open. Opening all four doors reduces the predicted onboard temperatures, however, the temperatures still exceed the acceptability criterion within few minutes. Since opening all four doors would introduce additional safety requirements and operational procedures, and does not bring significant improvements to onboard conditions, this option is not recommended.

The simulation incorporating the 4-car rolling stock with open wide gangways, but with all doors closed, showed that the fire follows the heat release rate curve of ignition source for about 5 minutes. The fire is predicted to decay shortly after 5 minutes and burn out completely in 13 minutes due to lack of oxygen within the rolling stock. During this incident, none of the windows are predicted to fail, and therefore no smoke could be extracted from the rolling stock, and no air entrainment is allowed. This case could be considered as hypothetical since obvious fatalities would occur, however the results showed how long the fire can survive under limited oxygen levels, and the importance of air entrainment for the fire to develop.

The simulations incorporating a time delay in opening the doors of the rolling stock during an incident showed that once the conditions are restored, fire development and flame spread patterns converge to the original case with the doors defined open at the beginning of the simulation. Two simulations of the same kind showed that once the doors are opened, there would be a sudden exchange of smoke trapped within the incident carriage and the running tunnel, during which an amount of air enters the carriage to ventilate the fire. In both cases, at that instant a sudden increase in the heat release rate is predicted. The considerable amount of combustion gases' being extracted from the incident carriage within a very short space of time is referred to a phenomenon called backdraft. In the simulations, the instantaneous peak heat release rates of 3.5MW and 8.3MW are predicted for the cases where the doors are defined to open at 3 and 6 minutes, respectively.

MECHANICAL VENTILATION

A set of simulations has been performed to investigate the effects of mechanical ventilation on fire development and flame spread within the underground rolling stock. In the simulations, in the absence of the full data set to identify the required minimum airflow velocity to control the movement of smoke, a mean velocity of 2.5m/s is assumed and applied at one of the tunnel boundaries.

The simulation incorporating an incident within the single carriage in the twin-track tunnel section with mechanical ventilation energized showed that the fire development and flame spread patterns are mostly identical to the case without the mechanical ventilation. The differences between the two cases become apparent once the window of the back end door fails, and air flows through the incident carriage. Until the failure of that window, airflows generated by the mechanical ventilation affect the conditions around the incident carriage, but do not alter the onboard conditions. The effect of the mechanical ventilation is predicted as a drop in the heat release rate, soon after the window of back end doors fails. The peak heat release rate for the incident incorporating mechanical ventilation is predicted to be 2.7MW, which is marginally greater than the value of 2.5MW predicted for the case with no ventilation.

The second of the two simulations incorporating mechanical ventilation involves an incident within the 4-car open train with open wide gangways in the single-track tunnel. The airflows generated by the mechanical ventilation directly affect the fire development and flame spread patterns, since the end doors are defined to be open for evacuation and ventilation. The peak heat release rate is predicted to be 2.0MW in the case where the ventilation is activated. The predicted peak heat release rate is considerably lower than 2.7MW, predicted with no ventilation, since airflows through the entire rolling stock not only reduce the onboard temperatures to impede the ignition of combustibles, but also prevent flames spreading in the upstream direction.

MESH SENSITIVITY

The accuracy of the predicted flame spread patterns and peak heat release rate values has been assessed through mesh sensitivity analysis. Two cases; an under-ventilated and a well-ventilated fire incident; have been simulated with the original and the refined grid sizes, and the predictions have been compared.

The simulations incorporating under-ventilated fire show that the combustible surfaces ignite slightly earlier in the case with the refined grid size. This resulted in the peak heat release rate value to be achieved slightly earlier compared to the same incident, where the original grid size is used. However, the peak heat release rate values are predicted to be quite similar; 2.6MW with the original grid size, and 2.5MW with the refined grid size. Overall, the variation of heat release rates and flame spread patterns are predicted to be similar for both cases.

The earlier ignition and slightly faster burning of the combustible surfaces in the case with refined grid size showed that burning behavior of the combustibles are altered with the change in element size in the computational domain. The material properties used in the initial and sensitivity simulations were calibrated using a cone calorimeter model that had grid sizes compatible with the original grid size used in the simulations. Consequently, refining the grid in the computational domain resulted in sharper responses to ignition and slightly faster combustion. This has become apparent in the flame spread patterns as a clear distinction between the burning and burnt-out items in the case with refined grid, compared to relatively smooth transition of burning of items in the case with the original grid size. However, it should be noted that the case with the original grid size captures all key parameters in the incident with minor differences to the same case with refined grid.

The second incident incorporating a well-ventilated fire showed that the overall variation of heat release rate and flame spread patterns agree reasonably well between the two cases with original and refined grid sizes. However, earlier ignition and slightly faster burning of the combustibles are also predicted during this incident. The changes in the burning behavior of the combustibles due to altered grid size increased the peak heat release rate slightly above the value predicted for the same incident with original grid size. The peak heat release rates are predicted to be 2.5MW and 3.0MW with the original and refined grid sizes, respectively.

In the second incident, both simulations predicted window failures. The case with refined grid size predicted failure of the two large windows in the premises of the ignition source slightly earlier. As the combustibles burn faster, and produce more heat, the temperature criterion for failure of these windows are achieved about 2 minutes earlier than predicted for the same case with original grid size. However, once the conditions within the incident carriage are stabilized, the total area of the ventilation openings are predicted to be the same between the

two cases.

Once again, the solution with the original grid size captures the key parameters of fire development and flame spread within the incident carriage, and represents accurately with minor differences the conditions predicted with the refined grid size.

The simulations show that halving the element sizes in longitudinal direction along the length of the incident carriage and in vertical direction along the height increases the required computational time significantly. The required computational time is estimated to be increased by 6.7 times for an incident in the single-track tunnel, and by 13 times for an incident in the twin-track tunnel.

It can be concluded that the results produced by the original grid size, which has been used in the initial and sensitivity simulations, are acceptable, reliable, and require much less computational time and effort compared to the same incidents with the refined grid size.

Table 6.4 summarizes the sensitivity cases simulated and the peak values of predicted heat release rate in each case.

Table 6.4: Summary of the sensitivity simulations with predicted peak heat release rates

Case ID	Ignition Source Characteristics	Tunnel Section	Rolling Stock Model	Ventilation Openings*	Predicted Peak HRR
Case-09a	Baggage fire on floor, releasing peak heat of 1.5MW following fast-growth curve	Twin-track tunnel (120m long)	1-car representing a train made up of physically separated carriages	2-side doors, on one side of carriage	2.6MW
Case-09b	Baggage fire on floor, releasing peak heat of 1.5MW following fast-growth curve	Single-track tunnel (120m long)	1-car representing a train made up of physically separated carriages	1-end door on the driver's cab end	6.4MW
Case-10	Baggage fire ignition source at the center of the second carriage, on floor	Single-track tunnel	4-car rolling stock, incorporating open wide gangways	2-end doors at each end of the rolling stock	5.5MW
Case-11a	Baggage fire on floor, releasing peak heat of 1.0MW following fast-growth curve	Single-track tunnel	1-car representing a train made up of physically separated carriages	1-end door on the driver's cab end	6.3MW
Case-11b-11f	Liquid fuel ignition source with volumes from 2.0lt to 10.0lt, on floor	Single-track tunnel	1-car representing a train made up of physically separated carriages	1-end door on the driver's cab end	1.7MW - 6.1MW (t_{fire}: 22s to 390s)
Case-12a	Baggage fire on floor, releasing peak heat of 1.5MW following fast-growth curve	Single-track tunnel	1-car representing a train made up of physically separated carriages	1-end door on the driver's cab end (limited window failure)	3.3MW
Case-12b	Baggage fire on floor, releasing peak heat of 1.5MW following fast-growth curve	Single-track tunnel	4-car rolling stock, incorporating open wide gangways	2-end doors at each end of the train (limited window failure)	4.8MW

* This column shows only the initial ventilation openings defined in the input files. The window failures are defined implicitly in all cases, in some of which failures are predicted as reported in the text above.

Table 6.4 Cont'd: Summary of the sensitivity simulations with predicted peak heat release rates

Case ID	Ignition Source Characteristics	Tunnel Section	Rolling Stock Model	Ventilation Openings*	Predicted Peak HRR
Case-13a	Baggage fire on floor, releasing peak heat of 1.5MW following fast-growth curve	Twin-track tunnel	1-car representing a train made up of physically separated carriages	2 doors per side, i.e. all 4 doors of carriage	2.6MW
Case-13b	Baggage fire ignition source at the center of the second carriage, on floor	Single-track tunnel	4-car rolling stock, incorporating open wide gangways	All doors in all carriages are defined to be closed	1.5MW (t_{fire}: 13 min.)
Case-13c,13d	Baggage fire on floor, releasing peak heat of 1.5MW following fast-growth curve	Twin-track tunnel	1-car representing a train made up of physically separated carriages	2-side doors, on one side of carriage (t_{delay}: 3, 6 min.)	3.5MW, 8.3MW (instantaneous)
Case-14a	Baggage fire on floor, releasing peak heat of 1.5MW following fast-growth curve	Twin-track tunnel	1-car representing a train made up of physically separated carriages	2-side doors, on one side of carriage (mechanical ventilation)	2.7MW
Case-14b	Baggage fire on floor, releasing peak heat of 1.5MW following fast-growth curve	Single-track tunnel	4-car rolling stock, incorporating open wide gangways	2-end doors at each end of the train (mechanical ventilation)	2.0MW
Case-15a, 15b	Baggage fire on floor, releasing peak heat of 1.5MW following fast-growth curve	Single-track tunnel	1-car model with refined computational domain grid size	1-end door on the driver's cab end no window failures	2.6MW, 2.5MW
Case-15c	Baggage fire on floor, releasing peak heat of 1.5MW following fast-growth curve	Twin-track tunnel	1-car model with refined computational domain grid size	2-side doors, on one side of carriage	3.0MW

* This column shows only the initial ventilation openings defined in the input files. The window failures are defined implicitly in all cases, in some of which failures are predicted as reported in the text above.

CHAPTER 7

FINAL SIMULATIONS

7.1 INTRODUCTION

The results of initial and sensitivity simulations revealed the variations in fire development and flame spread patterns in underground trains with respect to changes in the initial and boundary conditions, including changes in ignition source characteristics and ventilation conditions. However, in these simulations, the same material properties, which were taken from the previously published research study [20], have been used.

In the final simulations, the material properties proposed for the Class-378 rolling stock will be used. The seats and the floor will remain as the only combustible items in the rolling stock, walls and ceiling of the carriages remain non-combustible. Final simulations will include a set of selected cases, which have been shown to be eminent through initial and sensitivity simulations.

The burning characteristics of the materials proposed for Class-378 rolling stock are acquired through the results of Cone Calorimeter experiments undertaken by Bayer Industry GmbH & Co. laboratories. It should be noted that the raw experimental results are not in the form that can directly be used as input in the FDS simulations.

Consequently, the material properties that would be derived from the Cone Calorimeter experiments should have to be calibrated and rearranged in a form that can be used in the FDS simulations. In order for the material properties to be calibrated, an FDS model of the Cone Calorimeter has been built, simulations have been performed using this FDS model, and the predictions are checked against the experimental results until they reasonably match.

The Cone Calorimeter modelling and the calibrated material properties for the combustibles in the proposed Class-378 rolling stock are discussed in detail in Section C.1 of Appendix C. The final simulation results are discussed in Section 7.2 of this thesis.

7.2 SIMULATION RESULTS

A set of selected cases is simulated using the new set of combustible material properties. The cases are selected based on their eminent predictions during the initial and sensitivity simulations. The findings from the new simulations are summarized in the following Sub-sections.

7.2.1 A TEST CASE; CASE-16: 1-CAR, 1.5MW SOURCE, SINGLE-TRACK TUNNEL

The performance of calibrated material properties during an incident in a rolling stock is tested through a simulation of a baggage fire incident in the 1-car model. This case would be re-simulation of Case-05, and will be labelled as Case-16 in this thesis.

The simulation of Case-16 shows that the seats have not been ignited for the first 3 minutes from the ignition. At 4 minutes, the top section of back of seats closest to the ignition location is predicted to start burning. The flames are predicted to spread to the base of the seats and to the folded seats next to the side doors within the following minute. However, the simulation shows that the seats burn slowly and weakly, i.e. at burning rates much lower than 1.0 g/m^{2}s.

At the 8th minute, the seats closest to the ignition location, and the folded seats next to the side doors, are predicted to burn at their maximum burning rate. The seats at far end of the incident carriage are predicted to start burning at a very slow rate within this minute. Between the 9th and 11th minutes, the fire on the seats, which are ignited at the early stages of the incident, is predicted to die out. From the 11th minute and onwards, the fire starts to spread on the floor, and the seats at the center of the incident carriage become involved in the fire development. The seats at the central section of the incident carriage are predicted to burn between the 11th and the 13th minutes of this incident.

During this incident, the pair of small windows closest to the ignition location is predicted to fail at the 13th minute. This is followed by the failure of a single small window above the folded seats on one side of the carriage at 16 minutes from the ignition.

Fire on the floor is predicted to remain localized around the ignition location and the back end door. The simulation shows that flames spread in the downstream direction from 11 minutes and onwards, but they are not intense enough to make fire spread in the upstream direction towards the open end door.

The peak heat release rate is predicted to be 2.1MW for this incident. The predicted variation of heat release rate during this incident is given in Figure 7.1. The fire development, illustrated with the burning rate of the combustible surfaces is given in Figure 7.2.

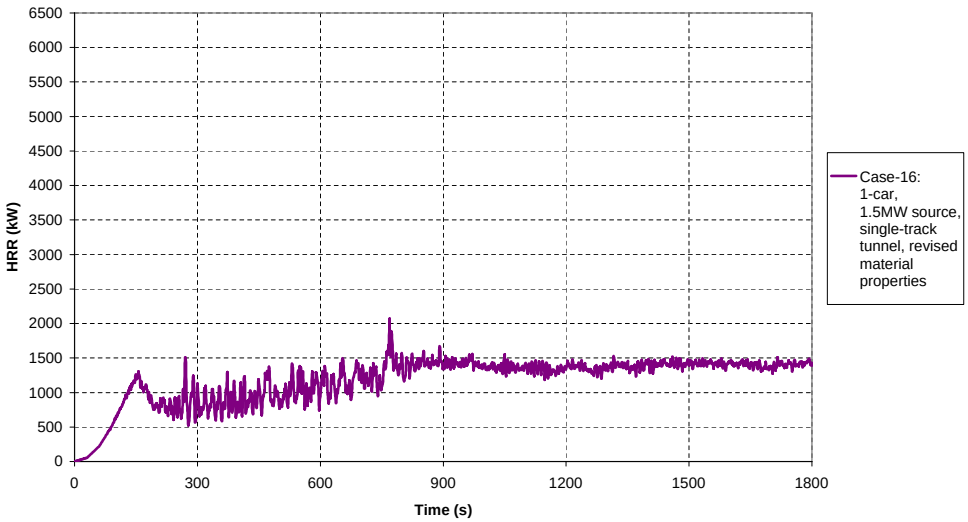

Figure 7.1: Heat release rate, 1-car, 1.5MW source, single-track tunnel, revised material properties

Once the simulation results have been investigated, it has come to attention that the flames from the ignition source are not intense enough to ignite the combustible surfaces within the rolling stock model. In other words, the calibrated material properties are too good to let the combustibles catch fire. This become apparent in the simulation results in terms of delayed ignition of seats, and very localized fire on floor.

Ignition

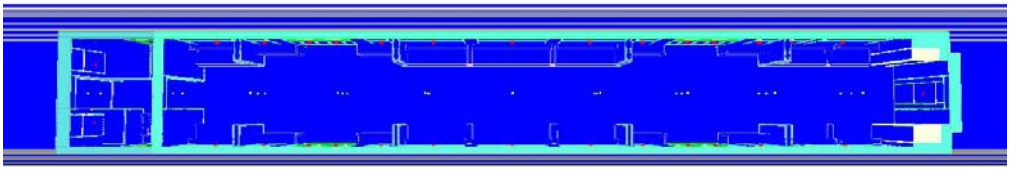

5 minutes

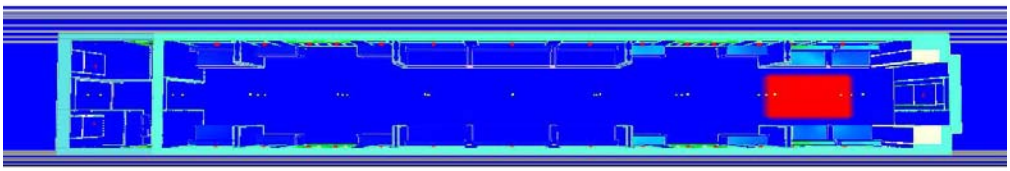

10 minutes

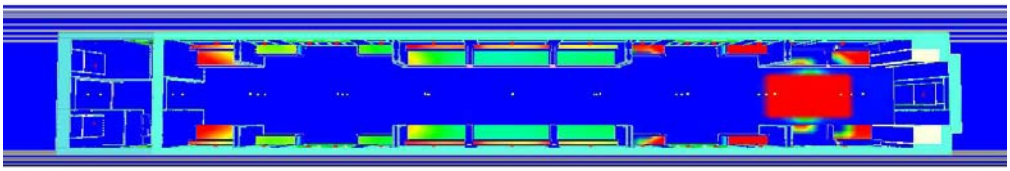

15 minutes

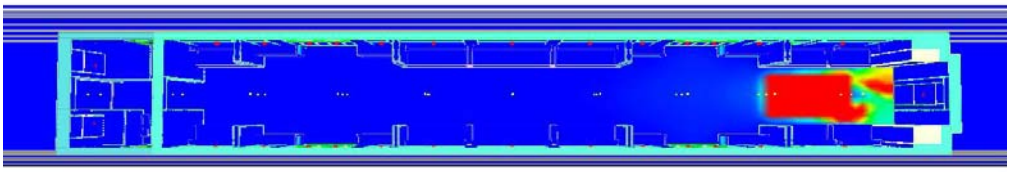

20 minutes

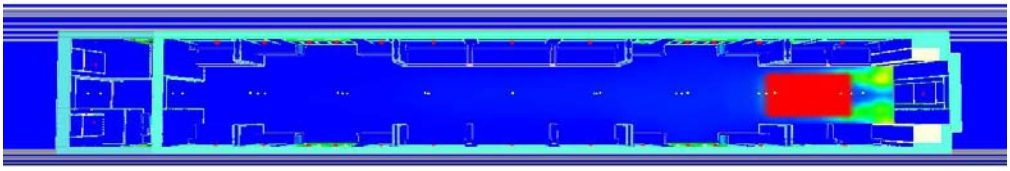

30 minutes

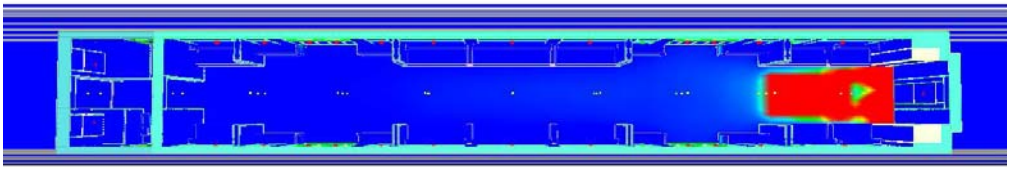

Figure 7.2: Fire spread, 1-car, 1.5MW source, single-track tunnel, revised material properties

However, once the initial and the calibrated material properties are compared, the following are expected based on the differences observed in variation of heat loads of combustibles as given in Figure 7.3:

- Seats
  - Slightly earlier ignition,
  - Shorter burning duration, and
  - Lower heat release rate.
- Floor
  - Similar or slightly earlier ignition times,
  - Longer burning duration, and
  - Higher heat release rate.

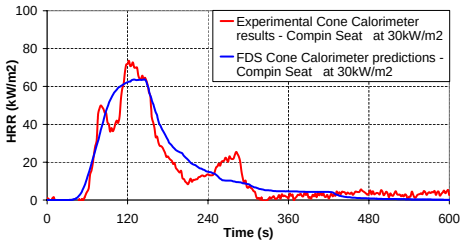

a. Cone Calorimeter results for calibrated seat material at 30kW/m^2

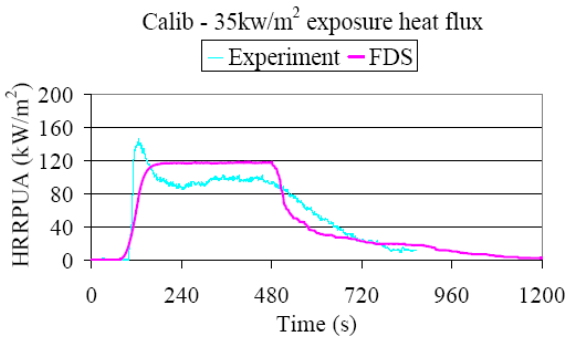

b. Cone Calorimeter results for seat material at 35kW/m^2 [20]

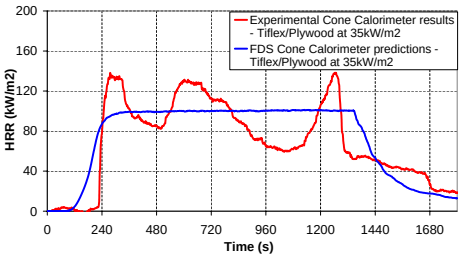

c. Cone Calorimeter results for calibrated floor material at 35kW/m^2

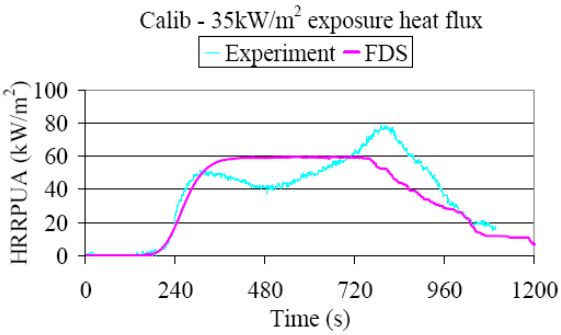

d. Cone Calorimeter results for floor material at 35kW/m^2 [20]

Figure 7.3: Comparison of the calibrated and the initial material properties used in the simulations

Consequently, it can be concluded that the assumed ignition temperatures are quite high for the calibrated seat and floor materials. In the absence of reported data, the ignition temperatures were selected to be 505°C and 560°C for seat and floor materials, respectively. These values have been selected during the calibration process based on their positive effect on matching the decay trend of heat load curves of the combustibles. The ignition temperatures for seat and floor materials in the initial simulations were taken to be 448°C and 419°C, respectively.

The temperatures are predicted to increase to about 740°C at 1.0m above the ignition, and to be between 580°C and 635°C in the rest of the carriage at the same height, during this incident. The predicted temperatures are not high enough to maintain continuous exposure of floor to temperatures at and above 560°C, for successful ignition and successive flame spread over the floor. Consequently, it has been decided to re-calibrate the combustibility characteristics of seat and floor materials with lower ignition temperatures. The findings from this analysis are summarized in Sub-section 7.2.2.

7.2.2 CALIBRATION OF MATERIAL PROPERTIES REVISITED

A large number of simulations has been performed during calibration of the combustible material properties. The following have been observed from the FDS cone calorimeter simulations:

- Increasing effective heat of combustion of the specimen;
  - Increases the peak value of the heat load (kW/m^2), and
  - Increases the rate of growth and decay, i.e. results in steeper slope in heat load predictions.
- Increasing heat of vaporization of the specimen;
  - Decreases the peak value of the heat load (kW/m^2), and
  - Decreases the rate of growth and decay, i.e. results in smoother slope in heat load predictions.
- Increasing the ignition temperature;
  - Delays the ignition of the specimen, i.e. the curve showing predicted heat load variation moves towards right along the time axis.

  - Slight reduction in the rate of growth and decay is also predicted during the FDS simulations.

- Increasing the product (ρ c δ) delays the ignition of the specimen.
- Increasing the thickness of the specimen increases the burning duration, i.e. the peak value of heat load is maintained longer.

In addition to the listed parameters above, maximum burning rate and the rate of burning at ignition are set in FDS simulations to prevent excessive pyrolysis and limit the peak value of heat load.

Consequently, one can find more than one set of parameters to replicate the experimental cone calorimeter predictions as far as the constraints allow to do so. Needless to say, one should consider the physical meaning of the parameters and apply reasonable limits in setting values for each of the parameters.

It was noted in Sub-section 7.2.1 that the ignition temperatures for the combustibles in the rolling stock model were selected to be too high in the first stage of the calibration process. Therefore, it has been decided to reduce the ignition temperatures and calibrate the remaining properties to match the experimental predictions. The combustible material properties obtained from the second stage of the calibration process are given in Table 7.1.

The predicted variation of heat loads of the combustibles are given in Figures 7.4 and 7.5 for comparison with the experimental data and the predictions of the first stage of the calibration process.

The performance of the re-calibrated material properties in the event of an incident has been assessed through re-simulation of Case-16, described above. The new case incorporates the re-calibrated material properties labelled as Set 2 in Table 7.1. The re-run of Case-16 is labelled as Case-16b.

Table 7.1: Calibrated material properties through FDS Cone Calorimeter simulations

	Compin/Pegasus Seats		Tiflex/Plywood Floor	
	Set 1	Set 2	Set 1	Set 2
Density, ρ † (kg/m^3)	121.4	121.4	944.4	944.4
Thermal conductivity ◇ (W/mK)	0.56	0.56	0.12	0.12
Specific heat*, c (kJ/kgK)	10.66	11.77	0.234	0.505
Thickness, δ* (m)	0.0017	0.0021	0.0235	0.0235
Ignition temperature* (°C)	505	435	560	430
Heat of vaporization* (kJ/kg)	4000	4000	4340	5520
Effective heat of combustion* (kJ/kg)	11350	9050	15430	12970
Maximum burning rate* (kg/m^{2}s)	0.0185	0.0185	0.018	0.018
Critical mass flux* (kg/m^{2}s)	0.012	0.012	0.009	0.009
ρ c δ* (kJ/m^{2}K)	2.2	3.0	5.2	11.2

†: Calculated from the Cone Calorimeter data by dividing the initial mass by the initial volume.
◇: Derived from the books. [8, 10]
*: Calibrated through a set of FDS Cone Calorimeter simulations.

The simulation of Case-16b shows that reducing the ignition temperatures of combustibles has insignificant effect on the predicted variation and the peak value of heat release rate, as far as the overall burning characteristics of the combustibles remain unchanged. As reported in Table 7.1, in order to match the experimental predictions, the effective heat of combustion is reduced and the product ρ c δ is increased, once the ignition temperatures are reduced. Therefore, although the individual parameters vary between the reported Set 1 and Set 2 material properties, the overall burning characteristics during an incident within a rolling stock remain unaffected.

The results of Case-16b show that the peak heat release rate increases to 1.8MW just after the 15th minute from the ignition. The overall flame spread characteristics and burning behavior of the combustibles in Case-16b are predicted to be similar to the predictions of Case-16. Minor differences are predicted between the two cases when the rate of burning of floor is examined closely. The reduction in ignition temperatures causes the materials to burn at slightly higher rates, which becomes apparent when the flame spread predictions of the two

cases are compared. However, key characteristics of the incident such as seats being burnt-out and fire being localized on floor around the ignition location remain unchanged.

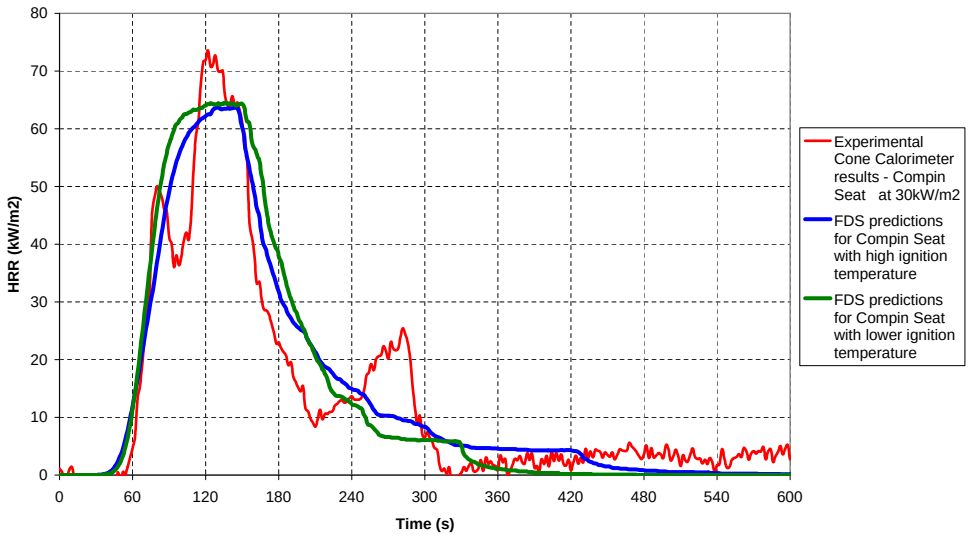

Figure 7.4: Heat release rate per unit area, Seat material with lower ignition temperature, FDS Cone Calorimeter calibration

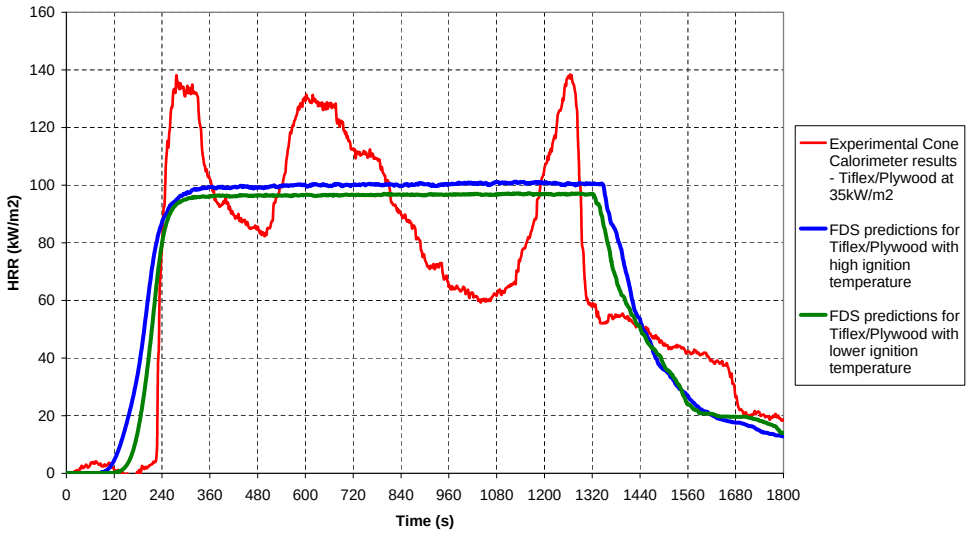

Figure 7.5: Heat release rate per unit area, Floor material with lower ignition temperature, FDS Cone Calorimeter calibration

The predicted variations of heat release rates for Cases 16 and 16b are given in Figure 7.6 for comparison.

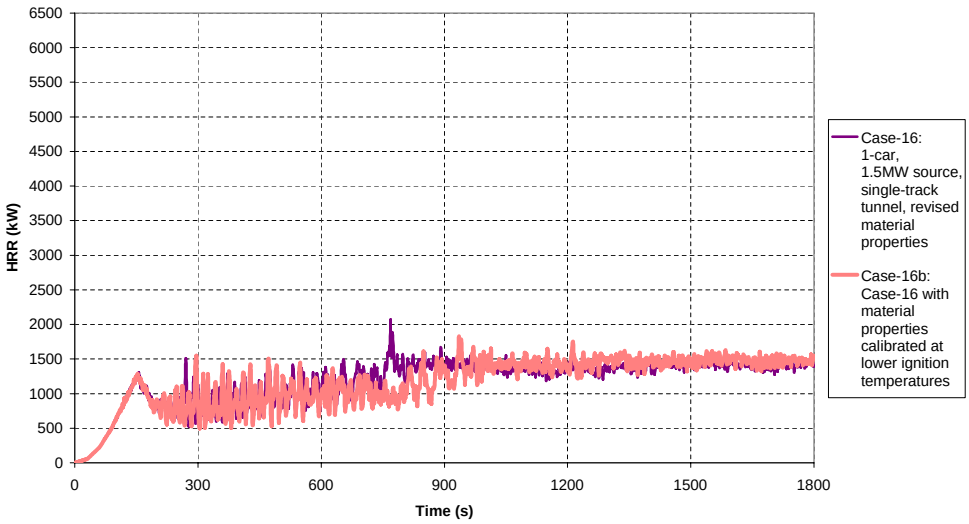

Figure 7.6: Heat release rate, 1-car, 1.5MW source, single-track tunnel, revised material properties with lower ignition temperatures

The fire development, illustrated with the burning rate of the combustible surfaces, in the incident carriage incorporating calibrated material properties with lower ignition temperatures is given in Figure 7.7.

It has been decided from the predictions of Cases 16 and 16b to use combustible material properties with lower ignition temperatures in the rest of the final simulations. The decision has been made based on predicted increase in burning rate of combustible surfaces within the carriage during an incident. In addition, revised ignition temperatures are closer to the values used in the initial and sensitivity simulations for FRP polyester seats and styrene butadiene floor, which would make comparisons of fire development predictions easier.

Although the ignition temperatures of the combustible materials are reduced in Case-16b, the fire development and flame spread within the incident carriage were found to be slow and steady. Another parameter that has been revised during the final simulations was the combustion reaction. The effects of the combustion reaction on the predicted flame spread and fire development have also been investigated, and the findings are reported in Sub-section 7.2.3.

Ignition

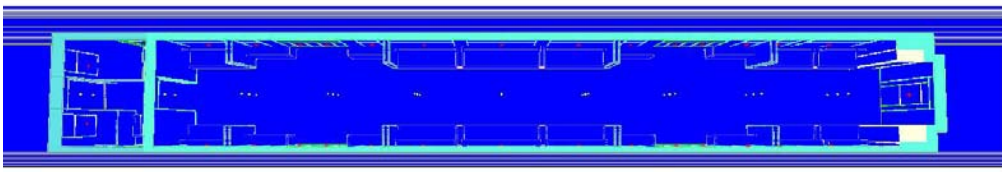

5 minutes

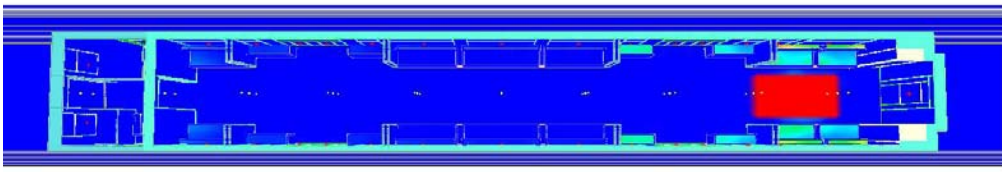

10 minutes

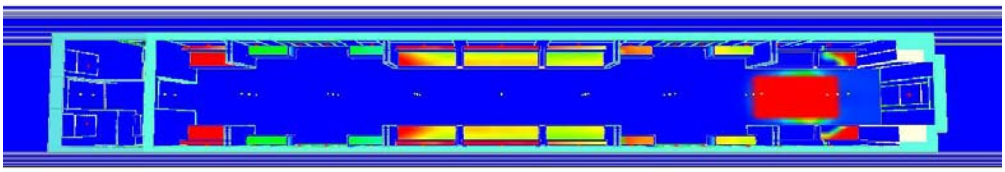

15 minutes

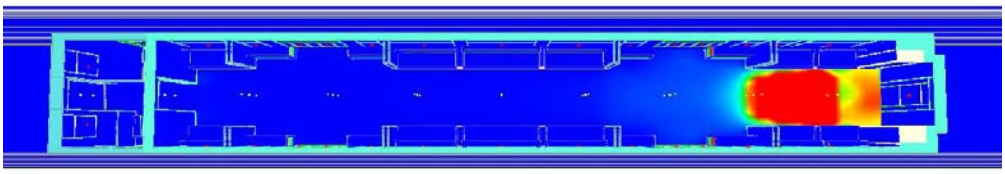

20 minutes

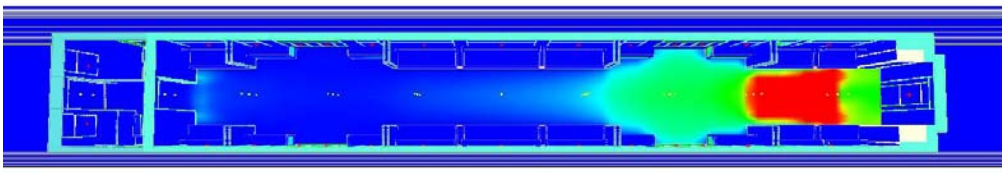

30 minutes

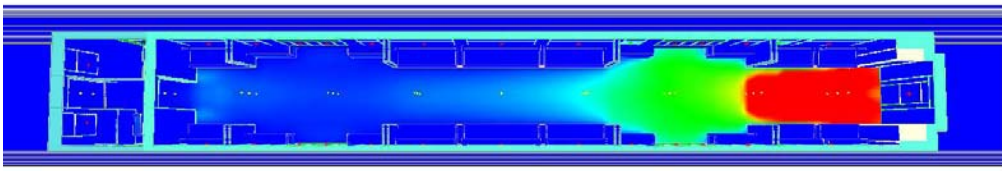

Figure 7.7: Fire spread, 1-car, 1.5MW source, single-track tunnel, revised material properties with lower ignition temperatures

7.2.3 COMBUSTION REACTION REVISITED

In Cases 16 and 16b, the combustion reaction was defined to be the chemical reaction of burning wood, since it was proposed that the fire development within the rolling stock is governed by flame spread over the floor. However, the proposed combustion reaction has lower energy release per unit mass of oxygen consumed and higher soot yield. Consequently, the energy released during burning of combustibles within the incident carriage is smaller compared to the same incident where chemical reaction of burning seats is used.

The seat manufacturer for Class-378 rolling stock, Compin, offers moquette as their basic surface finish on their Pegasus model seats [41]. Moquette is type of fabric with a thick, dense pile. Its durability makes moquette the preferred choice for carpeting and upholstery. The fire resistance of moquette fabrics could be increased by polyester additives. The polyester moquette fabrics in which the two ply yarns are arranged in ground portions meet the flame-retardant standard without a flame proof finish because they contain rayon, in addition to their high strength [42].

In Case-16c, the combustion reaction for wood floor material has been replaced by the reaction for polyester seats. The chemical reaction in the rest of final simulations, which was also used in the initial and sensitivity simulations, has the following form:

$$C_{5.77}H_{6.25}O_{1.63} + 6.5175\,(O_2 + 3.76N_2) \rightarrow\ 5.77\,CO_2 + 3.125\,H_2O + 24.5\,N_2$$

The key parameters for this combustion reaction can be listed as follows [20]:

- Soot yield: 0.062 kg/kg
- Carbon-monoxide yield: 0.0705 kg/kg
- Radiative fraction: 0.35
- Energy release per unit mass of oxygen consumed: 11900 kJ/kg.

Once again, using the same chemical reaction for initial and final simulations would make flame spread and fire development comparisons easier, and would show the differences in the performance of the combustible materials more distinctively.

The severe baggage fire incident is simulated using the single car model, where the calibrated material properties having reduced ignition temperatures and the combustion reaction for the seat material are used. This case is labelled as Case-16c in this thesis.

The simulation shows that in contrast to the predictions of Cases 16 and 16b, the seats closest to the ignition location start to burn and flames start to spread over the floor within the first 3 minutes of the incident. Increased value of energy release in the combustion reaction assisted earlier ignition of seats and floor, both of which burn at rates 1.0 g/m^{2}s or higher when ignited. It is predicted that within 5 minutes from the ignition, the seats closest to the ignition location are burnt out. This is expected since the burning duration of seats were found to be quite short from the cone calorimeter experiments.

The simulation also shows that the pair of large windows closest to the ignition location fail just after the 5th minute. This is followed by the failure of the back end door window just before the 7th minute. The failure of large windows allows fresh air entrainment to the incident carriage, which resulted in an instantaneous increase in the heat release rate. The peak heat release rate is predicted to be 3.1MW for this incident just after the 5th minute, when the largest number of seats are burning simultaneously with an increasing burning area over the floor.

It is predicted from the results that within the first 7 minutes of the incident, while some of the seats are being ignited by the flames, others that are ignited initially burn out. In addition, window failures ventilate the fire and reduce the rate of flame spread within the incident carriage. This resulted in fluctuations in the predicted heat release rate.

The results show that almost all seats are burnt out within the first 9 minutes of the incident. From the 9th minute and onwards flames spread slowly and steadily over the floor. It is predicted that one of the small windows closest to the ignition location fails just after the 15th minute. However, it has insignificant effect on the fire development. The simulation shows that only half of the floor area of the incident carriage is involved in fire within the first 30 minutes of this incident.

The fire development for this incident, illustrated with the burning rate of the combustible surfaces within the carriage, is given in Figure 7.8. The predicted variation of heat release rate during this incident is shown in Figure 7.9.

Ignition

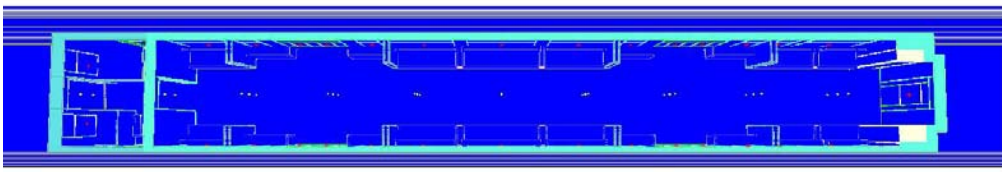

5 minutes

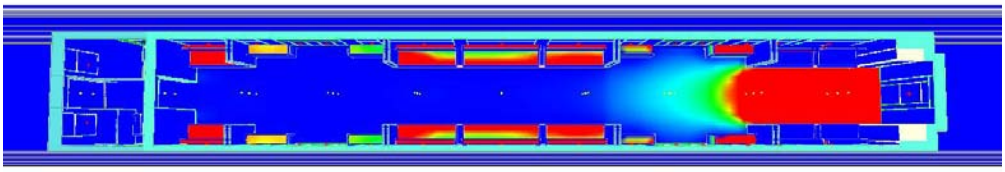

10 minutes

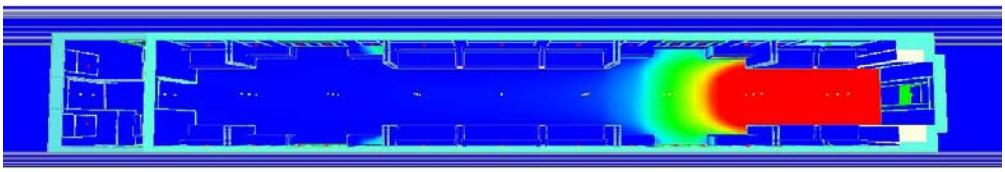

15 minutes

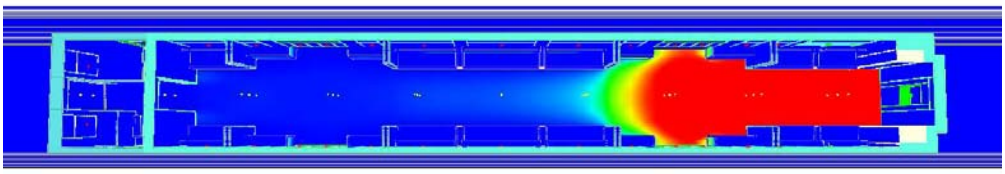

20 minutes

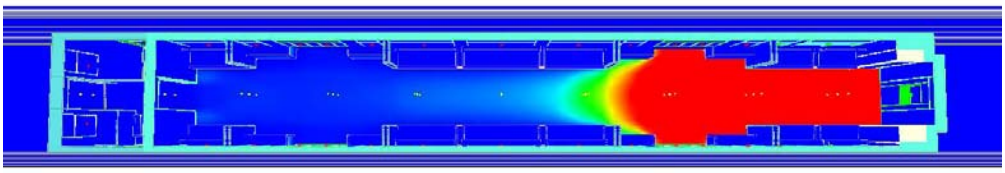

30 minutes

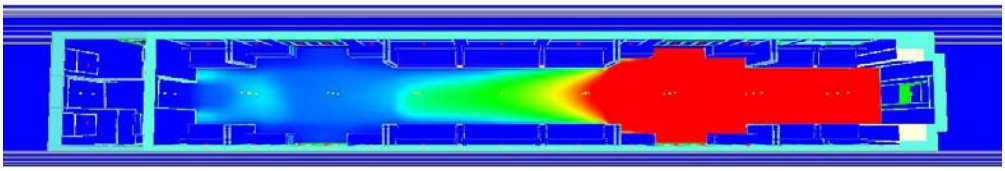

Figure 7.8: Fire spread, 1-car, 1.5MW source, single-track tunnel, combustibles with lower ignition temperatures and combustion reaction written for seats

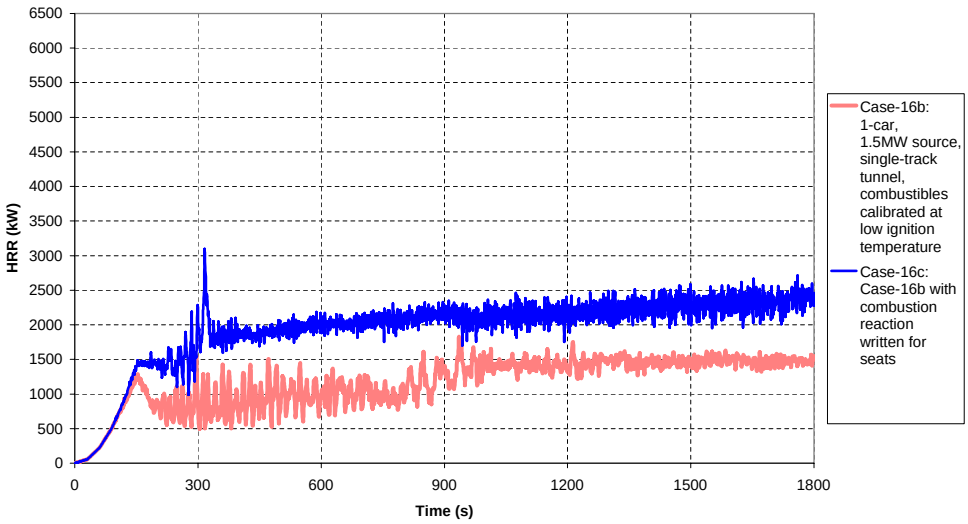

Figure 7.9: Heat release rate, 1-car, 1.5MW source, single-track tunnel, combustibles with lower ignition temperatures and combustion reaction written for seats

7.2.4 CASE-17: 1-CAR, 80kW SOURCE, SINGLE-TRACK TUNNEL

The performance of the revised material properties is also assessed through the design case, where an incident is simulated due to an 80kW arson fire ignition. This case would be re-simulation of Case-01 with the combustible material properties revised as given in set 2 of Table 7.1.

The simulation shows that the flame spread is limited to only a pair of seats around the initial ignition location. Simulation of this incident has confirmed that the 80kW source is not powerful enough to ignite the floor or the seats far away from the initial ignition location. The same conclusion was derived from the results of the simulated Cases 01 to 04 of the initial simulations.

The peak heat release rate during this incident is predicted to be 125kW. However, the overall heat release rate is in the order of 110kW, slightly less than the values predicted in Cases 01 to 04. This is expected since the revised properties of seats reflect smaller heat load and shorter burning duration. The predicted variation of the heat release rate during this incident is given in Figure 7.10, along with the heat release rate curve of Case-01 for comparison.

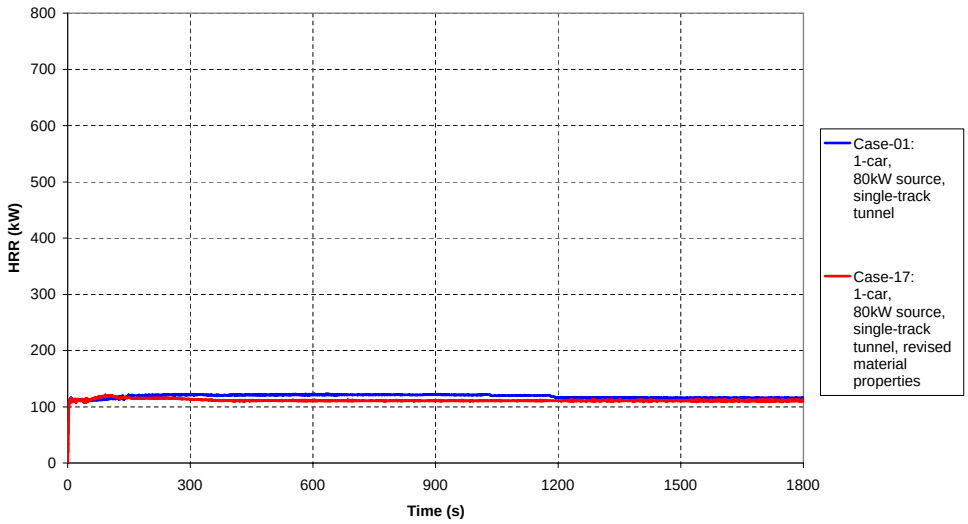

Figure 7.10: Heat release rate, 1-car, 80kW source, single-track tunnel, calibrated material properties

7.2.5 CASE-18: 4-CAR, 1.5MW SOURCE IN SECOND CARRIAGE, SINGLE-TRACK TUNNEL

It was predicted during the sensitivity simulations, reported in Chapter 6, that a severe baggage fire ignition source placed at the center of the second carriage produced the peak heat release amongst the other cases simulated using the 4-car rolling stock incorporating open wide gangways. This incident was simulated in a single-track tunnel, and was labelled as Case-10 in the sensitivity simulations.

The performance of the calibrated material properties during an incident has also been checked through re-simulation of Case-10 of the sensitivity simulations. The incident simulated using the revised material properties, given in set 2 of Table 7.1, is labelled as Case-18 in the final simulations.

The simulation shows that fire starts to develop by igniting the three pairs of seats at the center of the incident carriage and by spreading on floor in both upstream and downstream directions within the first 5 minutes of the incident. Between the 6th and the 9th minutes from the ignition, it is predicted that the three pairs of seats ignited at early stages of the incident are completely burnt out. However, within this interval, the remaining seats of the incident carriage are involved in fire, and fire continues to grow on floor in both directions.

One of the large windows is predicted to fail just before the 10th minute. While this window failure hinders the growth of fire in the downstream direction, it promotes flame spread in the upstream direction.

At the 11th minute, another window failure is predicted at the center of the incident carriage. This window lies on the upstream end of the incident carriage and prevents further spread of flame by reducing the intensity of the fire. This is reflected as a sudden drop in the predicted variation of heat release rate just after the 11th minute of the incident. By 11 minutes, all the seats in the incident carriage are found to be burnt out.

Fire regains its intensity and continues to spread in both upstream and downstream directions between the 11th and 16th minutes. In addition to fire development on floor of the incident carriage, some of the seats in the adjacent carriages are found to be ignited by the hot gases produced by the fire. However, the seats burn at a very slow rate within this interval. Another window failure at the center of incident carriage is predicted just after the 16th minute. However, this had insignificant effect on the fire development. This is followed by the failure of one of the remaining large windows at the center of the incident carriage just after the 20th minute.

By 20 minutes, the flames at the downstream end of the incident carriage are predicted to reach the adjacent carriage. Flames consume the remaining combustibles on the seats located at the end of the adjacent carriage closest to the incident. Between the 22nd and the 23rd minutes, three small windows, two on one side and the remaining one on the opposite side, next to the passenger doors at the downstream end of the incident carriage are predicted to fail. These failures brought fresh air to the fire, and promoted further flame spread at the downstream end.

The fire development and flame spread during this incident can be classified as steady and progressive. Although flames spread to most of the incident carriage and even spread to the adjacent carriage, sudden increase in heat release rate is not observed. The peak heat release rate for this incident is predicted to be 3.7MW. The fire development is deemed to continue further, when the simulation has stopped at 30 minutes. However, it is assumed that the fire brigade would arrive at the scene and control further development of fire within 30 minutes from the ignition.

The predicted variation of heat release rate for this incident is given in Figure 7.11, along with the predictions of same incident simulated within the scope of sensitivity simulations.

The flame spread within the rolling stock, illustrated with the burning rate of the combustibles, is given in Figure 7.12 for this incident.

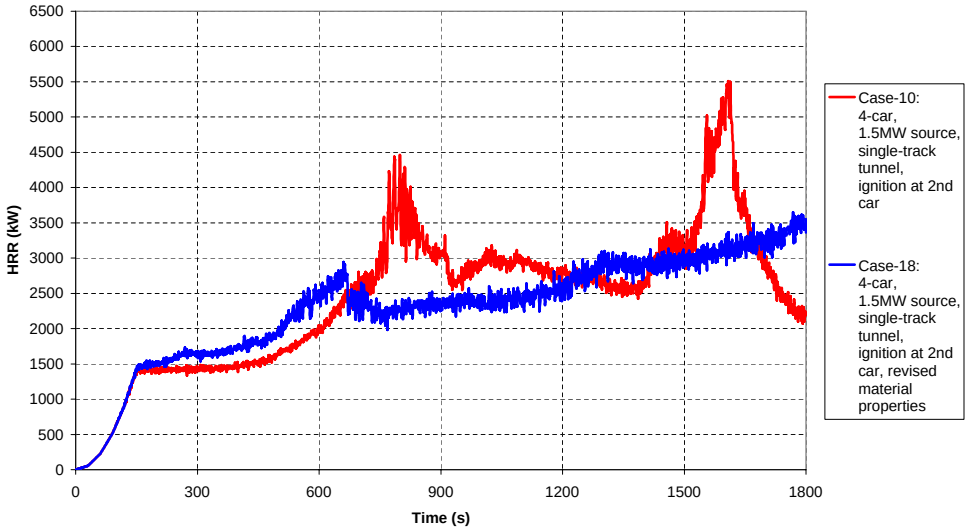

Figure 7.11: Heat release rate, 4-car, 1.5MW source, single-track tunnel, ignition at second car, revised material properties

7.2.6 CASE-19: 4-CAR, 1.5MW SOURCE, SINGLE-TRACK TUNNEL, LIMITED WINDOW FAILURE

It was predicted during the sensitivity simulations, reported in Chapter 6, that the failure of windows has a significant influence on the predicted fire development and flame spread within the rolling stock. It has been predicted that if windows on one side of the rolling stock are defined to be fail-safe, then the change in ventilation conditions results in the largest extent of flame spread within the rolling stock when a severe baggage fire incident is simulated in the 4-car open train in the single-track tunnel. This incident was labelled as Case-12b in the sensitivity simulations.

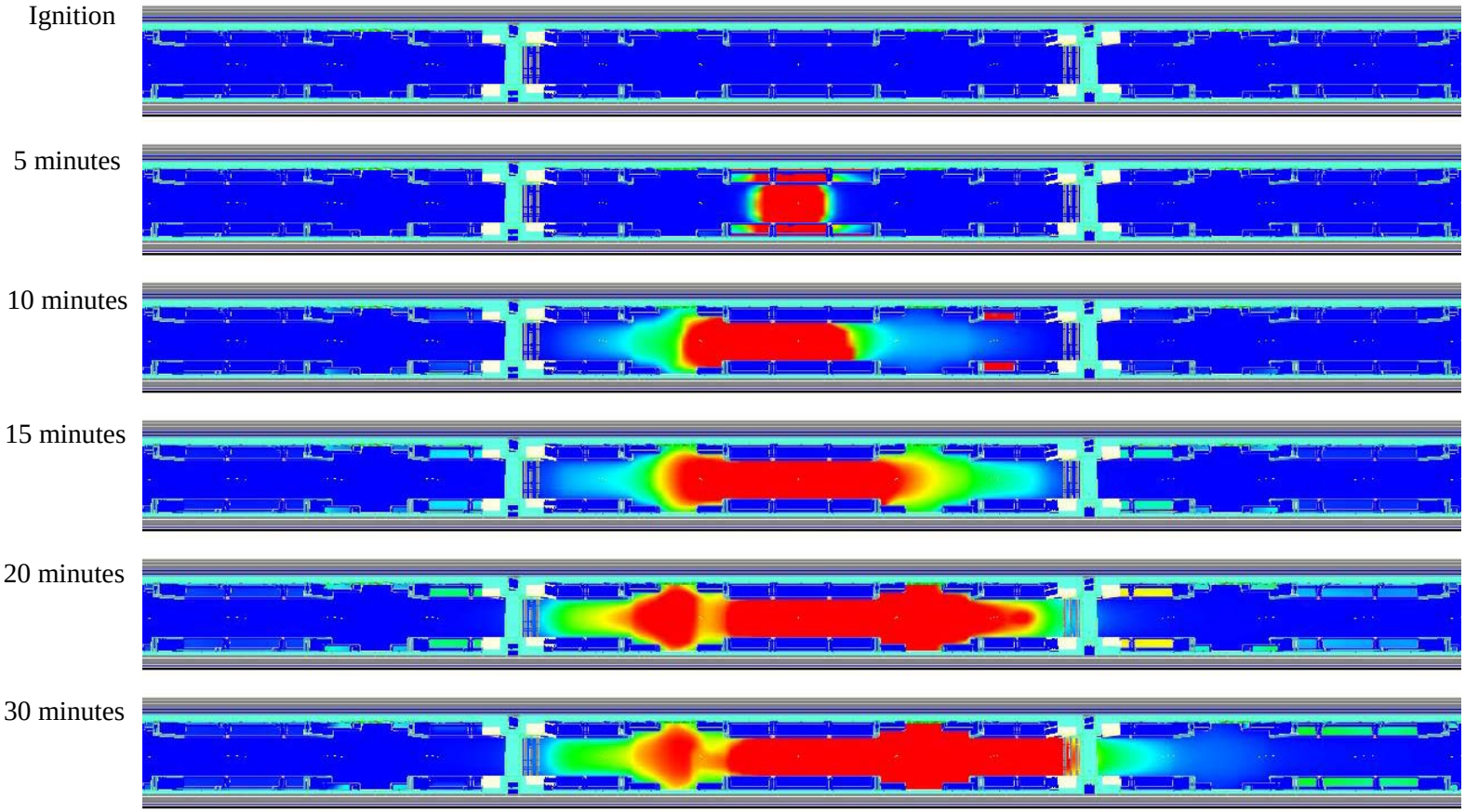

Figure 7.12: Fire spread, 4-car, 1.5MW source, single-track tunnel, ignition at second car, revised material properties

The performance of the calibrated material properties has been checked through re-simulation of the identical scenario defined in Case-12b. This incident is labelled as Case-19 in the final simulations, and involves revised material properties given in set 2 of Table 7.1.

The simulation shows that flames spread to the pair of seats adjacent to the ignition location, and fire starts to grow on the floor around the ignition source from the 3rd minute of the incident. Between the 5th and the 7th minutes from the ignition, while the seats that are ignited at the very early stages of the fire development burn out, flames propagate further on the floor in the upstream direction and ignite the folded seats next to the passenger side doors.

At the 9th minute of the incident, the seats at the center of the incident carriage are predicted to be involved in the fire development. In addition, flames continue to propagate in both upstream and downstream directions within this interval. Flames spread to the passenger doors area in the upstream direction, and reach gangway area in the downstream. At the 9th minute, the seats closest to the ignition source in the adjacent carriage are ignited. However, they burn at slow rates.

The first window failure is predicted just before the 10th minute. The large window closest to the ignition source fail, however this failure has insignificant effect on the fire development. By 12 minutes from the ignition, most of seats in the incident carriage are predicted to burn out. However, flames continue to propagate on floor, and involvement of seats of the adjacent carriage in fire development continues as fire retains its intensity.

The small window adjacent to the ignition location is predicted to fail at the 13th minute, which is followed by failure of the passenger door windows within the next minute. These window failures assist ventilation of smoke and bring fresh air to the fire. It is predicted that the failure of these windows promote flame spread, especially in the upstream direction. The simulation shows that most of the seats in the adjacent carriage are burnt out, and flames spread to three-quarters of the incident carriage and to about a quarter of the adjacent carriage by the 18th minute from the ignition. Within this minute, failure of two small windows on both sides of the passenger doors in the incident carriage and failure of a small window in the adjacent carriage are also predicted.

The simulation shows that fire reaches to its maximum extent by 25 minutes, when about one and a half carriage floor area is involved in the fire. Within this minute, multiple window failures are also observed in the adjacent carriage. In the rest of the simulation, while flames propagate further in the adjacent carriage in the downstream direction, the intensity of the fire at its upstream end is predicted to get smaller. Consequently, the extent of flame spread of one and a half carriage floor area remains as maximum.

The peak heat release rate during this incident is predicted to be 4.6MW. The variation of heat release rate is predicted to be quite similar to the predictions of Case-12b. Figure 7.13 shows the predicted variation of heat release rate during this incident.

The flame spread within the rolling stock, illustrated with the burning rate of the combustibles, is given in Figure 7.14 for this incident.

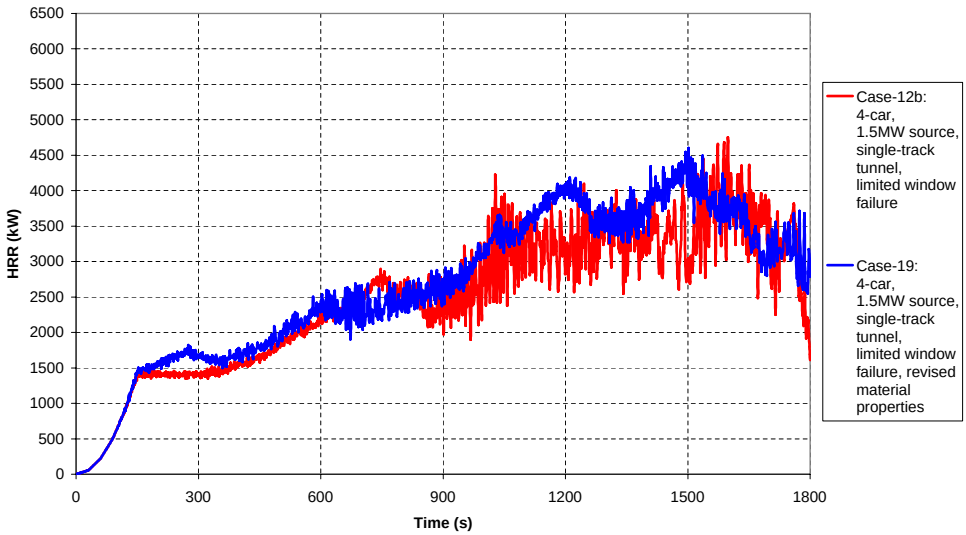

Figure 7.13: Heat release rate, 4-car, 1.5MW source, single-track tunnel, limited window failure, revised material properties

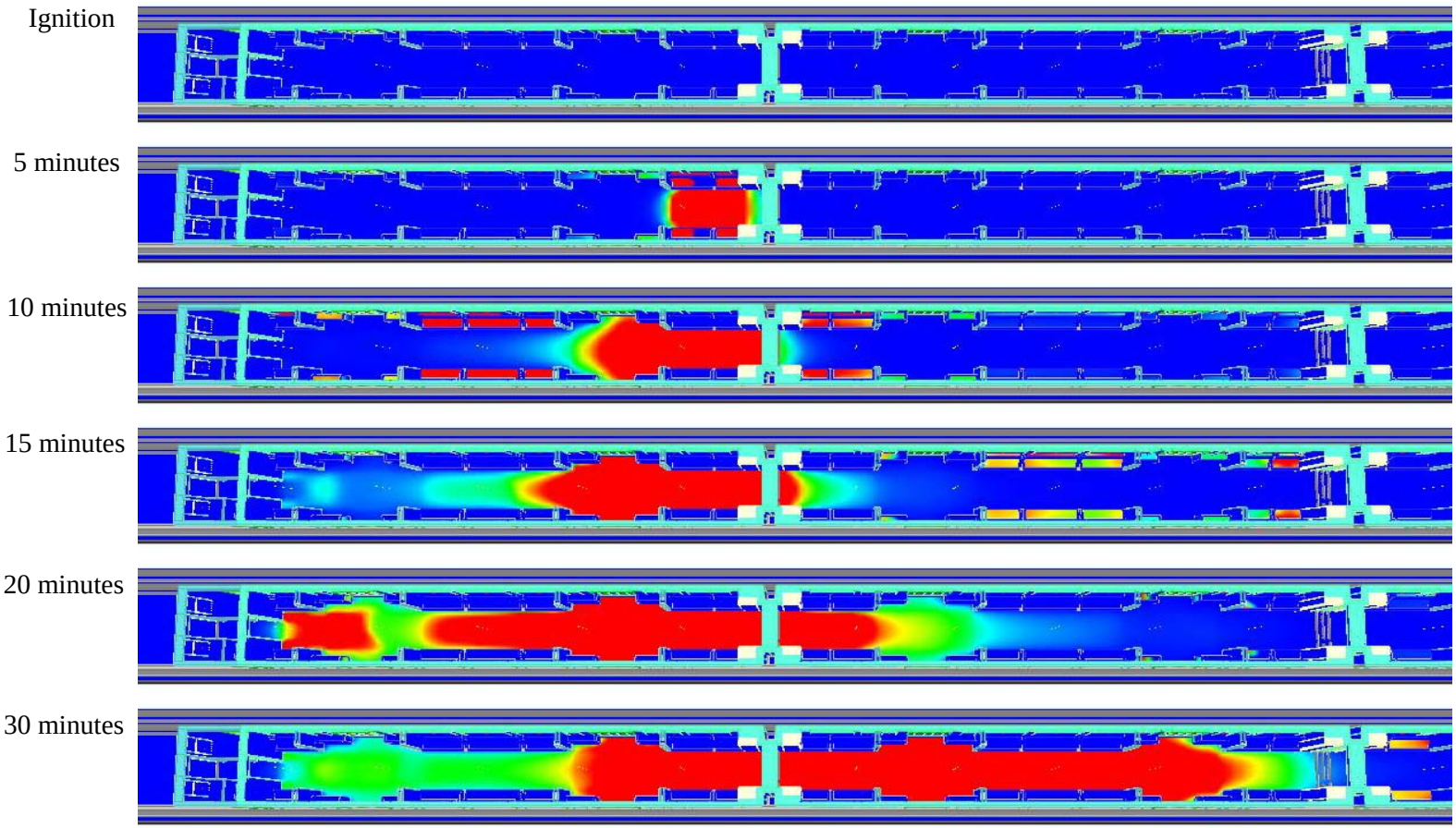

Figure 7.14: Fire spread, 4-car, 1.5MW source, single-track tunnel, limited window failure, revised material properties

7.2.7 SENSITIVITY ON FINAL SIMULATIONS

7.2.7.1 WINDOW FAILURE CRITERION

In all the simulations reported herein, the window failure criterion was defined to be 675°C. This value was claimed to be high regarding windows of Class-378 rolling stock by some of the authorities. Consequently, Cases 18 and 19 have been re-simulated with window failure criterion set to 400°C, as a part of the sensitivity analysis.

The simulation of the baggage fire incident at the center of the second carriage of a 4-car rolling stock showed that a pair of windows fail just after the 4th minute from the ignition. This is followed by two individual window failures between the 5th and the 7th minutes. The failure of windows in the close premises of the ignition source reduced the intensity of fire significantly. The fifth window failure at the center of the incident carriage is predicted to be just after the 11th minute. The fire is predicted to be too weak and remain localized around the initial ignition location. The growth rate of the fire is found to be too small due to effective ventilation of smoke during this incident. The peak heat release rate is predicted to be 2.5MW. Figure 7.15 shows the variation of heat release rate for this incident. The predicted flame spread within the rolling stock is given in Figure 7.16.

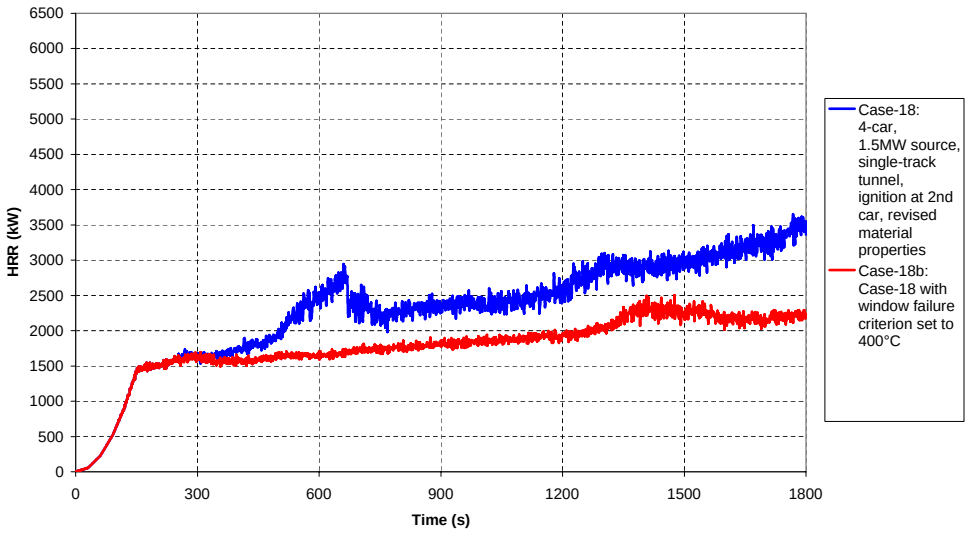

Figure 7.15: Heat release rate, 4-car, 1.5MW source, single-track tunnel, ignition at second car, revised material properties and window failure criterion

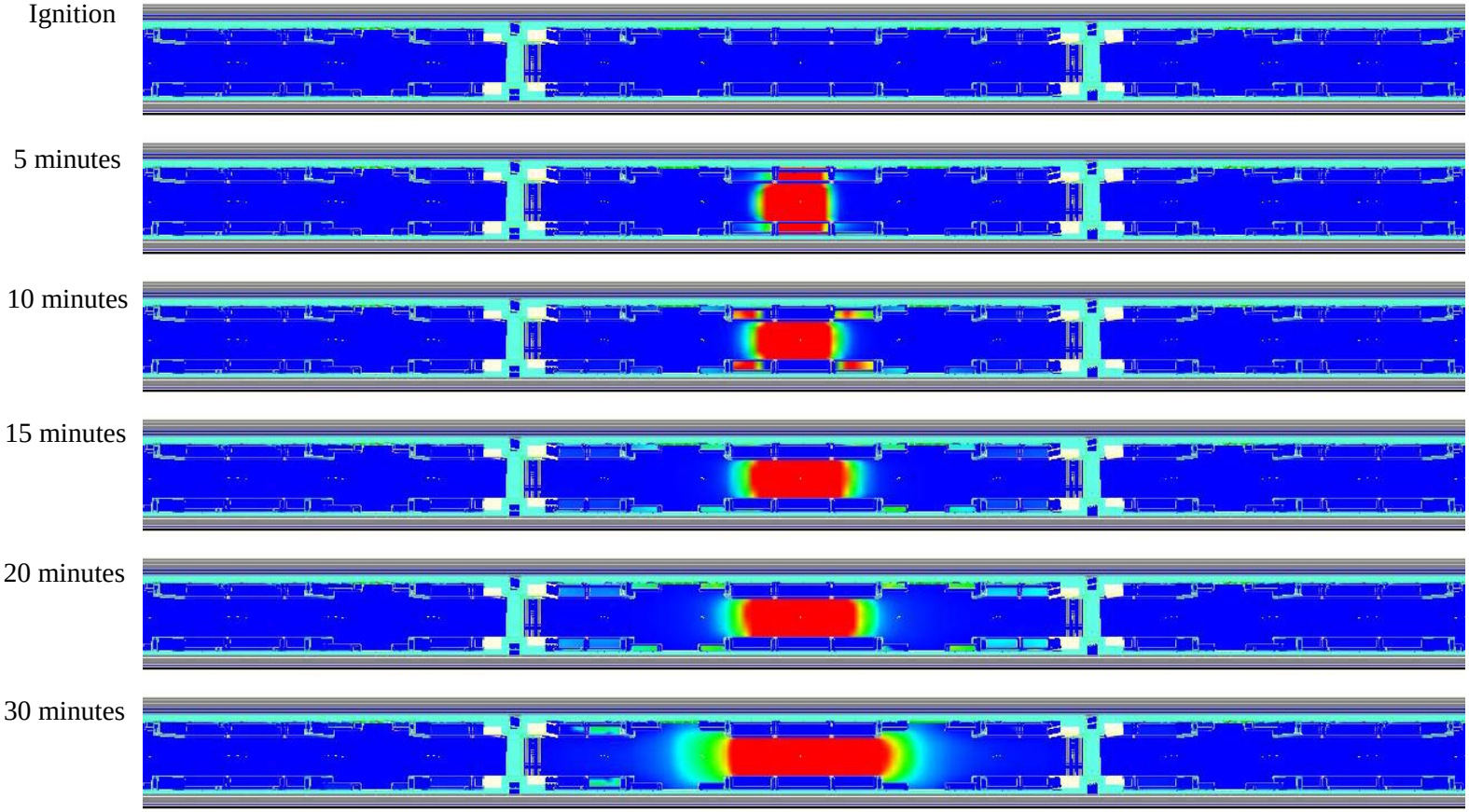

Figure 7.16: Fire spread, 4-car, 1.5MW source, single-track tunnel, ignition at second car, revised material properties and window failure criterion

The second of the sensitivity simulations involves Case-19, where the windows on one side of the rolling stock were defined to be fail-safe. The simulation showed that windows closest to the ignition location fail at the 4th and the 6th minutes. Although the failure of these windows slowed down the fire development, flames continue to spread over the floor at reduced rates. A group of windows is predicted to fail at the 10th minute, when a marginal reduction in the heat release rate is observed. The simulation shows that by 20 minutes from the ignition, all the windows on one side of the incident carriage fail along with four small windows and a large window of the adjacent carriage. As reported in the sensitivity simulations, gradual air entrainment to the rolling stock due to failure of windows promoted fire development and flame spread during this incident. However, the intensity of the fire is smaller in this case, compared to Case-19, due to slightly earlier failure of windows. Consequently, at 25 minutes the extent of flame spread was limited to half of the incident carriage and a small section of the adjacent carriage. The peak heat release rate is predicted to be 4.4MW during this incident. Figure 7.17 shows the variation of heat release rate for this incident. The predicted flame spread within the rolling stock is given in Figure 7.18.

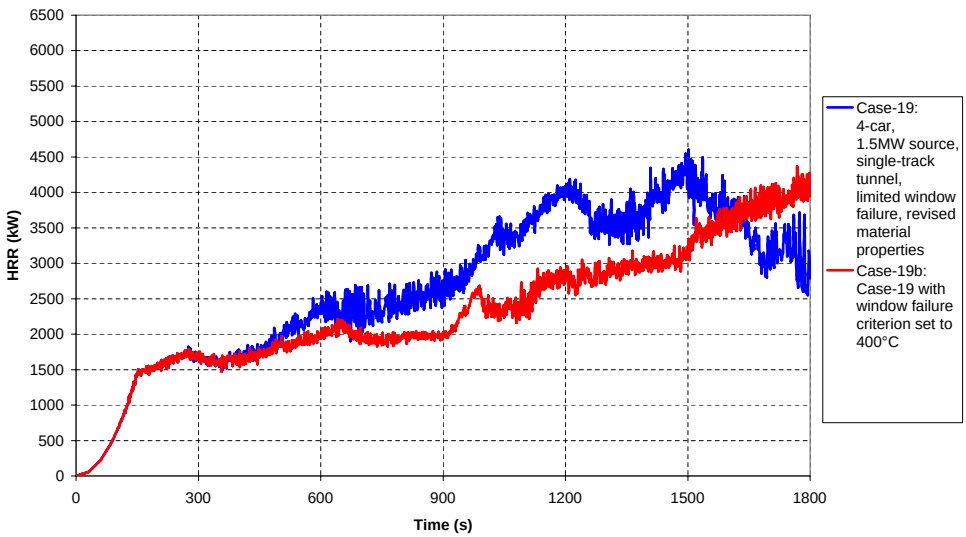

Figure 7.17: Heat release rate, 4-car, 1.5MW source, single-track tunnel, limited window failure, revised material properties and window failure criterion

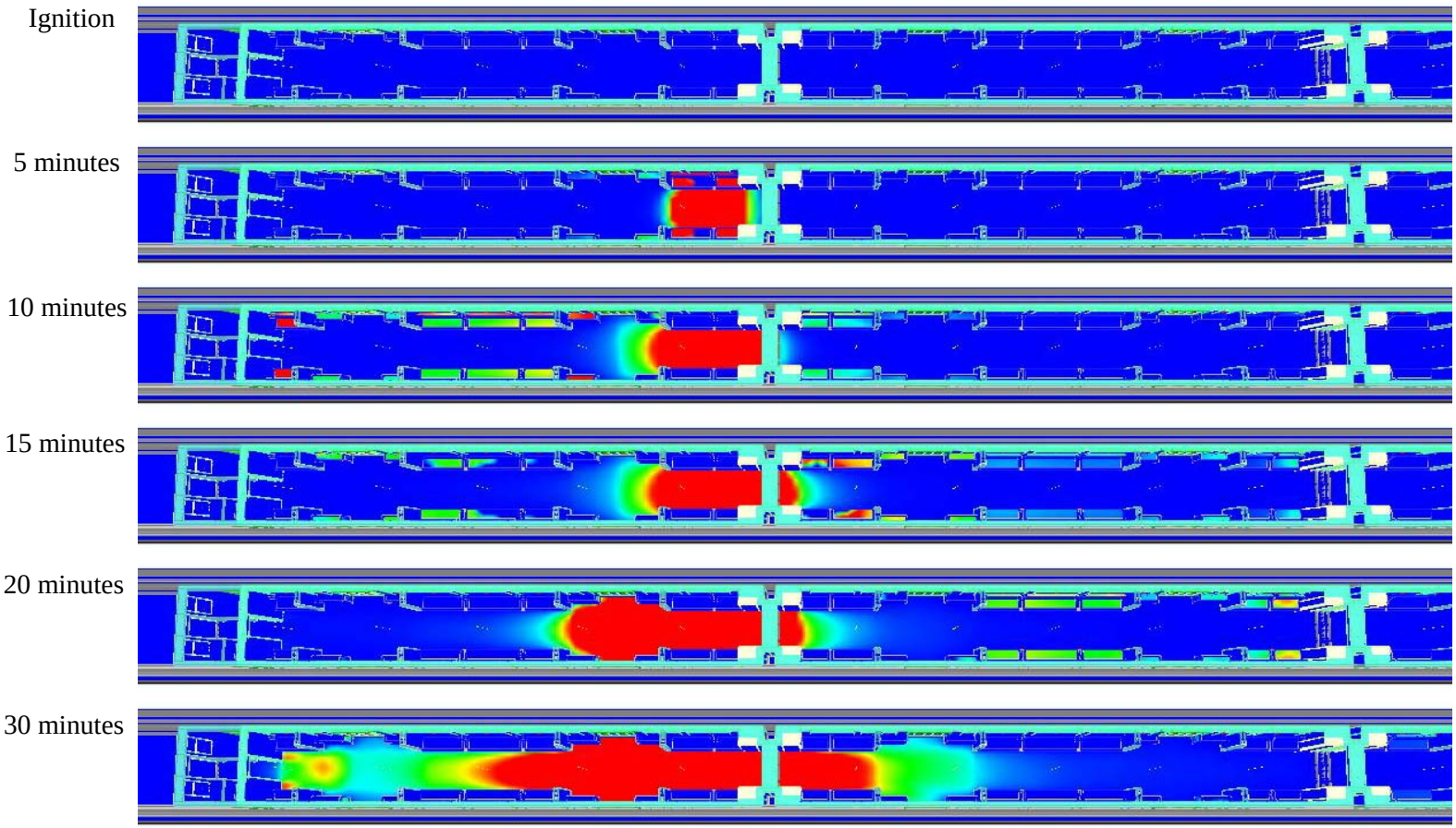

Figure 7.18: Fire spread, 4-car, 1.5MW source, single-track tunnel, limited window failure, revised material properties and window failure criterion

7.2.7.2 CONE CALORIMETER MODELLING

The combustible material properties that have been used in the initial and sensitivity case studies were calibrated through FDS cone calorimeter simulations incorporating a nominal element size of 8mm. This was claimed to reflect the burning behavior of the combustibles during an incident within the rolling stock with the assumption that the design fire size would be in the order of 10MW [20].

However, in the final simulations, combustible materials for Class-378 rolling stock were calibrated through FDS cone calorimeter simulations incorporating a nominal element size of 5mm. The grid size was revised based on the peak heat release rate predictions of about 6.5MW during the initial and sensitivity simulations. Consequently, a final attempt has been made to investigate the effect of the calibration model on the predicted fire development and flame spread within the rolling stock.

The inner wall temperatures of the cone calorimeter model are re-calibrated to impose the required surface heat flux on the combustible specimen, since the cone calorimeter model is revised to incorporate larger element sizes. The required inner wall temperatures of the new cone model are determined to be 693°C and 729°C in order to get surface heat flux levels of 30kW/m^2 and 35kW/m^2, respectively. The inner wall temperatures for the cone calorimeter model incorporating smaller element sizes were determined and reported to be 645°C and 680°C for the required surface heat flux levels, respectively, as given in Table C.2 in Appendix C.

The seat and the floor materials are re-calibrated using the revised cone calorimeter model, at surface heat flux levels of 30kW/m^2 and 35kW/m^2, respectively, due to reasons listed in Section C.1 of Appendix C. The re-calibrated material properties using the cone calorimeter model incorporating larger grid size are given as Set 3 in Table 7.2.

Initially, the material properties listed as Set 2 in Table 7.2, which were used in Cases 16b to 19b, have been tested using the revised cone calorimeter model. It is predicted from the simulations that the material properties given in set 2 result in reduced heat loads, when analyzed using the cone calorimeter model with increased element size.

Table 7.2: Calibrated material properties through FDS Cone Calorimeter simulations, 5mm and 8mm grid sizes

	Compin/Pegasus Seats		Tiflex/Plywood Floor	
	Set 2	Set 3	Set 2	Set 3
Density, ρ † (kg/m^3)	121.4	121.4	944.4	944.4
Thermal conductivity ◇ (W/mK)	0.56	0.56	0.12	0.12
Specific heat*, c (kJ/kgK)	11.77	15.56	0.505	0.568
Thickness, δ* (m)	0.0021	0.0018	0.0235	0.0220
Ignition temperature* (°C)	435	435	430	430
Heat of vaporization* (kJ/kg)	4000	4000	5520	5520
Effective heat of combustion* (kJ/kg)	9050	10150	12970	14900
Maximum burning rate* (kg/m^{2}s)	0.0185	0.0185	0.018	0.018
Critical mass flux* (kg/m^{2}s)	0.012	0.012	0.009	0.009
ρ c δ* (kJ/m^{2}K)	3.0	3.4	11.2	11.8

†: Calculated from the Cone Calorimeter data by dividing the initial mass by the initial volume.
◇: Derived from the books. [8, 10]
*: Calibrated through a set of FDS Cone Calorimeter simulations.

Consequently, it has become apparent that the effective heat of combustion of the materials have to be increased in order to match the desired peak heat load values. In addition, the thickness of the seat and floor materials are revised to match the burning durations predicted by the cone calorimeter experiments. Finally, the product ρ c δ is corrected to get an accurate representation of the ignition times.

The predicted variation of heat loads of the combustibles are given in Figures 7.19 and 7.20 for comparison with the experimental data. As noted during the calibration of material properties given in set 2 above, the re-calibration of the properties involve matching the overall trend of the experimental predictions and the corresponding energy release during combustion.

The performance of the material properties, given in Set 3 above, in the event of an incident has been analyzed through re-simulation of Case-16c. The incident in a single carriage, incorporating material properties listed as set 3 in Table 7.2, in the single-track tunnel is labelled as Case-20 in this thesis.

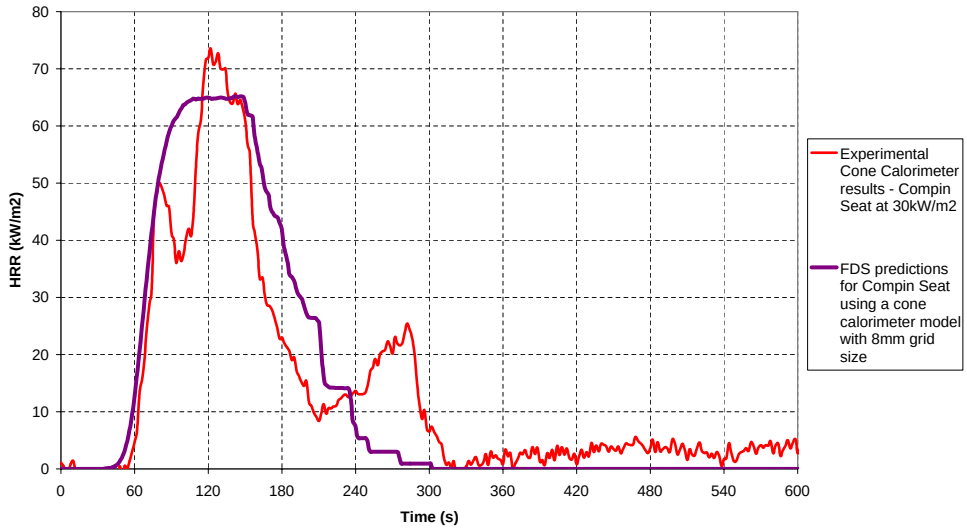

Figure 7.19: Heat release rate per unit area, Seat material, FDS Cone Calorimeter calibration with 8mm grid size

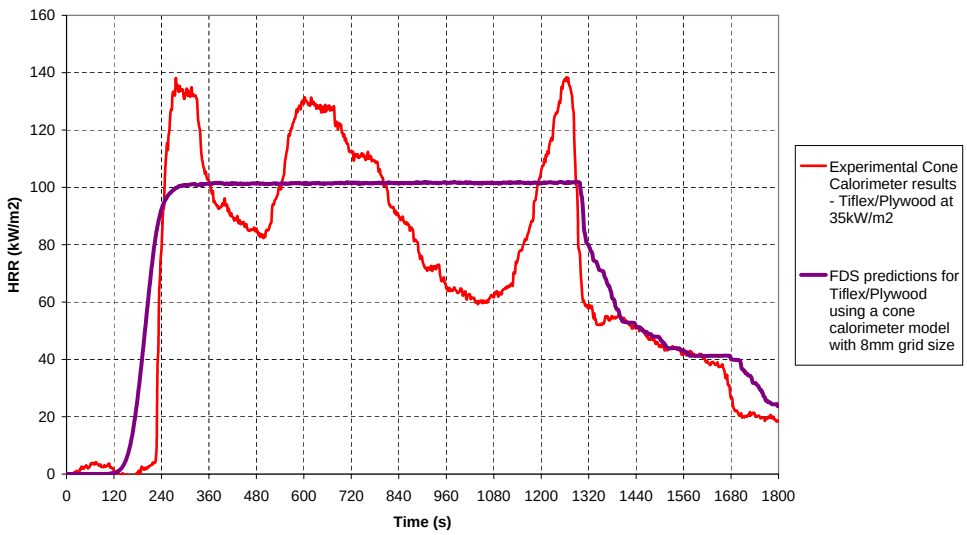

Figure 7.20: Heat release rate per unit area, Floor material, FDS Cone Calorimeter calibration with 8mm grid size

The simulation of Case-20 shows that the fire development and flame spread patterns are quite similar to the predictions of Case-16c, at least for the first 25 minutes of the incident. The ignition times and burning durations of the seats are observed to match principally in both cases. Within the first 25 minutes of the incident, only marginal differences between the predicted variations of the heat release rates are predicted. Slightly higher heat release rates are predicted in Case-20 due to higher effective heat of combustion of the floor material used in the simulation.

However, in Case-20 a significant increase in the heat release rate is predicted after the 27th minute of the incident. The intensity of the fire and the flame spread area over the floor are found to be greater in Case-20, compared to Case-16c, throughout the 30 minute long simulation. Consequently, the intensity of fire was found to be strong enough to maintain fire development and flame spread within the incident carriage. The sudden increase in heat release rate is predicted to be in conjunction with involvement of the upstream half of the incident carriage in fire development. The simulation shows that while the floor area ignited in the early stages of fire around the ignition source continue to burn, additional floor area is involved in fire as flames propagate further after the 27th minute, which resulted in an increase in the peak heat release rate. Figure 7.21 shows the predicted variation of heat release rates for Cases 16c and 20 for the 30 minute long simulations.

Following the predictions of 30 minute simulation of Case-20, it has been decided to increase the simulation time for further investigation of fire development in the incident carriage. It is worth noting that the curve for baggage fire ignition source given in Figure 4.3, is also extended for further 15 minutes in its decay period. The extended simulation covers an additional 15 minutes of analysis of fire development.

The extended simulation shows that the peak heat release rate, achieved at the 29th minute, remains almost constant for about 8.5 minutes. The peak heat release rate is reached when the most of the floor area is involved in fire and burning simultaneously. The decrease in the heat release rate is predicted once the combustibles on floor around the ignition source start to burn out. The peak heat release for this incident is predicted to be 4.9MW. The variation of heat release rate in Case-20 for the 45 minute long simulation is given in Figure 7.22. Figure 7.23 shows the fire development within the carriage during this incident.

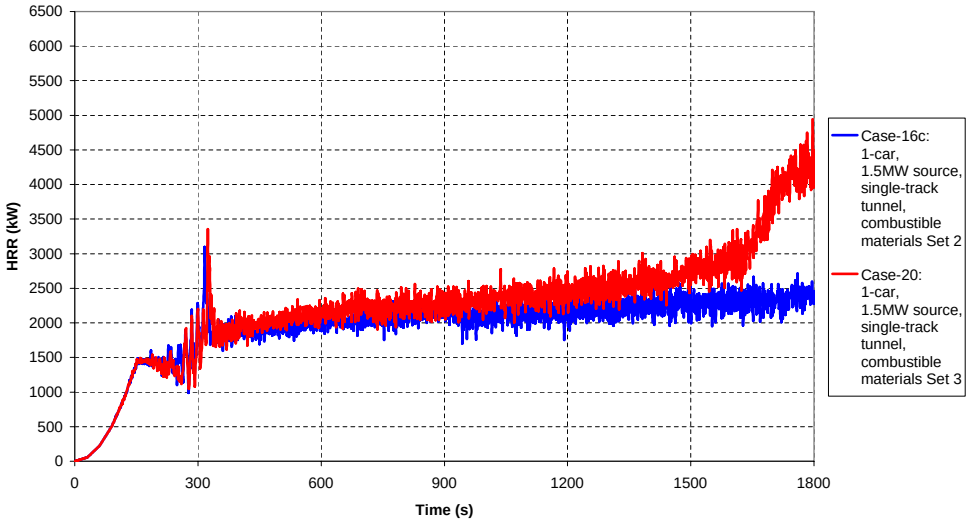

Figure 7.21: Heat release rate, 1-car, 1.5MW source, single-track tunnel, combustible material properties Set 2 and Set 3

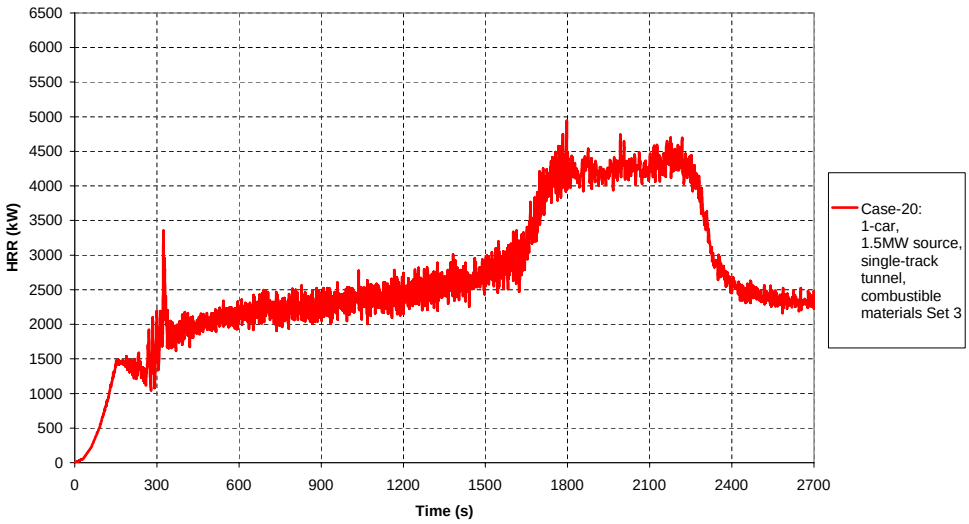

Figure 7.22: Heat release rate, 1-car, 1.5MW source, single-track tunnel, combustible material properties calibrated using cone calorimeter model with 8mm grid size

Ignition

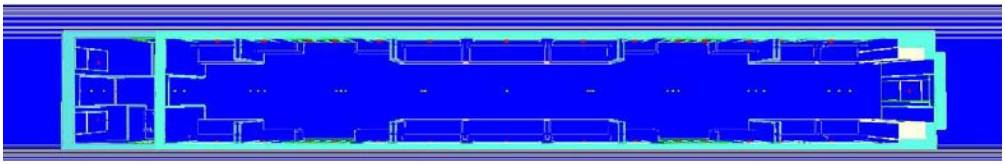

5 minutes

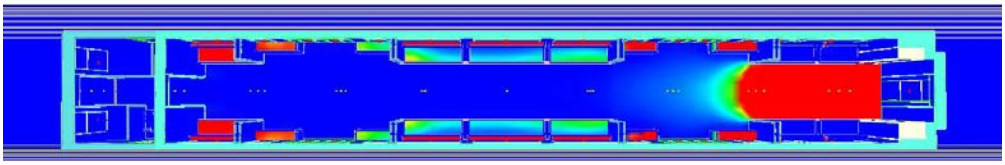

10 minutes

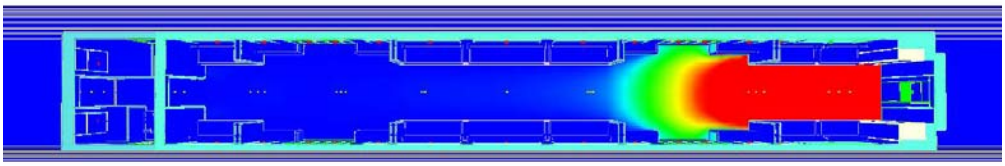

15 minutes

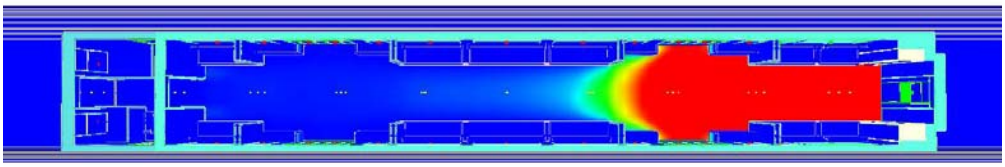

20 minutes

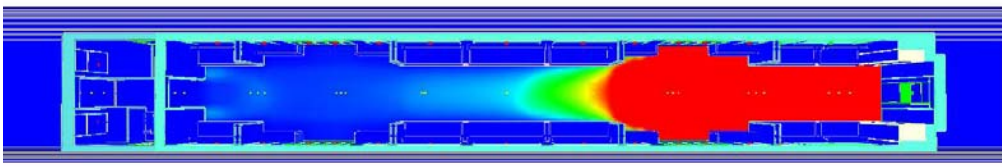

25 minutes

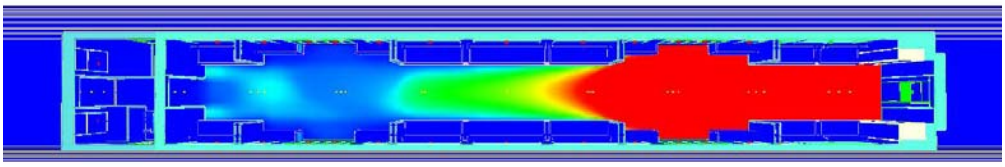

Figure 7.23: Fire spread, 1-car, 1.5MW source, single-track tunnel, combustible material properties calibrated using cone calorimeter model with 8mm grid size

30 minutes

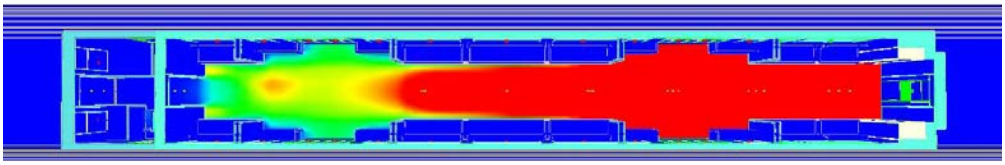

35 minutes

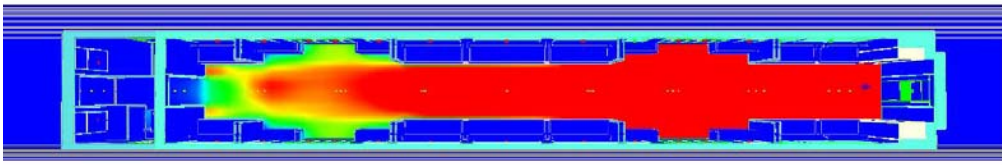

40 minutes

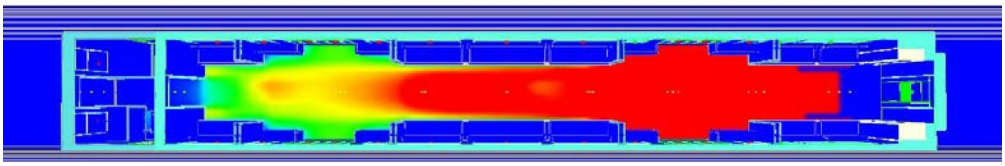

45 minutes

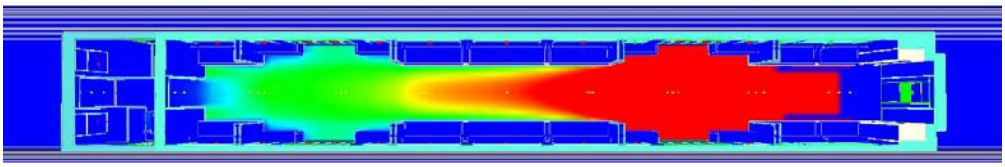

Figure 7.23 Cont'd: Fire spread, 1-car, 1.5MW source, single-track tunnel, combustible material properties calibrated using cone calorimeter model with 8mm grid size

The comparison of the simulated Cases 16c and 20 show that a slight increase in the heat of combustion of the materials increase the intensity of the fire and result in faster flame spread within the incident carriage. The faster flame spread resulted in simultaneous burning of most of the floor area of the single carriage model during an incident in the single-track tunnel. The prediction of sudden increase in the heat release rate and of the peak value amongst other cases simulated keep the single carriage model in the single-track tunnel as the design case, as noted in the initial and sensitivity simulations.

7.3 CONCLUDING REMARKS FROM FINAL SIMULATIONS

The final simulations involve revising the combustible material properties in the simulation model to reflect the burning behavior of seat and floor materials during an incident within the Class-378 rolling stock. In order to incorporate the properties of the proposed combustible materials in the simulations, a cone calorimeter model is built and parameters affecting the burning behavior of the materials are calibrated against the acquired cone calorimeter experimental results.

During the calibration of the material properties, it has been found that two different sets of parameters could lead to almost identical heat load curves. However, it is worth noting that one should pay attention to the physical meanings of the parameters and the associated limitations in assigning values to each property. Two sets of combustible material properties are derived for seat and floor materials in this thesis. The first set involves higher ignition temperatures than that defined for the second set. In order to match the experimental predictions, once the ignition temperatures are reduced, the effective heat of combustion values are decreased and the product ρ c δ is increased.

It has been predicted from the simulation results that the incidents involving either sets of material properties, i.e. with higher ignition temperatures or with lower ignition temperatures, result in quite similar predictions of heat release rate variations. Although, there are few differences predicted in flame spread patterns, overall trend and the peak heat release rate values are found to be marginally different. The peak heat release rates for these incidents are predicted to be as low as 2.1MW, with combustibles having high ignition temperatures, and 1.8MW, where combustibles have lower ignition temperatures.

Following the predictions of calibrated material properties, it has been decided to revise the combustion reaction. The combustion reaction is revised to involve the chemical reaction for seat material, which has higher energy release per unit mass of oxygen consumed and lower soot yield compared to the reaction for the floor. The simulations show that revised reaction produces enough energy to increase the intensity of the fire and promote flame spread within the carriage. The peak heat release rate for the identical incident case is predicted to increase from 1.8MW to 3.1MW, once the combustion reaction is revised from the one for floor to the one for the seats.

The simulation of an 80kW ignition source on a passenger seat is predicted to yield localized burning around the initial ignition location. The spread of flame or fire development are not predicted for this incident. The peak heat release rate is found to be about 125kW.

The simulation of an incident in the 4-car open train in the single-track tunnel, where the ignition source is at the center of the second carriage, shows that the flames tend to spread in the upstream direction towards the open end door at the early stages of fire development. However, the predicted window failures altered the intensity of the flame front through increased ventilation of smoke. Once the ventilation conditions are settled within the carriage, the flames are predicted to spread on both directions equally. It has been observed that the flames reach the adjacent carriages through spreading over the floor by 20 minutes from the ignition. The overall trend of the fire development is predicted to be steady, and the peak heat release rate for this incident is found to be 3.7MW.

The simulation performed to assess the performance of the revised material properties in the 4-car open train in the single-track tunnel showed that when all the windows on one side of the rolling stock are defined to be fail-safe, the fire develops steadily with increasing floor area involvement throughout the simulated 30 minute interval. The simulation shows that the seats in the adjacent carriage to the incident are involved in fire development within 9 minutes from the ignition. While the fire is predicted to grow predominantly in the incident carriage, it is predicted to spread to the adjacent carriage through open wide gangways, as well. The fire is predicted to reach its maximum area of influence by 25 minutes from the ignition, when it covers about one and a half carriages of floor area. The variation of heat release rate for this incident is found to be quite similar to the predictions of the same case simulated in the scope of sensitivity simulations given in Chapter 6, even though the flame spread patterns are observed to be different. The peak heat release rate is predicted to be 4.6MW for this incident.

A set of sensitivity simulations has also been performed to investigate the effect of window failures in the final simulations. The window failure criterion has been revised from 675°C to 400°C in the sensitivity cases. It has been predicted in the case, where the ignition source is placed at the center of the second carriage, that a number of windows at the center of the incident carriage fails at the very early stages of the fire development. These window failures increased effectiveness of the smoke ventilation, and reduced the rate of flame spread. The fire is predicted to remain localized, with peak heat release rate increasing only to 2.5MW,

during this incident.

The revised window failure criterion has also been simulated using the 4-car rolling stock model where all windows on one side are defined to be fail-safe. The simulation shows that successive failure of windows slowed down the flame spread within the rolling stock significantly. However, the intensity of the fire is found to be strong enough to sustain burning and to continue to spread even though the effectiveness of smoke ventilation is increased. The simulation resulted in reduced rate of increase of heat release rate, however, produced a peak value of 4.4MW, which is quite close to the predictions of the same incident with the original window failure criterion.

The simulations incorporating revised material properties showed that the burning characteristics tend to be steady and progressive, with slow rate of increase in the amount of heat released during the incidents. This is due to the low heat load and short burning durations of the seats, which lead to consumption within minutes of ignition during the incidents. Consequently, the fire development within the rolling stock is governed by the combustion of the floor material, effectively the burning of a single item, which results in progressive flame spread predictions.

A final attempt has been made to investigate the effect of cone calorimeter model on the calibrated values of material properties. The cone calorimeter calibration process, incorporating larger element size in the computational model, required an increased effective heat of combustion for the seat and floor materials in order to match the experimental predictions.

The performance of the re-calibrated material properties are tested during an incident in the single carriage model in the single-track tunnel. The re-calibrated material properties produced slightly increased heat release rates and flame spread areas throughout the simulation. One significant difference is predicted after the 27th minute of this incident. The intensity of the fire and the increased flame spread area over the floor are predicted to promote further flame spread to involve the upstream half of the incident carriage in fire. This resulted in significant increase in the heat release rate values. The peak heat release rate is predicted to be 4.9MW, which is observed to be maintained for about 8.5 minutes. This case showed that the incident in the single carriage model in the single-track tunnel remains the design case for the estimations of fire size, due to the predicted rapid increase in the rate of heat released.

Table 7.3 lists the final cases simulated and the predicted peak values of heat release rates.

Table 7.3: Summary of the final simulations with predicted peak heat release rates

Case ID	Ignition Source Characteristics	Tunnel Section	Rolling Stock Model	Ventilation Openings*	Predicted Peak HRR
Case-16,16b	Baggage fire on floor, releasing peak heat of 1.5MW following fast-growth curve	Single-track tunnel	1-car model with revised combustible materials & reaction for floor	1-end door on the driver's cab end	2.1MW, 1.8MW
Case-16c	Baggage fire on floor, releasing peak heat of 1.5MW following fast-growth curve	Single-track tunnel	1-car model with revised combustible materials & reaction for seat	1-end door on the driver's cab end	3.1MW
Case-17	Arson fire, releasing constant 80kW heat, located on a passenger seat	Single-track tunnel	1-car model with revised combustible materials & reaction for seat	1-end door on the driver's cab end	< 0.2MW
Case-18	Baggage fire ignition source at the center of the second carriage, on floor	Single-track tunnel	4-car rolling stock with revised combustibles & reaction for seat	2-end doors at each end of the rolling stock	3.7MW
Case-18b	Baggage fire ignition source at the center of the second carriage, on floor	Single-track tunnel	4-car rolling stock with revised combustibles & reaction for seat	2-end doors at each end of the train & window failure at 400°C	2.5MW
Case-19	Baggage fire on floor, releasing peak heat of 1.5MW following fast-growth curve	Single-track tunnel	4-car rolling stock with revised combustibles & reaction for seat	2-end doors at each end of the train (limited window failure)	4.6MW
Case-19b	Baggage fire on floor, releasing peak heat of 1.5MW following fast-growth curve	Single-track tunnel	4-car rolling stock with revised combustibles & reaction for seat	2-end doors at each end of the train, limited window failure at 400°C	4.4MW
Case-20	Baggage fire on floor, releasing peak heat of 1.5MW following fast-growth curve	Single-track tunnel	1-car model with reaction for seat & re-calibrated material properties	1-end door on the driver's cab end	4.9MW

* This column shows only the initial ventilation openings defined in the input files. The window failures are defined implicitly in all cases, in some of which failures are predicted as reported in the text above.

CHAPTER 8

EMPIRICAL METHODS APPROACH

8.1 DUGGAN'S METHOD

8.1.1 BACKGROUND INFORMATION

Duggan's method is a simplistic process carried out to estimate the peak heat release rate for a fire incident in a rolling stock, and is named after Gary J. Duggan's work for London Underground rolling stock [11, 17]. This method has been accepted by London Fire & Emergency Planning Authority (LFEPA) and widely used in the industry.

The method is commonly used to estimate the peak fire sizes of different types of rolling stock. However, the approach is pessimistic since it assumes that the entire load of combustible items becomes involved in fire development at the same time. In addition, the method makes no attempt to reflect how a fire might develop in terms of progressive fire spread from one item in the rolling stock to another component.

In this method, the major combustible surfaces within the rolling stock are identified as the first step. Then, these are grouped by type and orientation in accordance with the British Standard BS 6853 [6]. The power output of these combustible surfaces are obtained from cone calorimeter experiments, that have been carried out in accordance with ISO 5660-1 standard [12].

The cone calorimeter experiments generate a series of curves for the combustible surfaces where heat load (kW/m^2) vs time relationship is described. The data is then scaled for the nominal area of the surfaces within the rolling stock to obtain heat release rate (kW) vs time curve. Then these curves are summed to give the cumulative power vs time curve.

There is a requirement for the data in the final curve to be smoothed to merge peaks, remove noise and improve resolution of the data obtained from the cone calorimeter experiments in order for the final curve to reflect a real fire scenario. If too much smoothing is applied to the curve then the peaks can be continuously flattened giving a false view as to the scale of the incident. In order to avoid this, Duggan [11] suggests that the smoothing period should be selected so that peaks merged during the smoothing process are not demerged as the smoothing period is increased.

Duggan [11], in his assessment of peak fire size for London Underground rolling stock, and Hall [35], for the East London Line rolling stock, suggested using 60s as the smoothing interval to merge peaks in the final heat release rate curve. Duggan predicted some minor demerging of the peaks in the curves when 120s smoothing period is used. Consequently, a 60s smoothing interval will be used in this thesis in agreement with the earlier project reports on the same field.

8.1.2 DUGGAN'S METHOD TO VERIFY FDS PREDICTIONS OF HEAT RELEASE RATE

The Duggan's method explained in this chapter can be used to verify the design fire sizes predicted from the FDS simulations.

The heat release rate time history of the combustible items defined in the simulations will be used in the Duggan's analysis for verification of the peak heat release rate. The contribution of combustibles at particular sections of the rolling stock will be set in Duggan's analysis in agreement with the predicted burning rate of the surfaces in FDS simulations.

In the FDS simulations, details of which given in Chapter 4, two main combustible items, seats and the floor, are chosen for the analysis. The properties of the combustibles used in the simulations are taken from the cone calorimeter experiments performed at a surface heat flux of 35kW/m^2, as discussed in Chapter 4. The test results are given in Figure 8.1 for convenience.

The two cases, Case-05 and Case-12b, are analyzed in this section due to the extent of flame spread predicted in the simulations.

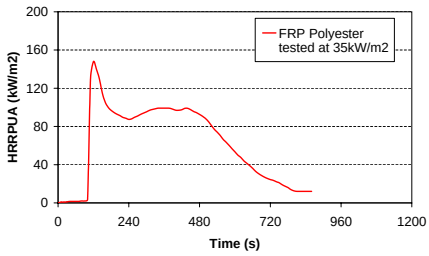

a. Cone Calorimeter results for FRP polyester to be used in Duggan's analysis

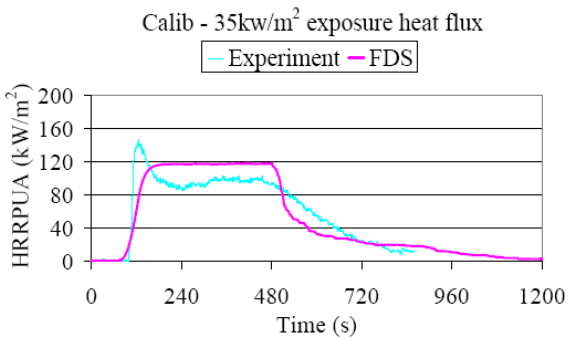

b. Cone Calorimeter results for FRP polyester at 35kW/m^2 [20]

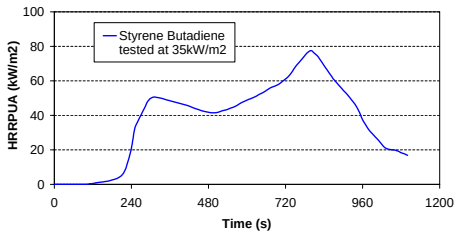

c. Cone Calorimeter results for styrene butadiene to be used in Duggan's analysis

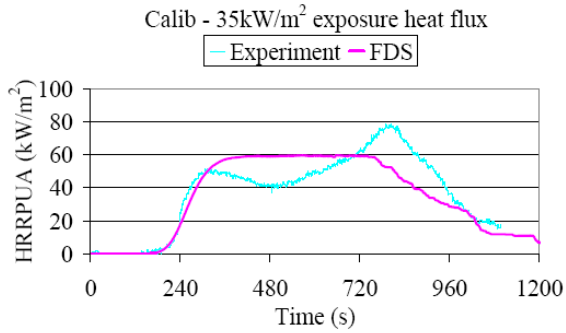

d. Cone Calorimeter results for styrene butadiene at 35kW/m^2 [20]

Figure 8.1: Cone calorimeter results used in verification of FDS simulations by Duggan's method

The areas of combustible items estimated from the 1-car simulation model is given in Table 8.1. It should be noted that there is a slight difference between the values listed herein and the areas provided by Bombardier for the actual rolling stock. The differences in areas are due to the assumptions and simplifications made during the FDS modelling. It should be noted that the discrimination for seat bases and seat backs is not necessary in this analysis, since both of them can only be represented with one characteristic curve in FDS simulations.

Initially, Case-05 is analyzed using the Duggan's method. The surface areas of the burning combustibles, which will be used in the analysis, are derived from the FDS predictions of flame spread represented by the burning rates of these surfaces. (See Figure 5.34)

Table 8.1: Areas of combustibles in the FDS model of DMOS carriage

	Area (m^2)
Standard Seats	18.0
Folded Seats	8.2
Saloon Floor	43.7
Drivers Cab Floor	3.3

The entire course of fire development is divided in intervals based on the observations of burning rates predicted from the simulation. The contribution of the combustibles in the fire development can be summarized as follows:

- 5 mins: seats: 6.1m^2 floor: 2.0m^2
- 10 mins: seats: 20.1m^2 floor: 3.2m^2
- 15 mins: seats: - floor: 19.7m^2
- 17 mins: seats: - floor: 5.8m^2

It should be noted that the surface areas given above represent the individual contributions to the overall fire development within the carriage, effective by the time defined from the ignition. In other words, the given areas do not represent the cumulative burning surface areas at a given time.

The breakdown of the contributions of the combustible items listed above defines all the seats are involved in the fire development at 10 minutes from the ignition. This assumption matches with the flame spread predictions given in Figure 5.34.

It should also be noted that not all the floor is involved in the Duggan's analysis. The careful examination of the FDS simulation predictions of fire spread showed that some of the surfaces under a number of seats are not ignited. These areas are excluded from the analysis for the purposes of comparison of two predictions.

The time at which the combustibles involved in the fire development is derived from the burning rates of these surfaces. The given times are based on the burning rates reaching 1.0 g/m^2s, in other words when the surfaces appear as red in Figure 5.34. Since the red surfaces show the combustibles are already ignited and burning, an assumption is made to correct the ignition times of the surfaces in the Duggan's analysis. It is assumed that it would

take one minute for the combustibles to reach 1.0 g/m^{2}s burning rate once they are ignited. Consequently, one minute is deducted from the times given above.

Another assumption is made on the contribution of the ignition source to the overall fire development. In the Duggan's method, neither is there a reference to the ignition source, nor is it included in the predictions of the design fire size. For the purposes of comparison of two methods, the ignition source will be included in the analysis, as it is defined in the FDS simulations.

The variation of heat release rate in time is given in Figure 8.2. The peak heat release rate is predicted to be 4.5MW with the Duggan's analysis.

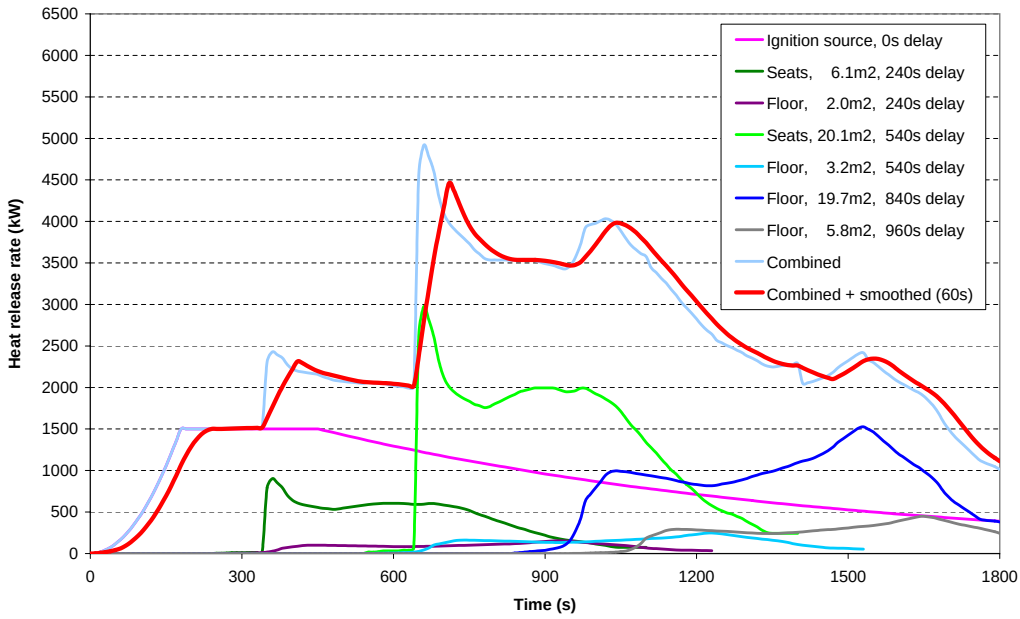

Figure 8.2: Predicted heat release rate variation using Duggan's method for single car, 1.5MW source, single-track tunnel

The comparison of the predictions of heat release rate variation is shown in Figure 8.3. The results show that the heat release rate variations predicted from the Duggan's analysis and FDS simulations match quite well for the first 11 minutes of the incident. However, Duggan's analysis predicts higher heat release rate between the 11th minute and the 14th minute from the ignition, and lower heat release rate between the 16th and the 19th minute when compared to the predictions of FDS simulations. The variations of predicted heat release rates follow a similar trend after the 19th minute, as the fire starts to decay.

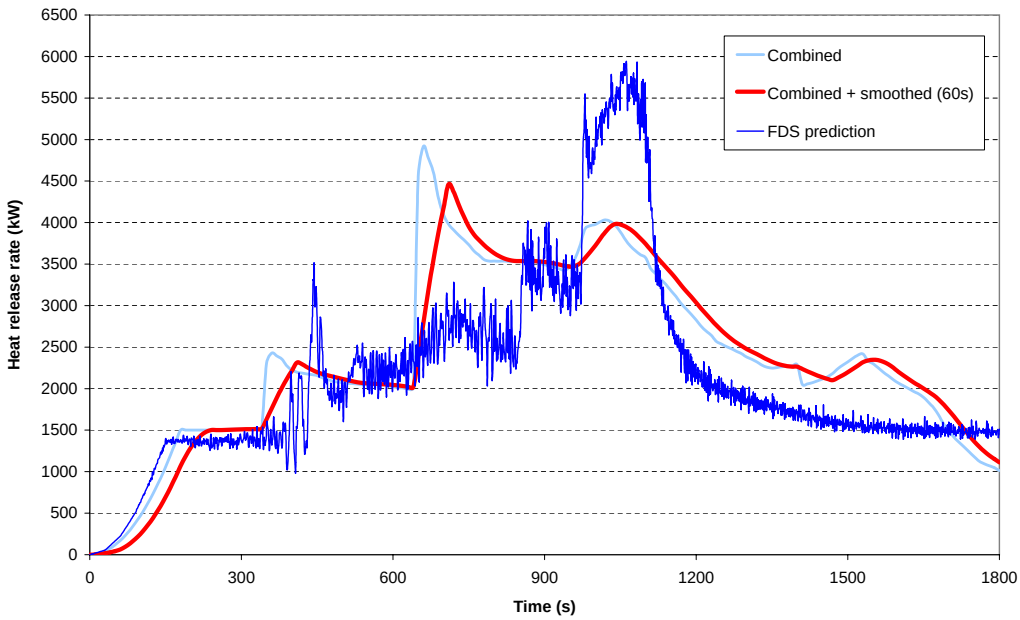

Figure 8.3: Comparison of the predicted heat release rate variations from the FDS simulation and the Duggan's analysis, 1-car model

The main difference between the Duggan's method and the FDS simulation is the predicted peak heat release rate. The Duggan's method for this particular case predicts the peak heat release rate 25% smaller than the value predicted from the FDS simulation. In addition, the peak heat release rate is predicted four minutes earlier than predicted by the simulation.

The reasons for differences in the predictions of two methods can be listed as follows:

1. In Duggan's analysis two characteristic curves for the combustibles are used, whereas in FDS simulations a set of data derived from these characteristic curves are used as input.
2. As a consequence of item 1, Duggan's analysis follows factoring these curves by the surface areas, whereas in FDS simulations the input data could lead different burning characteristics under different ventilation conditions and more importantly surface heat flux levels. The FDS simulations are the more sophisticated method as the burning rates of the surfaces depend on the heat feedback from the fire.
3. The method used herein to compare Duggan's analysis and the FDS simulation results depends on the observation and the assumptions made in contribution of the combustibles to the fire development.

Despite the differences in the comparison of two techniques, predictions of Duggan's analysis matched well with the overall trend of the variation of heat release rate predicted from the FDS simulation. However, it predicted lower peak heat release rate compared to the simulation results.

It has been estimated that in order to achieve the design fire size predicted by FDS simulation, the peaks of heat release rate curves for seats and the floor should match around 17 minutes from the ignition. This estimation does not match with the predicted burning rates of surfaces. However, the hypothetical combination leads to the possible maximum heat release rate to be predicted from this incident. This hypothetical combination of contribution of combustibles to fire development to replicate the FDS simulation results is given in Figure 8.4.

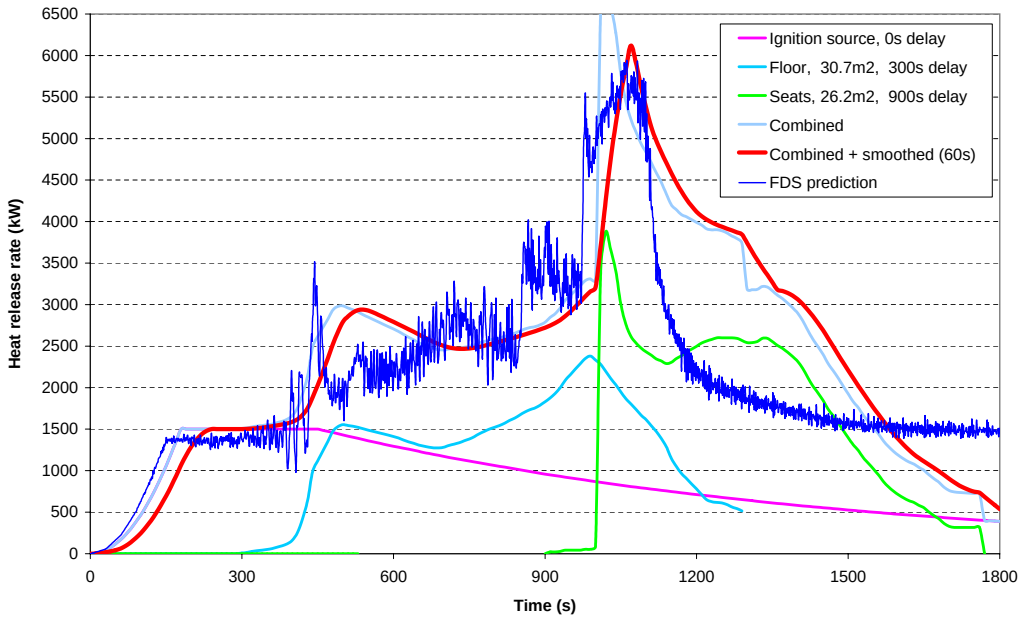

Figure 8.4: Hypothetical combination of curves in Duggan's analysis to match FDS predictions

In addition, a simple sum can also give an indication of the design fire size for this incident. However, it should be noted that the surface area of floor estimated from the simulation results is used in the equation, rather than the entire floor area.

$$Q_{peak} = \underbrace{148\ kW/m^2}_{\text{Peak HRR for seats}} \cdot 26.2\ m^2 + \underbrace{78\ kW/m^2}_{\text{Peak HRR for floor}} \cdot 30.7\ m^2 \cong 6.3\ MW \qquad (8.1)$$

The Duggan's method is also compared against FDS simulation predictions for a steady fire development. Case-12b, a baggage fire incident in a rolling stock with open wide gangways in a single-track tunnel, is selected for the analysis. The FDS simulation shows that with the limited window failure, fire develop steadily and spread to the adjacent carriage to the incident.

The contribution of the combustibles is derived from the FDS predictions of burn rates of the surfaces (See Figure 6.13). The areas of the combustible surfaces that are involved in the fire development during this incident can be listed as follows:

- 5 mins: seats: - floor: 2.5m^2
- 8 mins: seats: 5.1m^2 floor: 0.5m^2
- 11 mins: seats: 5.7m^2 floor: 3.0m^2
- 14 mins: seats: 13.9m^2 floor: 2.7m^2
- 19 mins: seats: 7.5m^2 floor: 18.6m^2
- 23 mins: seats: - floor: 9.8m^2
- 28 mins: seats: 16.0m^2 floor: 5.1m^2
- 29 mins: seats: 3.0m^2 floor: -

Once again, the given surface areas represent the individual contributions of the combustibles to the overall fire development at the specified time during the course of the incident.

In this analysis, the total surface area of the burning seats is predicted to be 51.2m^2, which includes all seats in the incident carriage and most of the seats in the adjacent carriage to the incident. It is predicted that the first set of seats in the incident carriage is involved in fire at the 8th minute from the ignition. The remaining seat surfaces are involved in fire gradually until the 19th minute. The surface area given at the 19th minute includes the remaining 1.5m^2 of the seats in the incident carriage and 6.0m^2 of the seat surfaces from the adjacent carriage. The reported seat areas after the 19th minute correspond to the seats in the adjacent carriage.

Similar to the seats, the floor of the adjacent carriage is also involved in fire during this incident. The simulation shows that the flames progress on floor to the adjacent carriage after 23 minutes from the ignition. The first significant contribution of floor of the adjacent carriage is predicted at the 28th minute during the course of the incident.

In the analysis of this case, it is assumed that it would take one minute for the combustibles to

reach 1.0 g/m^{2}s burning rate once they are ignited, as it was assumed in the analysis of 1-car model. Consequently, one minute is deducted from the times given above, as before.

The variation of heat release rate in time is given in Figure 8.5. The peak heat release rate is predicted to be 4.7MW with the Duggan's analysis, which was predicted to be 4.8MW through FDS simulation.

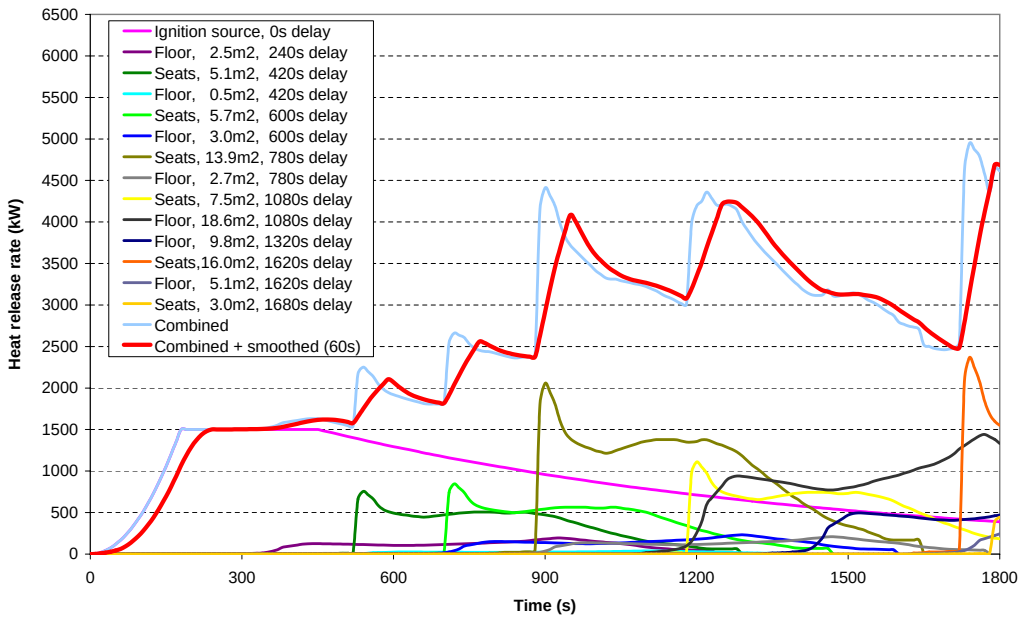

Figure 8.5: Predicted heat release rate variation using Duggan's method for 4-car rolling stock, 1.5MW source, single-track tunnel

The comparison of the predictions of heat release rate variation is shown in Figure 8.6. The results show that the heat release rate variations predicted from the Duggan's analysis match quite well with the predictions of FDS simulation. In addition, two methods predict almost the same value for the design fire size for this incident. However, differences are predicted between the 25th and the 29th minute during this incident. In this interval Duggan's analysis predicts lower heat release rates than the FDS predictions by almost 1.0MW. The reasons for the differences in predictions are the same as listed for the analysis of single car model. Despite the differences in the two methods and the simplicity of the Duggan's analysis, the predictions are within the acceptable margins for verification.

It can be concluded that the Duggan's analysis predicts the heat release rate variation reasonably well for the steadily developing fire incidents.

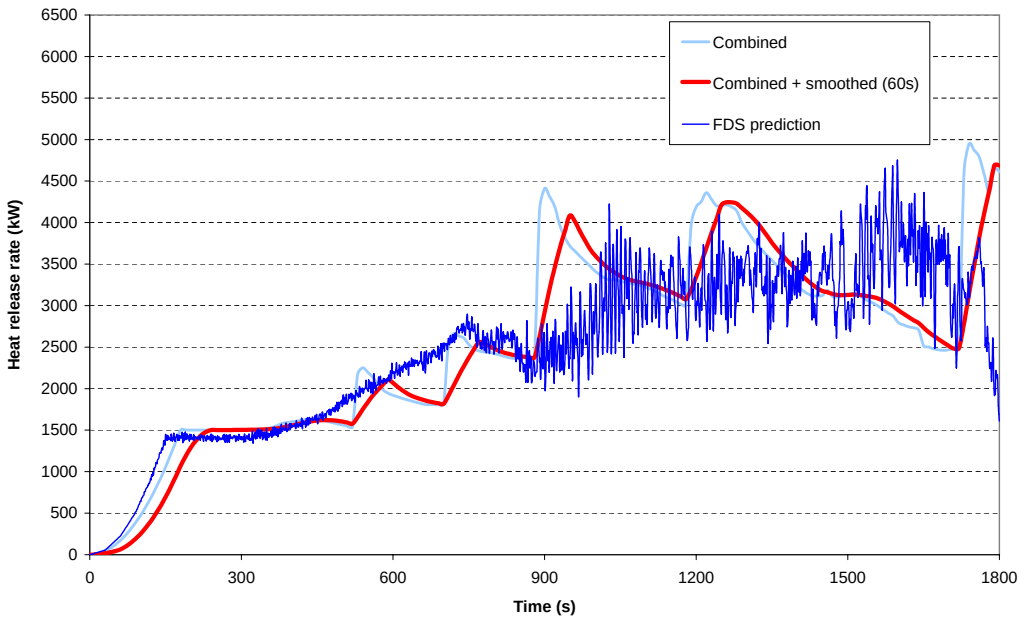

Figure 8.6: Comparison of the predicted heat release rate variations from the FDS simulation and the Duggan's analysis, 4-car model

If the flashover conditions are achieved within the rolling stock then most of the combustible surfaces would be involved in fire at once. In that case Duggan's analysis predicts slightly lower design fire sizes than expected, since the method relies upon the cone calorimeter results of the individual combustibles. In order to match with the expected design fire size, the Duggan's method requires the peaks of the heat release rate curves of combustibles coincide at one instance during the course of the incident.

It should be noted that the Duggan's method relies on the observations of FDS predictions when it is being used for the verification of results. If the simulation results are not present then the method relies upon the assumptions on the contribution of the combustible surfaces. However, an advantage of the method is it's allowing different heat release rate curves for the combustibles to be used during the analysis, to account for different heat flux levels that the surfaces are exposed during a fire incident.

8.2 CFAST SIMULATIONS

8.2.1 BACKGROUND INFORMATION

CFAST, Consolidated Model of Fire Growth and Smoke Transport, simulation program is a two-zone fire model used to calculate the evolving distribution of smoke, fire gases and temperature throughout compartments of a constructed enclosure during a fire incident. In CFAST, each compartment is divided into two gas layers. [22, 23]

The zone models, like CFAST, use two control volumes to describe a compartment - an upper layer and a lower layer. The two-layer approach has evolved from observation of such layering in real-scale fire experiments. The zone modelling relies upon hot gases being collected at the ceiling to form upper layer, and filling the compartment from the top in time. While the real-scale fire experiments show some variation in conditions within the layers, these are small compared to the differences between the layers. Therefore, the zone models can produce realistic results under many common conditions.

The CFAST model consists of a set of ordinary differential equations to compute the environment in each compartment and a collection of algorithms to compute the mass and enthalpy source terms required by the differential equations.

The modelling equations used in CFAST take the mathematical form of an initial value problem for a system of ordinary differential equations. These equations are derived using the conservation of mass, the conservation of energy, the ideal gas law and relations for density and internal energy. These equations predict pressure, layer height and temperatures as functions of time, given the accumulation of mass and enthalpy in the two layers.

The CFAST input files contain information about:

- the enclosure geometry such as compartment sizes, material properties, and materials of construction,
- the openings such as doors, windows, vertical flow openings in ceilings, and mechanical ventilation connections,
- the fire properties such as fire size and species production rates,
- the specifications for detectors and sprinklers, such as position, size, and heat transfer and flow characteristics where applicable.

Materials are defined by their thermal conductivity, specific heat, density, thickness, and burning behavior in CFAST simulations.

The outputs of CFAST are the sensible variables that are needed for assessing the environment in an enclosure subjected to a fire. These include temperatures of the upper and lower gas layers within each compartment, the ceiling/wall/floor temperatures within each compartment, the visible smoke and gas species concentrations within each layer, target temperatures and sprinkler activation time where applicable.

The CFAST model has been subjected to extensive validation studies by the National Institute of Standards and Technology (NIST). Although some differences between the model and the experiments were evident in these studies, they are typically explained by limitations of the model and uncertainty of the experiments. The most well-known difference was found during the studies to be the overprediction of gas temperature often attributed to uncertainty in soot production and radiative fraction. Still, studies typically show predictions accurate within 10% to 25% of measurements for a range of scenarios. Like all predictive models, the best predictions come with a clear understanding of the limitations of the model and of the inputs provided to the calculations.

8.2.2 CFAST SIMULATIONS TO VERIFY FDS PREDICTIONS OF ONBOARD CONDITIONS

A set of CFAST simulations has been performed to predict onboard conditions in the event of a fire incident within the rolling stock, and to compare the findings against the FDS predictions.

As discussed in Sub-section 8.2.1, CFAST predicts the conditions for two layers; the upper layer and the lower layer. The layer height within the rolling stock depends on the smoke production rate of the predefined heat release rate history of the ignition source. Consequently, the layer height changes with the size of the domain simulated and the defined ignition source. In the CFAST simulations, since fire spread has not been simulated the heat release rate predictions of FDS simulations will be input for comparison of onboard conditions.

In the CFAST simulations only the interior of the rolling stock is modelled as a simple volume, as opposed to the detailed model of rolling stock in a section of tunnel used in the FDS simulations. This approach is acceptable since simple smoke-filling method is used in CFAST

and the onboard conditions are the main interest rather than conditions within the tunnels. The ventilation openings, such as open doors and window failures, are modelled in the CFAST simulations.

Two different train models are used in the analysis. These are 1-car model and the 4-car model with open wide gangways. The single carriage is modelled as a 2.2m high, 2.5m wide and 20.0m long rectangular volume. The 4-car model is constructed by joining four of these volumes one after another. The end doors or the side doors are defined to be open depending on the case being simulated.

8.2.2.1 80kW IGNITION SOURCE

The two significant cases, one with the single carriage model and the other with the 4-car open train, have been simulated using the 80kW arson fire ignition source for the comparison of onboard conditions.

The FDS simulations predict a constant heat release rate of 125kW in all the cases simulated with the arson ignition source. Consequently, the fire in the CFAST simulations is defined to be constant at 125kW during the course of the incident.

The FDS simulations predict the smoke spread within the carriages, however, they do not discriminate volumes within the carriages as upper layer and lower layer. The conditions in the rolling stock are recorded at the center of the carriages at 1.0m, 1.5m and 2.0m above the floor level. Consequently, in order to compare the CFAST predictions against the FDS predictions the first step is to identify the layer heights in the carriages.

Figures 8.7 and 8.8 show that the hot smoke layer, also referred as the upper layer, remains above 1.0m from the floor level in the carriages in most of the cases simulated. The exception is predicted at the second car of a 4-car train, when only two end doors open for ventilation. However, in that case, the upper layer temperature increases to the order of 50°C which might be considered to be too low to define a hot smoke layer. Similarly, the layer heights in the third and the fourth carriages are also predicted to decrease to 0.6m measured from the floor level. The upper layer temperatures are predicted to be in the range of 30°C to 40°C in these carriages. Therefore, the distinction between the upper layer and the lower layer should be made in agreement with the predicted layer temperatures.

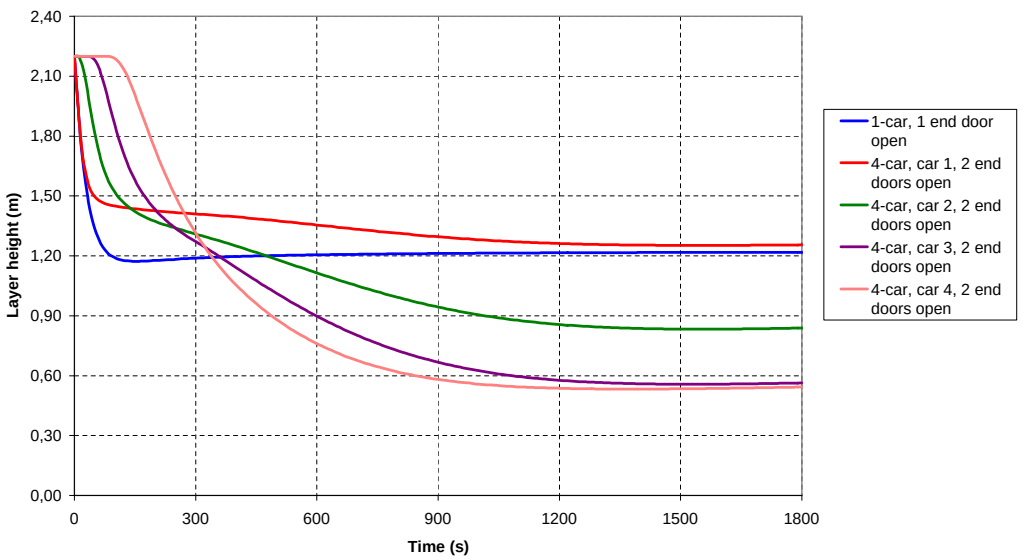

Figure 8.7: Layer height predictions for 1-car and 4-car models in a single-track tunnel

Consequently, it is assumed that the upper layer conditions predicted by the CFAST simulations reflect the conditions at a point 2.0m above the floor level in the FDS simulations. Similarly, the lower layer conditions will be compared against the predictions of FDS simulations at 1.0m above the floor level.

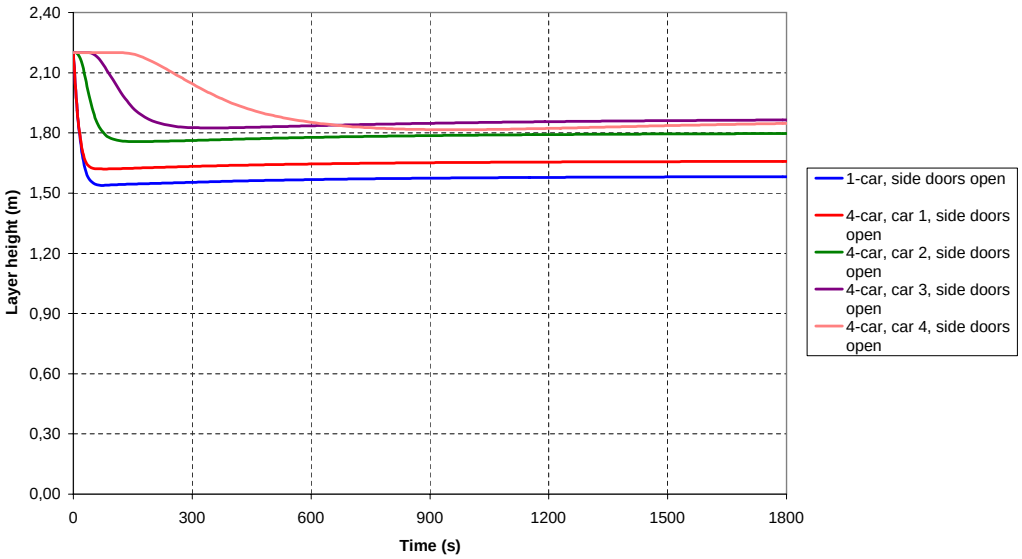

Figure 8.8: Layer height predictions for 1-car and 4-car models in a twin-track tunnel

The smoke spread from the incident carriage to the adjacent carriages can be predicted through the variations in layer height. It is worth noting that the results of CFAST simulations given in Figures 8.7 and 8.8 can be used to identify the effects of ventilation openings on smoke-filling of the carriages of a rolling stock incorporating open wide gangways.

1-CAR, SINGLE-TRACK TUNNEL

The comparison of the temperature predictions for CFAST and FDS simulations is shown in Figure 8.9, and the results are summarized in Table 8.2. The results show that FDS predicts higher temperatures at a point 2.0m above the floor level than the upper layer temperatures predicted by the CFAST simulation. However, the predicted upper layer temperatures match quite well with the FDS predictions at a point 1.5m above the floor.

In the CFAST program, each of the carriages is treated as a volume of two layers. However, in the FDS program, the computational domain is defined by a number of cells in three dimensions, which allows predictions of variables at different points along the length, width and the height of the rolling stock. Consequently, FDS predicts more accurate results with gradual changes in the parameters within the computational domain, rather than giving a value that corresponds to a proportion of the total volume of the enclosure as in the CFAST simulations.

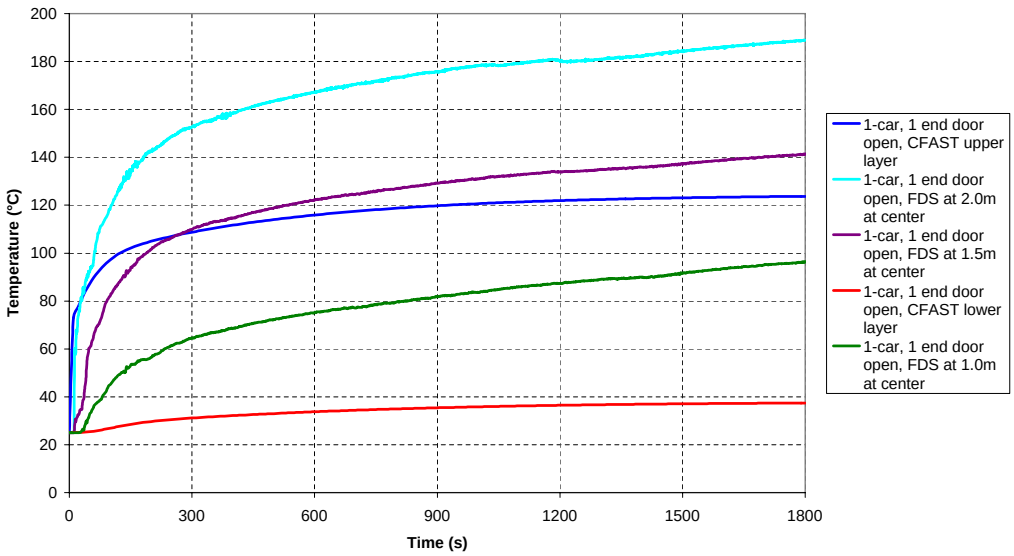

Figure 8.9: Comparison of CFAST and FDS predictions of temperature for 1-car model with 1 end door open

Table 8.2: Comparison of CFAST and FDS predictions of temperature for 1-car model with 1 end door open

		Max Temperature (°C)	Average Temperature (°C)
CFAST	Upper layer	124	116
	Lower layer	37	34
FDS	At 2.0m center	189	167
	At 1.5m center	141	122
	At 1.0m center	96	78

The gradual change in the temperature along the height of the carriage can be observed in Table 8.2. The layer height for this case is predicted to be about 1.25m from the CFAST simulations when the fire has reached the steady state conditions. Therefore, the reported upper layer temperature is the average temperature of the volume above 1.25m from the floor level.

Since the hot layer accumulates at high level and the temperature of the layer drops as the height decreases, it is reasonable to compare the predictions of FDS at 1.5m above the floor level with the CFAST predictions of the upper layer conditions.

The upper layer temperature is predicted to increase to 124°C in the CFAST simulation. The FDS simulation shows that the peak temperature increases to 141°C at the center of the carriage at 1.5m above the floor level. The difference between the temperatures is about 17°C, which is acceptable when the differences in the treatment of the computational domain and the solution methodology are considered. The difference corresponds to a 14% variance in the predictions.

The CFAST simulation predicts a maximum temperature of 37°C in the lower layer. However, FDS simulation predicts higher values of temperatures with 96°C at a point 1.0m above the floor level. The difference between the predicted maximum temperatures by the two simulation programs, once again, depends on the definition and the treatment of the computational domains. Since the layer height is predicted to be 1.25m, the temperatures predicted from the FDS simulation are influenced by the hot layer above the target point, where the temperatures are measured.

The predictions of the lower layer temperatures by the two methods will be shown to match

well for the layer heights well above 1.0m from the floor level in the following cases.

4-CAR, TWIN-TRACK TUNNEL

The comparison of the upper layer and lower layer temperature predictions from the CFAST and FDS simulations of an arson fire incident in a 4-car open train at a twin-track tunnel section are given in Figures 8.10 and 8.11, respectively.

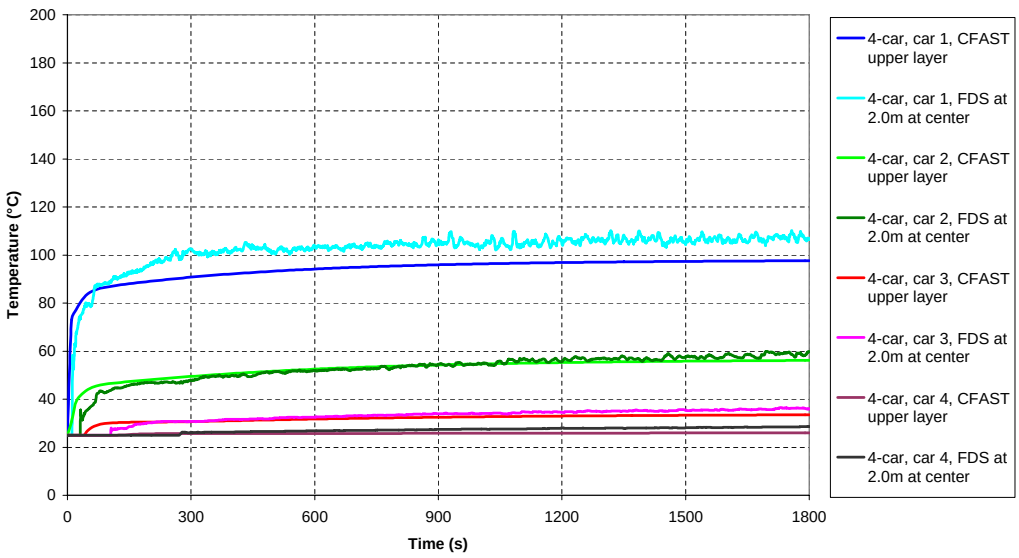

Figure 8.10: Comparison of CFAST and FDS predictions of the upper layer temperature for 4-car model with 8 side doors open

The layer heights for all the carriages are predicted to be above 1.6m by the CFAST simulation. This indicates that the incident is well ventilated and the hot smoke layer remains at high level in all carriages, including the incident carriage. The results also show that there is only a slight change in the temperatures within the fourth carriage, farthest to the incident location, due to effective ventilation of smoke produced by the fire. Consequently, it can be expected for this case that the temperature predictions of FDS program at 2.0m and 1.0m should agree well with the CFAST predictions of upper and lower layer temperatures, respectively.

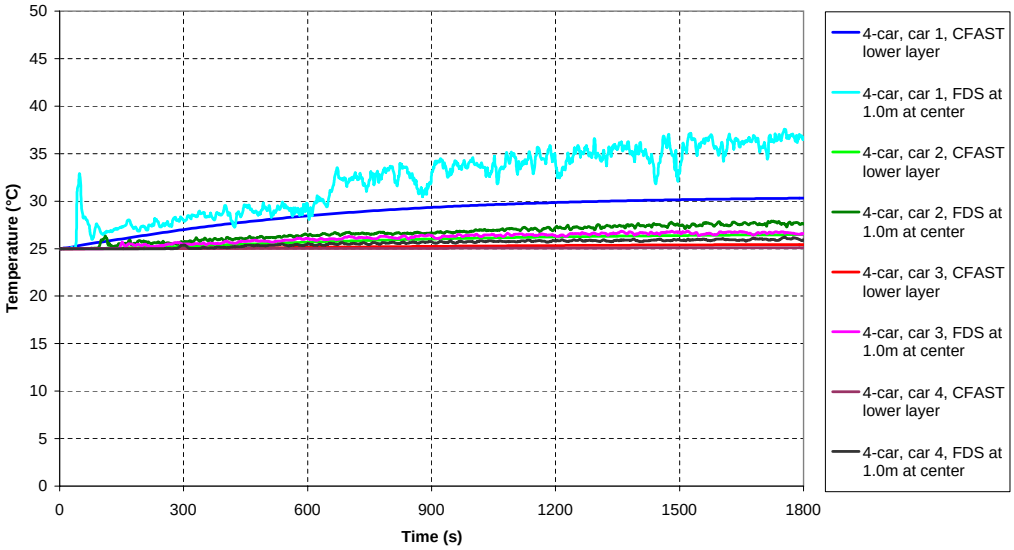

Figure 8.11: Comparison of CFAST and FDS predictions of the lower layer temperature for 4-car model with 8 side doors open

Table 8.3: Comparison of CFAST and FDS predictions of temperature for 4-car model with 8 side doors open

			Max Temperature (°C)	Average Temperature (°C)
CFAST	Upper layer	Car 1	98	94
		Car 2	56	53
		Car 3	34	32
		Car 4	26	26
FDS	At 2.0m center	Car 1	110	102
		Car 2	60	53
		Car 3	37	33
		Car 4	29	27
CFAST	Lower layer	Car 1	30	29
		Car 2	26	26
		Car 3	25	25
		Car 4	25	25
FDS	At 1.0m center	Car 1	38	32
		Car 2	28	27
		Car 3	27	26
		Car 4	26	26

The summary of the temperature predictions of the two simulation programs for this case is given in Table 8.3. The results show that the FDS predictions of maximum temperature at the center of the carriages at 2.0m above the floor match quite well with the CFAST predictions of upper layer temperatures, as expected. In addition, the temperatures recorded at 1.0m through FDS simulation agree very well with the CFAST lower layer temperature predictions.

In most cases, the difference between the temperature predictions of two simulation programs is as small as 5°C. The exception is predicted for the temperatures within the incident carriage. However, the differences are only about 8 - 12°C, which are acceptable considering the differences in the methodology.

The following conclusions can be drawn from the comparison of the temperature predictions of the FDS and CFAST simulations:

- FDS records the temperature history at the user defined points throughout the course of the incident, whereas CFAST divides the volume into two layers, and predicts and updates the temperatures of the layers as the layer height varies.
- The temperature predictions match well in most of the cases, especially when the target points in FDS lie within the upper and lower layers predicted from the CFAST simulations. However, as FDS predicts gradual variation of the temperature along the height of the rolling stock, some differences are predicted between the results of the simulation programs, especially when the layer height is below 1.5m.
- Almost perfect matches in the results are predicted for the 4-car open train with open side doors, since the layer heights are predicted above 1.5m. Consequently, the temperatures recorded at 2.0m and 1.0m agree very well with the upper layer and lower layer temperatures of CFAST, since the points lie almost exactly at the centers of the layers.
- The difference between the predictions depends on how well the target point represents the temperature of the layers. For example, if the layer height is found to be less than 1.0m, then the temperature predictions of FDS at a point well below 1.0m should be used in comparison of lower layer temperatures.

8.2.2.2 1.5MW IGNITION SOURCE

All four cases described in Chapter 5 are simulated with the 1.5MW ignition source. From the FDS simulations incorporating the baggage fire ignition source, the fire is predicted to spread within the rolling stock and produce different variations of heat release rate under different ventilation conditions. As discussed earlier in Sub-section 8.2.1, the fire development is not analyzed in the CFAST simulations, hence the predicted heat release rate histories from the FDS simulations are used as the fire curves in the CFAST cases simulated. In addition, in order for the correct representation of the ventilation in the rolling stock, window failures predicted from the FDS simulations are incorporated in the individual CFAST cases.

1-CAR, SINGLE-TRACK TUNNEL

The heat release rate history predicted from the FDS simulation of a baggage fire incident in a 1-car model in the single-track tunnel is analyzed and replicated in the CFAST simulation of the same case. The heat release rate curve is simplified by a set of data points which are input to the CFAST run. The heat release rate variations obtained from the two simulation programs are given in Figure 8.12 for information and comparison.

FDS simulations predicted rapid spread of smoke and hot gases, leading to untenable conditions fairly quickly within the rolling stock. This prediction could be confirmed by the CFAST simulation through careful observation of the predicted layer height for this incident. The predicted layer height is given in Figure 8.13.

Figure 8.13 shows that the layer height for this incident drops below 0.5m within the first three minutes from the ignition. The layer height is predicted to drop further to 0.3m within the consecutive four minutes. The first relaxation on the layer height is predicted between the 7th and 8th minutes when the pairs of windows on both sides of the carriage, closest to the ignition source, fail as predicted by the FDS simulation. The failure of the windows is predefined in the CFAST simulation, in agreement with the predictions of the FDS simulation.

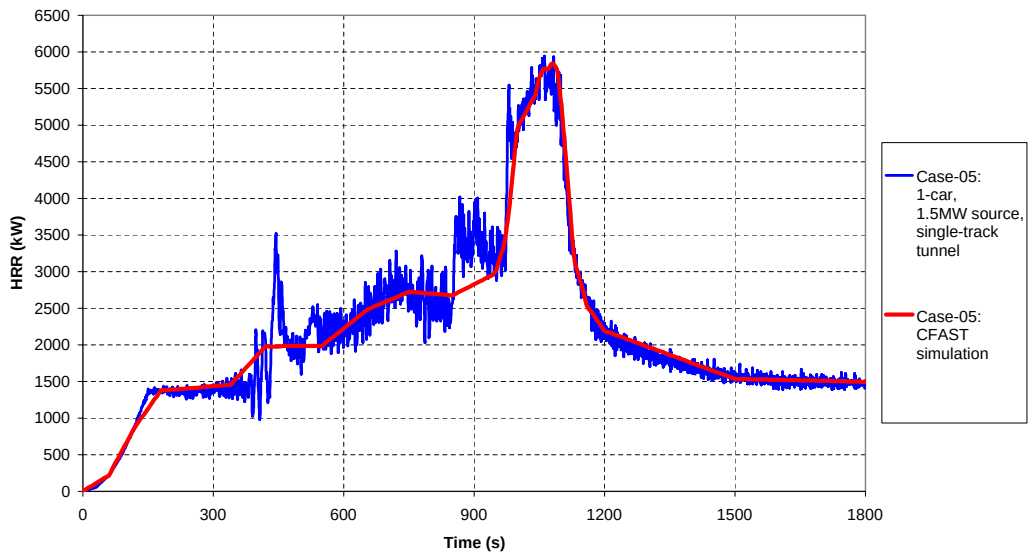

Figure 8.12: The heat release rate histories obtained from the FDS and CFAST simulations for baggage fire in a 1-car model in the single-track tunnel

Once the layer height drops below 1.5m within the first minute, it is predicted to remain below 1.5m for the rest of the simulation. The thickness of the hot smoke layer changes during the course of the incident as the heat release rate changes and the window failures are introduced.

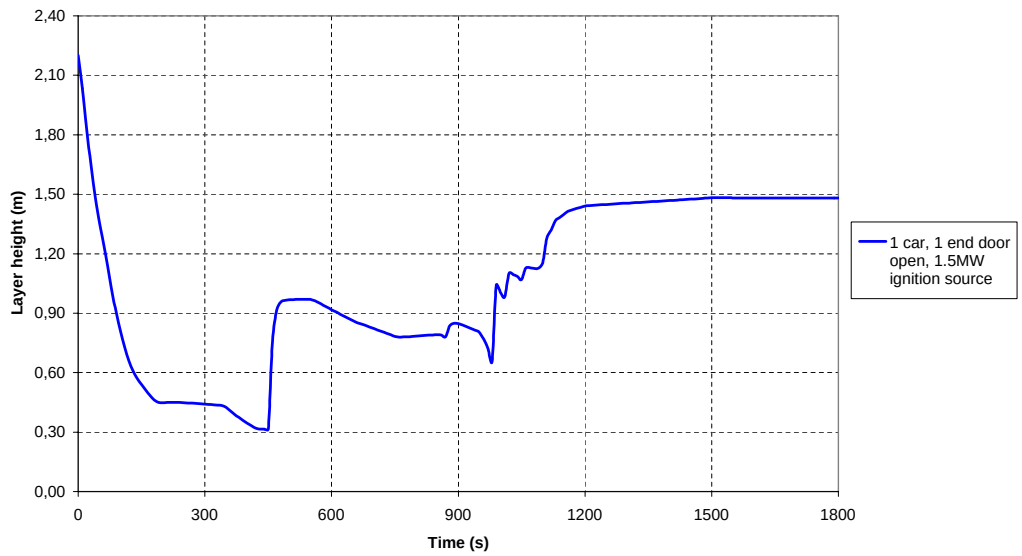

Figure 8.13: Layer height prediction for 1-car model in a single-track tunnel for baggage fire incident

The comparison of the temperature predictions for CFAST and FDS simulations is shown in Figure 8.14. The figure shows that the variation of temperature at 1.0m, 1.5m, and 2.0m above the floor level increases rapidly as the smoke and hot gases fill the carriage during the initial development of the fire. The upper layer temperature of the CFAST simulation is predicted to follow the same trend with similar values predicted from the FDS run.

The predicted upper layer temperature matches quite well with the FDS predictions at the initial stages of the fire development. The decrease in the temperature, just after the failure of the first pair of windows between the 7th and 8th minute from the ignition, is well captured by the CFAST simulation. However, between the 8th and the 18th minute CFAST predicts slightly lower temperatures compared to the FDS predictions. Within this interval, due to the consecutive window failures, the layer height varies with time, but does not go beyond the 1.0m mark.

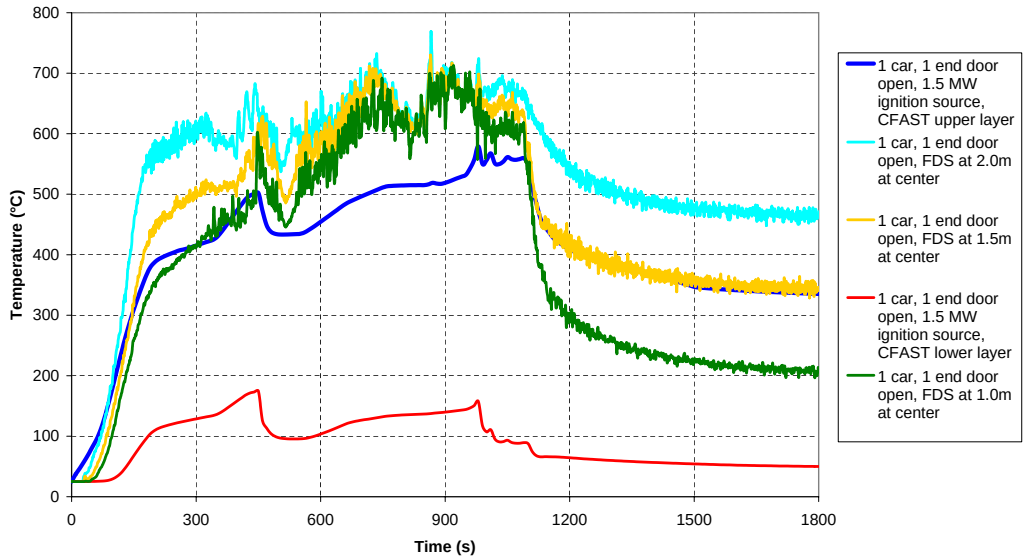

Figure 8.14: Comparison of CFAST and FDS predictions of temperature for a baggage fire incident in 1-car model in a single-track tunnel

After the 18th minute, the layer height is predicted to be constant around 1.5m above the floor level, when the amount of smoke produced becomes equal to the amount that is being extracted. The temperature profiles predicted by the FDS simulation at 1.5m and by the CFAST simulation for the upper layer are predicted to match significantly well, in the last stages of this incident.

As discussed earlier, the temperature histories of the points below 1.0m are not recorded in the FDS simulations. Consequently, there is no reference for comparison of the lower layer temperatures predicted by the CFAST simulation, however, it can be concluded that the temperature in the lower layer exceeds the tenability limit of 60°C most of the time during the course of the incident. The layer heights being as low as 0.3m with temperatures increasing to 180°C, this incident results in untenable conditions within the carriage.

1-CAR, TWIN-TRACK TUNNEL

The baggage fire incident in the 1-car model has also been simulated in a twin-track tunnel, where the smoke and hot gases are ventilated through the open side doors. The analysis of fire spread through FDS simulations showed that the fire is localized around the ignition source, and produce much less heat release rate compared to an incident in the single-track tunnel. Consequently, the fire source in the CFAST simulations is redefined for this case to represent the predicted heat release rate from the FDS simulation. The heat release rate histories of FDS and CFAST simulations are given in Figure 8.15.

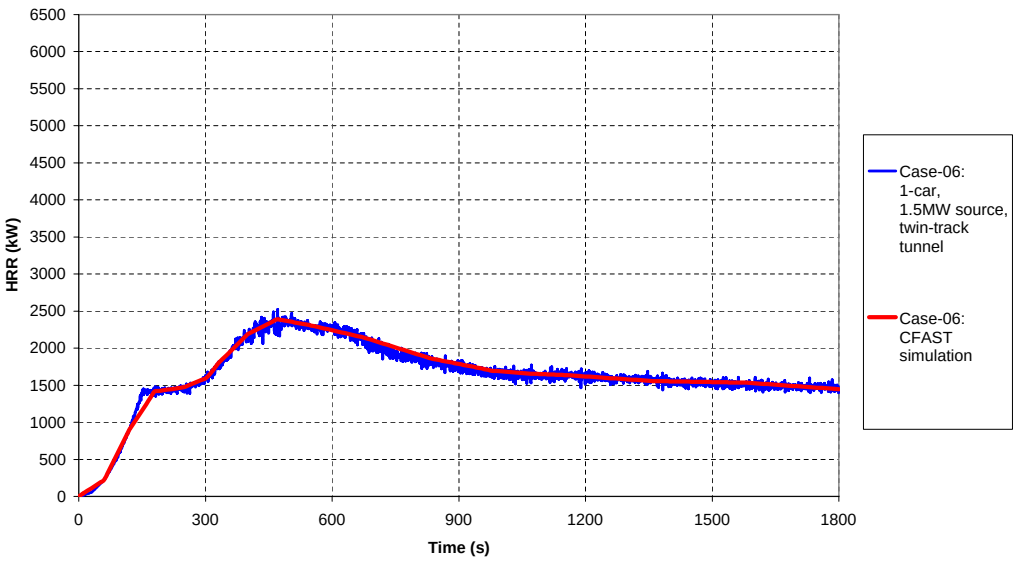

Figure 8.15: The heat release rate histories obtained from the FDS and CFAST simulations for baggage fire in a 1-car model in the twin-track tunnel

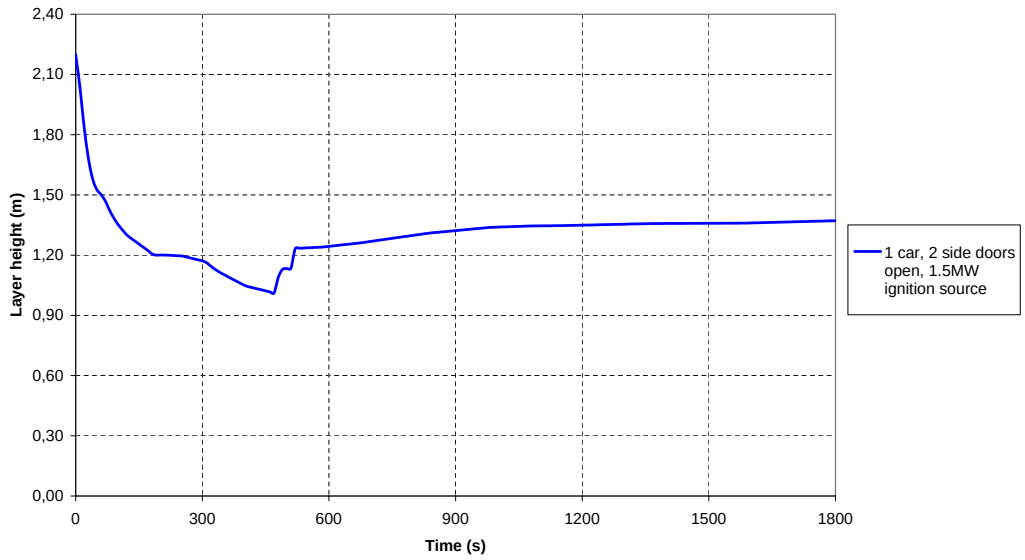

Figure 8.16: Layer height prediction for 1-car model in a twin-track tunnel for baggage fire incident

The predicted variation in the layer height is given in Figure 8.16. The figure shows that the layer height within the carriage drops to about 1.0m within the first 8 minutes from the ignition. The predicted failure of the windows between the 8th and 9th minutes improved ventilation of smoke, resulting in an increase in the layer height.

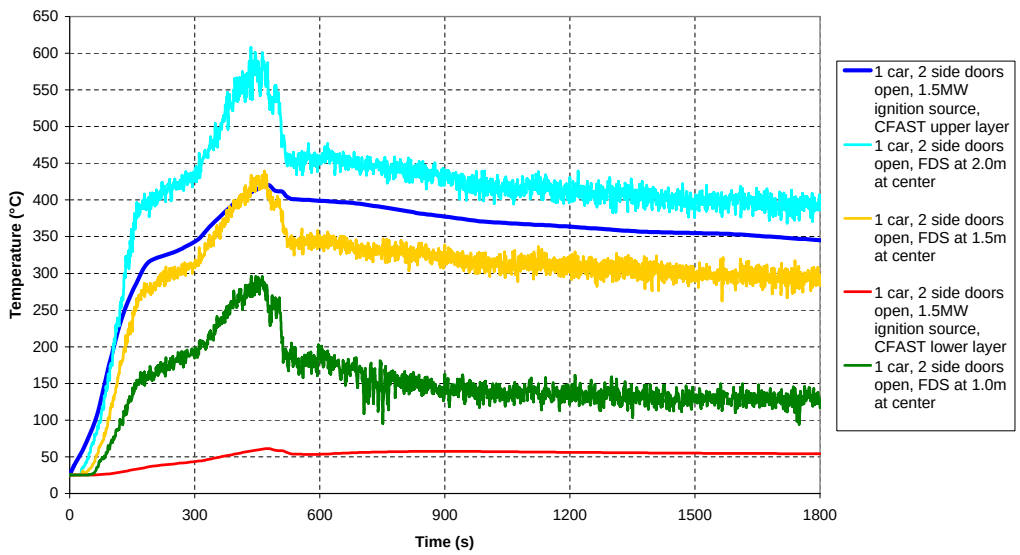

Figure 8.17: Comparison of CFAST and FDS predictions of temperature for a baggage fire incident in 1-car model in a twin-track tunnel

It is predicted from the layer height variation that almost steady state conditions have been achieved after 15 minutes from the ignition. After the 15th minute, only a slight change in the layer height is observed.

The predicted temperature histories are shown in Figure 8.17. The variations of temperature agree with the failure of windows between the 8th and 9th minutes, during which reduction in temperatures is predicted. The effects of window failure on temperatures are more significant in the results of FDS simulation, whereas CFAST results show a slight reduction. This is due the CFAST simulations averaging the temperature over the upper layer volume. However, FDS simulations record the values of temperature at specific points.

The upper layer temperature predicted from the CFAST simulations agrees very well with the FDS predictions at 1.5m above the floor level, within the first 8 minutes. Since then, the window failures change the layer height and the corresponding upper layer volume. As the layer height increases, the temperature is averaged within a smaller volume, which results in higher temperatures than predicted at 1.5m by the FDS simulation. As the midpoint of the upper layer lies between 1.5m and 2.0m, the values of predicted upper layer temperature are between the FDS predictions of temperature at 1.5m and 2.0m above the floor level.

The lower layer temperature is predicted to increase to 61°C from the CFAST simulation. However, the temperature values at 1.0m above the floor level predicted by the FDS simulation are much higher than the CFAST predictions. FDS predicts gradual temperature variation along the height of the carriage, however CFAST predicts temperature for the lower layer volume. Consequently, since 1.0m mark is too close to the interface height between the upper and lower layers, higher temperature values are expected than the volume averaged lower layer temperature. For a better comparison, temperatures well below 1.0m should have been checked against the CFAST predictions.

Further analysis showed that the FDS predictions of temperature at 1.0m above the floor match very well with the average of the upper and lower layer temperatures of the CFAST predictions for the first 8 minutes. Since the layer height is about 1.0m until the windows fail, the average temperature represents similar values with the FDS predictions at 1.0m. After the 15th minute, as the layer height increases to about 1.4m, the FDS predictions of temperature at 1.0m are lower than the average of the upper and lower temperatures of the CFAST run. Consequently, the temperature variations predicted by two simulation software match well

where data can be compared directly, and produce expected and acceptable results where direct comparison is not possible.

4-CAR, SINGLE-TRACK TUNNEL

Following the baggage fire incidents in the single car model, the simulations have also been performed using the 4-car rolling stock incorporating open wide gangways. The first of the two cases involves a train stopping in a single-track tunnel, where the evacuation and ventilation are through the detrainment doors at each end of the rolling stock. The heat release rate variation predicted from the FDS simulation for this case is defined as input in the CFAST simulation. The heat release rate variations predicted from the two simulation programs are given in Figure 8.18.

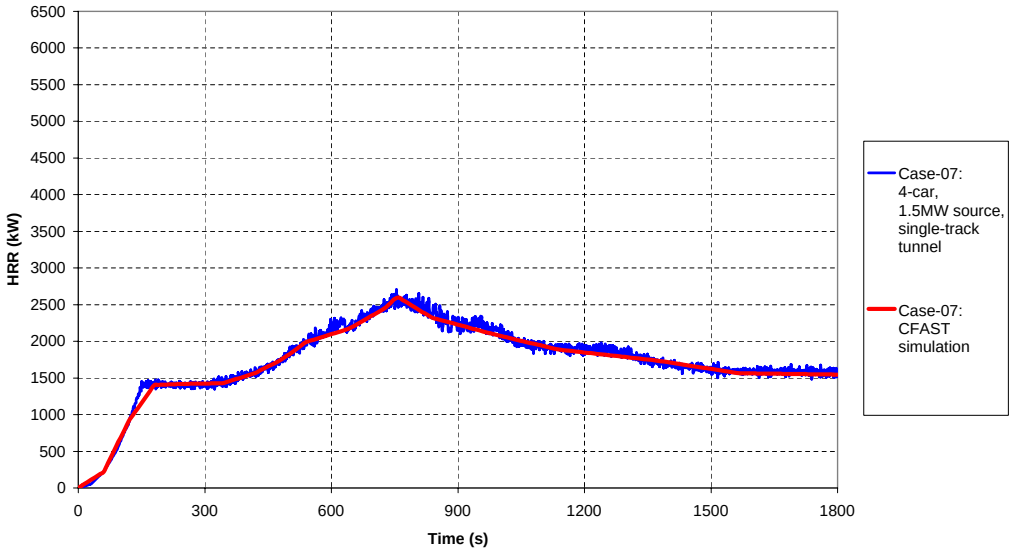

Figure 8.18: The heat release rate histories obtained from the FDS and CFAST simulations for baggage fire in a 4-car model in the single-track tunnel

The predicted layer heights for this incident, given in Figure 8.19, show that the smoke and hot gases spread to all carriages fairly quickly. It is predicted that the layer height in the incident carriage drops to about 0.8m within the first 5 minutes from the ignition. The layer heights in all carriages drop to 0.5m, measured from the floor level, within 10 minutes from the start of the fire.

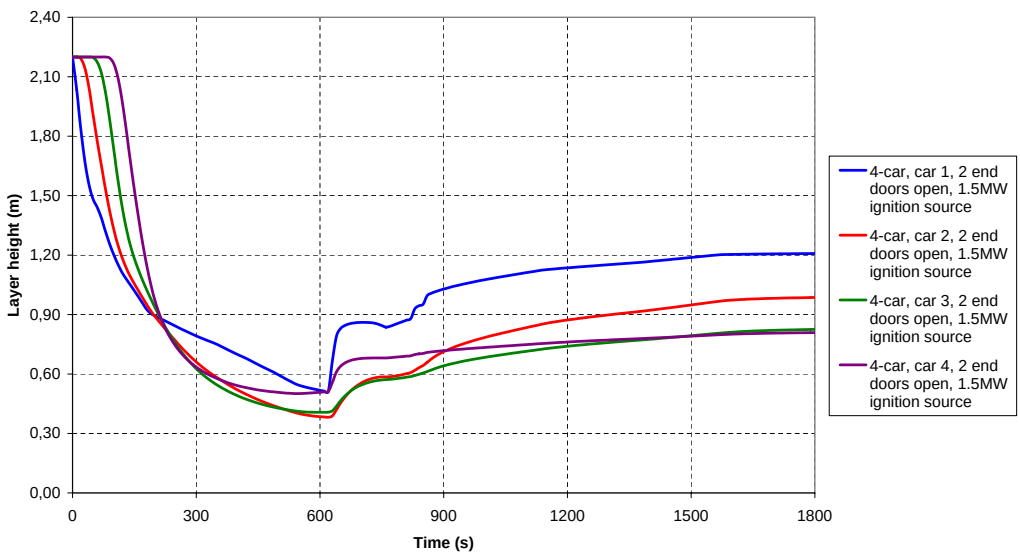

Figure 8.19: Layer height prediction for 4-car model in a single-track tunnel for baggage fire incident

The first pair of windows are predicted to fail between the 10th and the 11th minute from the FDS simulations. The window failure results in an increase in the layer heights as the amount of smoke extract increases. The second pair of windows fail between the 13th and 14th minute, during which further increase in the layer heights are predicted. The layer heights then increase slightly towards the end of the simulation, as the fire loses its intensity.

The predicted temperatures from the two simulation programs are given in Figures 8.20 and 8.21. The FDS predictions of temperature at a point 2.0m above the floor in the incident carriage are too high compared to the volume averaged upper layer temperature predictions of CFAST simulation, since the layer height in the incident carriage remains below 1.2m during most of the simulation time. However, the results show that the upper layer temperature predictions from the CFAST simulation match very well with the values of temperature at 1.5m predicted by the FDS program for the incident carriage. In the rest of the rolling stock, the upper layer temperatures are lower than the temperatures predicted at 1.5m from the FDS simulation.

The results show that the lower layer temperatures predicted from the CFAST simulation are much lower than the temperatures predicted at 1.0m by FDS.

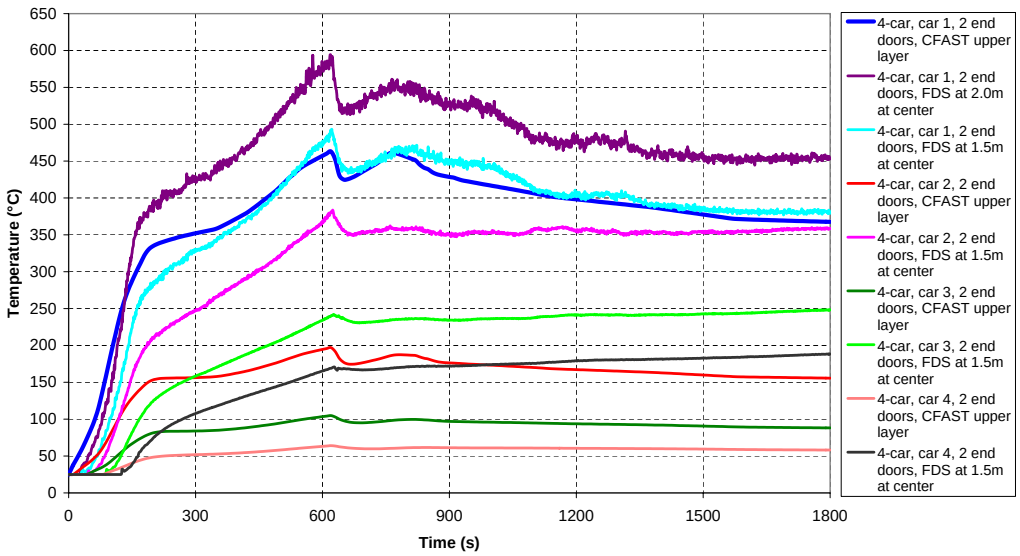

Figure 8.20: Comparison of CFAST and FDS predictions of the upper layer temperature for a baggage fire incident in 4-car model in a single-track tunnel

Once again, since the layer heights in all carriages are either close to or below 1.0m mark, the lower layer temperatures should have been compared against values well below 1.0m. However, the gradual temperature predictions by FDS confirm that the values are as expected and acceptable.

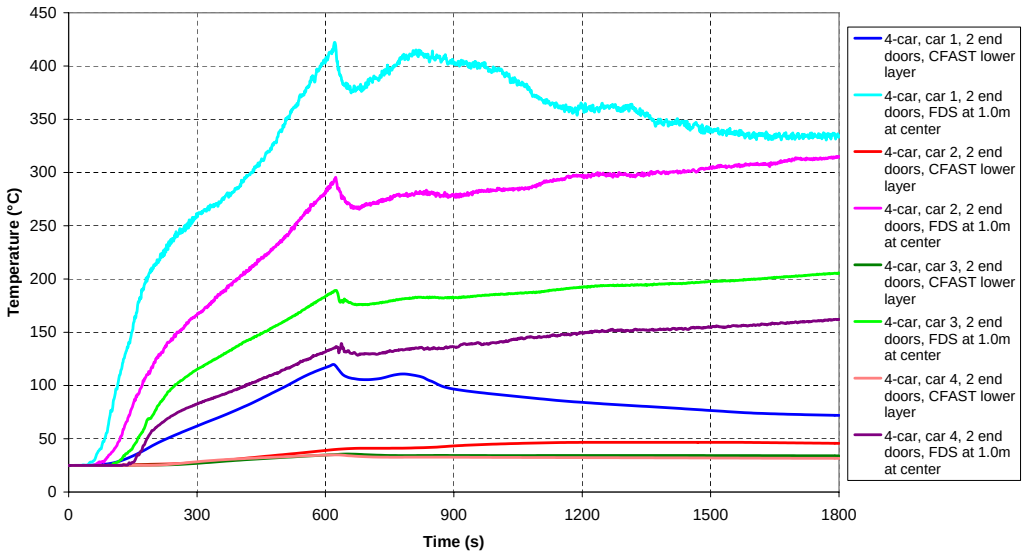

Figure 8.21: Comparison of CFAST and FDS predictions of the lower layer temperature for a baggage fire incident in 4-car model in a single-track tunnel

4-CAR, TWIN-TRACK TUNNEL

The heat release rate histories obtained from the simulations of a baggage fire incident in a twin-track tunnel using the FDS and CFAST programs are given in Figure 8.22. The heat release rate curve is predicted from the FDS simulation and is simplified by a set of data points which are input to the CFAST run, as noted for the previous cases.

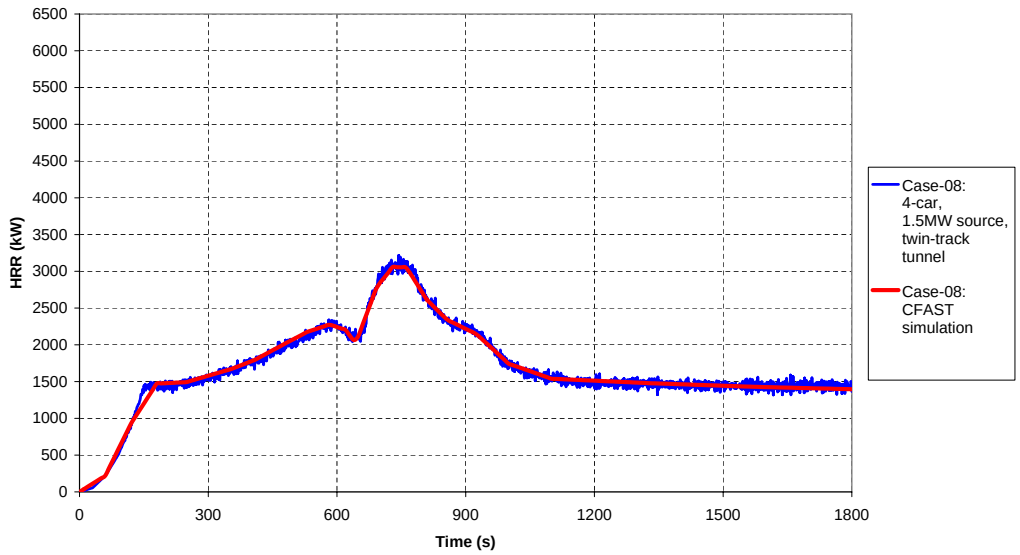

Figure 8.22: The heat release rate histories obtained from the FDS and CFAST simulations for baggage fire in a 4-car model in the twin-track tunnel

The predicted layer heights for the carriages in this incident are given in Figure 8.23. The results show that the layer height in the incident carriage varies between 1.0m and 1.5m during most of the simulation. The increase in the layer height just after 10 minutes and 13 minutes are due to the window failures defined for this case, as predicted from the FDS simulation. The layer heights are predicted to be above 1.5m in the rest of the rolling stock.

The variation of layer heights shows that the smoke is ventilated more effectively when the side doors are open compared to a case in which the ventilation is through the open end doors.

The predicted upper and lower layer temperatures are shown in Figures 8.24 and 8.25. The results show that upper layer temperature for the incident carriage matches very well with the FDS predictions of temperature at 2.0m. The upper layer temperature for the second car is found to be between the temperatures predicted at 1.5m and 2.0m from the FDS simulation.

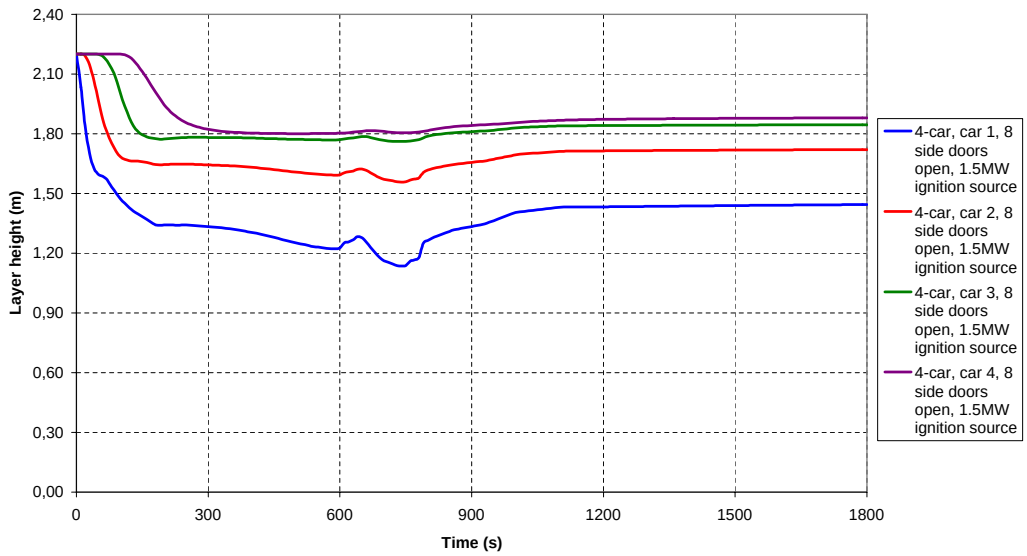

Figure 8.23: Layer height prediction for 4-car model in a twin-track tunnel for baggage fire incident

The predicted upper layer temperature in the third carriage matches very well with the predictions of temperature at 1.5m from the FDS simulations. In the fourth carriage, upper layer temperature is less than the values obtained from FDS at 1.5m.

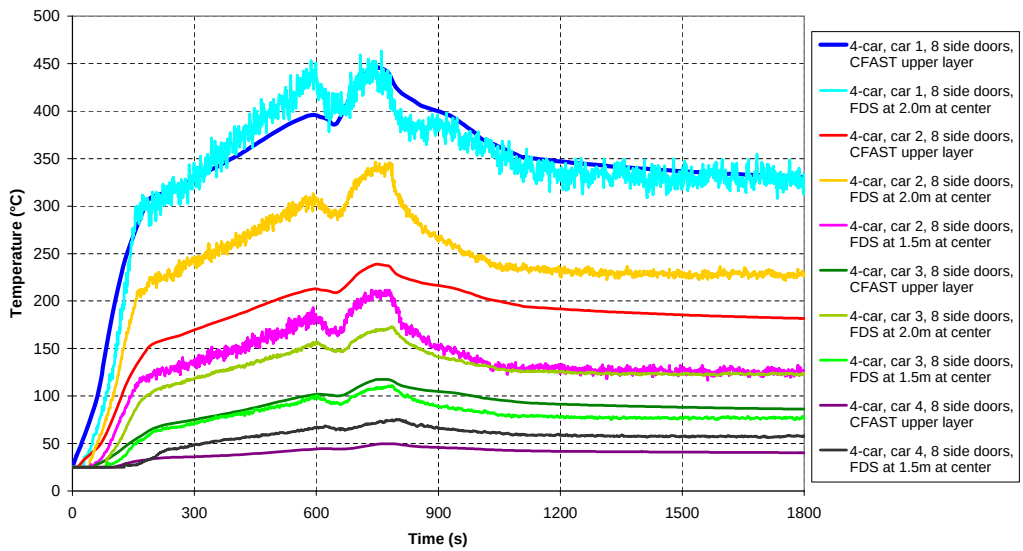

Figure 8.24: Comparison of CFAST and FDS predictions of the upper layer temperature for a baggage fire incident in 4-car model in a twin-track tunnel

The comparison of temperatures shows that as the target point moves away from the incident carriage in the rolling stock, the upper layer temperatures match better with the FDS predictions at points away from the ceiling. This statement agrees with the predicted layer heights in the incident and the adjacent carriages. However, the layer heights are predicted to be above 1.8m in the third and the fourth carriages, where the upper layer temperatures match with the FDS predictions at 1.5m or lower. This is due to the CFAST programs' predicting the upper layer temperatures lower than the predictions of FDS program, since CFAST gives a temperature for the upper layer volume whereas FDS predicts temperatures at specific target points.

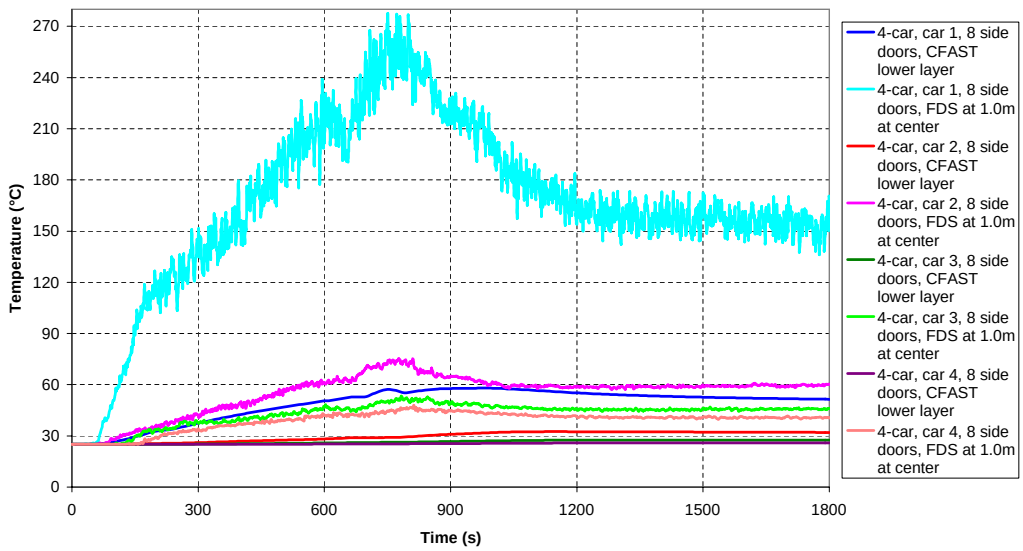

Figure 8.25: Comparison of CFAST and FDS predictions of the lower layer temperature for a baggage fire incident in 4-car model in a twin-track tunnel

The lower layer temperatures for this incident are predicted to be below 60°C from the CFAST simulations. FDS predicts significantly high temperatures at 1.0m above the floor level in the incident carriage. This is due to the gradual temperature predictions of the FDS program. The hot smoke layer in the incident carriage drops below 1.2m, which causes FDS to predict high temperatures at 1.0m. For the rest of the rolling stock, FDS predictions of temperature at 1.0m match well within the acceptable limits with the lower layer temperature predictions of CFAST program.

8.2.2.3 CONCLUDING REMARKS

The comparison of the predictions of CFAST and FDS shows that the results match quite well for most of the time, especially for the upper layer temperature. This has been shown for a set of simulations including various parameters. (Refer to Figures 8.10, 8.14, 8.20, and 8.24)

CFAST predicts temperature values for the upper and lower layer volumes, whereas FDS predicts temperature values at specific predefined target points. Therefore, some differences in the temperature values are also predicted, especially when the layer volumes are large, or the height of the points defined in FDS simulations do not agree well with the layer height predictions.

It should be noted that although CFAST program uses empirical relations, it is reliable in predicting indicative smoke spread in the event of a fire in the rolling stock. Therefore, it is acceptable to use CFAST to compare the predictions of FDS program.

In addition, the run-time for a CFAST simulation is as low as few minutes, which makes it superior compared to any other simulation software. However, if a more detailed analysis is required, the FDS program is the preferred software, especially if fire spread modelling or prediction of design fire size is required.

CHAPTER 9

DISCUSSION & CONCLUSION

9.1 INTRODUCTION

The purpose of this research study is to investigate fire development and flame spread within the underground rolling stock using 3-dimensional simulation methods. A set of simulations is performed using FDS simulation software with various initial and boundary conditions to achieve this aim. This study is focused on fire incidents within the passenger compartments of the underground railway carriages.

The cases simulated are divided into three groups of simulations in this thesis; the initial, the sensitivity, and the final simulations. The purpose of the initial simulations is to identify the developing fire incidents and gain an insight on how the fires might develop within underground rolling stock. The sensitivity simulations incorporate variations in the ignition source characteristics and the ventilation conditions, and investigate their effects on fire development and flame spread. The final simulations include re-running of the selected cases from the initial and sensitivity simulations with revised material properties. The final simulations are performed to investigate the effects of the change in combustible material properties on flame spread characteristics and on the peak value of heat release rate.

The design fire size, in other words the peak heat release rate, in the event of a fire incident in the underground rolling stock has also been investigated using empirical methods. The Duggan's method, named after Gary J. Duggan's work for London Underground rolling stock, is chosen and implemented in this study. In addition, the predictions of FDS simulations for the selected cases are checked against the predictions of the Duggan's method.

In the initial set of simulations, the onboard conditions have also been predicted and re-

ported. The predicted onboard conditions are verified using the CFAST program, a two-zone fire model used to calculate the evolving distribution of smoke, fire gases and temperature throughout compartments of an enclosure during a fire incident.

The predictions and the conclusions derived from them are summarized in the following Sections.

9.2 COMMENTS ON FDS SIMULATIONS

9.2.1 INITIAL SIMULATIONS

The predictions from the initial simulations are discussed under two headings; fire development and onboard conditions. The findings are summarized in the following Sub-sections.

9.2.1.1 FIRE DEVELOPMENT

The simulations incorporating an 80kW arson fire ignition source show that the fire is localized around the initial ignition location and would not spread to the adjacent combustible items or would not grow to involve the entire carriage of an underground rolling stock. It has been shown in four different case studies that the fire remains localized, only igniting the very adjacent seats to the initial ignition location, irrespective of the rolling stock model or the ventilation option selected.

The 80kW arson ignition source is compliant to the British Standard BS 6853, and referred to as the design condition by the rolling stock manufacturers. It is assuring that with this ignition source the fire would be localized with peak heat release rate of about 135kW.

A set of simulations incorporating a severe baggage fire ignition source, following fast growth rate and reaching to 1.5MW at its peak, show that the fire would grow and, if the conditions allow, could lead to flashover phenomenon. Amongst the simulated cases, an incident in a single carriage with only one end door open results in the highest peak heat release rate of 6.0MW. In this case, the severity of the ignition source along with the change in ventilation conditions, by means of window failures, promote the fire to develop and involve the entire carriage, where the flashover is predicted.

It has been predicted from the remaining set of simulations that if the initial ventilation openings are large enough to ventilate the smoke effectively, or the volume of the enclosure is large enough to dilute the smoke within the rolling stock, as in the 4-car train with open wide gangways, the fire burns locally and the risk of flashover is reduced significantly. The peak heat release rates are predicted to be between 2.5MW and 3.2MW, in these cases.

9.2.1.2 ONBOARD CONDITIONS

The simulations incorporating an 80kW arson fire ignition source show that the number and size of the ventilation openings are crucial in assessing the onboard conditions. The incident case in a single carriage with only one end door open resulted in untenable conditions for the passengers onboard due to high temperature and high level of carbon-monoxide concentration.

However, the onboard conditions are predicted to be within the acceptability criteria, defined for temperature and carbon-monoxide concentrations by the British and NFPA Standards, at a height 1.0m and below, measured from the floor level, for incidents involving a single carriage with open side doors and a 4-car rolling stock with open wide gangways and open end doors. Exceptions are predicted locally in these cases where temperature and carbon-monoxide levels exceed the defined criteria marginally. However, these remain acceptable when evacuation periods of 15 minutes to 20 minutes are considered. The 80kW arson fire incident in a 4-car rolling stock with open wide gangways and open side doors resulted in tenable conditions at 1.5m and below, measured from the floor level, within the first 30 minutes from the ignition. An increased number and area of the open doors, and a larger enclosure in the cases of 4-car open train, assisted effective ventilation and dilution of the smoke produced, maintaining the conditions tenable longer.

The visibility levels at 1.5m in all the cases simulated drop fairly quickly below the recommended acceptability criterion of 5m. However, it should be noted that the reduction in visibility does not directly cause fatalities, but it would hinder the evacuating passengers.

The initial simulations incorporating a severe baggage fire ignition source show that the conditions become untenable within the incident carriage, and in the rest of the rolling stock for the 4-car train with open wide gangways, within few minutes from the ignition. The temperatures

within the incident carriage are found to exceed the acceptability criterion within the first two minutes, whichever the rolling stock model is used or ventilation strategy is implemented.

It has been predicted that for the 4-car open train, with the smoke being ventilated through the open end doors, a severe baggage fire incident would result in loss of tenability in the entire rolling stock within the first 4 minutes of the incident. The simulation results show that the tenable conditions are maintained for 9 minutes in the adjacent carriage to incident, and for 30 minutes in the carriages farthest away from the ignition, if the side doors are opened in the 4-car open train. Once again, the number and the area of the ventilation openings define whether the onboard conditions would be tenable or not.

It can be concluded that

- in order to maintain the onboard conditions tenable longer, and to reduce the risk of flashover, a fire should be taken care of before it grows in size and starts to spread.
- opening side doors, as far as doing so is reasonably safe, would reduce the risk of flashover and would assist effective ventilation of smoke from the fire.
- the recommended ignition source of 80kW for design considerations is suitable to check the onboard conditions.
- a severe ignition source is required for the fire to develop within the rolling stock and to assess the design fire size of an incident.

9.2.2 SENSITIVITY SIMULATIONS

The sensitivity simulations have been performed to investigate the individual effects of the computational domain length, the location of the ignition source, a change in the ignition source characteristics, the window failures, a change in the amount of air entrained through the open doors, the mechanical ventilation, and the grid size in the computational domain, on the fire development and flame spread patterns within the underground rolling stock. The predictions from the sensitivity simulations are discussed and the conclusions derived from the analysis are summarized in the following Sub-sections.

9.2.2.1 TUNNEL LENGTH

The simulations showed that an incident in the twin-track tunnel section produces almost identical heat release rate curves for domain lengths of 40m and 120m. The cross-section of the twin-track tunnel is large enough to accommodate most of the smoke produced during the incident, which reduces the effects of portal ventilation significantly.

The simulation of an incident in the 120m long single-track tunnel showed that increasing the domain length increases the peak heat release rate marginally, and results in slightly earlier prediction of the peak value, compared to an incident in the 40m long domain. It is predicted from the simulations that the peak heat release rate increases from 6.0MW to 6.4MW, with the peak value being achieved 2.5 minutes earlier, when the domain length is increased from 40m to 120m.

The simulations also showed that increasing the domain length three-fold increases the computational time required to achieve the solution by a factor of 2.3 for an incident in the single-track tunnel, and by a factor of 2.8 for an incident in the twin-track tunnel.

It has been concluded that increasing domain length does not affect the predicted fire development and flame spread patterns significantly, yet requires additional computing power. Consequently, it has been decided to perform the simulations involving the single carriage using the short tunnel model.

9.2.2.2 LOCATION OF IGNITION SOURCE

The simulation of an incident where the ignition source is moved from one end of the carriage to the center in a 4-car rolling stock with open wide gangways showed that the incident produces much greater peak heat release rate when the source is placed at the center of the carriage. The rate of fire development, and therefore increase in the heat release rate, is predicted to be quite similar in the early stages of the fire development for both cases, with ignition source located either at one end or at the center of a carriage. However, the incident develops further, since an increased surface area of combustibles is readily available in the premises of the ignition source, when the fire is assumed to begin at the center of the carriage.

It has also been predicted from the simulations that the fire starts to spread in both directions

within the rolling stock. As the fire develops, it tends to spread further in one direction as far as the conditions are favorable. The simulation showed that the failure of windows in the direction of fire spread slows down and even stops further propagation of flames, as the temperatures are reduced in the vicinity of broken windows. However, as fire loses its intensity in the initial direction of spread, the flames regroup and start to spread in the reverse direction. Consequently, during such an incident two peak values of heat release rate are predicted from the simulation. The peak heat release rate during the initial development of fire is predicted to be 4.5MW. A second peak of 5.5MW is predicted after the flames regroup and fire regains its intensity. Both of the values are much higher than the fire size of 2.7MW, predicted for an incident with the ignition source is located at one end of the carriage.

9.2.2.3 IGNITION SOURCE CHARACTERISTICS

The simulation incorporating a modified baggage fire ignition source, defined to release 1.0MW heat at its peak, show that this ignition source is powerful enough to promote flame spread and to sustain burning in the rolling stock. The simulation incorporating 1-car model in a single-track tunnel with modified baggage fire ignition source predicted flashover conditions and produced quite similar results to the same incident with the original baggage fire source. The peak heat release was predicted to be 6.3MW, when the flashover conditions were achieved with the modified baggage fire source.

The set of simulations involving liquid fuel showed that the intensity of the fire depends on volume and spillage area of the fuel. The simulations predicted that for an assumed volume of fuel, increasing the spill area results in higher heat release rates but shorter burning durations. The peak heat release rates for a volume of fuel varying between 2.0 and 10.0 liters are predicted to vary between 1.7MW and 6.1MW, with burning durations ranging from 22s to 390s. The spillage area in the simulations were taken to be between 0.5 and 2.0m^2.

9.2.2.4 WINDOW FAILURES

The simulations showed that the flame spread and fire development within the incident carriage and in the rest of the rolling stock depend strongly on ventilation through the failed windows. The simulation of an incident within a single carriage, where the windows along

one side of the carriage and the window of the back end door are defined to be fail-safe, showed that altered ventilation conditions change the fire development pattern from flashover conditions to steady burning behavior. The peak heat release rate for this incident is predicted to be 3.3MW, with steady burning conditions at 10 minutes from the ignition and onwards. Although the failure of windows provided fresh air entrainment into the incident carriage and assisted ventilation of smoke, the rate of exchange was found to be sufficient only to sustain burning. Limited oxygen concentration within the carriage prevented achieving flashover onset conditions.

The incident in a 4-car rolling stock with open wide gangways and fail-safe windows on one side of the rolling stock showed that the extent of flame spread exceeds a single carriage. The fire development in this incident was found to be identical for the same case with normal window failures for the first 13 minutes of the incident. However, differences in the window failure patterns changed the ventilation conditions by the 15th minute, after which gradual increase in air entrainment and smoke extract from the incident carriage have been predicted in the limited window failure case. This gradual change in ventilation conditions sustained burning longer and promoted flame spread, however, the fire development is predicted to be progressive rather than sudden. The peak heat release rate for this incident is predicted to be 4.8MW.

9.2.2.5 NUMBER OF OPEN DOORS

The sensitivity of fire development and flame spread within the underground rolling stock to the number of open doors has been investigated through an incident within the twin-track tunnel section, where all four doors of the incident carriage are assumed to be open. The simulation incorporating an incident in an individual carriage showed that opening all four doors slightly delays the development of fire, however, has insignificant effect on the predicted peak heat release rate. In an incident caused by a severe ignition source, opening all four doors of the incident carriage marginally altered the onboard conditions, and was not sufficient to maintain the conditions within the tenability criteria. Consequently, opening all four doors of the incident carriage in the event of an incident is not recommended, since the benefits are marginal and doing so would introduce additional safety and operational requirements.

Another incident simulated using the 4-car rolling stock with open wide gangways, but all

doors defined closed, has shown that fire follows the ignition source development curve for the first five minutes, after which it starts to decay and dies out within the next eight minutes due to lack of oxygen within the rolling stock. This simulation could be considered as a hypothetical case but has confirmed that if there is no flow exchange between the rolling stock and the running tunnel, the temperatures at the face of windows do not increase to the predefined failure criterion. Consequently, smoke and toxic gases produced by the fire fill the entire carriage and consume all the available oxygen. This case verifies the importance of the air entrainment in development of fire within the constant volume enclosures.

Two additional cases have been simulated where a time delay of three and six minutes have been applied in opening the doors of the rolling stock during an incident. The simulations showed that once the flow exchange and onboard conditions are restored, fire development and flame spread patterns converge to the original cases where the doors were defined open at the beginning of the simulation. In both cases, once the doors are opened, a sudden exchange of smoke and fresh air between the incident carriage and the running tunnel has been predicted, which has led to an instantaneous increase in the predicted heat release rates. The two cases showed examples of the backdraft phenomenon, caused by considerable amount of combustion gases' being extracted from the incident carriage within a very short space of time. The instantaneous peak heat release rates are predicted to be 3.5MW and 8.3MW, where the doors are defined to open at three and six minutes, respectively.

9.2.2.6 MECHANICAL VENTILATION

The simulation of an incident in an individual carriage in a twin-track tunnel showed that the effect of mechanical ventilation on fire development and flame spread within the incident carriage is insignificant until the window of back end door fails. Failure of that window allows forced air to flow through the incident carriage, and reduces the rate of heat released by the fire. It has been concluded that the mechanical ventilation system, modelled as a mean airflow velocity at the tunnel boundary, ventilates smoke effectively, preventing any further flame spread within the incident carriage.

A second case simulated to investigate the influence of mechanical ventilation on fire development involves an incident within the 4-car rolling stock with open wide gangways in the single-track tunnel. In this case, forced airflows penetrate through the entire rolling stock,

since the end doors are defined to be open for evacuation and ventilation. The airflows prevent flames spreading in the upstream direction and ventilate smoke effectively retaining the heat release rate at significantly lower values. The peak heat release rate is predicted to be 2.0MW in this case, which is considerably lower than 2.7MW, predicted under natural ventilation conditions.

9.2.2.7 MESH SENSITIVITY

The accuracy of the fire development and flame spread predictions has been assessed through the grid sensitivity simulations. An under-ventilated and a well-ventilated fire incident have been re-simulated with element sizes halved in the longitudinal direction along the length, and in the vertical direction along the height of the rolling stock.

The variations of heat release rates and flame spread patterns predicted from the simulations incorporating refined grid size were found to be quite similar to the predictions of identical cases simulated with the original grid. A common exception has been predicted for both cases during the growth period of the fire. In both cases, the rate of increase in heat release rate is found to be higher in the results of simulations with refined grid. The cause of the predicted differences highly relies on the change of the burning behavior of combustible materials within the incident carriage, due to alteration in the grid size.

The combustible material properties had been calibrated using a cone calorimeter model that had grid size compatible with the original grid size used in the initial and sensitivity simulations reported in this thesis. Consequently, refining the grid in the mesh sensitivity analysis resulted in sharper responses to ignition and slightly faster combustion. However, predictions of overall trend of fire development and flame spread match well between the simulated cases incorporating different grid sizes. The peak heat release rate is predicted to be 2.5MW for the under-ventilated incident, and 3.0MW for the well-ventilated fire, from the simulations with refined grid sizes. The peak heat release rates were found to be 2.6MW and 2.5MW for under-ventilated and well-ventilated incidents incorporating the original grid size, respectively.

The simulations of mesh sensitivity analysis have also shown that halving the element sizes in longitudinal and vertical directions in the computational domain increases the computational time required to achieve a 30-minute solution by 6.7 times for an incident in the single-track

tunnel, and by 13 times for an incident in the twin-track tunnel.

It can be concluded that original grid size used in the initial and sensitivity simulations captures the key parameters of fire development and results in reliable peak heat release rate estimates within reasonable computational time and effort.

9.2.3 FINAL SIMULATIONS

The final simulations incorporate the revised material properties to reflect the combustible seat and floor materials proposed for the Class-378 rolling stock. The combustible materials that are input in the final simulations are calibrated through FDS cone calorimeter simulations against the acquired experimental predictions. Their performance during an incident in the rolling stock has been assessed through selected set of simulations.

In the first stage of the calibration process, ignition temperatures for the combustible seat and floor were chosen to be 505°C and 560°C, respectively, in the absence of the specified values in the experimental data. Once the calibrated material properties have been tested through an incident in the single car model in the single-track tunnel, it has been found that the surfaces resist ignition, and even when ignited burn at very slow rates. The incident is predicted to produce a peak heat release rate of 2.1MW.

In the second stage of the calibration process, ignition temperatures for seats and the floor are reduced to 435°C and 430°C, respectively. As the ignition temperatures were reduced, the effective heat of combustion of the materials had to be reduced, and the product ρ c δ had to be increased to match the experimental predictions. The calibration process has shown that two different sets of material properties could yield quite similar burning characteristics and heat loads, as far as all the parameters used in the set of properties are within the physical limitations. It is predicted that the same incident in the rolling stock, mentioned above for the first stage of the calibration process, produces a peak heat release rate of 1.8MW when the material properties with lower ignition temperatures are incorporated in the model. However, an increased area of ignited combustibles is observed.

In the two simulations performed using different sets of calibrated material properties, a combustion reaction for the floor material was used, since the initial and sensitivity simulations identified that the fire development within the rolling stock is governed by the flame spread

over the floor. The simulations were predicted to yield much lower heat release rate values than predictions of the initial and sensitivity simulations. Consequently, the combustion reaction has been revised from floor material to the seat material, due to increased energy release per unit mass of oxygen consumed during the combustion of seats. The same incident, mentioned above in two cases of the final simulations, is predicted to produce a peak heat release rate of 3.1MW with much larger surface area involvement in fire, when the calibrated material properties having lower ignition temperatures and reaction for seats are incorporated in the model. Therefore, it has been decided to use the combustion reaction for seats and material properties with lower ignition temperatures in the rest of the final simulations.

An 80kW arson fire ignition source in the single carriage model in the single-track tunnel has been simulated with the revised material properties to assess their performance for the design case. It is predicted from the simulation results that the fire is localized on seat around the initial ignition location and produces a peak heat release rate of 125kW during this incident.

The performance of the calibrated material properties has also been checked through the simulation of an incident within the 4-car rolling stock in the single-track tunnel, where the ignition source is placed at the center of the second carriage. This case was selected, since it was predicted to produce the highest peak heat release rate for the 4-car open train amongst the cases simulated in the initial and sensitivity simulations. The simulation shows that flames spread evenly in both upstream and downstream directions within the incident carriage, with an exception predicted at the early stages of the incident where flames tend to spread in the upstream direction towards the front end of the train. The fire development is predicted to be steady with peak heat release rate of 3.7MW. The flames are predicted to reach the adjacent carriages within 20 minutes from the ignition, during this incident.

The simulation of an incident in the 4-car rolling stock in the single-track tunnel, with all the windows on one side of the train defined fail-safe, showed that the heat release rate from the fire increases steadily with progressive flame spread over the floor within the rolling stock. The flames are predicted to spread mainly in the incident carriage, however, involvement of adjacent carriage in fire is also observed during this incident. The seats in the adjacent carriage are predicted to be involved in the fire development within 9 minutes from the ignition. The peak heat release rate for this incident is predicted to be 4.6MW at the 25th minute of the incident, when the extent of fire reaches to its maximum value of about one and a half

carriages. Even though the flame spread patterns are observed to be different, the variation of heat release rate for this incident and the same incident simulated with the initial material properties are found to be quite similar.

In all the simulations reported herein, the window failure criterion was defined to be 675°C. It has been claimed by some of the authorities that this value is too high for the proposed window material and composition for the Class-378 rolling stock. Two incidents within the 4-car rolling stock incorporating open wide gangways, described above under the final simulations, have been re-simulated with the revised window failure criterion of 400°C. The simulation of the incident at the center of the second carriage showed that a number of windows in the premises of the ignition source fails at the very early stages of the fire development. These failures result in increased effectiveness of ventilation of smoke, localized flame spread, and a peak heat release rate of 2.5MW. The simulation of the incident, incorporating fail-safe windows on one side of the 4-car rolling stock, showed that the windows fail in a successive manner, and the fire retains its intensity and sustains flame spread within the rolling stock. The failure of windows reduced the rate of flame spread and fire growth significantly, however, the peak heat release rate is predicted to be 4.4MW, which is quite close to the value predicted for the same incident with original window failure criterion.

A final attempt has been made to investigate the effects of cone calorimeter model on the calibrated material properties. The cone calorimeter simulations incorporating larger element sizes resulted in the requirement to increase the effective heat of combustion values for seats and floor in order to match the experimental predictions. The last simulation incorporating the re-calibrated material properties in a single carriage in the single-track tunnel showed that increased heat of combustion of the materials increases slightly the predicted heat release rate during the incident, due to slightly increased area of influence of the fire. However, a significant increase in the heat release rate is predicted at the 27th minute of the incident, when the flames spread further to involve the upstream half of the incident carriage. The peak heat release rate during this incident is predicted to be 4.9MW, maintained constant over 8.5 minutes, after which fire starts to decay.

It can be concluded from the final simulations that due to the short burning duration and low heat loads of the seats, the values of the peak heat release rates highly depend on the rate of flame spread over the floor. The seats were found to be consumed fairly quickly after

the ignition, therefore floor solely acts as the dominant combustible within the rolling stock. In addition, the simulations show that the single carriage model in the single-track tunnel remains the design case for estimation of the design fire size of the rolling stock, due to predicted sudden increases in the values of heat release rate.

9.3 COMMENTS ON EMPIRICAL METHODS

The most important benefit of the empirical methods and the two-zone fire model simulations is their reliable predictions within a relatively short period of time, compared to the detailed FDS simulations. On the other hand, the accuracy of the predictions mostly relies on the initial conditions and the assumptions being made during the analysis. The conclusions derived from the analysis with the empirical methods are summarized in the following Sub-sections.

9.3.1 DUGGAN'S METHOD

The Duggan's method is an empirical approach that is being used to predict the design heat release rate of a rolling stock in the event of a fire incident, and is widely accepted by the industry. The Duggan's method uses the experimental cone calorimeter predictions of fire load, i.e. heat release rate per unit area, of the combustible items in a rolling stock. However, how much of the total area of combustibles and when they are involved in fire development in a rolling stock depend on the engineering judgement.

In this thesis, the Duggan's method has been used to verify the FDS predictions of heat release rate variations during an incident within the rolling stock. Two cases; an incident in a single carriage with only one end door open, and an incident in the 4-car rolling stock incorporating open wide gangways but with limited window failure; have been analyzed. These cases are selected since the incident in the single carriage produces the peak heat release rate, and the incident in the 4-car rolling stock results in the largest flame spread area amongst the other cases simulated. The flame spread areas are estimated from the images of burning rates of the combustibles produced by the FDS simulations. The cone calorimeter curves are factored by the estimated areas, and their contributions to the overall heat release rate are introduced at certain instances derived from the FDS predictions. The contribution of the ignition source is also added in the predictions of variation of overall heat release rate. This is introduced to the

Duggan's method in order to get the heat release rate estimates accurately for the verification of results, since the ignition source is already included in the FDS simulations.

The analysis of Duggan's method for the two cases described to verify the FDS predictions show that the empirical method predicts the variation of heat release rate reasonably well for an incident with steady burning behavior. The peak heat release rate of the incident within the 4-car open train with steady burning characteristic and progressive flame spread is predicted to be 4.7MW by Duggan's method and 4.8MW by the FDS simulation. However, in a flashover case, the Duggan's method estimated the peak heat release rate much lower than the FDS prediction. It has been noted that in order to get the peak value of heat release rate accurately in a flashover case, the peak values of the two individual burning curves of combustibles should match at the same instant. With that assumption the peak heat release rate can be predicted within 5% accuracy.

There are two main disadvantages of this verification method that should be noted. The accuracy of the verification methodology relies upon the accuracy of the observation and the frequency of the data input in the empirical analysis. The second drawback is the Duggan's methods' allowing a number of curves tested under different heat flux levels for the same material, such as seat bases and seat backs. In FDS simulations, a set of properties has been used to reflect the behavior of the combustibles and to account for the heat feedback from the fire. Consequently, under certain circumstances, minor variations between the two methods might be expected.

9.3.2 CFAST SIMULATIONS

A set of CFAST simulations has been performed to predict the onboard conditions in the event of a fire incident within the rolling stock. The results have been used to verify the predictions of FDS simulations for the identical incident scenarios.

One advantage of the CFAST program is its' producing reliable results in a very short space of time. However, the program divides each compartment into two layers and predicts values averaged over the upper and lower layer volumes. Therefore, the results highly depend on the layer heights, which separate the upper and lower layers, predicted for each carriage. On the contrary, onboard conditions can be monitored and recorded at any point within the computational domain in FDS simulations. For the purposes of this research, onboard conditions were

recorded at 1.0m, 1.5m, and 2.0m above the floor level in the FDS simulations. The CFAST program can not predict flame spread and fire development within the carriages. Therefore in order to create the same onboard conditions, the heat release rate variations predicted for each case by the FDS simulations are input as the ignition source in CFAST case studies. Similarly, the window failures are considered in CFAST simulations by introducing new openings in agreement with the FDS predictions.

The simulations of an 80kW arson fire ignition source showed that almost identical variations of temperature are predicted, between the CFAST and FDS software, for an incident in the 4-car open train with open side doors. The layer heights for this incident are predicted to be higher than 1.5m, therefore the temperatures recorded by the FDS target points at 2.0m and 1.0m above the floor agree very well with the upper layer and lower layer temperature predictions of CFAST, respectively.

However, slight differences between the temperature predictions of the two softwares are observed especially for the incident in the single-track tunnel. For an incident in the single-track tunnel, the smoke ventilation openings are limited to the open end doors, which inevitably alter the effectiveness of smoke extract and the predicted layer heights. The simulation of an incident in the single carriage model shows that the upper layer temperatures match reasonably well with the FDS predictions at 1.5m above the floor level. However, lower layer temperatures are predicted to be much lower than the temperatures at 1.0m obtained from the FDS simulations. These variations are acceptable, since ineffective ventilation of an incident in the single-track tunnel causes layer heights to drop, and therefore the target points in FDS do not lie within the center of the layers of the CFAST case anymore. In such cases, the lower layer temperatures should be checked against FDS predictions of temperature recorded at target points lower than 1.0m height.

Similar to the observations and comments made for the cases involving an 80kW ignition source, temperature predictions of the two softwares are found to agree very well with each other in cases involving a severe ignition source, when the target points in FDS model match the centerline of the layers defined by the CFAST program. The results show that upper layer temperatures match reasonably well with the FDS predictions in the incident carriage at 1.5m above the floor level, when the incident is in the single-track tunnel. The upper layer temperatures in the incident carriage are found to match with the predictions of FDS at 2.0m,

when the incident is at the twin-track tunnel section. In cases involving 4-car open train, as the target points move away from the incident carriage, few differences are observed between the predictions of two program. These differences are solely due to the change in the layer heights, and therefore are acceptable.

It is worth noting that the incident carriage and all the carriages of an open train are filled with smoke fairly quickly during incidents involving severe ignition source. Consequently, the layer heights during these incidents were predicted to be as low as 0.3m in some cases. Therefore, in most of these cases, the lower layer temperatures were found to be too low even for the temperature predictions of FDS at 1.0m above the floor level. As noted above, these temperatures should be checked against the predictions at target points much lower than 1.0m for better agreement.

It can be concluded that FDS predicts gradual variation, and therefore results in more accurate description of temperature distribution within the rolling stock in the event of a fire incident. However, CFAST delivers temperature values averaged over the two volumes defined by the smoke layer height, and therefore results in approximate predictions. In addition, CFAST can not solve flame spread and fire development within the rolling stock. Consequently, in order to predict onboard conditions, either estimated variations of heat release rates should be implemented or design fire size should be used as a conservative approach. Nevertheless, the ease of modelling and the speed of obtaining results, to have an idea of what might be expected during an incident scenario, shall not be overlooked.

9.4 CONCLUDING REMARKS

Fire development and flame spread within the underground trains have been studied extensively through computer simulations. The following conclusions have been drawn from the predictions of the simulations:

- Ignition Source:
  - An arson fire ignition source on a passenger seat releasing 80kW heat, representing a trash bag filled with paper, is not intense enough to promote flame spread within the rolling stock. This source is to be used in assessing the onboard conditions for tenability.

- A severe baggage fire ignition source on floor, following the fast growth curve and releasing 1.5MW heat at its peak, is powerful enough to ignite the seats and promote flame spread over the floor. This source is to be used in assessing the design fire size of an incident in the rolling stock. This source can yield flashover conditions within the rolling stock if the ventilation conditions and material properties are in favor of rapid fire development.
- The modified baggage fire source on floor, releasing 1.0MW heat at its peak, is found to be sufficient to achieve flashover conditions within the underground rolling stock. Consequently, it is recommended to suppress the fire before it reaches to 1.0MW whenever it is possible to do so to prevent flashover.

- Rolling Stock Model:
  - In a train made up of physically separated carriages, the volume of enclosure and the areas of ventilation openings are smaller compared to a train incorporating open wide gangways. The individual enclosures limit the extent of flame spread to a single carriage. However, the temperatures and toxic gas concentrations would be higher in the event of an incident, and even an arson fire source could result in untenable conditions within the incident carriage. Smaller enclosure, when combined with limited ventilation, could also yield flashover conditions if the ignition source and material properties are in favor of rapid fire development.
  - In the event of an incident in a rolling stock incorporating open wide gangways, the smoke produced by the fire spreads from the incident carriage to the entire rolling stock fairly quickly. If the incident produces high volumes of smoke and toxic gases, the conditions could be untenable in the entire rolling stock. However, open wide gangways allow passengers to move away from the incident carriage to a safe haven faster than a train made up of physically separated carriages. On the other hand, the open wide gangways also allow flame spread over the floor in the incidents involving a powerful ignition source, unless a fire barrier on floor between the carriages has been implemented. However, the extent of flame spread is generally found to be limited to a single carriage through the simulations with only one exception. The rolling stock incorporating open wide gangways behave as a single vestibule diluting the smoke from fire, and therefore moderating the temperatures within the incident carriage. Consequently, the results of simulations

showed that the risk of flashover is reduced significantly when the open wide gangways are implemented.

- Ventilation:
  - It has been predicted through simulations in this research that ventilation has a significant effect on fire development within an underground rolling stock. In a typical twin-track tunnel where the side walkways are present, opening side doors for evacuation of passengers and ventilation of smoke helps maintaining onboard conditions tenable for longer durations in the event of a small size fire incident. Increased effectiveness of smoke ventilation through opening side doors in the event of a severe incident results in reduced onboard temperatures yielding localized burning, and therefore reduced risk of flashover.
  - For incidents in tunnel sections with relatively small cross-sectional area, the development of fire is found to be highly dependent on window failures, i.e. supplementary ventilation of smoke. It has been predicted that if windows are defined to be highly fire retardant, the fire burns steadily with relatively low heat release rates, due to limited oxygen levels within the incident carriage and in the rest of the rolling stock. However, successive failures of windows ventilate smoke from the incident carriage and deliver relatively fresh air to the fire, which promote flame spread and fire development. It has been predicted that successive window failures could lead to flashover phenomenon through a change in the characteristics of fire from fuel-controlled to ventilation-controlled.
  - In most of the modern railway systems, mechanical ventilation is provided to achieve and maintain control over the movement of smoke in the event of an incident. The case studies show that once the mechanical ventilation is energized to provide a mean airflow velocity of 2.5m/s at the tunnel cross-section, the forced ventilation controls the development of fire and reduces the rate of heat released if the airflows penetrate through the rolling stock. The simulations show that mechanical ventilation has insignificant effect on the fire development until the forced air flows through the incident carriage over the developing fire. It has been concluded that activation of mechanical ventilation at rates sufficient to gain control over the smoke movement would slow down the fire development and keep heat release rates at relatively low values, reducing risk of flashover.

- Risk of Flashover:
  - The case studies simulated to assess the individual effects of the parameters that have influence on the fire development and flame spread within underground rolling stock show that a number of conditions have to be satisfied to achieve flashover phenomenon. A powerful ignition source and favorable ventilation conditions that would promote flame spread in a rolling stock are required essentially. The incidents involving a rolling stock incorporating open wide gangways showed steady burning behavior and often localized flame spread around the ignition location. The resistance of combustible materials to fire also has a significant effect on flame spread behavior within the rolling stock leading either to steady burning or flashover.

    Amongst a number of cases simulated only one combination of parameters has led to flashover phenomenon. Therefore, it can be concluded that the risk of flashover is quite small compared to all possible variations of incidents, but it could still occur however small the chance is. Figure 9.1 shows the necessary conditions required for an ignition source to yield flashover conditions.
- Design Fire Size:
  - The results of the case studies show that fire spreads progressively within a rolling stock incorporating open wide gangways. However, flashover conditions could be achieved during an incident in a rolling stock made up of physically separated carriages, which would lead to the prediction of the peak heat release rate. Consequently, the design case for the prediction of fire size is the incident in a single carriage.
  - The incident cases simulated in this thesis, using typical combustible materials for an underground rolling stock, resulted in a peak heat release rate of 6.3MW. It can be concluded that the predictions have confirmed the proposed design fire size of 8.0MW for Bombardier Class-378 type rolling stock. It should be noted that in predictions of the design fire size, spread of flame to under-carriage and failure of rubber bellows or roof structure have not been considered. It has been assumed that the fire barrier between the floor and the under-carriage would prevent any flame spread between two regions, and the integrity of the bellows and roof structure are not compromised within the first 30 minutes from the ignition.

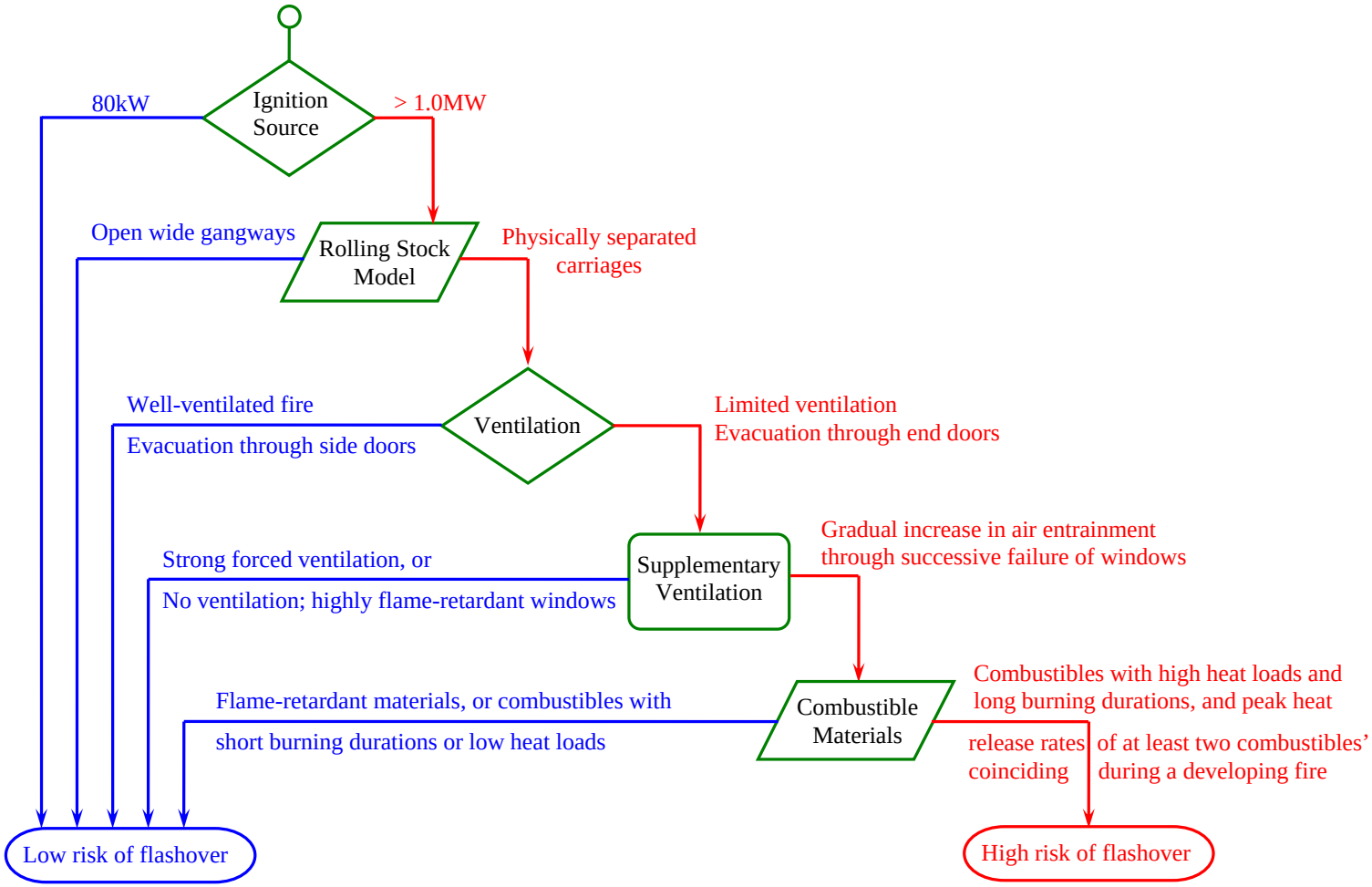

Figure 9.1: Parameters that affect fire development and their relation to risk of flashover

REFERENCES

[1] British Standards, “Fire tests on building materials and structures. Part 15: Method for measuring the rate of heat release of products”, BS 476:1993

[2] Kennedy W.D., Gonzales J.A., Sanchez J.G., “Derivation and Application of the SES Critical Velocity Equations”, ASHRAE Transactions: Research, v.102, 1996

[3] Incropera F.P., DeWitt D.P., “Fundamentals of Heat and Mass Transfer”, Fourth edition, 1996

[4] Weckman E.J., Strong A.B., “Experimental Investigation of the Turbulence Structure of Medium-scale Methanol Pool Fires”, Combustion and Flame, v.105, 1996

[5] Drysdale D., “An Introduction to Fire Dynamics”, Second edition, 1999

[6] British Standards, “Code of practice for fire precautions in the design and construction of passenger carrying trains”, BS 6853:1999

[7] Peacock R.D., Braun E., “Fire Safety of Passenger Trains; Phase I: Material Evaluation (Cone Calorimeter)”, National Institute of Standards and Technology (NIST) IR 6132, 1999

[8] Karlsson B., Quintiere J.G., “Enclosure Fire Dynamics”, 2000

[9] Briggs P., Métral S., Le Tallec Y., Troiano D., Messa S., Breulet H., “Firestarr - Final Report”, Firestarr Consortium, 2001

[10] DiNenno P.J., “The SFPE Handbook of Fire Protection Engineering”, 2002

[11] Duggan G.J., “Indication of flashover power output: Generic LUL tube stock: ISO 5660-1 source data”, Report 20D02-43400, 2002

[12] International Standard, “Reaction-to-fire tests - Heat release, smoke production and mass loss rate. Part 1: Heat release rate (cone calorimeter method)”, ISO 5660:2002

[13] Ferziger J.H., Perić M., “Computational Methods for Fluid Dynamics”, Third edition, 2002

[14] British Standards, “Application of fire safety engineering principles to the design of buildings. Part 1: Initiation and development of fire within the enclosure of origin”, PD 7974:2003

[15] Hostikka S., Axelsson J., “Modelling of the radiative feedback from the flames in cone calorimeter”, Nordtest Technical Report No. 540, 2003

[16] British Standards, “The application of fire safety engineering principles to fire safety design of buildings. Part 6: Human factors: Life safety strategies”, PD 7974:2004

[17] Duggan G.J., “Indication of underbody fire power output: Generic LUL tube stock: ISO 5660-1 source data”, Report 20D04-12300, 2004

[18] Hietaniemi J., Hostikka S., Vaari J., “FDS simulation of fire spread - comparison of model results with experimental data”, VTT Building and Transport research paper, 2004

[19] Iqbal N., Salley M.H., Weerakkody S., “Quantitative Fire Hazard Analysis Methods for the U.S. Nuclear Regulatory Commission Fire Protection Inspection Program Final Report”, NUREG - 1805, 2004

[20] Chiam B.H., “Numerical Simulation of a Metro Train Fire”, Fire Engineering Research Report 05/1, Dept. of Civil Engineering, Univ. of Canterbury, 2005

[21] Beard A., Carvel R., “The Handbook of Tunnel Fire Safety”, 2005

[22] Jones W.W., Peacock R.D., Forney G.P., Reneke P.A., “CFAST - Consolidated Model of Fire Growth and Smoke Transport (Version 6) Technical Reference Guide”, National Institute of Standards and Technology (NIST), 2005

[23] Peacock R.D., Jones W.W., Reneke P.A., Forney G.P., “CFAST - Consolidated Model of Fire Growth and Smoke Transport (Version 6) User’s Guide”, National Institute of Standards and Technology (NIST), 2005

[24] McGrattan K., “Fire Dynamics Simulator (Version 4) Technical Reference Guide”, National Institute of Standards and Technology (NIST), 2006

[25] McGrattan K., Forney G., “Fire Dynamics Simulator (Version 4) User’s Guide”, National Institute of Standards and Technology (NIST), 2006

[26] U.S. Nuclear Regulatory Commission research report, “Verification and Validation of Selected Fire Models for Nuclear Power Plant Applications, Volume 1: Main Report”, NUREG - 1824, 2006

[27] U.S. Nuclear Regulatory Commission research report, “Verification and Validation of Selected Fire Models for Nuclear Power Plant Applications, Volume 6: Fire Dynamics Simulator (FDS)”, NUREG - 1824, 2006

[28] NFPA Standards, “Standard for Fixed Guideway Transit and Passenger Rail Systems”, NFPA 130:2007

[29] Wen J.X., Kang K., Donchev T., Karwatzki J.M., “Validation of FDS for the prediction of medium-scale pool fires”, Fire Safety Journal, v.42, 2007

[30] Hasib R., Kumar R., Shashi, Kumar S., “Simulation of an experimental compartment fire by CFD”, Building and Environment, v.42, 2007

[31] Kim E., Woycheese J.P., Dembsey N.A., “A Study of Fire Dynamics Simulator Version 4.0 for Tunnel Fire Scenarios with Forced Longitudinal Ventilation”, 11th International Conference on Fire Science and Engineering (InterFlam) Proceedings, 2007

[32] Rinne T., Hietaniemi J., Hostikka S., “Experimental Validation of the FDS Simulations of Smoke and Toxic Gas Concentrations”, VTT Technical Research Centre of Finland, 2007

[33] NFPA Standards, “Standard for Road Tunnels, Bridges, and Other Limited Access Highways”, NFPA 502:2008

[34] Bombardier, “Schedule of Finishes - NLR/ELR”, Report 3EER400007 - 8549, 2008

[35] Hall R.C., “Assessment of Train Fire Size”, East London Line Project Report ELM-TEC-226-14-08-0001, 2008

[36] Hall R.C., Musluoglu E., “Smoke Modelling of Interior of Rolling Stock”, East London Line Project Report ELM-TEC-226-14-08-0002, 2008

[37] Kim J.S., Jeong J.C., Cho S.H., Seo S.I., “Fire resistance evaluation of a train carbody made of composite material by large scale tests”, Composite Structures, v.83, 2008

[38] Hjohlman M., Försth M., Axelsson J., “Design fire for a train compartment”, SP Technical Research Institute of Sweden, Brandforsk project 401-051 report no. 2009:08, 2009

[39] Wikipedia - The Free Encyclopedia, “2008 Channel Tunnel fire”, http://en.wikipedia.org/wiki/2008_Channel_Tunnel_fire, updated: 12 August 2009, accessed: 22 August 2009

[40] Wikipedia - The Free Encyclopedia, “British Rail Class 378”, http://en.wikipedia.org/wiki/Class_378, updated: 21 August 2009, accessed: 22 August 2009

[41] Compin Group, “Compin Seats Pegasus”, http://www.compin.com/pages/uk/pdf/pegasus.pdf, updated: 3 November 2008, accessed: 22 August 2009

[42] Patent Storm LLC., “Pile fabric - US Patent 6537640 Description”, http://www.patentstorm.us/patents/6537640/description.html , accessed: 22 August 2009

Appendix A

BOMBARDIER CLASS-378 ROLLING STOCK

A.1 SECTIONAL AND PLAN VIEWS OF THE MODELLED ROLLING STOCK

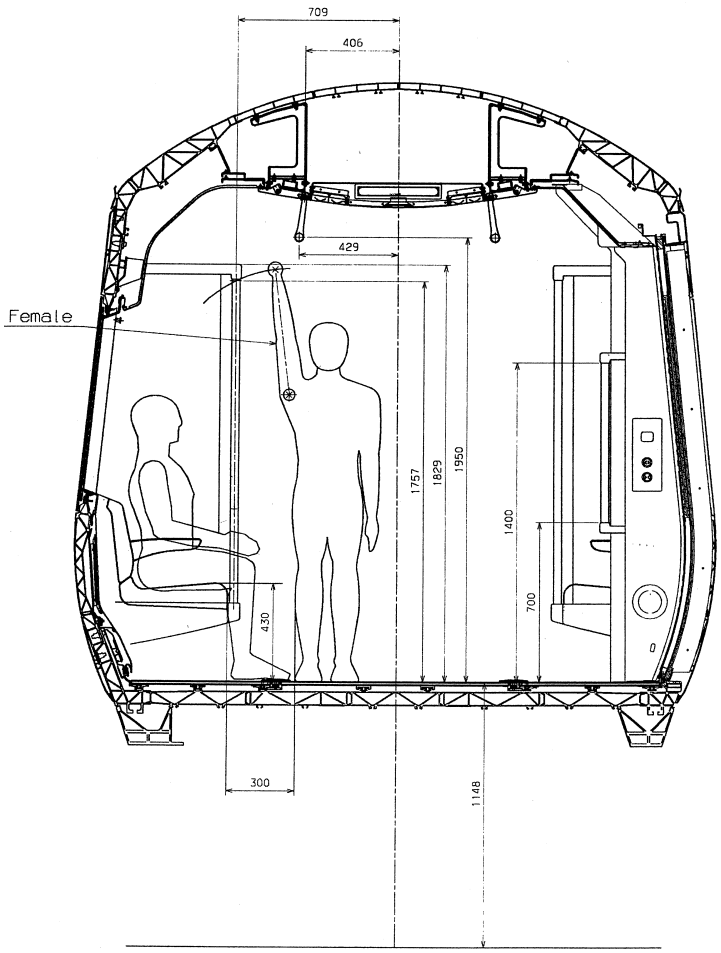

Figure A.1: Sectional view of the typical carriage

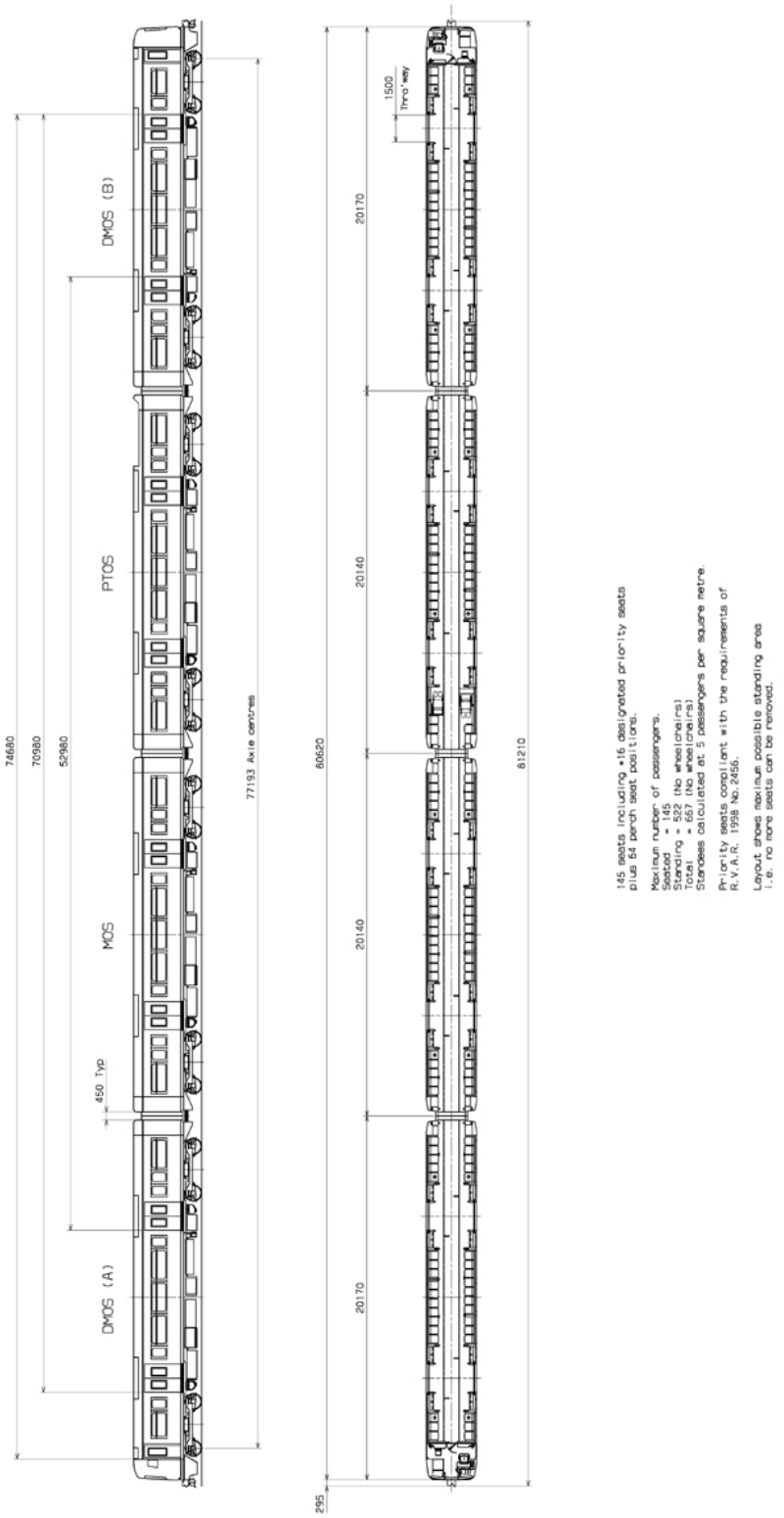

Figure A.2: Overall view of the rolling stock

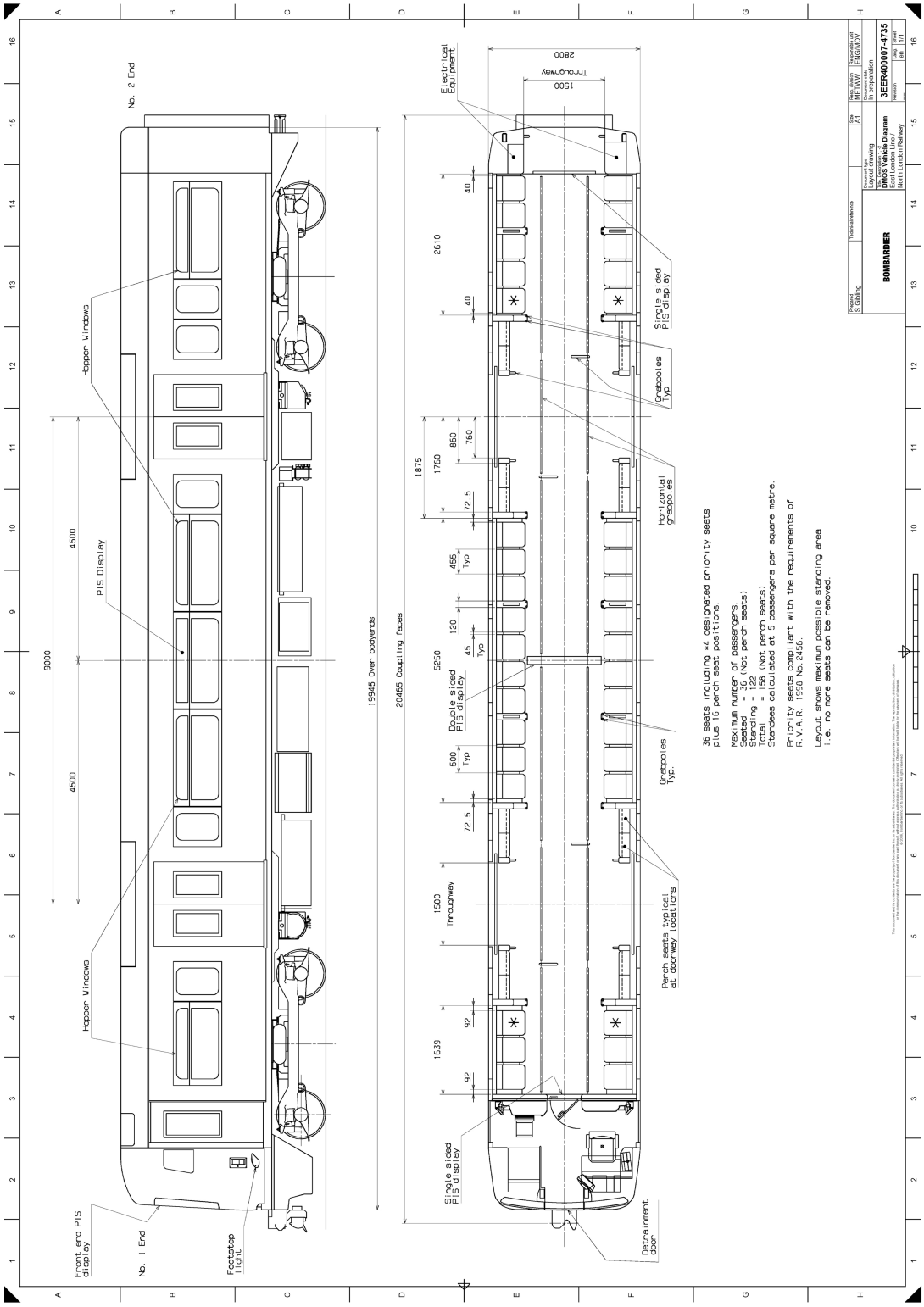

Figure A.3: Plan view of the DMOS type carriage

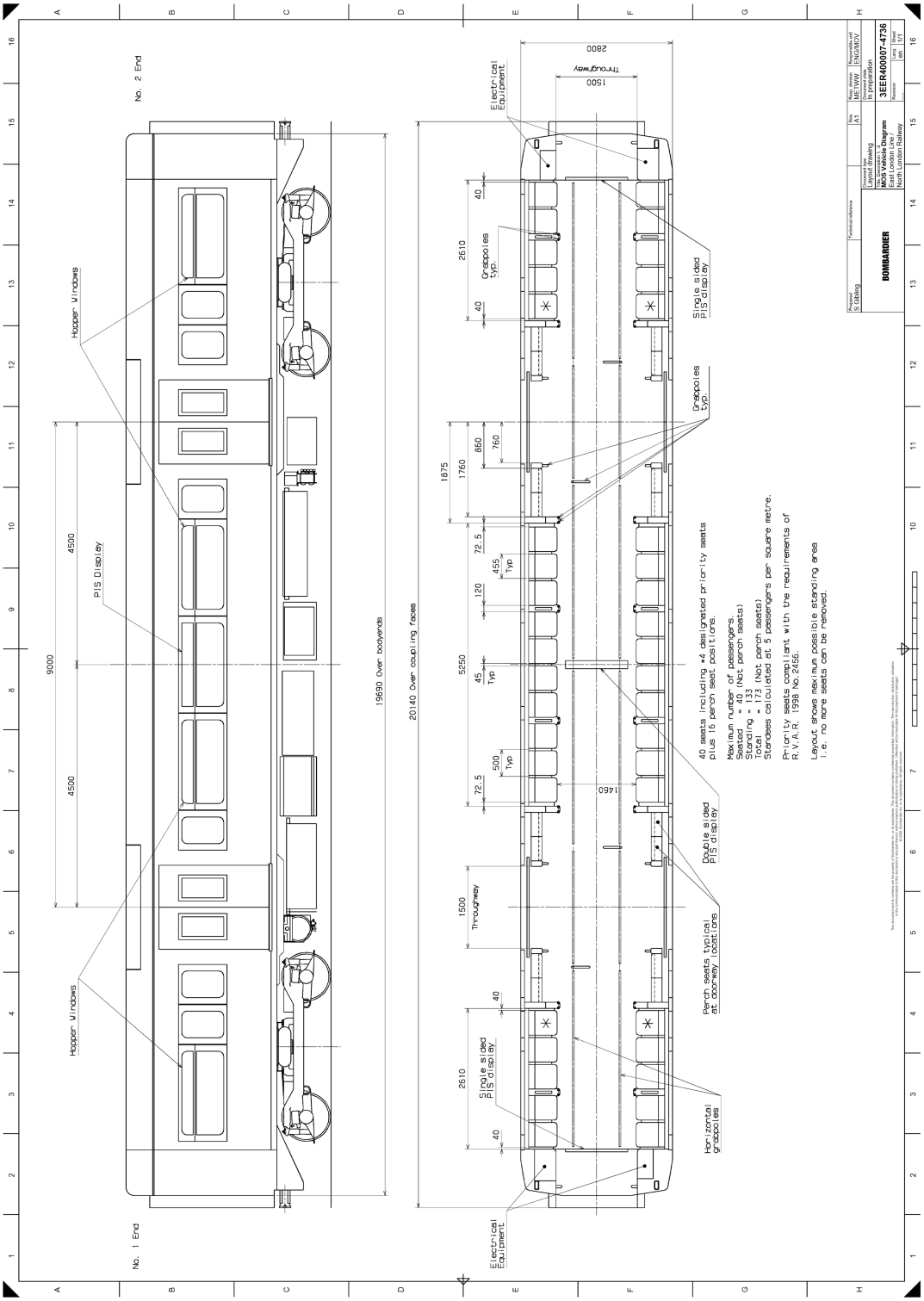

Figure A.4: Plan view of the MOS type carriage

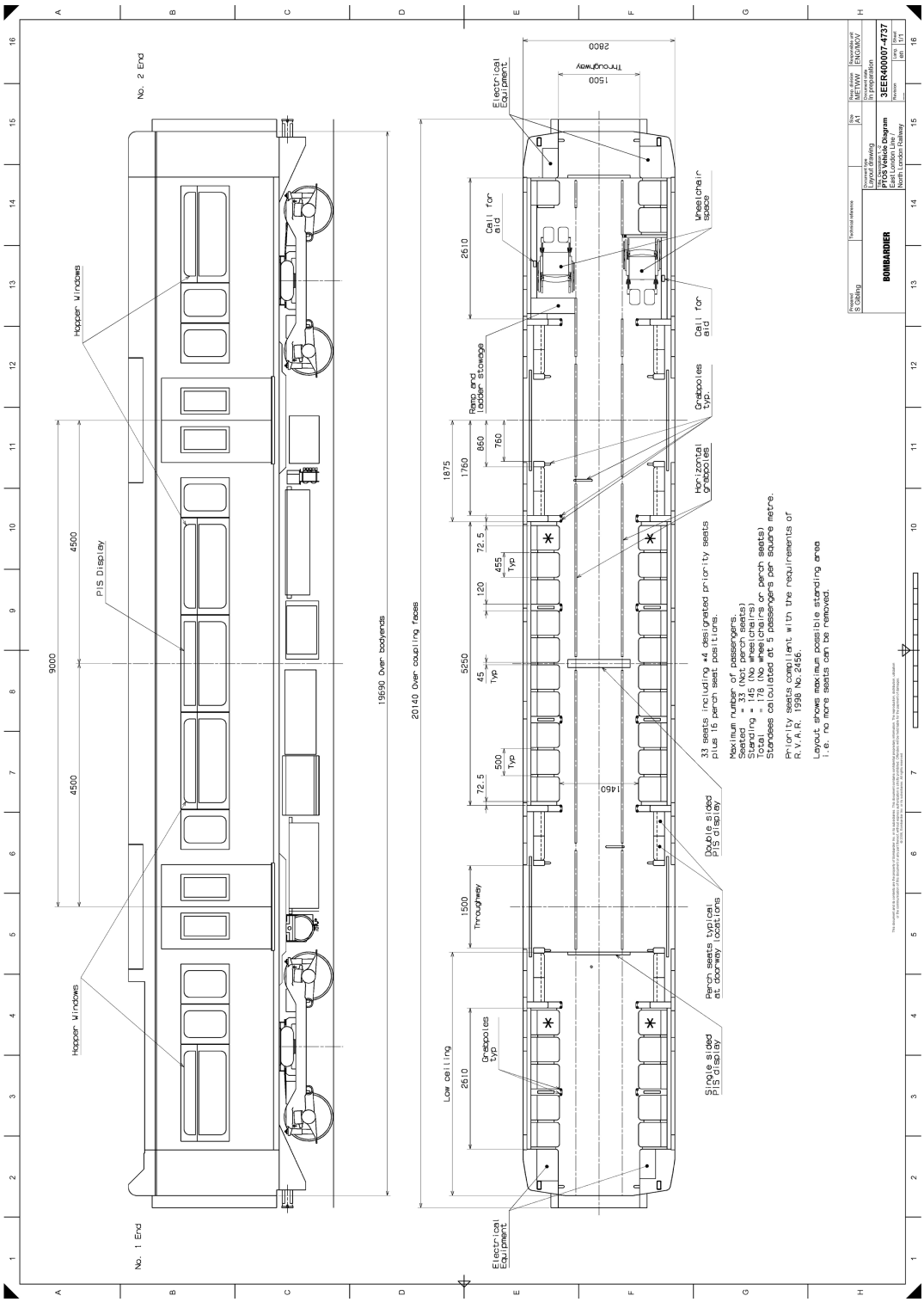

Figure A.5: Plan view of the PTOS type carriage

Appendix B

FIGURES: INITIAL SIMULATION RESULTS

B.1 CASE-01: 1-CAR, 80kW SOURCE, SINGLE-TRACK TUNNEL

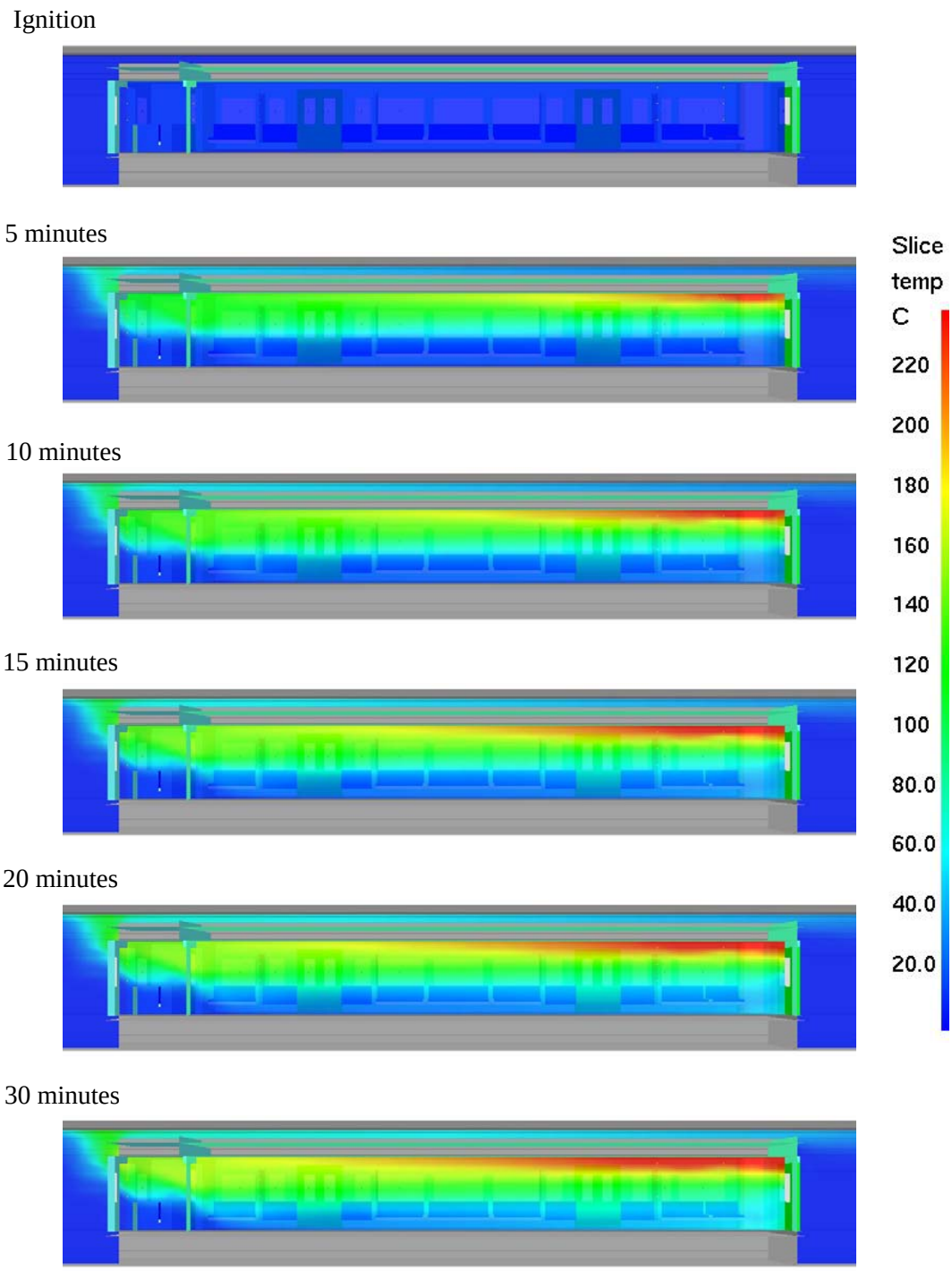

Figure B.1: Temperature, 1-car, 80kW source, Single-track tunnel

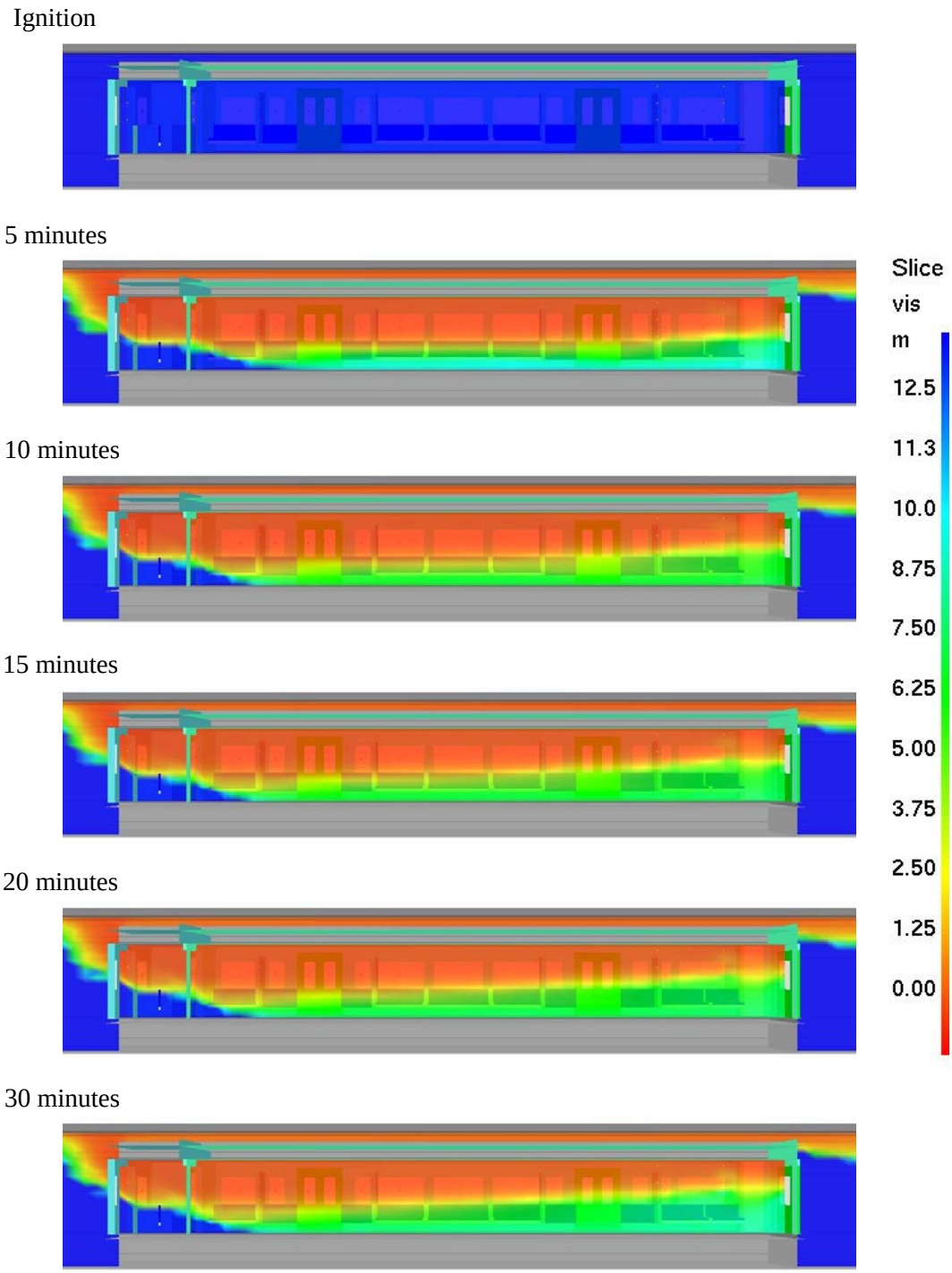

Figure B.2: Visibility, 1-car, 80kW source, Single-track tunnel

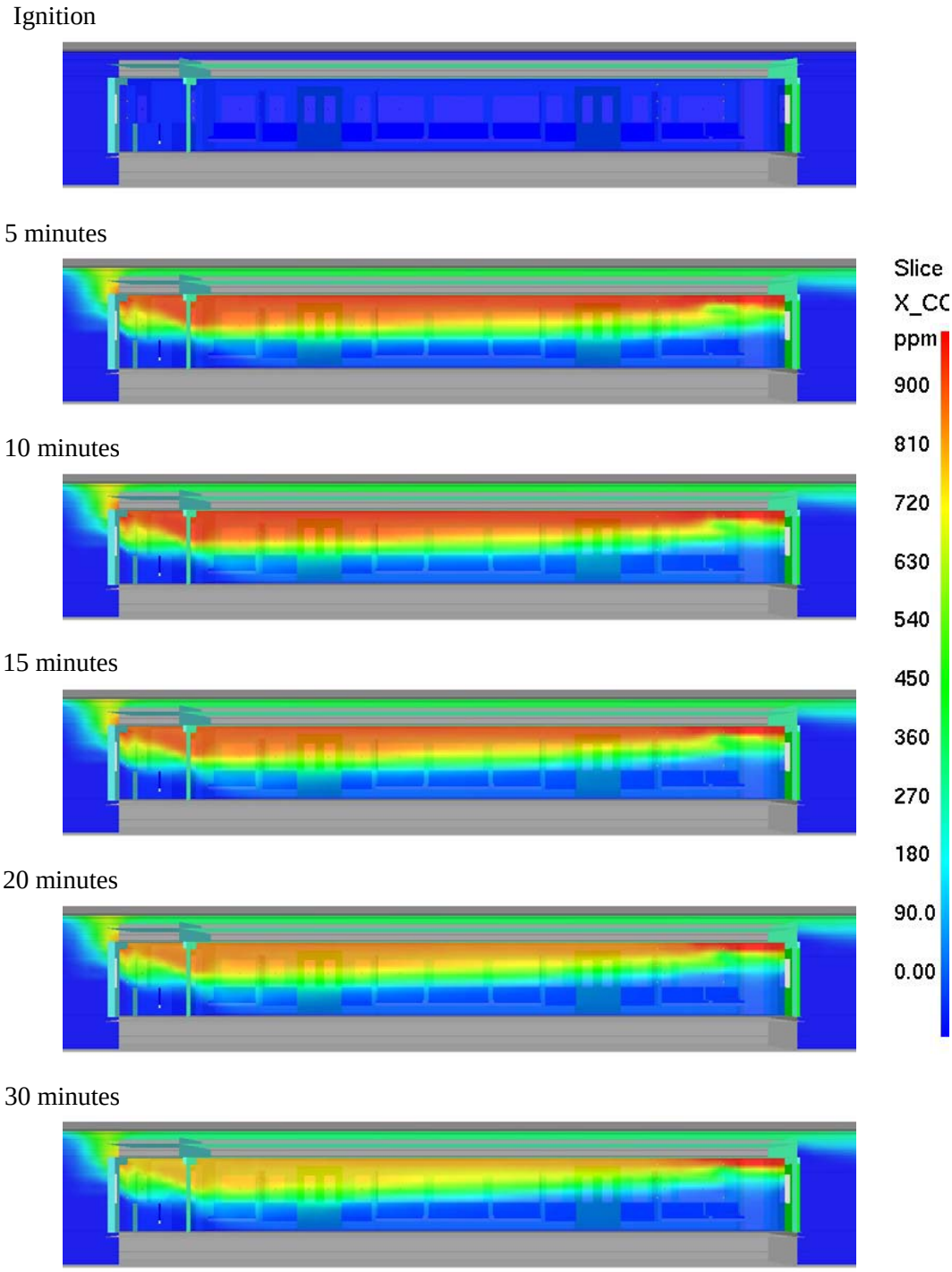

Figure B.3: Carbon-monoxide concentration, 1-car, 80kW source, Single-track tunnel

B.2 CASE-02: 1-CAR, 80kW SOURCE, TWIN-TRACK TUNNEL

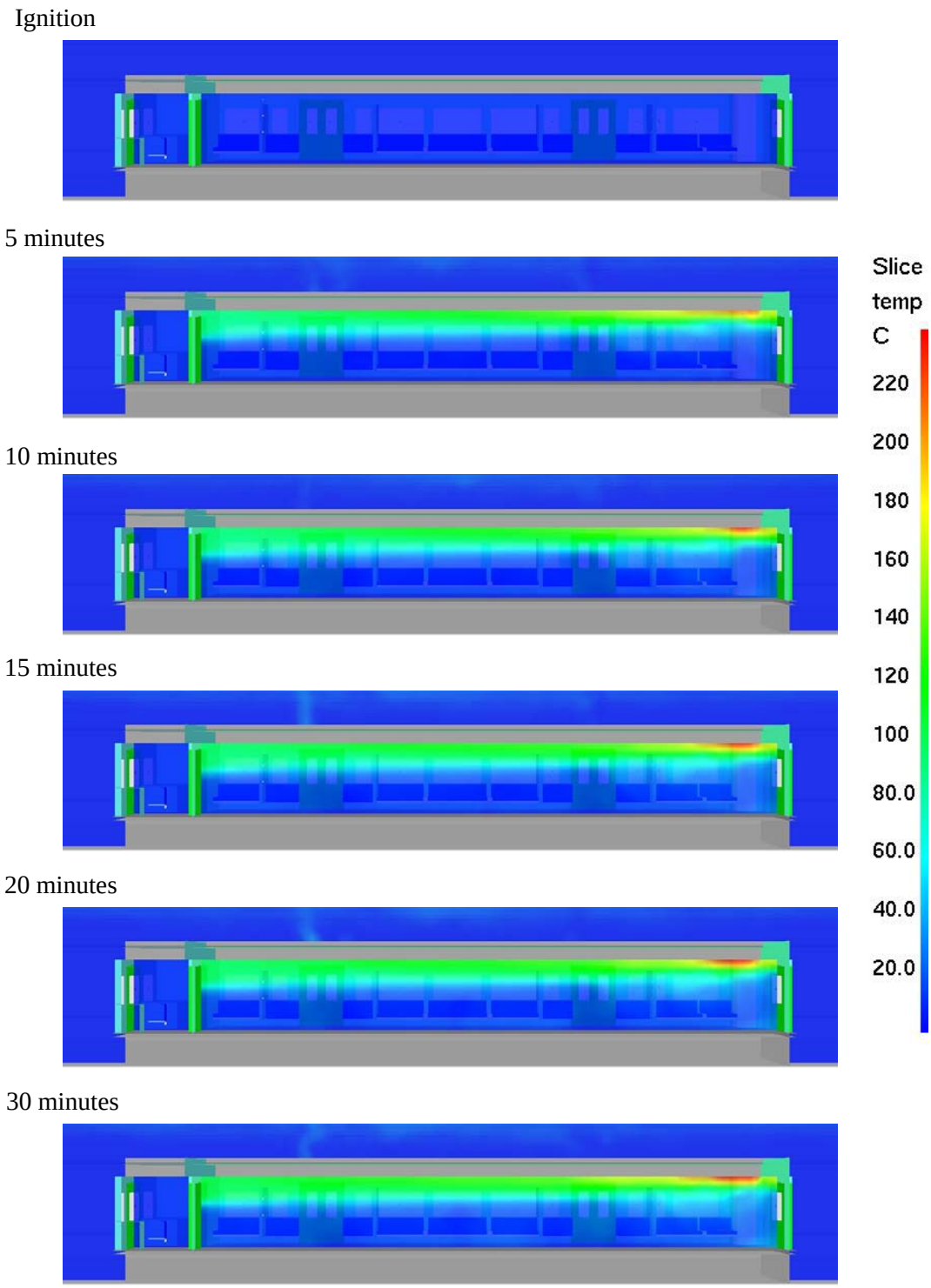

Figure B.4: Temperature, 1-car, 80kW source, Twin-track tunnel

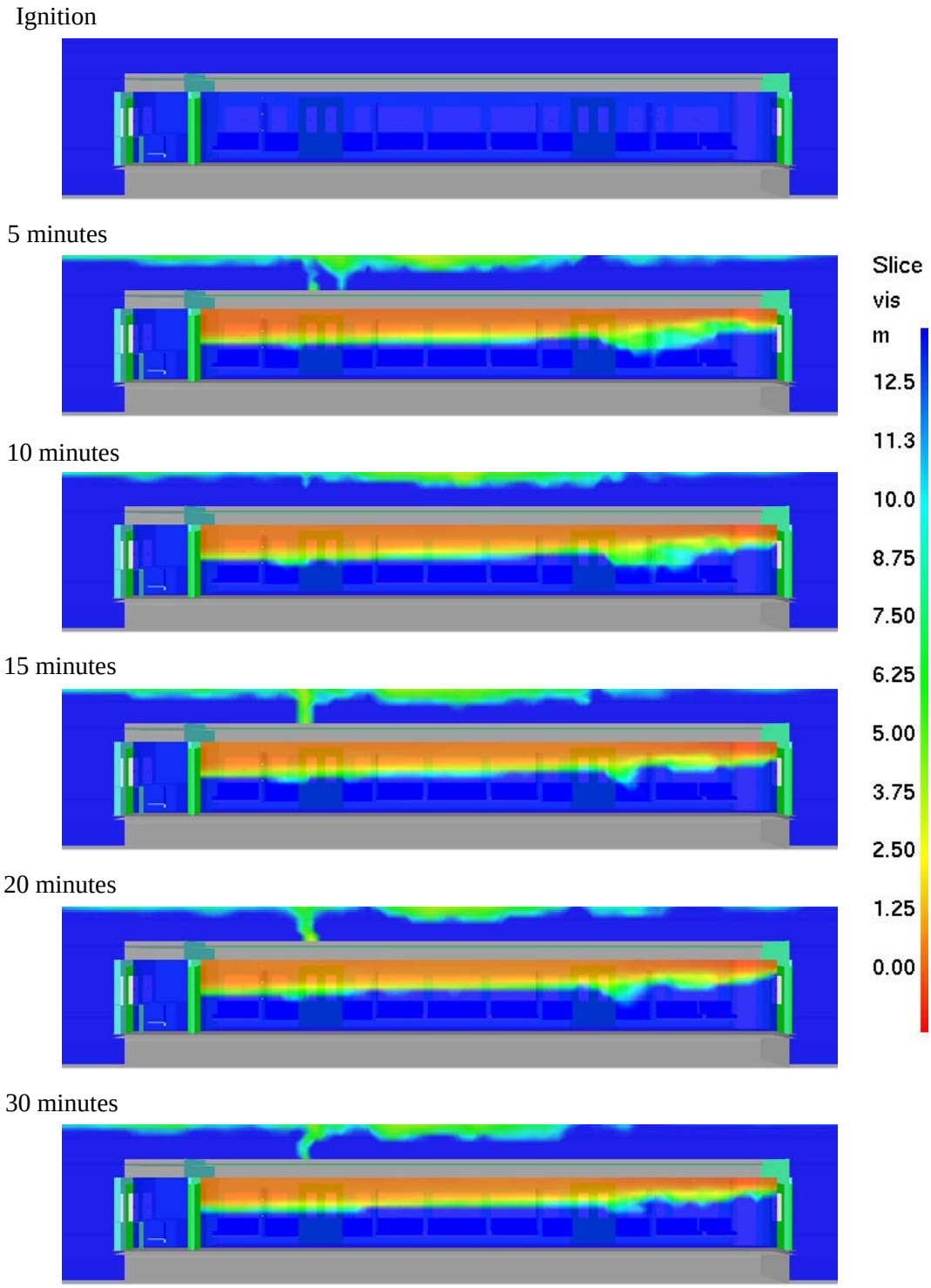

Figure B.5: Visibility, 1-car, 80kW source, Twin-track tunnel

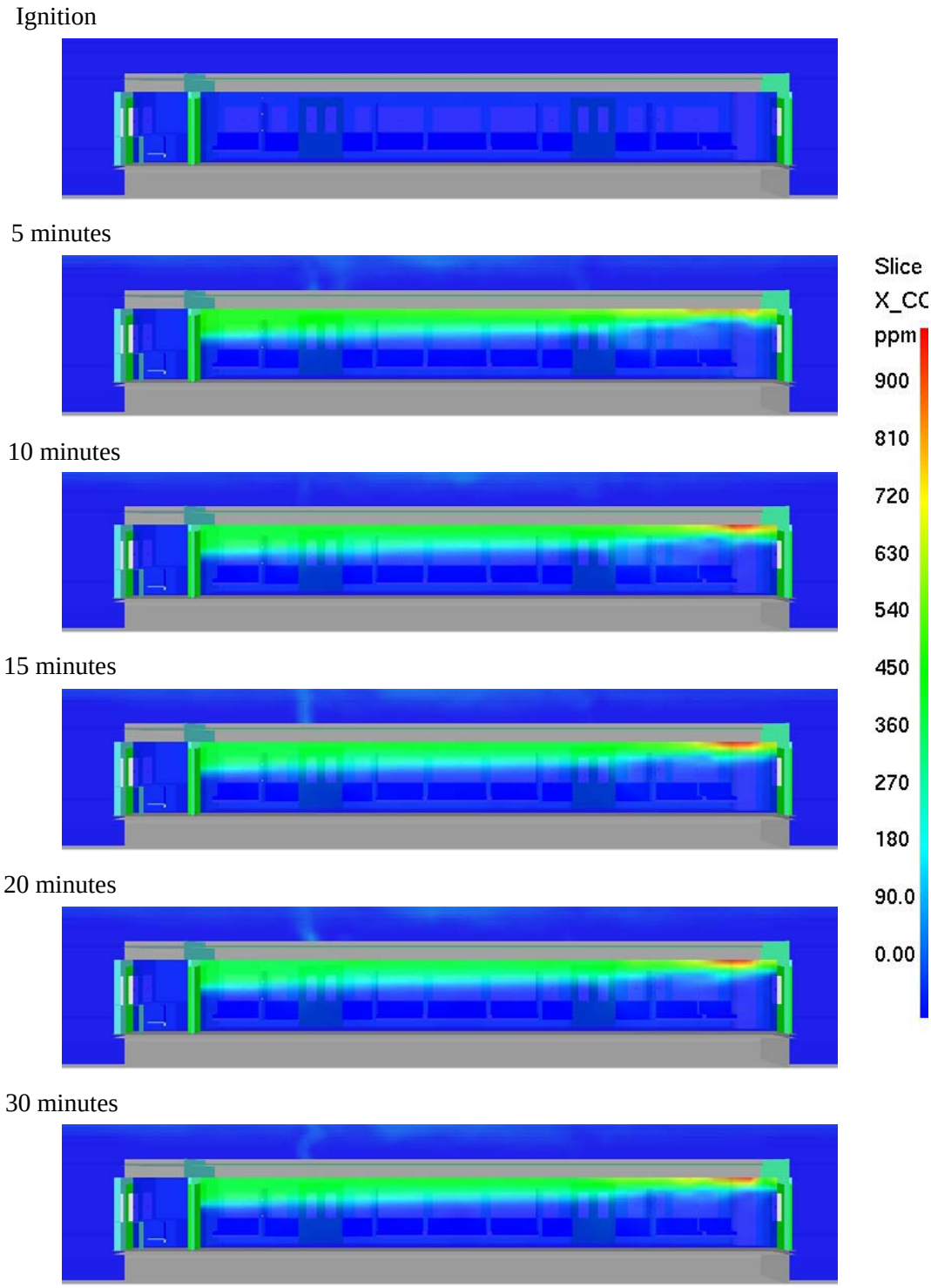

Figure B.6: Carbon-monoxide concentration, 1-car, 80kW source, Twin-track tunnel

B.3 CASE-03: 4-CAR, 80kW SOURCE, SINGLE-TRACK TUNNEL

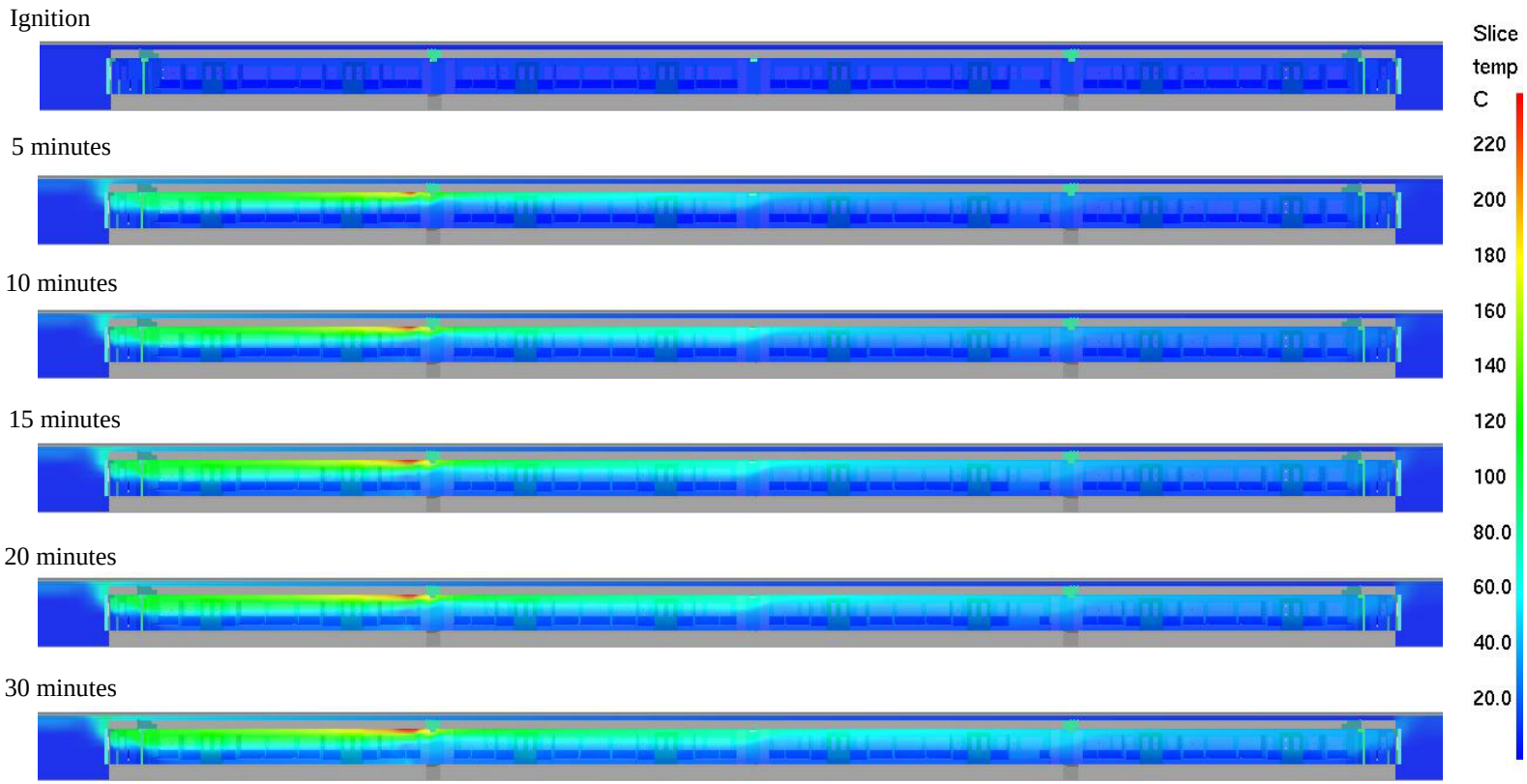

Figure B.7: Temperature, 4-car, 80kW source, Single-track tunnel

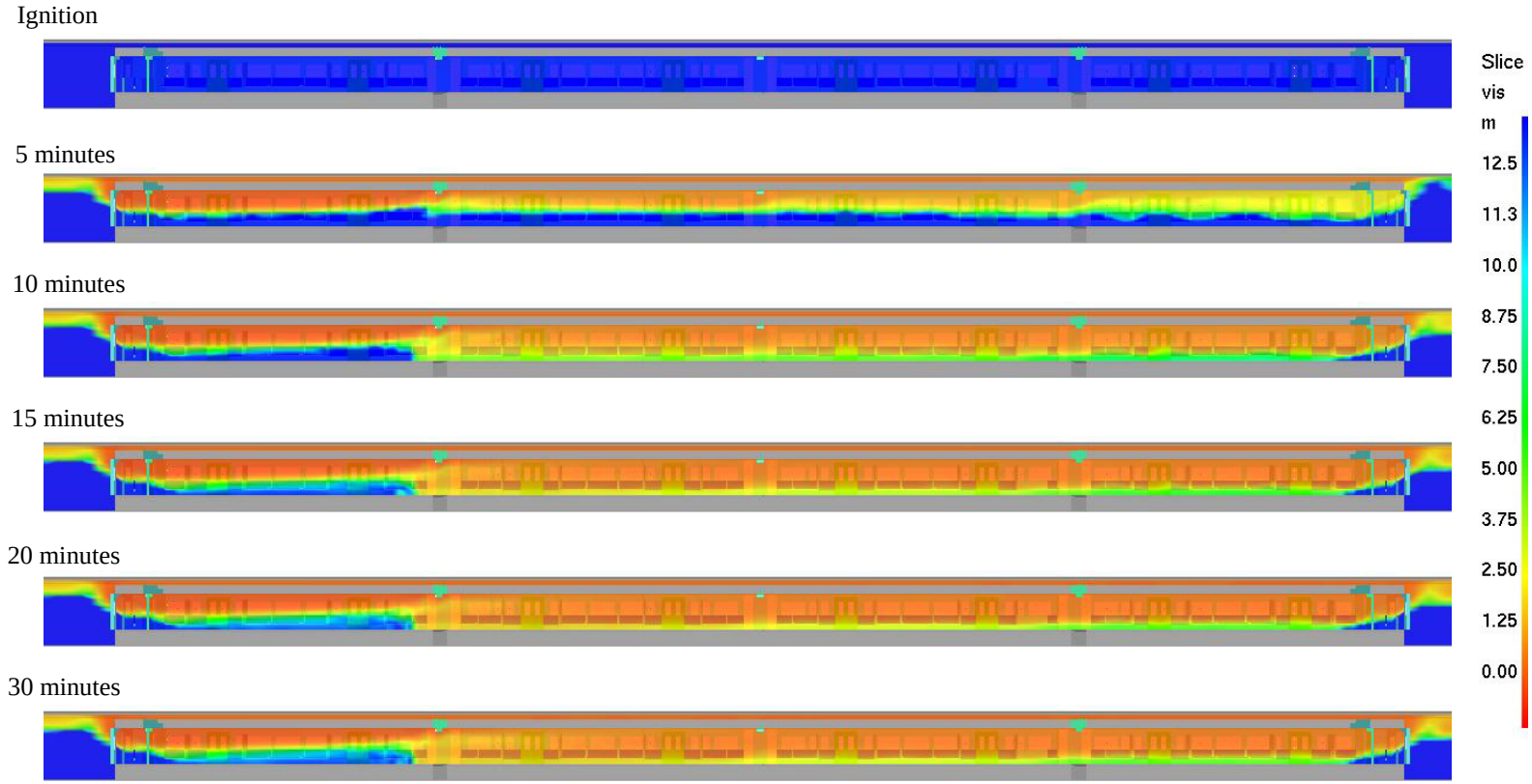

Figure B.8: Visibility, 4-car, 80kW source, Single-track tunnel

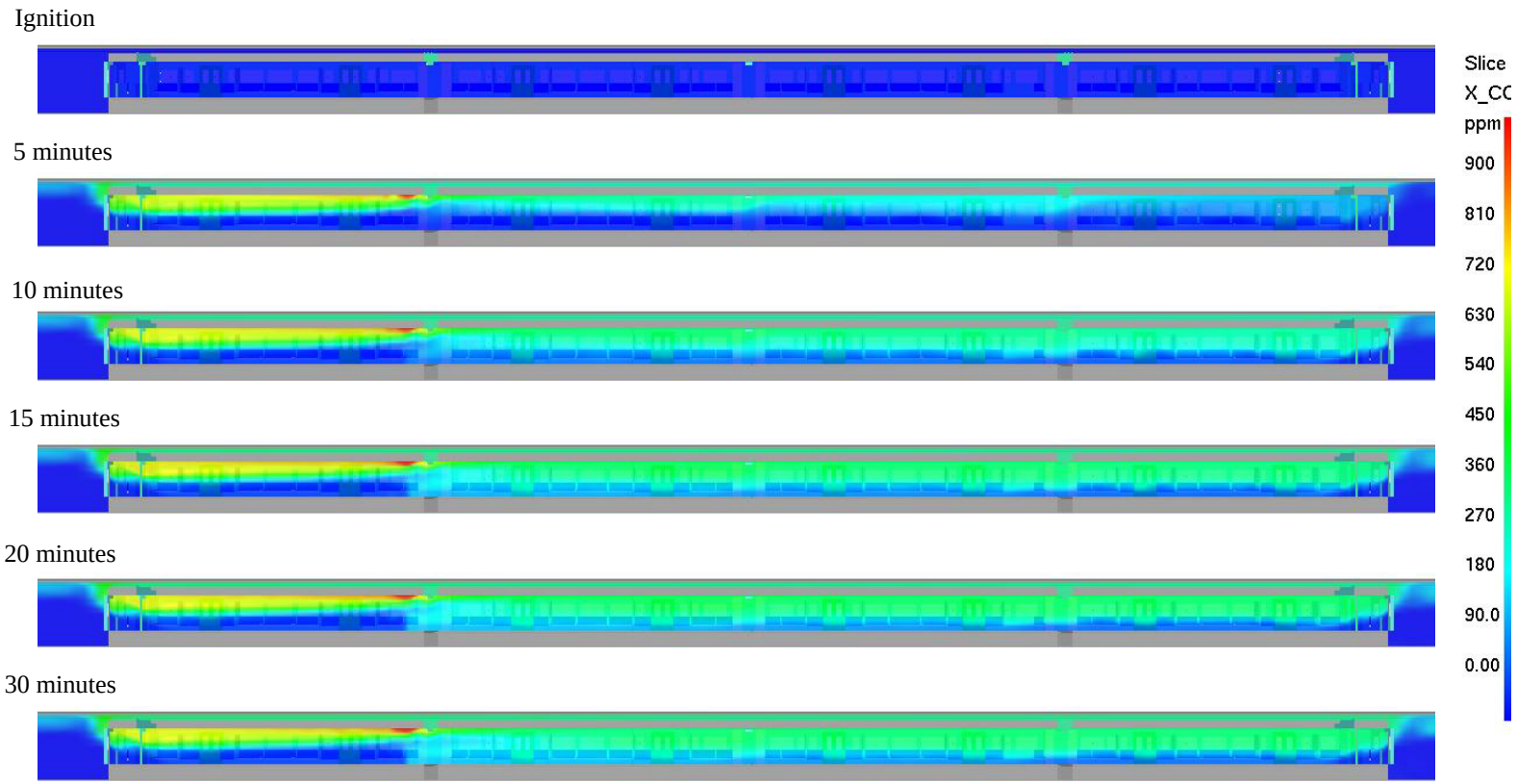

Figure B.9: Carbon-monoxide concentration, 4-car, 80kW source, Single-track tunnel

B.4 CASE-04: 4-CAR, 80kW SOURCE, TWIN-TRACK TUNNEL

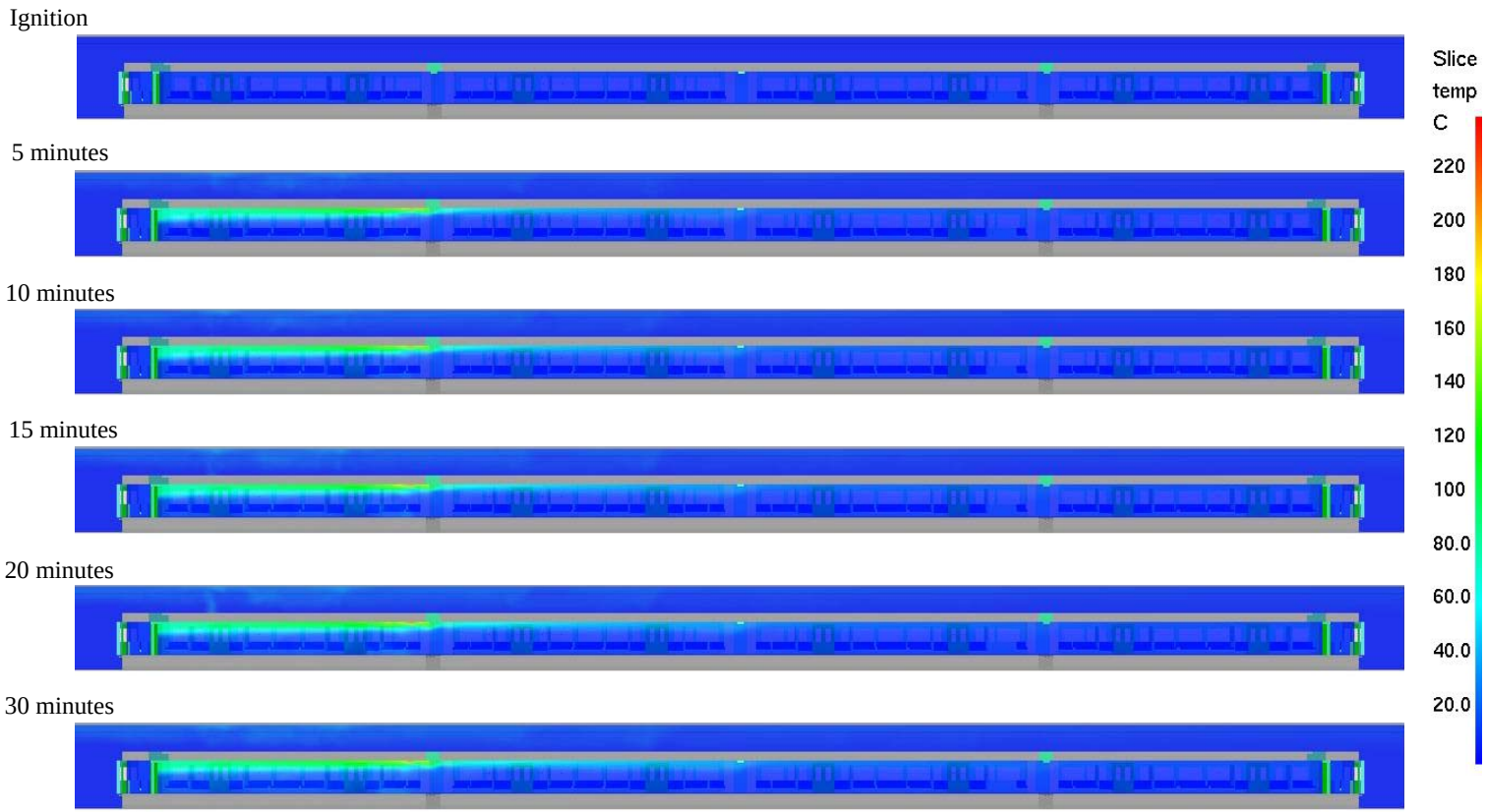

Figure B.10: Temperature, 4-car, 80kW source, Twin-track tunnel

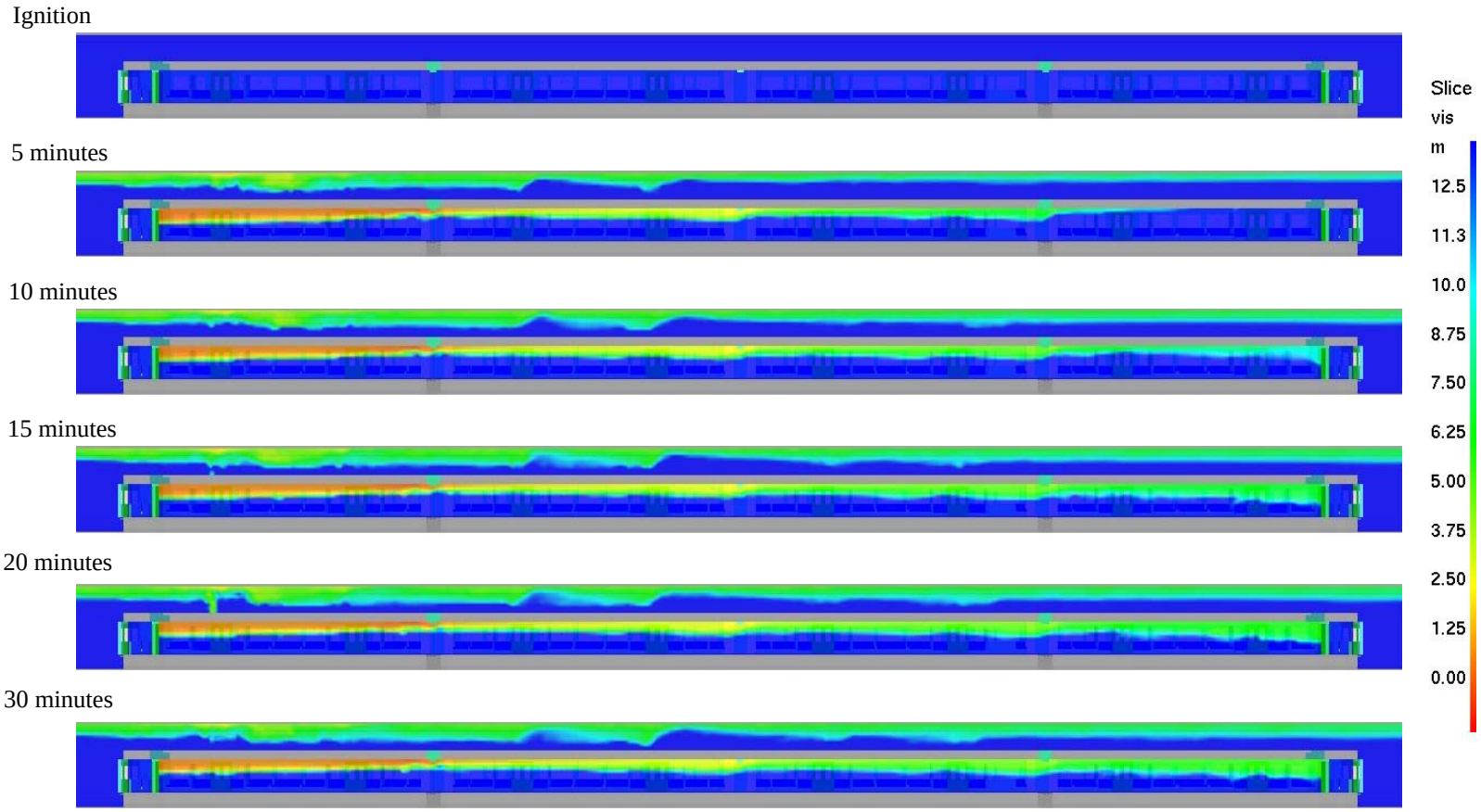

Figure B.11: Visibility, 4-car, 80kW source, Twin-track tunnel

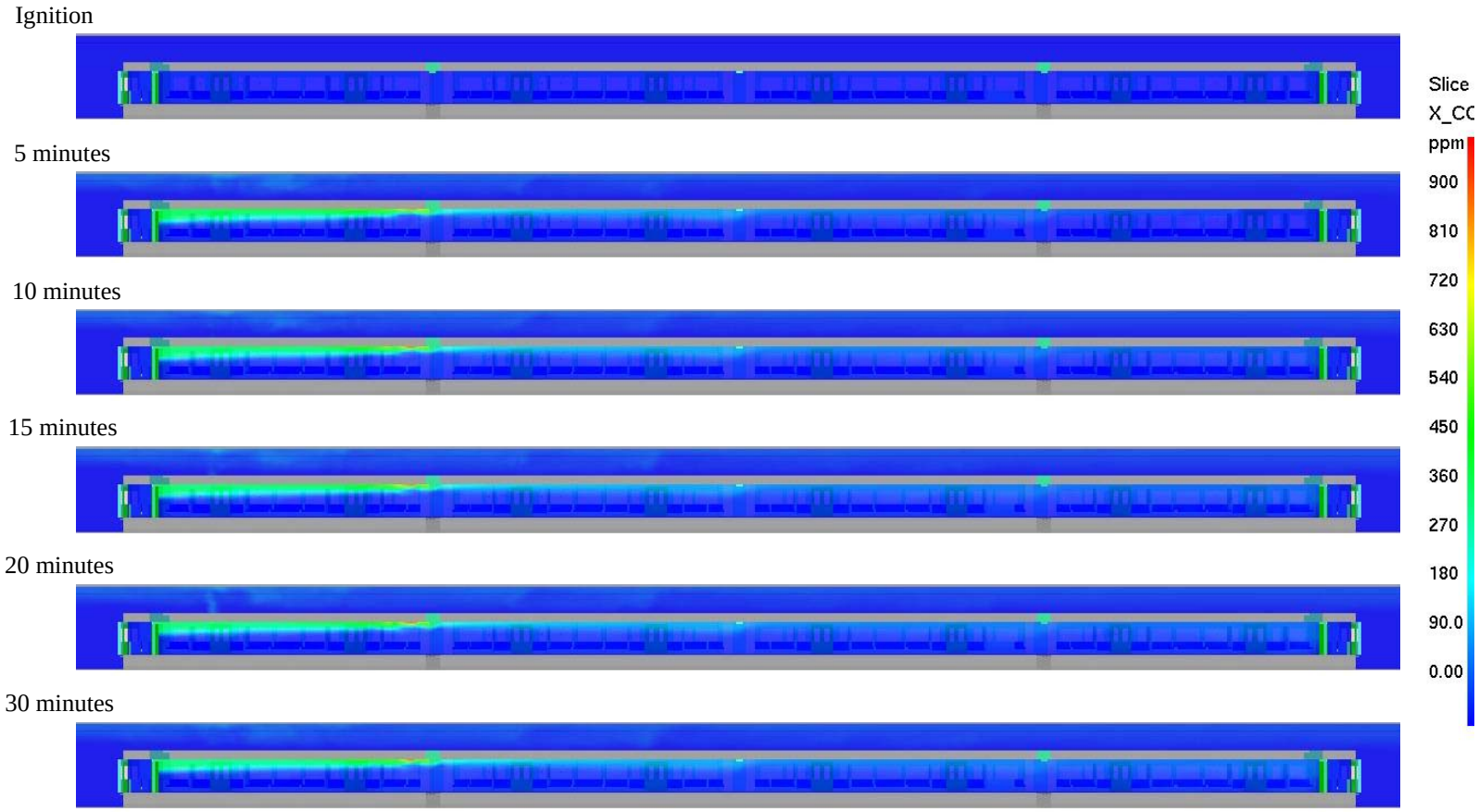

Figure B.12: Carbon-monoxide concentration, 4-car, 80kW source, Twin-track tunnel

B.5 CASE-05: 1-CAR, 1.5MW SOURCE, SINGLE-TRACK TUNNEL

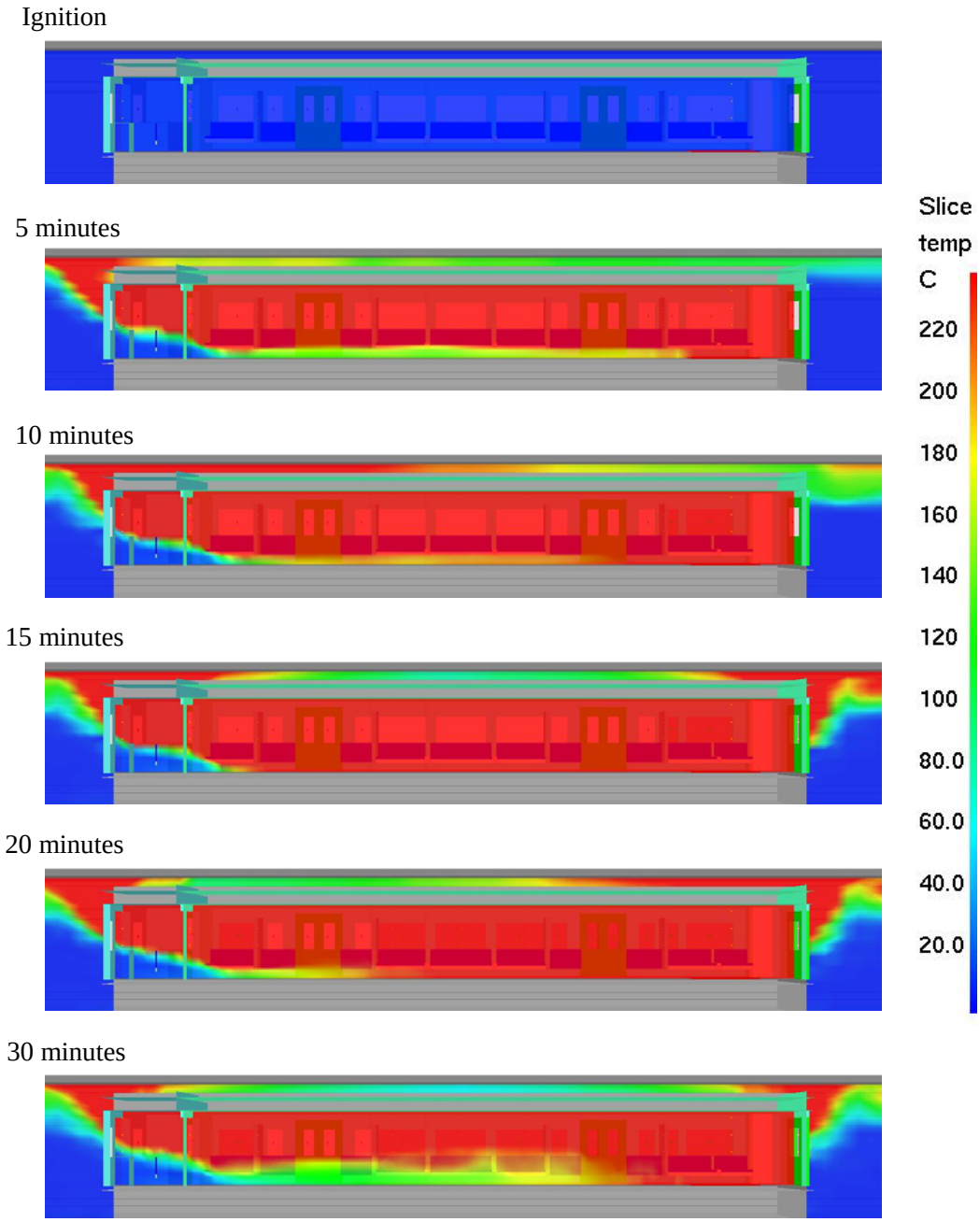

Figure B.13: Temperature, 1-car, 1.5MW source, Single-track tunnel

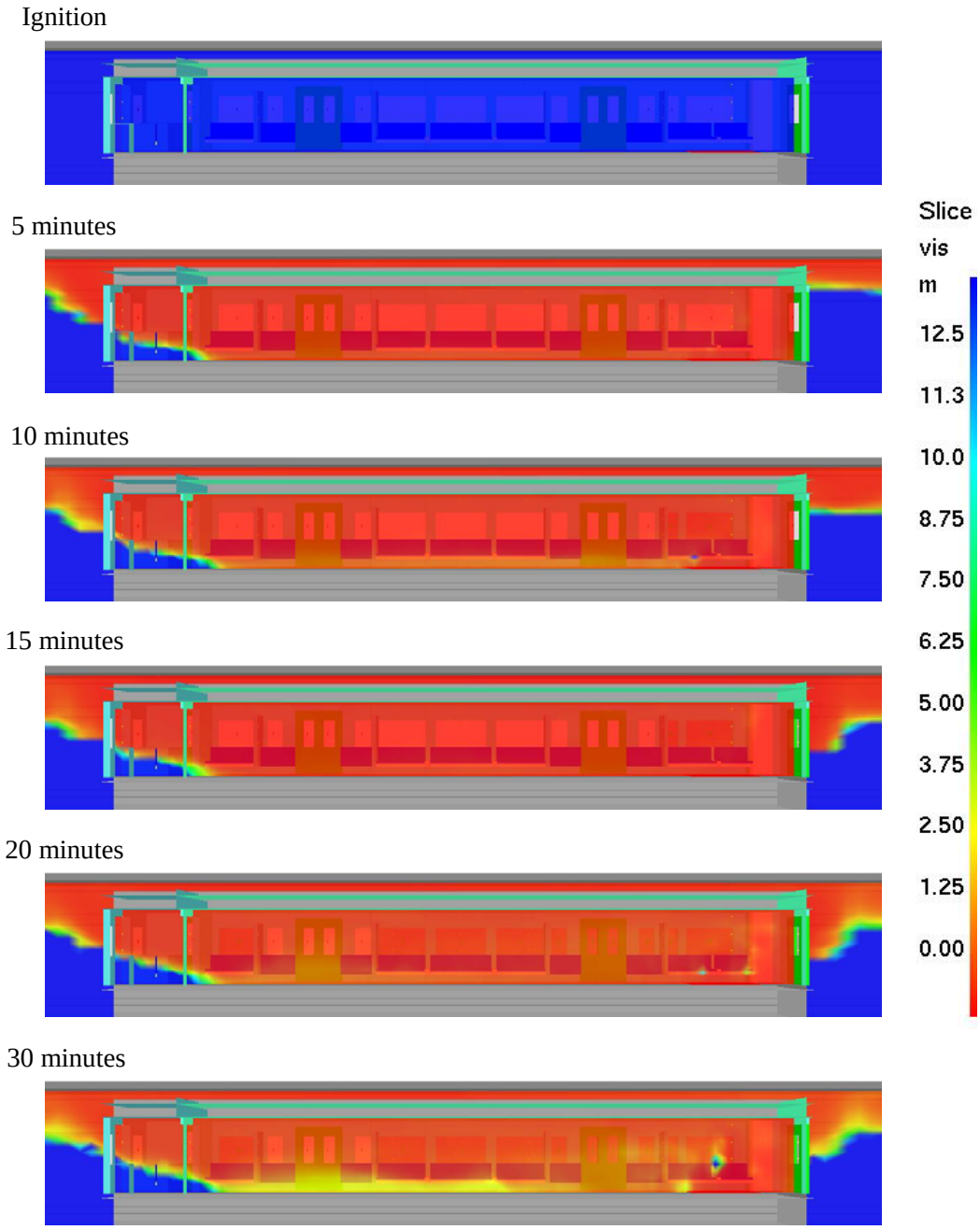

Figure B.14: Visibility, 1-car, 1.5MW source, Single-track tunnel

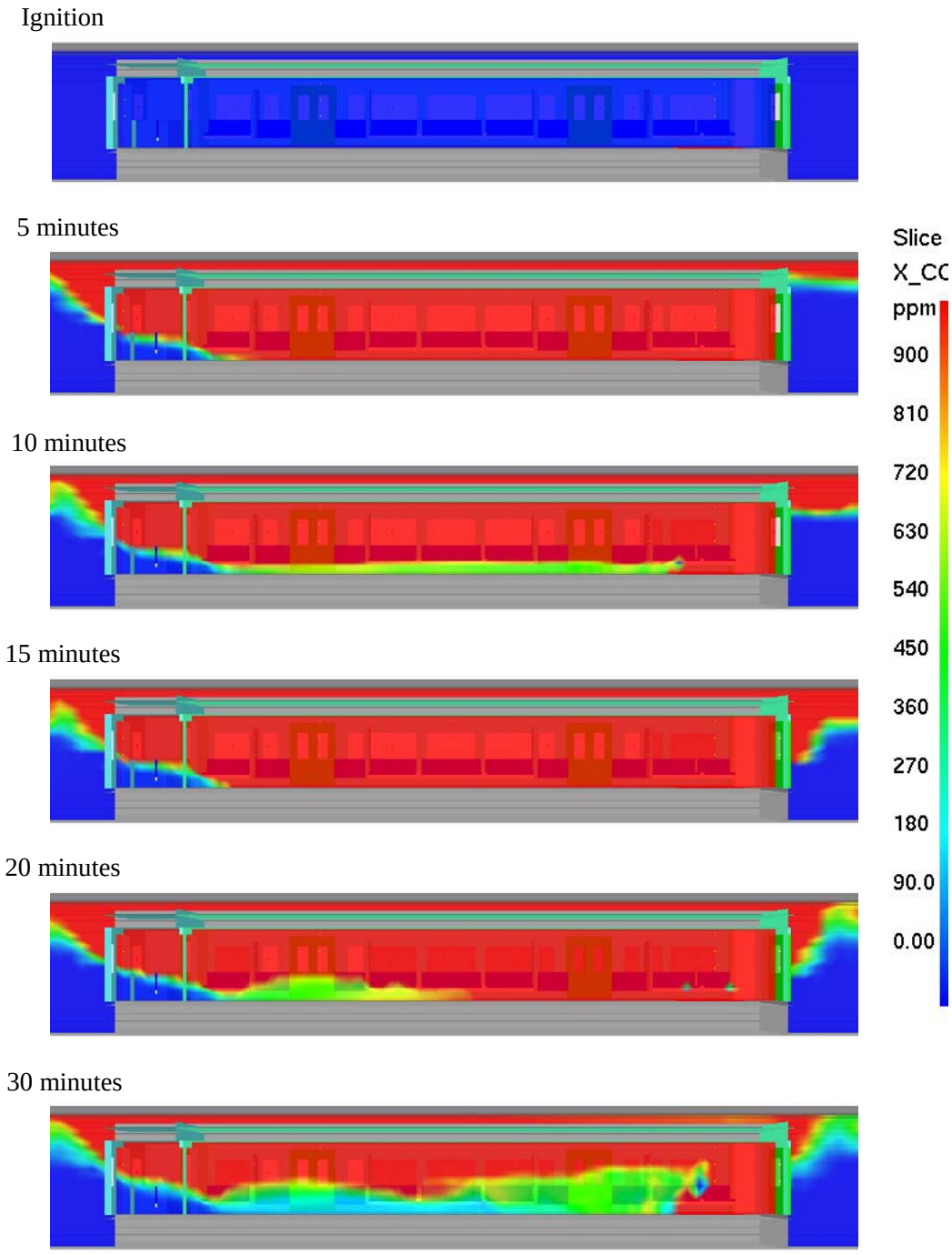

Figure B.15: Carbon-monoxide concentration, 1-car, 1.5MW source, Single-track tunnel

B.6 CASE-06: 1-CAR, 1.5MW SOURCE, TWIN-TRACK TUNNEL

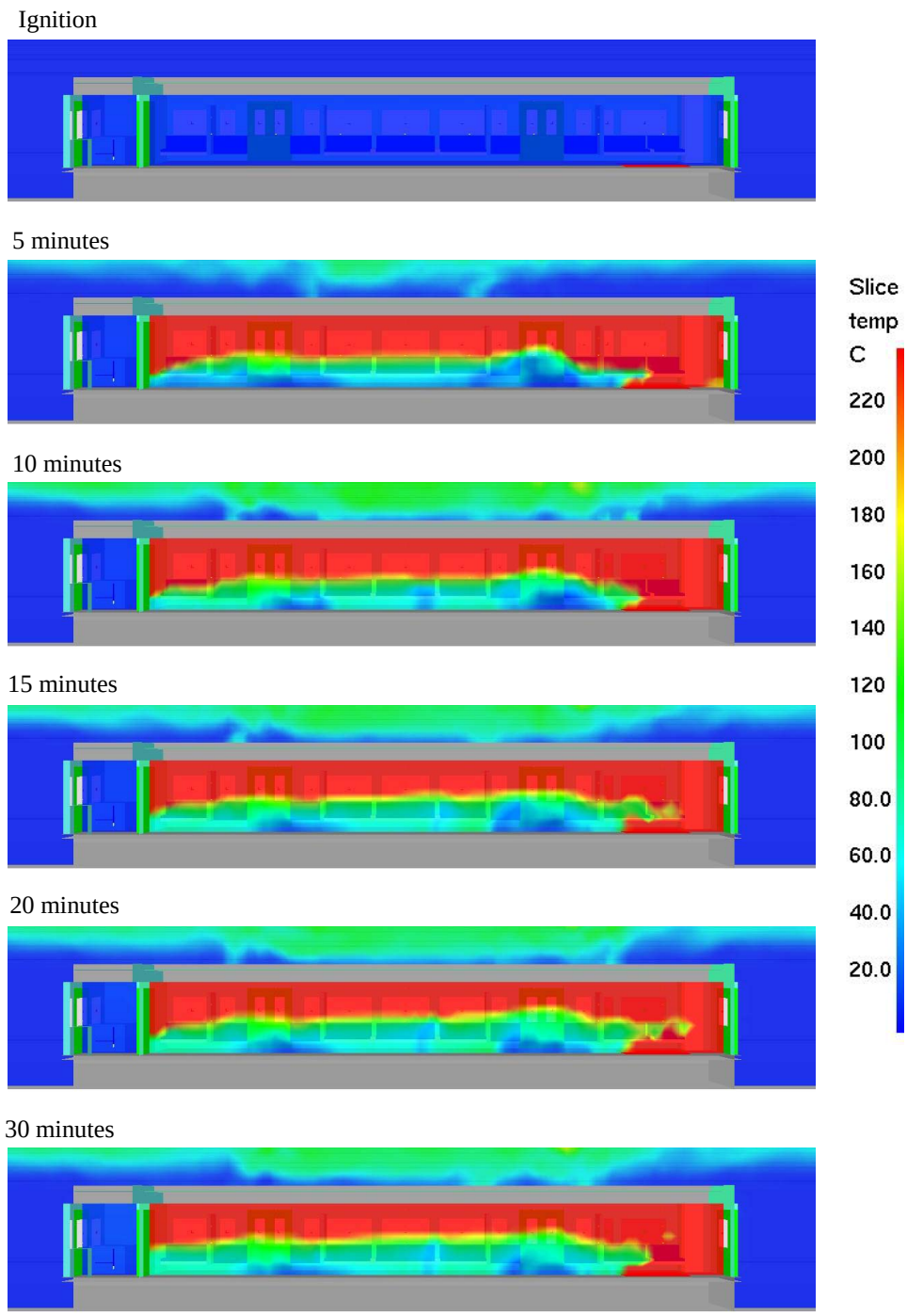

Figure B.16: Temperature, 1-car, 1.5MW source, Twin-track tunnel

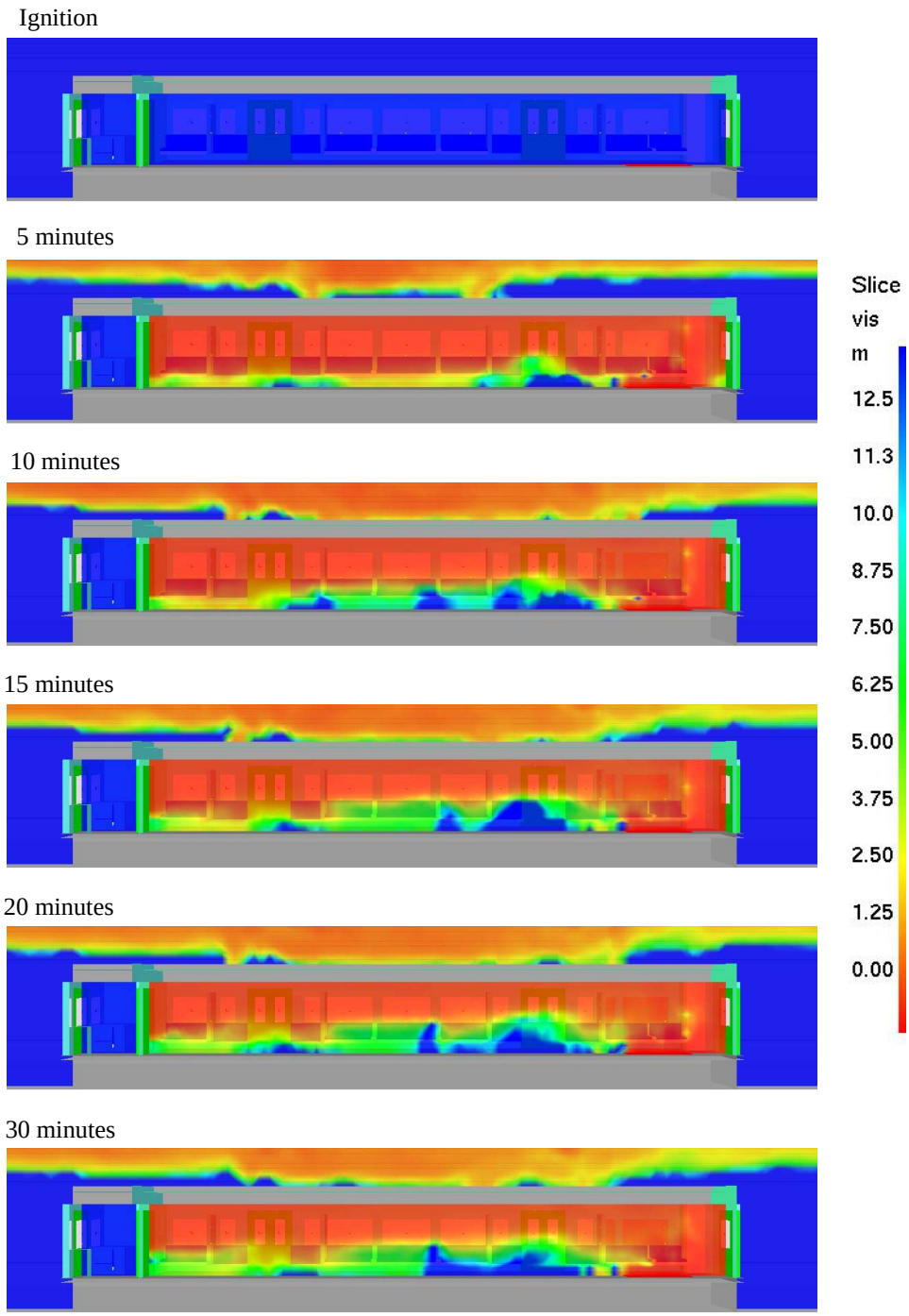

Figure B.17: Visibility, 1-car, 1.5MW source, Twin-track tunnel

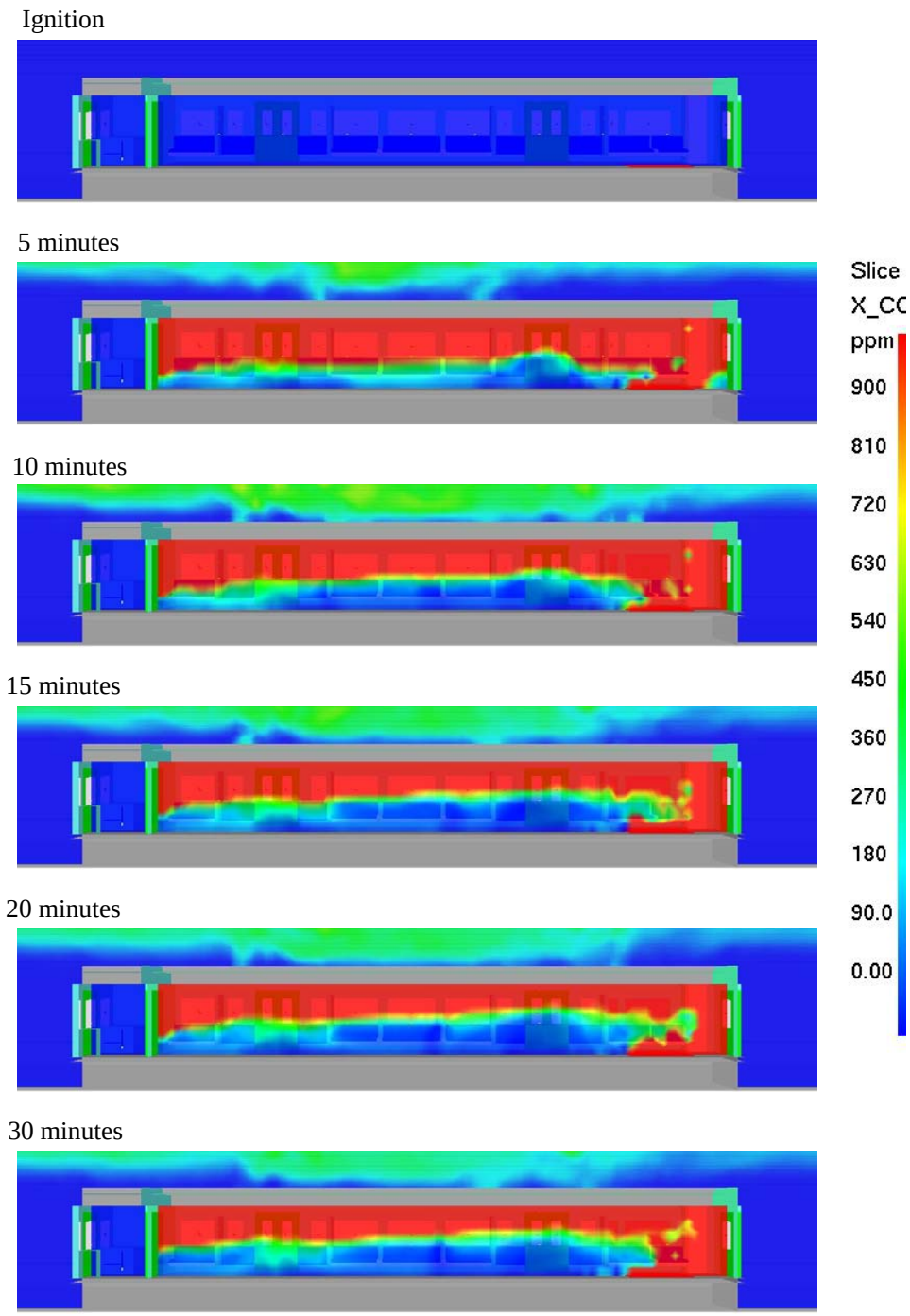

Figure B.18: Carbon-monoxide concentration, 1-car, 1.5MW source, Twin-track tunnel

B.7 CASE-07: 4-CAR, 1.5MW SOURCE, SINGLE-TRACK TUNNEL

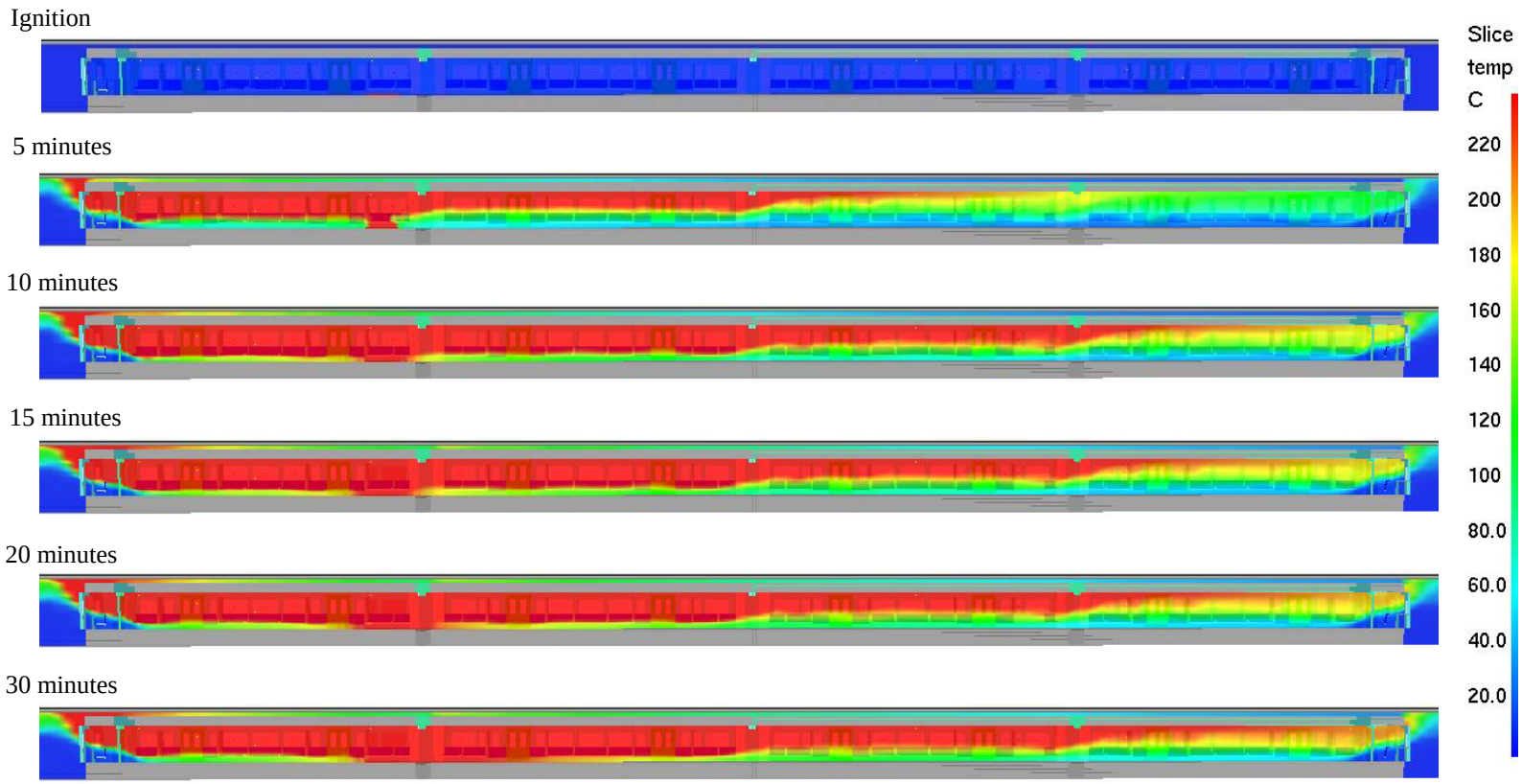

Figure B.19: Temperature, 4-car, 1.5MW source, Single-track tunnel

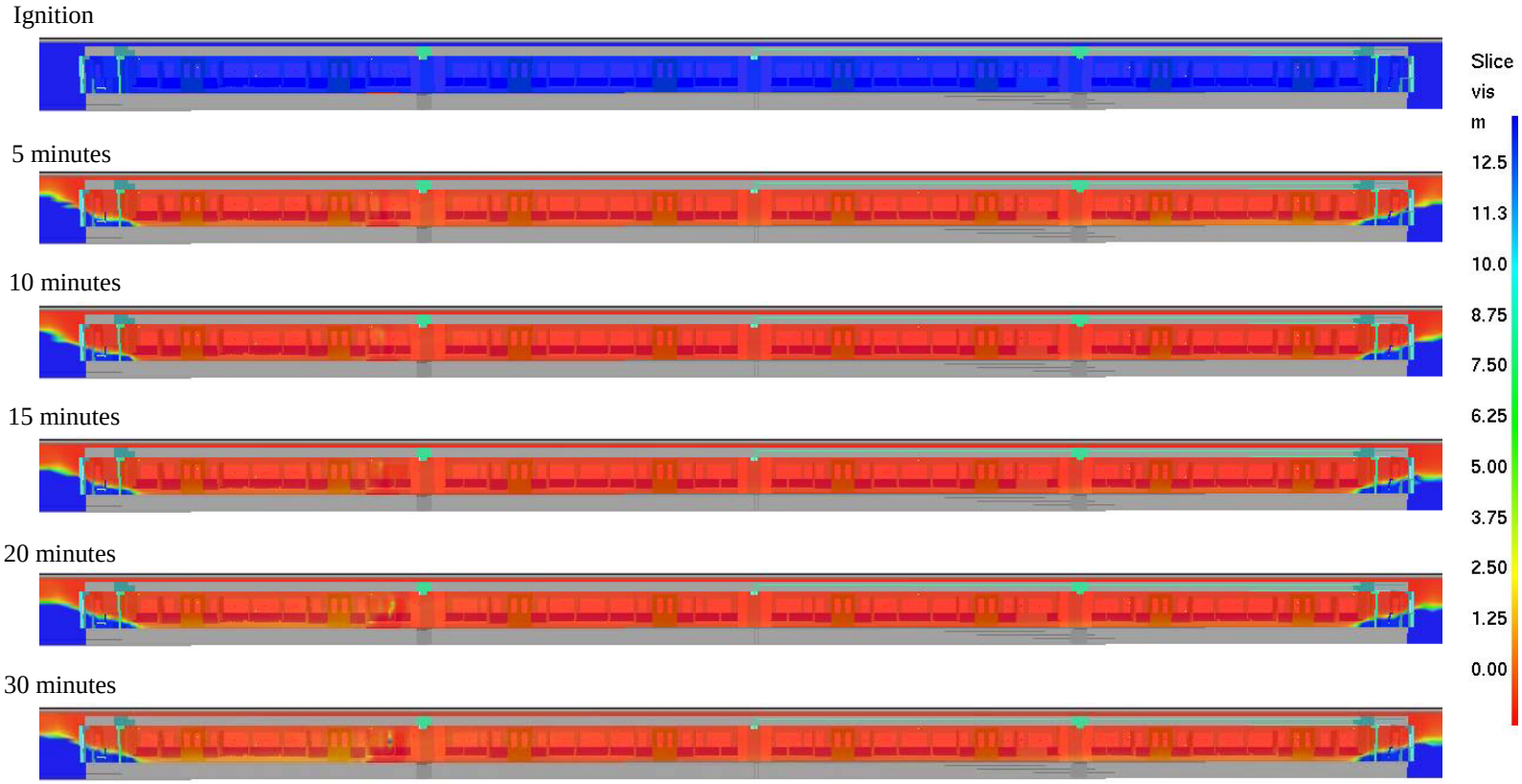

Figure B.20: Visibility, 4-car, 1.5MW source, Single-track tunnel

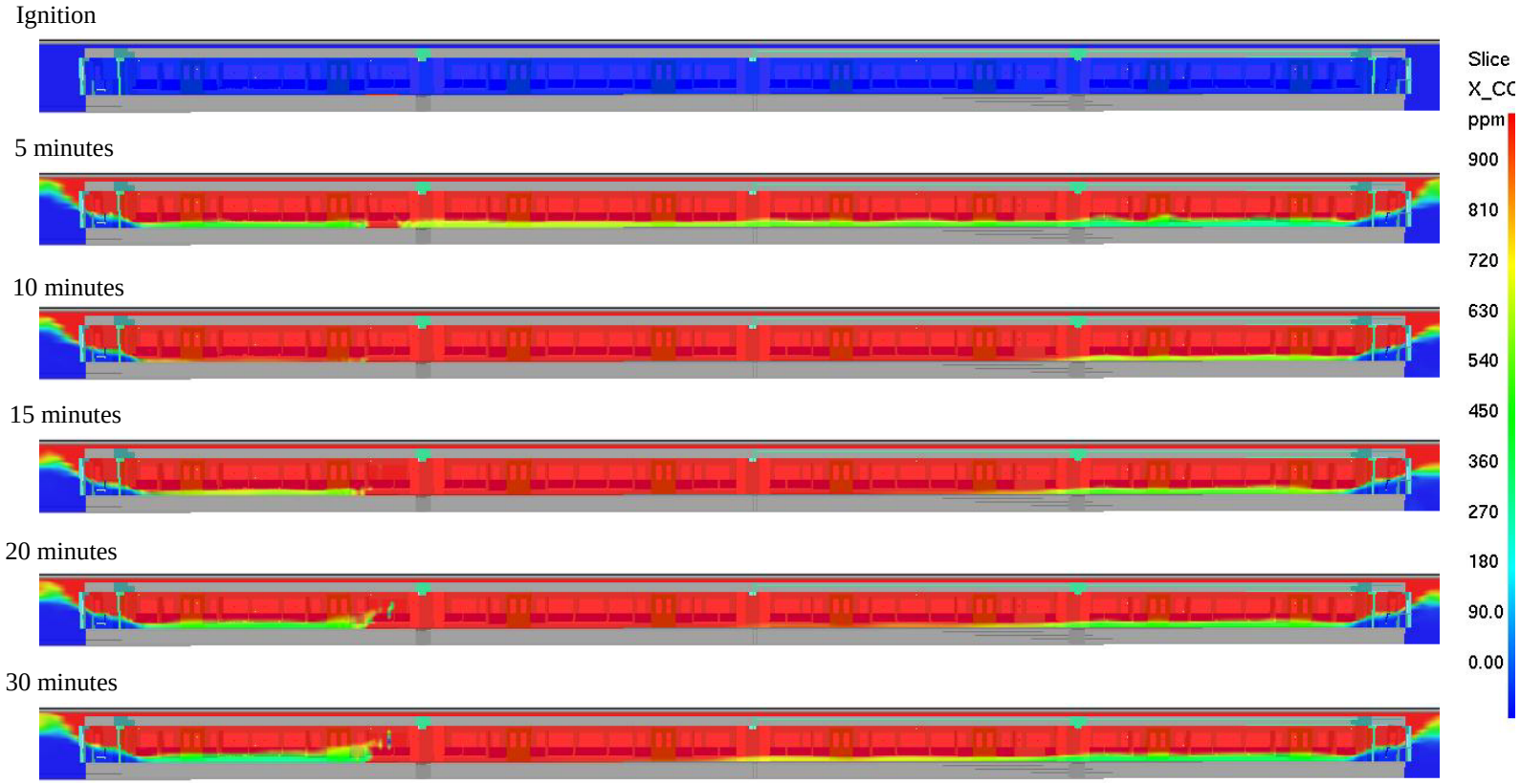

Figure B.21: Carbon-monoxide concentration, 4-car, 1.5MW source, Single-track tunnel

B.8 CASE-08: 4-CAR, 1.5MW SOURCE, TWIN-TRACK TUNNEL

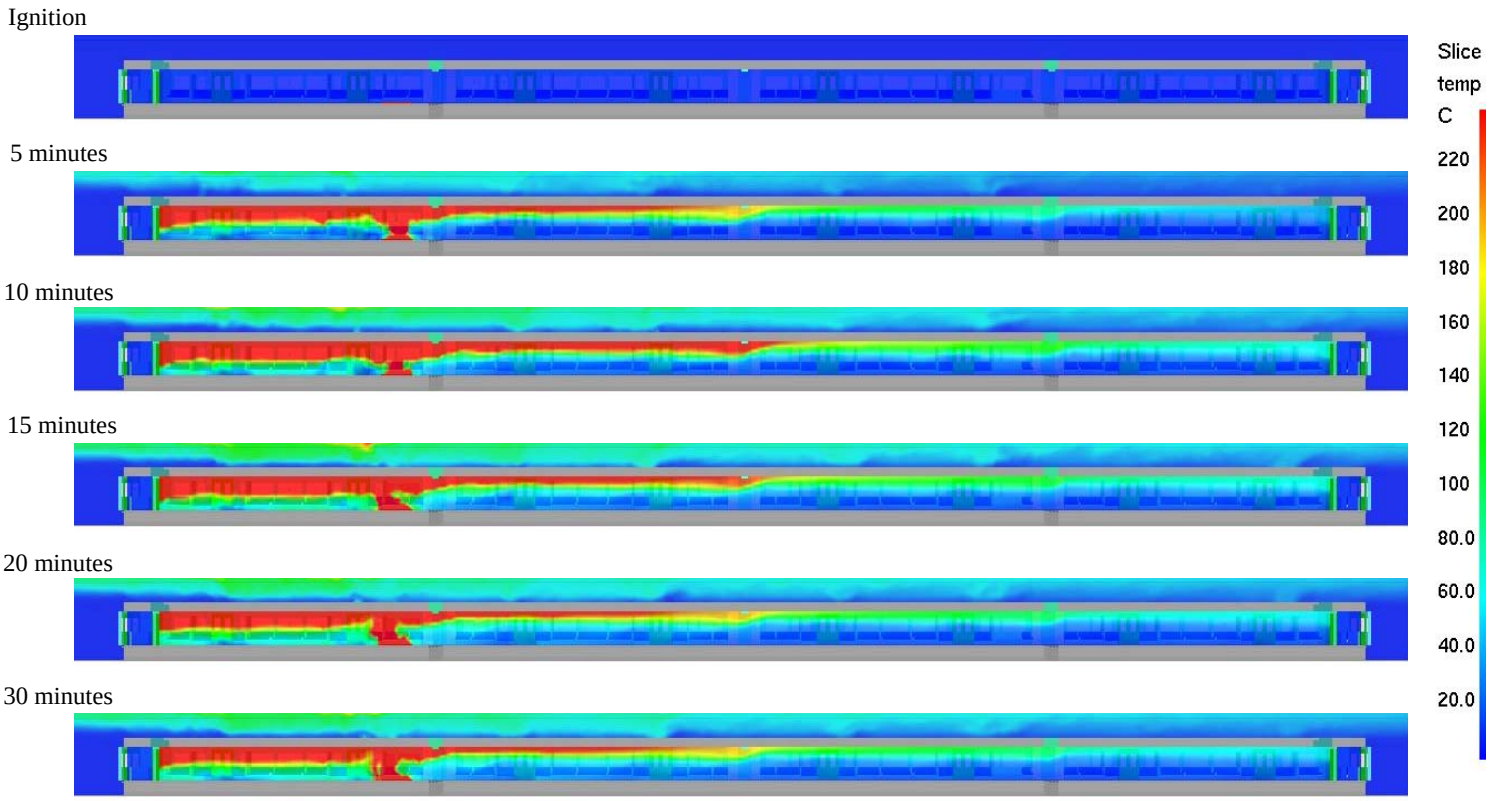

Figure B.22: Temperature, 4-car, 1.5MW source, Twin-track tunnel

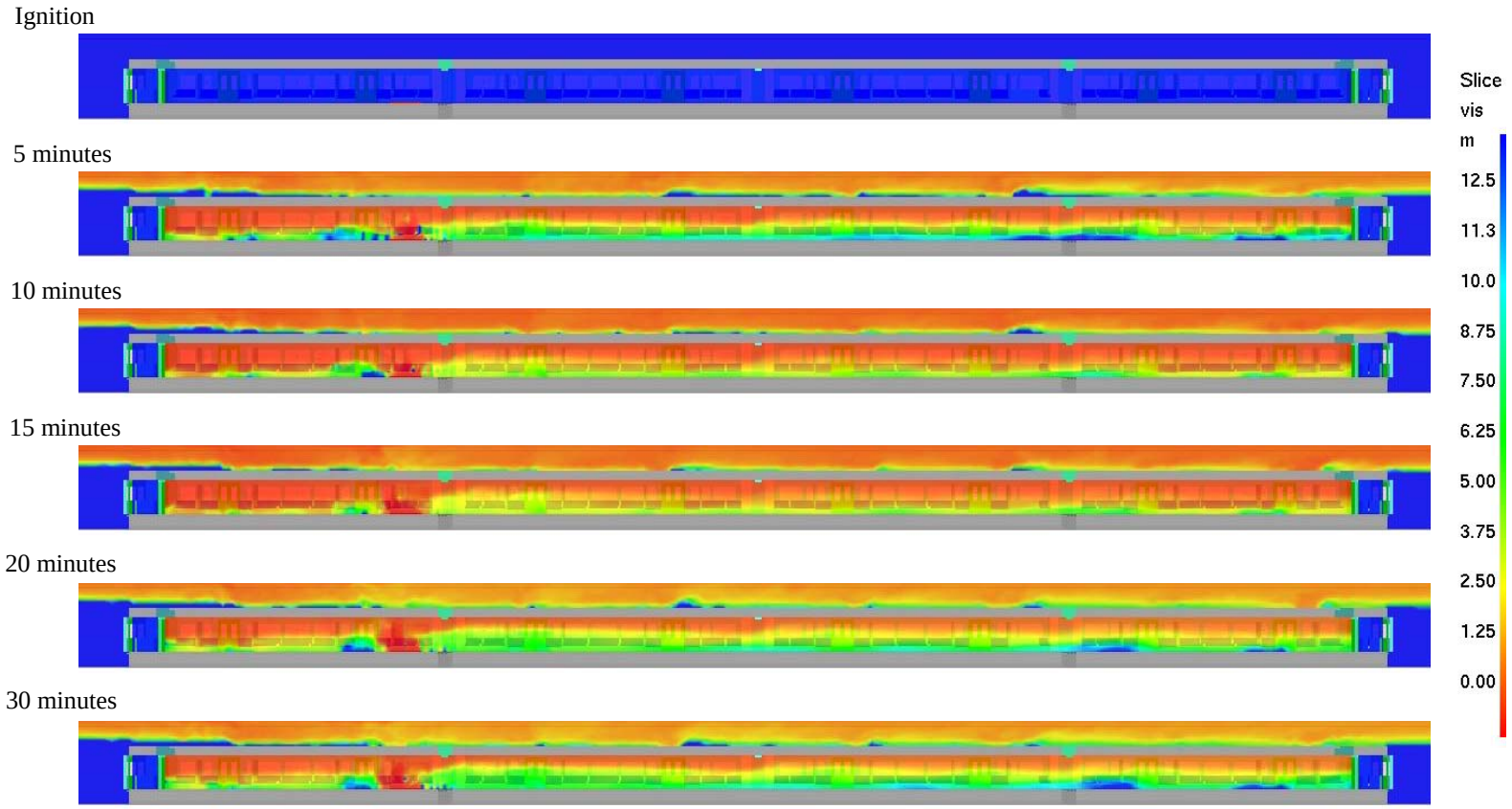

Figure B.23: Visibility, 4-car, 1.5MW source, Twin-track tunnel

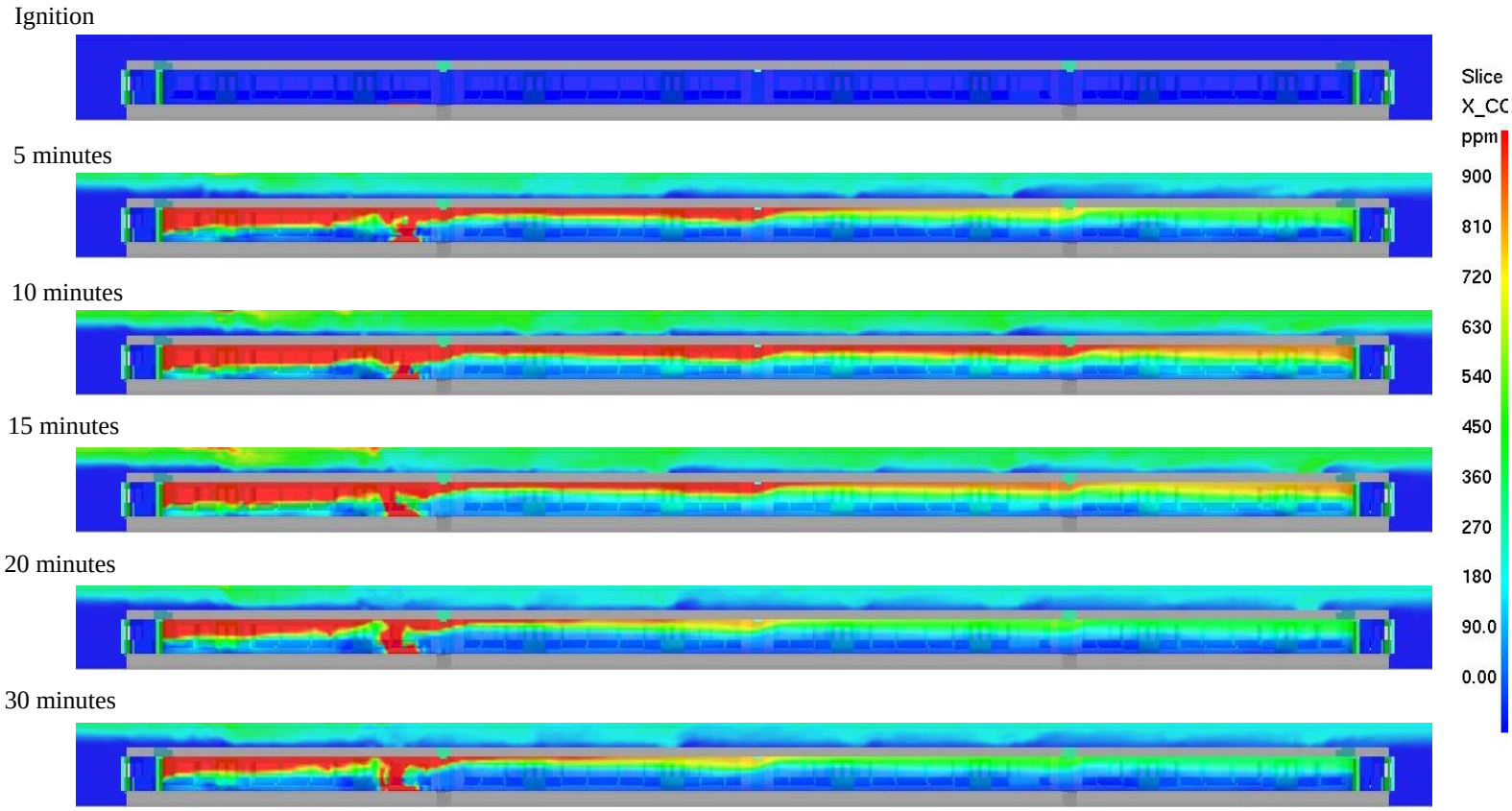

Figure B.24: Carbon-monoxide concentration, 4-car, 1.5MW source, Twin-track tunnel

Appendix C

CONE CALORIMETER MODELLING

C.1 CONE CALORIMETER MODELLING

For the analysis of fire development in a confined space, such as rail car interior, the ignition properties and the heat release rates of the materials involved in fire should be analyzed. The combustibility characteristics of passenger train car materials are measured using the Cone Calorimeter setup. A sample set of measurements for rail car materials is published by the National Institute of Standards and Technology (NIST) [7].

The Cone Calorimeter is a single test apparatus which provides a measurement of heat release rate (HRR), specimen mass loss, smoke production, and combustion gases. The ASTM E 1354 standard for the Cone Calorimeter defines the design and operational details of the apparatus. The general view of the Cone Calorimeter is given in Figure C.1.

The design and the data of Cone Calorimeter are based on an engineering understanding of fire; therefore the device has wider applicability and better assessment of flammability compared to the traditional test methods.

Test specimens are nominally 100x100mm and up to 50mm thick. For materials that expand during the burning process, a wire grid is placed over the specimen surface to prevent the material from expanding into the cone heater and increasing the burning rate and heat release rate. Smoke measurements are made on the effluent flow by means of a helium-neon laser beam projected across the exhaust duct. This results in an instantaneous measure of the optical smoke density.

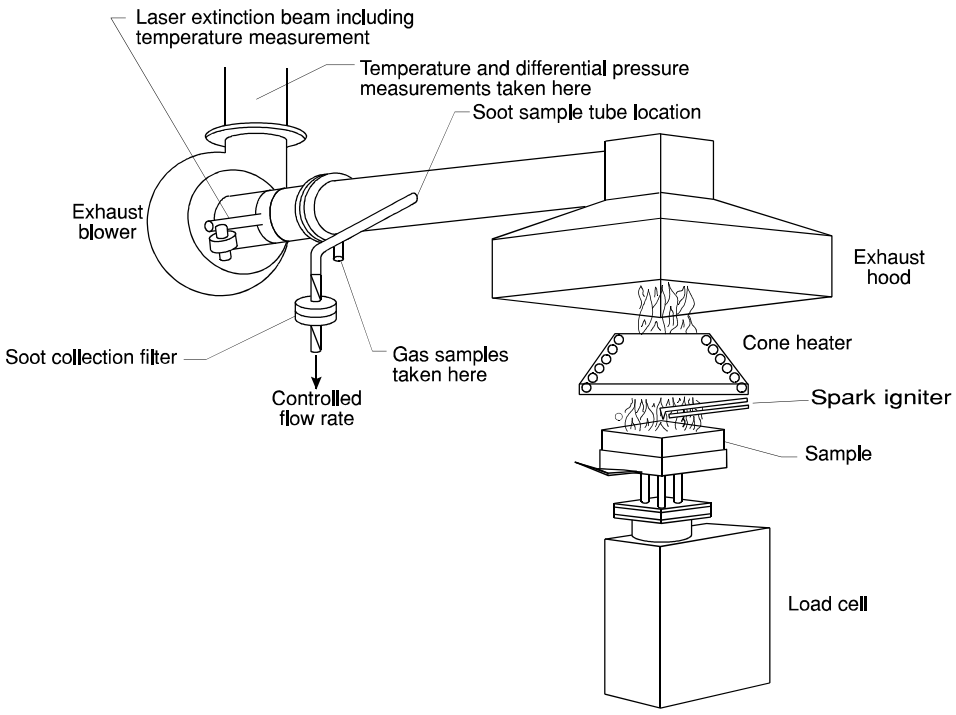

Figure C.1: General view of the Cone Calorimeter [7]

The characteristic data measurements obtained from the Cone Calorimeter include:

- Ignition time: a measure of how easily a material can be ignited,
- Time to peak HRR: a measure of the speed of fire growth,
- Peak HRR: a measure of how large a fire will result from a burning material,
- Specific extinction area: a measure of smoke production of the material, and
- Effective heat of combustion: a measure of the amount of heat released from a burning material per unit mass of sample burned.

The British Standard BS 476 part 15 and International Standard ISO 5660 also give information on Cone Calorimeter apparatus and explain the test procedure to measure the rate of heat release of the materials [1, 12]. Figures C.2 and C.3 show the sectional view of the conical heater and the overall view of the Cone Calorimeter, respectively. In the figures presented the nominal dimensions in millimeters are also indicated.

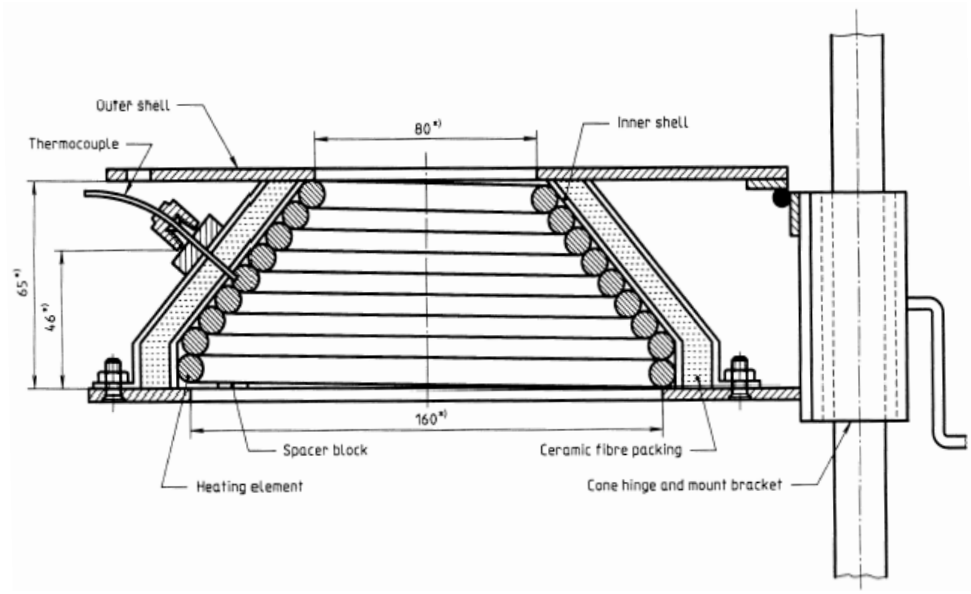

Figure C.2: Sectional view through the heater [1]

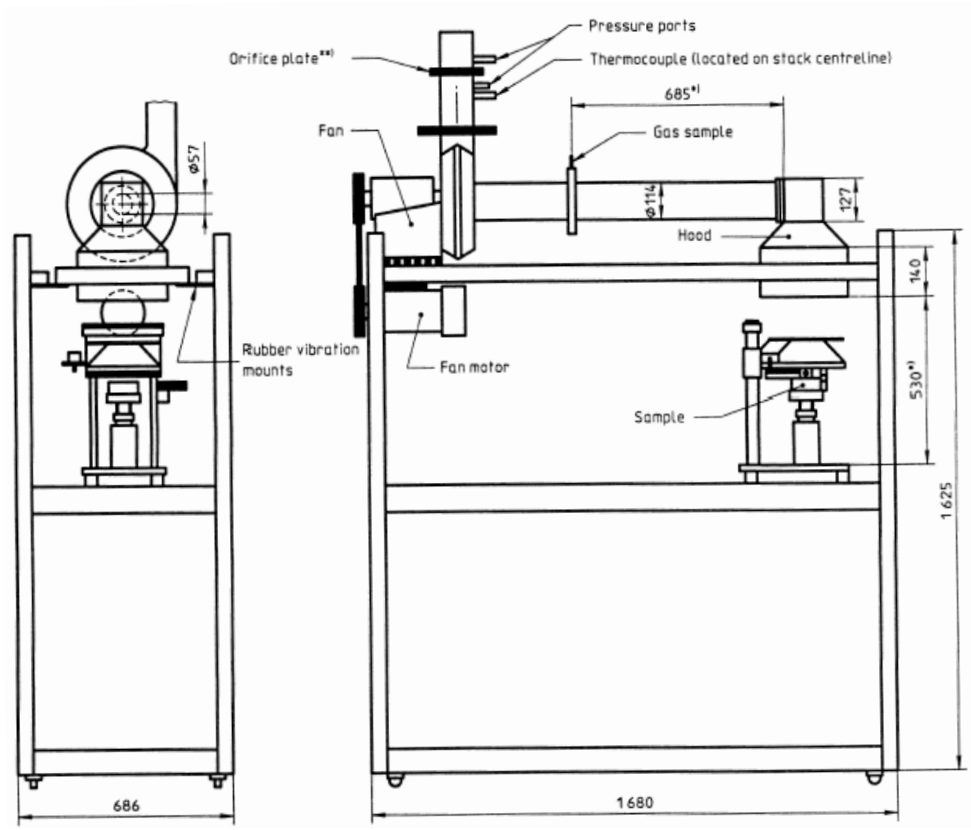

Figure C.3: Overall view of Cone Calorimeter apparatus [1]

Based on the dimensions provided in BS 476 part 15, an FDS model of Cone Calorimeter is built. For the purpose of the study, only the conical heater and the test specimen under examination are modelled. The dimensions of the domain are defined as 0.2m x 0.2m x 0.2m, and the cell edge length is selected to be 5.0mm in all three dimensions.

The cell edge length, used in the Cone Calorimeter model, is selected in agreement with the nominal cell edge length used in the model to predict the heat release rate variation of a train fire. The cell edge length in two models should be selected so that the fractions of characteristic fire diameter over the nominal cell edge length in two models would be the same.

The relation between the characteristic fire diameter and the heat release rate from a fire is given as follows:

$$D^* = \left(\frac{\dot{Q}}{1100}\right)^{\frac{2}{5}} \tag{C.1}$$

where D^* is the characteristic fire diameter in meters, and $\dot{Q}$ is the heat release rate from fire in kW.

The nominal peak heat release rate from a train fire is predicted to be about 6.5MW. The nominal cell edge length in computational domain used in the FDS simulations of a train fire is 0.175m. The Cone Calorimeter simulations show that the peak heat release rate from the specimen is about 1.0kW. Consequently, a nominal cell edge length of about 5.0mm is acceptable in modelling the Cone Calorimeter. The grid size derivation is summarized in Table C.1. The values of $D^*/\delta x$ in two models should match for better representation. However, in order to match 11.66, an edge length of 5.2mm should be used in the Cone Calorimeter model. Since, an accuracy of 0.2mm in the grid size is unrealistic in terms of numerical computation, a nominal cell edge length of 5.0mm is used in the Cone Calorimeter model.

Table C.1: Comparison of grid sizes between the train fire domain and the Cone Calorimeter domain

	Train fire	Cone Calorimeter
$\dot{Q}$ (kW)	6500	1
D^* (m)	2.04	0.06
δx (m)	0.175	0.005
$D^*/\delta x$	11.66	12
δx: nominal cell edge length		

The FDS cone calorimeter model will be used to calibrate the properties of the combustible materials to reflect the correct ignition time, and correct amount of heat release from the materials in an event of fire in the carriage. The results of FDS cone calorimeter simulations will be checked against the cone calorimeter experiments of combustible materials, and the burning characteristics of the materials will be calibrated in the FDS input files. The cone calorimeter model would allow simulating different set of materials to examine the effects of material properties on the fire development. The prepared FDS model of the cone calorimeter is shown in Figure C.4, with representations of computational grid and brief explanations.

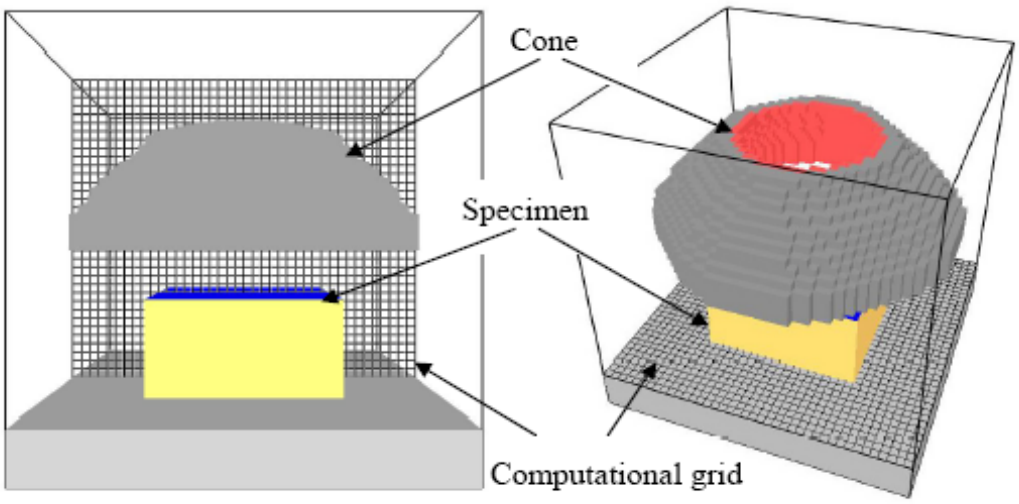

a. Front view of Cone Calorimeter

b. Isometric view of Cone Calorimeter

Figure C.4: Views of the FDS Cone Calorimeter model

The calibration process starts with setting the correct inner wall temperature of the cone to get the required heat flux on the surface of the specimen. The combustible materials are often tested at heat fluxes of 25 to 50kW/m^2 measured at the surface of the specimen, as recommended by the standards [1, 6, 12].

The inner wall temperatures of the cone, which would give the desired surface heat flux values on the specimen, are determined after trial-error simulations . Table C.2 shows the estimated wall temperatures of the cone calorimeter. During the prediction of the surface heat fluxes, the specimen is assumed to be non-combustible to prevent any interference in the predicted heat flux values due to the ignition of specimen.

Table C.2: Cone Calorimeter wall temperatures and predicted surface heat fluxes on specimen

Inner wall temperature of the cone (°C)	Surface heat flux on specimen (kW/m^2)
600	25
645	30
680	35
710	40
770	50

Once the temperature is adjusted to give the required heat flux on the specimen, the following combustibility parameters are to be calibrated in the FDS cone calorimeter simulations against the experimental data acquired:

- ignition temperature,
- the product of specific heat, thickness and density of the combustible ($c\,\delta\,\rho$),
- maximum burning rate, and critical mass flux at ignition temperature,
- heat of vaporization, and heat of combustion.

The combustion properties of the materials, listed above, play a significant role in predicting the flame spread within the rolling stock, since they would define whether the materials are flame-retardant or could easily be ignited at low temperatures. Although the flammability properties of the combustible materials are fixed for a certain material, the behavior of the material changes under different surface heat fluxes.

However, in an FDS simulation, only one set of material properties could be defined for combustibles predicted under certain heat flux level. For example, a set of properties is selected for seats, say calibrated under 30kW/m^2 heat flux. Although the seats could behave in a different manner under various heat flux levels, a compromising value of surface heat flux, at which the material properties are to be calibrated , should be selected in agreement with the observations from the full-scale experiments.

It is reported in the literature [20] that at lower heat flux levels, the single representative characteristic could lead slightly under-predicted heat release rate values, and would predict earlier ignition. At higher heat flux levels, the representative characteristic could over-predict heat release rate, but would delay the ignition. Consequently, as mentioned briefly in Section 4.2.5, in order to overcome this drawback, two additional properties for the combustibles, namely critical mass flux and the maximum burning rate, are defined in the simulations. These parameters would control the mass loss rate of the combustible surface at ignition temperature and limit the burning rate to prevent excessive heat release rates.

The maximum burning rate is used to limit the mass loss rate of the fuel to its measured maximum. This parameter is often used to prevent excess pyrolysis to predict the correct amount of heat release from the combustion of fuels. The 'burning_rate_max' parameter in FDS is used to set the maximum heat release rate of a specimen in cone calorimeter simulations, in accordance with the experimental data acquired.

As mentioned earlier in the text, only the seats and the floor are considered to be combustible within the rolling stock that is being studied. The selection of surface heat flux levels, at which the material properties are going to be calibrated, is based on the recommendations of British Standards' code of practice for fire precautions in the design and construction of passenger carrying trains, BS 6853 [6]. The standard suggests that the burning characteristics of

- downward facing surfaces should be tested at a heat flux of 50kW/m^2,
- vertical surfaces should be tested at a heat flux of 35kW/m^2, and
- upward facing surfaces should be tested at a heat flux of 25kW/m^2.

It should be noted that although the standard provides guidance on testing, it may not always be possible to apply the recommendations to the simulation work. For example, the passenger seats consist both horizontal and vertical sections, namely bases and backs. Consequently, if a set of material properties is to be used for seats in the simulations, an average surface heat flux value is to be selected. Therefore, the material properties of the seats are calibrated at 30kW/m^2 heat flux in this thesis.

According to the recommendations of BS 6853, the floor material should be tested at a surface heat flux of 25kW/m^2. However, the acquired experimental results only include a range of surface heat flux values between 30kW/m^2 and 50kW/m^2. Once the experimental predictions are investigated, it has been found out that the floor material has different burning characteristics at 30kW/m^2 than the remaining test results, which are all in agreement implicitly. The experimental results of floor material tested at 30kW/m^2 show a significant spike about 22nd minute through the testing.

The proposed floor material, Tiflex/Plywood, for Class-378 rolling stock is composed of three layers; Tiflex layer, an epoxy glue, and the plywood as the third layer. Bayer laboratories noted that the spike predicted during the experiments at 30kW/m^2 heat flux corresponds to the stage when the epoxy glue starts to burn. Consequently, if these experimental results were used in the simulations, the combustion characteristics would be based on burning of the internal epoxy glue layer rather than the composite floor material. The heat release rate results predicted from the experiments performed at surface heat flux levels of 35kW/m^2 and above do not show this behavior. In addition, the experimental results do show combustion of all three layers of the composite floor. Consequently, the material properties of the floor are calibrated at 35kW/m^2 heat flux in this thesis.

Figure C.5 shows the results of FDS cone calorimeter simulation with the calibrated seat material properties at 30kW/m^2 surface heat flux, along with the acquired experimental results, given for comparison.

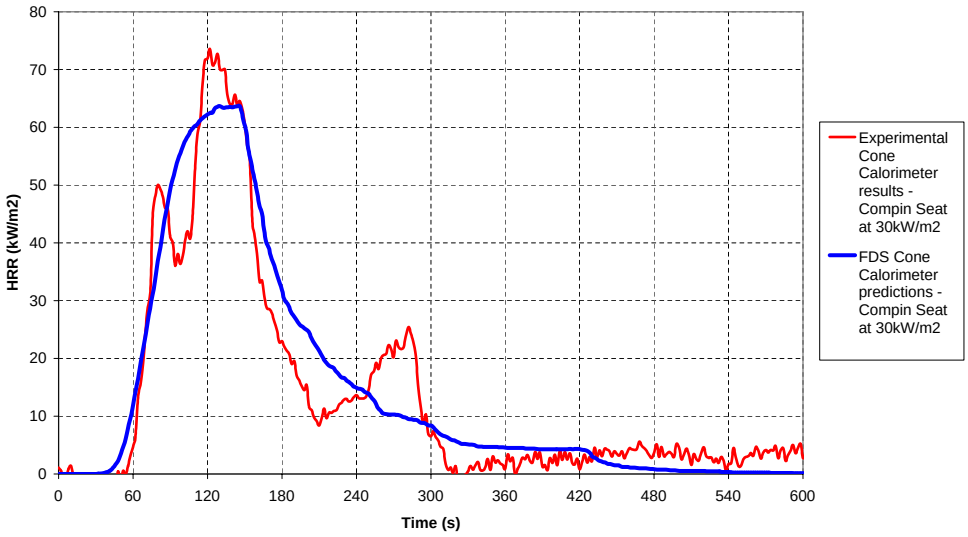

Figure C.5: Heat release rate per unit area, Seat material, FDS Cone Calorimeter calibration

Once the experimental results are examined, it can be seen that there are more than one peak in the predicted variation of heat release rate. This is due to combustion of different layers of materials in the composite form of passenger seat. However, since only one set of parameters can be defined in FDS, the cone calorimeter simulations would only give one peak value for heat release rate.

Consequently, the calibration process is based on the total energy released per unit area of the specimen. In other words, although the peak values in heat release curves of simulation and experimental data might not match, the area under the curves should reasonably agree each other. Therefore, in the calibration of seat material, although the highest peak value and the second peak are not achieved in the simulations, predicted results in FDS match reasonably well with the experimental findings in terms of shape of the curve and the area under it.

Figure C.6 shows the results of FDS cone calorimeter simulation with the calibrated floor material properties at 35kW/m^2 surface heat flux, along with the acquired experimental results, given for comparison.

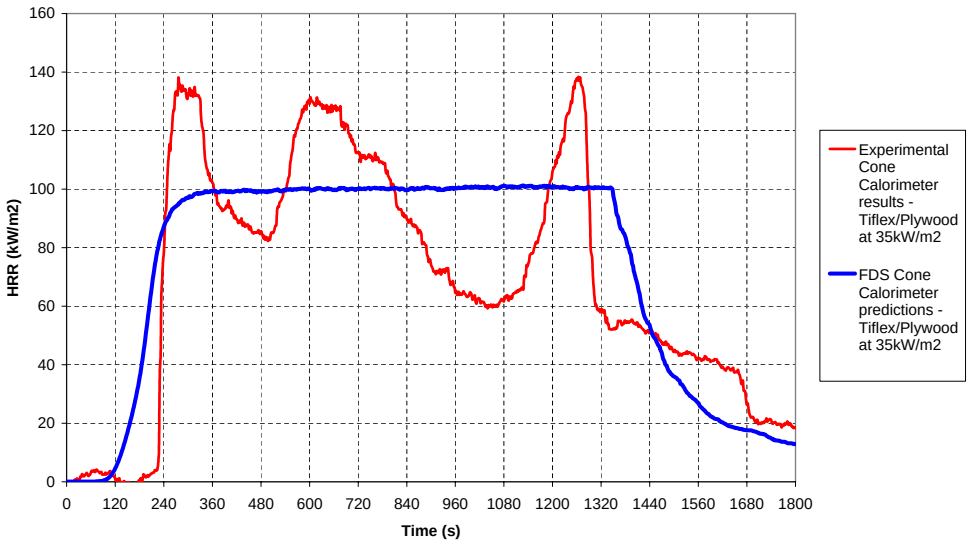

Figure C.6: Heat release rate per unit area, Floor material, FDS Cone Calorimeter calibration

Similar to the discussion above, since only one set of material properties can be defined for the composite floor material, the peaks in heat release rate observed during experimental work can not be obtained in FDS simulations. The three peaks predicted in the experiments correspond to the combustion of three layers of the floor specimen. During calibration of floor material in FDS, a representative peak heat release rate value and the trend of decay conditions are sought. Once again, the material properties are selected so that the amount of energy released in the experiments match reasonably well with the predictions of the simulations.

The calibrated material properties are given in Table C.3. The properties of non-combustible surfaces, such as walls and ceiling, are kept as defined in the initial simulations, since they represent reasonably well the non-combustible surfaces in Class-378 rolling stock.

Table C.3: Material properties used in the final simulations

	Combustible Materials		Non-combustible Materials				
Location	Seats	Floor	Tunnel Walls	Train Walls	Train Ceiling	Doors	Windows
Material	Compin/Pegasus	Tiflex/Plywood	Concrete	Glass wool sandwich between aluminum panels			Laminated safety glass
Density, ρ (kg/m^3)	121.4†	944.4†	2100	119	176	276	1380
Thermal conductivity (W/mK)	0.56$^\diamond$	0.12$^\diamond$	1.1	0.038	0.038	0.038	0.049
Specific heat, c (kJ/kgK)	10.66*	0.234*	0.88	0.68	0.68	0.68	0.84
Thickness, δ (m)	0.0017*	0.0235*	0.7	0.1	0.06	0.035	0.023
Ignition temperature (°C)	505*	560*	-	-	-	-	-
Heat of vaporization (kJ/kg)	4000*	4340*	-	-	-	-	-
Effective heat of combustion (kJ/kg)	11350*	15430*	-	-	-	-	-
Maximum burning rate (kg/m^{2}s)	0.0185*	0.018*	-	-	-	-	-
Critical mass flux (kg/m^{2}s)	0.012*	0.009*	-	-	-	-	-
ρ c δ (kJ/m^{2}K)	2.2*	5.2*	-	-	-	-	-

†: Calculated from the Cone Calorimeter data by dividing the initial mass by the initial volume.
$^\diamond$: Derived from the books. [8, 10]
*: Calibrated through a set of FDS Cone Calorimeter simulations.

In an FDS simulation, in addition to the combustible material properties, a chemical reaction should be defined for the combustion, where the soot and carbon-monoxide yields can be defined along with the amount of energy released per unit mass of oxygen consumed during the combustion reaction.

In the initial and sensitivity simulations, the combustion reaction for the seat material was used in agreement with the comments from the published research study, from which the calibrated material properties were taken [20]. The reaction for the seat material, i.e. for FRP Polyester, was given as:

$$C_{5.77}H_{6.25}O_{1.63} + 6.5175\,(O_2 + 3.76N_2) \rightarrow 5.77\,CO_2 + 3.125\,H_2O + 24.5\,N_2$$

For this reaction, the following additional parameters were defined [20]:

- Soot yield: 0.062 kg/kg
- Carbon-monoxide yield: 0.0705 kg/kg
- Radiative fraction: 0.35
- Energy release per unit mass of oxygen consumed: 11900 kJ/kg.

In the final simulations, since the material properties are calibrated to reflect the combustible surfaces in Class-378 rolling stock, the combustion reaction and the associated parameters have to be revised accordingly.

The initial and sensitivity simulations show that the flame spread over the floor defines the extent of the fire development, and indicates whether flashover conditions are achieved or not. Consequently, it can be concluded that the fire development within the rolling stock is governed by the combustion of the floor material. Following on from this discussion, the combustion reaction is revised based on Tiflex/Plywood material as follows:

$$CH_{1.7}O_{0.74} + 1.055\,(O_2 + 3.76N_2) \rightarrow\ CO_2 + 0.85\,H_2O + 3.97\,N_2$$

In the absence of detailed chemical composition of the Tiflex/Plywood floor material, the chemical reaction for wood [10], given above, is used in the final simulations. It should be

noted that the chemical composition has very little influence on the heat release rate variation and onboard conditions predicted from the simulations.

The amount of energy release per unit mass of oxygen consumed for the assumed reaction is calculated using the following equation [25]:

$$\Delta H \approx \frac{\nu_{O_2} M_{O_2}}{\nu_f M_f} \Delta H_{O_2} \tag{C.2}$$

where ΔH is the heat of combustion; 12400 kJ/kg for wood [10]; ν_{O_2} is the stoichiometric coefficient of oxygen; 1.055 for the assumed reaction; and M_{O_2} is the molecular weight of oxygen; 32 g/mol. If the appropriate values for the stoichiometric coefficient of fuel; 1; and molecular weight of fuel; 25.5 g/mol; are inserted in Equation C.2, then the energy release per unit mass of oxygen consumed during this reaction can be found to be about 9370 kJ/kg.

The soot and carbon-monoxide yields during the combustion of seat and floor materials within the Class-378 rolling stock are derived from the experimental cone calorimeter data. The experiments have produced the following results:

- Compin/Pegasus seat tested at 30kW/m^2 surface heat flux
  - Mean carbon-monoxide yield: 0.067 kg/kg
- Tiflex/Plywood floor tested at 35kW/m^2 surface heat flux
  - Mean carbon-monoxide yield: 0.031 kg/kg

The relationship between the carbon-monoxide yield and the soot yield is given by the following equation [25]:

$$y_{CO} = \frac{12\,x}{M_f\,\nu_f}\,0.0014 + 0.37\,y_s \tag{C.3}$$

where x is the number of carbon atoms in a fuel molecule, and y_{CO} and y_s are the carbon-monoxide and soot yields, respectively. It should be noted that Equation C.3 refers to well-ventilated fires. In the absence of reported data for soot production during the combustion of seat and floor materials in cone calorimeter experiments, soot yield for the combustion reaction will be estimated from Equation C.3 and defined in the final simulations.

As noted earlier, only one combustion reaction can be defined in an FDS simulation. However, the rolling stock simulation model incorporates two combustible surfaces, seat and floor, each of which has different yields of hazardous combustion products. Consequently, a compromising value for carbon-monoxide and soot yields are estimated and input in the FDS simulations.

The carbon-monoxide concentration for the reaction in the final simulations is defined based on the area-averaged yields of the two combustibles. The carbon-monoxide concentration is calculated, based on a DMOS type carriage, to be:

$$y_{CO-total} = \frac{y_{CO-seats} \cdot A_{seats} + y_{CO-floor} \cdot A_{floor}}{A_{seats} + A_{floor}}$$

$$y_{CO-total} = \frac{0.067 \cdot 22.7 + 0.031 \cdot 39.6}{22.7 + 39.6} = 0.044$$

The soot yield is calculated using Equation C.3 and area-averaged carbon-monoxide yield as:

$$y_s = (y_{CO} - \frac{12\,x}{M_f\,\nu_f}\,0.0014)\ /\ 0.37$$

$$y_s = (0.044 - \frac{12 \cdot 1}{25.5 \cdot 1}\,0.0014)\ /\ 0.37 = 0.117$$

To summarize, the following parameters have been used in the final simulations for the combustion reaction:

- Soot yield: 0.117 kg/kg
- Carbon-monoxide yield: 0.044 kg/kg
- Radiative fraction: 0.37 [10]
- Energy release per unit mass of oxygen consumed: 9370 kJ/kg.

CURRICULUM VITAE

PERSONAL INFORMATION

Surname, Name: Musluoğlu, Eren

Nationality: Turkish (TC)

Date and Place of Birth: 18 February 1979 , Ankara

Marital Status: Single

Phone: +90 532 482 07 01, +44 777 550 12 83

Fax: +44 208 681 57 06

email: erenmusluoglu@gmail.com

EDUCATION

Degree	Institution	Year of Graduation
MS	METU Mechanical Engineering	2003
BS	METU Mechanical Engineering	2000
High School	TED Ankara College	1996

WORK EXPERIENCE

Year	Place	Enrollment
2005-Present	Mott MacDonald Ltd., UK	Tunnel Ventilation Engineer
2002-2005	Ostim Investment Co.	Mechanical Engineer
2000-2005	METU Department of Mechanical Engineering	Teaching Assistant

FOREIGN LANGUAGES

Advanced English

PUBLICATIONS

1. Eralp O.C., Başeşme E., Kayılı S. and Musluoğlu E. "A CFD Analysis of Station Fire Incidents and Determination of Passenger Evacuation Scenarios", International Congress on Safety Innovation Criteria Inside Tunnels (2005)
2. Eralp O.C., Musluoğlu E. and Kayılı S. "CFD Analysis of Fire Incidents around Cross-over Located on the Tunnels Connecting ODTÜ and Bilkent Stations in Ankara Metro System", International Congress on Safety Innovation Criteria Inside Tunnels (2005)
3. Eralp O.C., Musluoğlu E. "YeraltıToplu Taşıma Sistemlerinde Acil Durum Havalandırması", VI. Ulusal Tesisat Mühendisliği Kongresi ve Sergisi (2003)